The Ann Arbor Road Profilometer Meeting

Final Report

M. W. Sayers
T. D. Gillespie

April 1986

1. Report No. FHWA/RD-86/100	2. Government Accession No.	3. Recipient's Catalog No.
4. Title and Subtitle THE ANN ARBOR ROAD PROFILOMETER MEETING		5. Report Date April 1986
		6. Performing Organization Code
7. Author(s) M.W. Sayers and T.D. Gillespie		8. Performing Organization Report No. UMTRI-86-19
9. Performing Organization Name and Address Transportation Research Institute The University of Michigan 2901 Baxter Road Ann Arbor, Michigan 48109		10. Work Unit No. 31W3 062
		11. Contract or Grant No. DTFH61-83-C-00123
12. Sponsoring Agency Name and Address Federal Highway Administration U.S. Department of Transportation Washington, D.C.		13. Type of Report and Period Covered Final 11/84-11/85
		14. Sponsoring Agency Code
15. Supplementary Notes FHWA Contract Manager: Rudolph R. Hegmon, HNR-20		

16. Abstract

The Road Profilometer Meeting was held in Ann Arbor in September 1984. In this meeting, 11 agencies used their profilometer equipment to provide measures over 27 test sites. Overall, 13 independent instruments were used, including static rod and level measures on 10 of the sites. Analyses of the profiles obtained in the experiment were used to determine and compare some of the performance characteristics of profilometers in use today. The profiles from each system were processed to yield quarter-car roughness, RMSVA roughness, power spectral density functions, and waveband indices. Plots of filtered profiles were also compared. These results were used to determine the performance limits of the profilometers, in terms of operating speed, surface type, and roughness level. Most of the profilometers were demonstrated to measure valid profiles over a full range of pavement roughness, with varying degrees of accuracy that depend on the particular profilometer and the analysis used. Some of the profiles submitted were not valid, indicating that better data-checking methods need to be adopted.

17. Key Words Longitudinal profile, Profilometer, Road roughness, Quarter-car, Power spectral density, RMSVA	18. Distribution Statement No restrictions. This document is available to the public through the National Technical Information Service, Springfield, Virginia 22161		
19. Security Classif. (of this report) Unclassified	20. Security Classif. (of this page) Unclassified	21. No. of Pages 237	22. Price

ii

Approximate Conversions to Metric Measures

| Symbol	When You Know	Multiply by	To Find	Symbol
LENGTH				
in	inches	*2.5	centimeters	cm
ft	feet	30	centimeters	cm
yd	yards	0.9	meters	m
mi	miles	1.6	kilometers	km
AREA				
in²	square inches	6.5	square centimeters	cm²
ft²	square feet	0.09	square meters	m²
yd²	square yards	0.8	square meters	m²
mi²	square miles	2.6	square kilometers	km²
	acres	0.4	hectares	ha
MASS (weight)				
oz	ounces	28	grams	g
lb	pounds	0.45	kilograms	kg
	short tons (2000 lb)	0.9	tonnes	t
VOLUME				
tsp	teaspoons	5	milliliters	ml
Tbsp	tablespoons	15	milliliters	ml
fl oz	fluid ounces	30	milliliters	ml
c	cups	0.24	liters	l
pt	pints	0.47	liters	l
qt	quarts	0.95	liters	l
gal	gallons	3.8	liters	l
ft³	cubic feet	0.03	cubic meters	m³
yd³	cubic yards	0.76	cubic meters	m³
TEMPERATURE (exact)				
°F	Fahrenheit temperature	5/9 (after subtracting 32)	Celsius temperature	°C
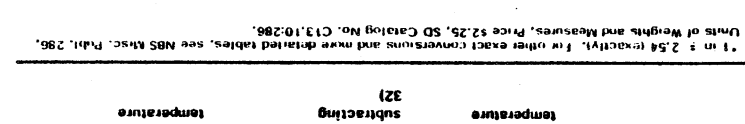
*1 in = 2.54 (exactly). For other exact conversions and more detailed tables, see NBS Misc. Publ. 286, Units of Weights and Measures, Price $2.25, SD Catalog No. C13.10:286.

Approximate Conversions from Metric Measures

Symbol	When You Know	Multiply by	To Find	Symbol
LENGTH				
mm	millimeters	0.04	inches	in
cm	centimeters	0.4	inches	in
m	meters	3.3	feet	ft
m	meters	1.1	yards	yd
km	kilometers	0.6	miles	mi
AREA				
cm²	square centimeters	0.16	square inches	in²
m²	square meters	1.2	square yards	yd²
km²	square kilometers	0.4	square miles	mi²
ha	hectares (10,000 m²)	2.5	acres	
MASS (weight)				
g	grams	0.035	ounces	oz
kg	kilograms	2.2	pounds	lb
t	tonnes (1000 kg)	1.1	short tons	
VOLUME				
ml	milliliters	0.03	fluid ounces	fl oz
l	liters	2.1	pints	pt
l	liters	1.06	quarts	qt
l	liters	0.26	gallons	gal
m³	cubic meters	35	cubic feet	ft³
m³	cubic meters	1.3	cubic yards	yd³
TEMPERATURE (exact)				
°C	Celsius temperature	9/5 (then add 32)	Fahrenheit temperature	°F

°F   -40   0   32   98.6   160   200   212
°C   -40   -20   0   20   37   40   60   80   100

cm   inches

TABLE OF CONTENTS

TABLE OF CONTENTS (continued)

LIST OF FIGURES

LIST OF FIGURES (continued)

LIST OF FIGURES (continued)

LIST OF TABLES

LIST OF TABLES (continued)

ACKNOWLEDGEMENTS

INTRODUCTION

Background

This report presents the analysis and findings from a Road Profilometer Meeting (RPM) held in Ann Arbor, Michigan on September 11 to 13, 1984. The program was conducted by The University of Michigan Transportation Research Institute (UMTRI) with the participation of a number of organizations owning and/or operating road profilometer equipment. The program was sponsored by the Federal Highway Administration (FHWA) as a task under the project, "Methodology for Road Roughness Profiling and Rut Depth Measurement," Contract No. DTFH61-83-C-00123.

A road profilometer is a vehicle-mounted instrumentation system intended to measure vertical deviations of the road surface along the direction of travel. They have been in existence for over two decades, with many millions of dollars spent thus far on their purchase and operation. In recent years, the variety in profilometer hardware and design available to the highway community has increased dramatically. The most universal purpose for road profile measurements at the present time is to assess the roughness of the surface encountered by motor vehicles. In the future, as their capabilities expand, profilometers are expected to play a role of ever-increasing importance as an engineering tool for pavement condition evaluation, including a key role in the Strategic Highway Research Program.

The inertial profilometer, originally invented by Spangler and Kelly at the General Motors Research Laboratories (GMRL) 20 years ago, allowed measurement of the longitudinal profile of a road at speeds of 60 km/h on typical paved roads.[1] However, the instrumentation available at that time was relatively expensive and difficult to maintain. In this design, a vertically mounted accelerometer serves as an inertial reference by which the vertical motions of the vehicle body are measured. A second measure of the instantaneous height of the vehicle above the road is added to the vehicle body motions to obtain the profile of the road surface.

As newer instrumentation and computer equipment have become available, the original GM design concept has been retained, although incorporating many varieties of analog and digital computers to combine the transducer signals and compute the profile. The mechanical follower wheels originally used for measuring distance to the road surface have

been replaced in more recent systems with a variety of noncontacting sensors that use ultrasound, laser beams, visible lights, or infrared light to detect the road surface.

In Europe, profilometers based on different design concepts have been developed. The Longitudinal Profile Analyser (APL), developed by the Laboratoire Central des Ponts et Chaussees (LCPC), France, is a towed trailer that uses a special rotational pendulum as an inertial reference.[2] The British Transport and Road Research Laboratory (TRRL) laser profilometer uses a rigid beam with laser sensors mounted along its length. The laser signals are processed to cancel the beam motions that occur as it is towed over the road at highway speeds.[3]

Common to all designs is the limitation that the measurements are confined to a wavelength range. The limits on long wavelengths cause the measured profiles to exclude constant slopes and geographic features (hills and valleys). The true profile of the road (measured on a scale of absolute elevation) includes these features. Thus, profiles from a profilometer cannot be compared directly to the true profile in a meaningful way. Different profilometers were designed to capture different wavelength ranges. For example, the GM-type inertial profilometer is designed to measure the wavelengths that have significant influence on the vibrations of road-using vehicles.

Presuming the instrumentation is functioning correctly, it is proper to expect that all profilometers measure a profile. However, the profiles from different equipment will vary in quality with regard to the accuracy and bandwidth of the measurement. In evaluating the quality of a measure, it must be remembered that the profile itself has no direct meaning. Only when it is processed for some specific application can the quality be judged, and then only with regard to the accuracy of the results obtained in that particular application. It is therefore expected that any given profilometer design will be valid for some applications, but not for others.

With all of the different design concepts of the profilometers in use today there has not yet been an objective and independent study of their performance capabilities. The program reported here was conceived out of the need to obtain an objective evaluation of the performance of the various types of road profilometry equipment available, capitalizing on the fact that similar tests were being designed and organized to validate the profilometer built for FHWA under this project.

The Road Profilometer Meeting (RPM) was held in Ann Arbor in September, 1984. In this meeting, 11 agencies used their profilometer equipment to provide measures over 27

test sites. Overall, 13 independent instruments were used, including manual rod and level measures on 10 of the sites.

Objective

The objective of the Road Profilometer Meeting was to determine and compare some of the performance characteristics of profilometers in use today. A necessary part of that objective was to determine just how profilometers can be meaningfully compared with regard to measuring various aspects of road roughness. Because most profilometers measure a "filtered" form of the profile (normally excluding long wavelengths), the profiles cannot be compared at the simple visual level. Rather, the profiling ability of the systems must be compared in the context of the applications for the profile data.

An aspect of this objective was to determine the performance limits of the profilometers, in terms of operating speed, surface type, and roughness level. Many profilometers are capable of measuring valid profiles under some conditions. However, their reliable use for routine purposes by highway departments further dictates that they be functional and valid over the full range of anticipated road conditions. At a minimum, if a profilometer cannot measure validly under some conditions, then the profilometer records should clearly reflect the fact that questionable data are being obtained.

It is emphasized here that the objective of the Road Profilometer Meeting was validation. It was not a "correlation" program, nor was it a "calibration" program as commonly held for various types of pavement measuring equipment. This is because profilometers are calibrated by certain functional checks and adjustments of the equipment to ensure valid measurements in routine use. Thus, the intent here was to validate the ability of the different profilometers to measure profile as they are routinely used, and to determine the limits on the validity. Although a number of profile analyses were applied to the data, the intent was simply to see whether the various profilometers were appropriate for that analysis. Correlations between the results from the various analyses were not investigated, although the results have been tabulated in an appendix as a resource for the interested reader.

Report Organization

The report is divided into five sections. An overview of the Road Profilometer Meeting was covered by the previous introductory material in this section. The research methodology is described in the next two sections, "Experiment" and "Analyses," which

3

separately cover the testing activities and the analytical work, respectively. The results of the experiment are presented in the section "Results," including a description of each profilometer and the findings regarding its performance. The "Results" section is organized such that the material pertaining to each piece of equipment is fairly independent of the material pertaining to the other equipment. This is intended to aid the reader who is interested primarily in the findings related to one particular instrument. In order to fully appreciate the findings, it is recommended that the reader be familiar with the material in the "Experiment" and "Analyses" sections. The results are summarized and compared in the "Conclusions" section.

Engineering Units

With the equipment and analyses used in the RPM, a mixture of both English and metric units are commonly used. Test speeds may have been selected in miles per hour (mi/h) or kilometers per hour (km/h). Some instruments are set up to sample or perform analysis at intervals of feet, while others are set up on metric measures. Metric units have been selected as the preferred choice in the text and figures, with English equivalents indicated immediately thereafter in parentheses where appropriate.

EXPERIMENT

Participants

In order to obtain the broadest representation possible, the Road Profilometer Meeting (RPM) was considered open to any and all devices in the world that are said to measure road profile. Evaluation is simplified for systems that both measure *and* record the profile, although devices that do not include the additional (and expensive) hardware necessary to record the data can also be validated if the details of the data reduction method are known. Invitations were sent to those who owned and operated these kinds of equipment, and/or to the developers of the equipment. Table 1 lists the organizations that participated in the RPM, and also indicates some important design elements of the profilometers that will be discussed below.

Personnel participating from each organization are listed in appendix A. In addition to the participants, a number of people from other organizations visited to observe the program. The observers are also listed in the appendix.

Overview of Profilometer Concepts

At the time of the program planning, a number of generic profilometer types were known to exist, as described below:

GM-type Inertial Profilometers

The profilometers in most common use today are of the inertial design developed by General Motors Research in the mid-1960's. The General Motors Corporation, the Michigan Department of Transportation, and the South Dakota Department of Transportation each have units that they have built themselves. K. J. Law Engineers, Inc. commercially manufactures these profilometers under a patent license, and has incorporated improvements in the design. The original GM design was such that profile measurements had to be made at a constant speed. The more recent models from K. J. Law Engineers, Inc. use improved software with "spatial" filtering that compensates for speed variations during measurements.

5

Table 1. Summary of participants and equipment in the Road Profilometer Meeting.

Agency	Profilometer Manufacturer/model	Type	Profile storage	Onboard profile
Colorado DOH (with K. J. Law)	K. J. Law 8300 Roughness Surveyor	GM — ultrasound	none	yes
FHWA (UMTRI) Selcom system Infrared system Rod and level	FHWA contract with UMTRI	GM — laser GM — optical Static survey	tape cartridge tape cartridge field notes	no no —
General Motors Proving Grounds	built in-house	GM — laser	9-track tape	no
LCPC (with CRR and MAP Sarl)	LCPC and MAP APL Trailer	APL	analog tape	yes
Michigan DOT	built in-house	GM — optical	analog tape	yes
Minnesota DOT	K. J. Law 690 DNC	GM — optical	9-track tape	yes
Novak, Dempsey & Assoc.	VTI Road Surface Tester	GM/VTI — laser	floppy disk	no
Ohio DOT	K. J. Law 690 DNC	GM — optical	9-track tape	yes
Pennsylvania State Univ. (Penn. Trans. Inst)	K. J. Law 690 (modified)	GM — follower wheel	analog tape	no
South Dakota DOT	built in-house	GM — ultrasound	floppy disk	yes
West Virginia DOT	K. J. Law 690 DNC	GM — optical	9-track tape	yes

K. J. Law units have been purchased by the States of Pennsylvania, Ohio, West Virginia, Minnesota, Kentucky, and Texas. Invitations were sent to all of the above. The General Motors Corporation, Michigan DOT, South Dakota DOT, Ohio DOT, West Virginia DOT, Minnesota DOT, and Pennsylvania State University (operating the unit from the Pennsylvania DOT) were able to participate. The profilometer being designed and built for the Federal Highway Administration (FHWA) by UMTRI is also an inertial-type profilometer and participated in the program with two configurations of road-follower hardware.

K. J. Law, Inc. also builds an instrument based on the same concepts, called the Model 8300 Roughness Surveyor. It does not include the equipment to record profile, but instead calculates quarter-car statistics from profile during measurement. A unit was purchased by the Colorado Department of Highways (DOH), and Colorado was invited. The system, which had not yet been delivered to Colorado at the time of the RPM, was operated by personnel from K. J. Law Engineers, Inc.

APL

The Laboratoire Central des Ponts et Chaussees (LCPC, France) has developed a towed trailer with a combination of instrumentation and built-in mechanical properties that allow it to measure profile. It uses an inertial pendulum in lieu of an accelerometer to provide the profile reference. The same unit is used by the Centre de Recherches Routieres (CRR, Belgium), although each organization has its own method for processing the profile data obtained. Both organizations were invited to participate. By agreement between them, LCPC personnel came to Ann Arbor with an APL profilometer. The CRR sent staff to observe the experiment and take copies of the profile data home for separate processing.

Swedish VTI Laser Road Surface Tester

The Swedish Road and Traffic Research Institute (VTI) has developed a system for noncontact measurement of pavement condition. One unit is in the United States and is operated by Novak, Dempsey & Associates, Inc. (NDA) (it is now operated by IMS, Inc.). Both VTI and NDA were invited to participate. By agreement between the two organizations NDA brought a unit to participate in the program. Postprocessing of the data records was performed by VTI, who then copied the computed profiles onto a 9-track digital tape that was sent to UMTRI for analysis.

ARAN

Highway Products International (Ontario, Canada) builds a pavement condition monitoring system that includes an accelerometer mounted on a road-wheel for measuring profile. HPI was invited, but was unable to attend.

TRRL Laser Profilometer

The Transport and Road Research Laboratory (TRRL) in England has developed a unique laser profilometer. Distance to the road surface is sensed at three points along the length of a trailer. As the trailer progresses forward, road elevation at the leading sensor is referenced to that at the other sensors so that a continuing profile can be developed. TRRL was invited but was unable to arrange participation.

Overview of Profilometer Design Considerations

To exercise the different profilometers over the full range of their capabilities, it is necessary to include test sites with surfaces that might challenge the various systems. The profilometers are described individually in the "Results" section, but an overview of the major design considerations is included here, to aid the reader in appreciating the various challenges posed by certain types of pavement surfaces to the different profilometers.

All of the participating profilometers, except the French APL trailer, are based on the concept of the GM-type inertial system. In this design, a vehicle is instrumented with an accelerometer and a height sensor. The accelerometer senses the vertical motions of the vehicle body, relative to an inertial reference. The height sensor follows the road by sensing the distance between the vehicle and the road surface. The signals from the accelerometer and the height sensor are used together to compute the profile of the road, relative to an inertial reference, by eliminating the vehicle reference. This profile computation is a form of data processing that is specific to GM-type profilometers, and requires some type of computer capability. Within the concept of the GM-type profilometer, the designer is faced with an array of possible choices for the data acquisition system, the height sensor, and the computer system.

Data Acquisition Systems

Systems that process and record the signals from the various sensors can be classified as analog or digital. An analog data acquisition system processes signals using electronic

circuits, and stores data signals as continuously varying voltages, using a device such as an FM tape recorder. Profile computations are made using an analog computer, which is essentially a system of precision electrical components. Analog systems are limited in range and accuracy. Voltages that are too high will saturate operational amplifiers, while voltages that are too low are lost in a background of electronic noise. The amplitudes in a road profile are approximately proportional to wavelength, such that a profile containing wavelengths over the range of 1- to 100-m will contain information covering a range of 100 to 1. This allows little margin for error in setting the amplifier ranges for the right roughness level, especially when considering that roughness varies along the length of a road. Thus, users of analog systems must be very careful to keep all of the amplifiers set close to the optimum at all stages in the system—from the transducers, to the profile computation, to the tape storage.

Because of these amplitude limitations, analog systems can be challenged by roads that are very rough or very smooth, or which include a few rough sections in an otherwise smooth surface.

Digital systems use one or more components to process data numerically, using arithmetic operations. A digital tape recorder stores a signal as a sequence of numbers, rather than as a continuously varying voltage. Digital systems are based on computer technology, and are fairly recent. Once a voltage has been digitized (converted from a voltage to a number), ranging problems can be eliminated. There is no background noise to deal with, and the maximum range of a digital computer can be set much higher than any measurement that would be encountered. Digital systems are also convenient for gathering data that will eventually be entered into a computer system for further processing. A potential problem with digital systems is that there is no information about what happened to the signal between the samples. For example, if a profile signal is digitized every 0.5 meter, a tar strip that falls between samples will not be represented in the sequence of numbers that represents the profile. Usually, when an analog signal from a transducer is digitized, an anitialiasing filter is used to eliminate the high-frequency component of the signal. This approach eliminates the potential problem of missing information between samples. (For example, a tar-strip between samples would cause the filtered signal to include the frequencies of the tar-strip that can be seen by the system.) However, some of the noncontacting height sensors used in profilometers never produce an analog signal, so conventional antialiasing filters cannot be used.

Most of the data aquisition and processing portions of the profilometer systems are unique, and can be expected to show different strengths and weaknesses under different conditions.

The original GM-type Profilometer used a mechanical follower wheel, spring-loaded against the ground.[1] In this design, the position is sensed with a conventional potentiometer, placed between the wheel and the vehicle body. The follower-wheel assembly and tire have dynamic properties that influence the quality of the measurement. Probably the biggest problem with a follower-wheel system is that it can sometimes bounce when it hits a bump or hole. The result is that the profile obtained will trace the path of the wheel through the air, rather than the surface. The design of follower wheels used on GM-type profilometers has limited their valid measurement range to exclude rough roads, and imposes limits on the operating speed on even slightly rough roads. (The APL trailer, which is not a GM-type of profilometer, also uses a mechanical follower wheel. However, it has a suspension that is more effective at keeping the wheel on the ground—even on very rough roads.)

The mechanical follower wheels have been replaced in many of the newer profilometers by noncontacting sensors which measure height using ultrasound, laser beams, or optical images.

Height can be measured using ultrasound in several ways. A speaker can emit a short burst of sound, and the time needed for the sound to reach the pavement and be reflected back to a microphone can be measured.[4] By knowing the speed of sound through air, the distance can be computed from the time interval. Another method involves the continuous measurement of phase in the reflected sound, using a steady tone for the source.[5] Measuring height with ultrasound requires that a number of problems be solved that have nothing to do with the surface quality, such as effects of wind and changes in air pressure. Surface condition can also challenge an ultrasonic system if it is a poor reflector of sound. None of the sensors can function unless a detectable sound is returned to the microphone. Generally, open texture and bumps with sharply sloping surfaces are poor reflectors, which might cause an ultrasonic sensor to lose the signal. Smooth roads also pose a challenge, because the ultrasound sensors typically have limited resolution—an effect that adds a small amount of roughness to the measurement.

Laser beams are used in other systems to measure vehicle height by triangulation. A laser beam is projected straight down onto the surface resulting in a small, bright spot of light. The spot is seen by a photodetector mounted to the side. Optics and a linear detector are used to relate the light spot location to an angle, from which the distance from the vehicle to the ground is determined.[3, 6] The laser uses a single frequency (monochromatic light), and the detector can include filters to exclude effects of ambient

10

light. Thus the system may be made insensitive to variations in light intensity, both the ambient and that reflected from the laser. One problem that can occur with a laser sensor is that the spot can go into a crack or hole, where it cannot be seen by the detector. Another property of this design is that it may include texture in the measure, which can add a random error to a profile if not properly dealt with in the digital data system. Thus, surfaces with open textures or significant cracking might challenge this type of device.

Instead of the small image projected by a laser, a larger patch of light can be projected onto the surface to reduce the incidence of signal loss when the light beam drops into a crack or hole. However, the size of the image makes its precise location harder to pinpoint, particularly when the size is changing due to surface topography, and the intensity changes due to surface reflectiveness. A noncontact sensor of this type was developed by Southwest Research using an infrared light beam with two photodetectors viewing the image from an angle.[7, 8] The relative amount of illumination falling on detectors is used to establish the angle to the light spot, and hence the distance from the detector to the road surface. Surfaces that exhibit abrupt changes in reflectiveness (for example, painted stripes, black tar strips in Portland Cement Concrete joints, oil stains) might challenge this type of sensor.

The design of the noncontacting sensor used by K. J. Law Engineers, Inc. and the Michigan DOT also employs a large spot of visible light, with modifications to overcome the difficulties mentioned above. The image on the road surface is rectangular, with a short dimension in the direction of travel to better define the location of measurement. The angle to the light spot is also measured with a system that includes a detector and rotating mirror, designed to eliminate error due to variations in surface reflectivity.

Site Selection

The philosophy of comparing profilometers "as they are normally used" required that the comparative tests be conducted on actual road surfaces (rather than, for example, a laboratory dynamic test). Ideally, the crews would operate the profilometers in their routine fashion, modified only as necessary to obtain the data required.

In order to put numbers on the accuracy obtainable with each system, it is essential to have reference measures for some of the profiles. Only a static method, such as rod and level, was appropriate for this task. The static method, while laborious, is very straightforward and contains no surprising sources of error. It is trivial to specify the requirements for accuracy and sample interval to exceed the capabilities of the

11

profilometers. For this program, the sample interval was 76 mm (0.25 ft), and the accuracy was better than 0.5 mm (0.02 inch).

It is not trivial to obtain the profile measurements with rod and level, however. The process is time consuming, taking about five hours to measure a profile 161 meters long (1/10th mile). Because of the time that a traffic lane must be closed to traffic, it was not feasible in this study to obtain rod and level measures on public roads. The General Motors Proving Grounds (GMPG) offered the use of their facilities for this program on nine sites that could be closed off for rod and level measurement. These sites were built by General Motors to evaluate new vehicles under a variety of road conditions, and therefore they encompass a wide range of surface types and roughness levels. (In this case, they are maintained to keep the same properties, not to improve rideability as with normal highways.)

Knowing the characteristics of profilometer instruments and, in particular, areas in which the various designs might be limited, additional test sites were selected from the public roads in the Ann Arbor area to address the following areas of performance:

- roughness limits (can the profilometers handle the large amplitudes encountered on rough roads?)

- smoothness limits (can the profilometers maintain linearity on smooth roads, when vehicle vibrations and background instrumentation noise are significant?)

- texture (can the laser and ultrasonic profilometers provide a measure on open surfaces that could "lose" a dot image or reflect ultrasound poorly?)

- reflectiveness changes (can the optical systems tell the difference between a color change and a bump?)

- reflectiveness levels (can the optical sensors operate on highly reflective (white) new PCC, on nonreflective (black) new asphalt, or combinations of the above?)

- wavelength range (are wavelengths accurately "seen" by the profilometers at various test speeds?)

- singularities (can the profilometers handle singular features such as tar strips, open joints, and patches?)

The site selection also reflected the practical consideration that sites should be located within reasonable proximity to each other, so that the profilometers could perform the

12

measurements within a moderate amount of time. A second concern was the need for sites where the profilometers could maintain a constant speed, thereby excluding roads within the city that experience stop-and-go traffic conditions. It should be noted that the limitation of constant measurement speed is inherent to many, but not all, of the profilometers that participated in the program. In particular, the newer K. J. Law profilometers are designed to allow speed variations during a profile measurement. Because the older systems do not allow speed variation during a measurement, the experiment was not designed to isolate and evaluate the effect of speed variation.

Eventually, 18 public road sites were selected which could be covered in a few hours. Table 2 provides a description of each site, along with characteristics (in parentheses) that might challenge some of the systems. Table 3 provides similar descriptions of the nine sites located within the GMPG.

Site Identification

The experiment was designed around the philosophy of evaluating the ability of the road profilometers to measure comparable profiles. Though it is desirable to assess the differences between profilometers as operated by their normal crew, that does not extend to the differences in interpretation of what is the wheeltrack. Thus, the experimental design included considerable effort to ensure that the profilometers were measuring profile on the same section of road.

White reference marks were painted along the left wheeltrack of many of the public road sites. On these sites, the operators were requested to make the profile measurement one foot to the right of the marks, as shown in figure 1 below.
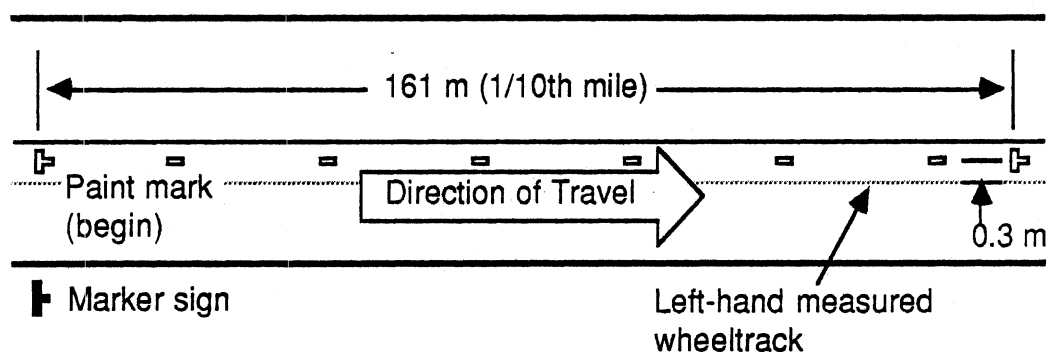
Figure 1. Diagram of the site identification markings.

Table 2. Descriptions of test sites on public roads.

Site No.	Length (meters)	Description
1	483	Very rough bituminous with cracks and patches (patches and cracks might challenge some of the height sensors; roughness level might cause out-of-range problems; roughness might cause bouncing of mechanical systems; patching might challenge digital systems)
2	483	Patched and rolling bituminous; manhole cover (rolling features might cause out-of-range problems; manhole cover might cause bouncing of mechanical systems; surface of manhole cover might challenge non-contacting height sensors)
3	322	Railroad crossing (speed limit of 55 km/h was suggested) (optical sensors might be confused by white painted lines on pavement; all height sensors might be challenged crossing rails; digital systems might miss rails)
4	1127	Surface treatment road, with long- and medium-waves (has no specific features that would challenge systems)
5	644	Surface treatment road with moderate roughness (has no specific features that would challenge systems)
6	805	Asphaltic concrete road with moderate roughness (has no specific features that would challenge systems)
7	966	Transition from old maintained asphalt to asphalt with deep longitudinal cracking (longitudinal cracks might confuse laser sensors)
8	644	Surface treatment road with minor corrugations and some big repairs underlying the most recent surface treatment (open texture and some loose gravel might challenge all of the non-contacting height sensors; corrugations might confuse some height sensors)
9	805	Good PCC construction, surface has lateral grooves (grooves might confuse laser and ultrasound sensors; grooves might cause aliasing problems with digital systems)
10	805	Good PCC construction, surface has lateral grooves (different contract than site 9) (grooves might confuse laser and ultrasonic sensors; grooves might cause aliasing problems with digital systems)
11	805	Good PCC with visible tar-strips flush at joints (extreme reflectivity change at tar strips might trigger erroneous response from optical height sensors)

Table 2. Descriptions of test sites on public roads. (continued)

Site No.	Length (meters)	Description
12	322	Brief section of smooth blacktop, bounded on each end by PCC surface (extreme and sustained reflectivity change might challenge optical and laser sensors)
13	805	PCC road with faulting, open joints, and patches at joints (joints might cause out-of-range errors; joints might cause bouncing of mechanical systems; reflectiveness changes at joints might trigger erroneous response from optical systems; open joints might cause dropout problems with all noncontacting sensors; digital systems might miss joints)
14	483	PCC surface that was grooved laterally and ground to reduce roughness, leaving grooves in both lateral and longitudinal directions (crisscrossing grooves might challenge laser and ultrasonic sensors; changes in reflectiveness in ground areas might challenge optical sensors)
15	966	Rough bituminous with lots of cracking and patching (roughness levels might cause out-of-range problems; patches might cause bouncing of mechanical systems; cracks might challenge noncontacting sensors; patches might be missed by digital systems)
16	805	PCC surface with open areas at joints (open joints might lose signals for all noncontacting height sensors; out-of-range problems might occur; mechanical systems might bounce; reflectiveness changes might challenge optical sensors; digital systems might miss joints)
17	805	Very smooth bituminous overlay (background noise in profilometer might override the low profile amplitudes)
18	483	Bridge crossing, bituminous to PCC (abrupt step change in height might cause bouncing in mechanical systems; reflectiveness change together with step might challenge optical sensors)

15

Table 3. Descriptions of test sites at General Motors Proving Grounds (GMPG).

Site No.	Length (meters)	Description
19	483	Very rough bituminous with periodic "joints" and patches (patches and "joints" might challenge some of the height sensors; roughness level might cause out-of-range problems; roughness might cause bouncing of mechanical systems. Patching might challenge digital systems)
20	483	Very rough bituminous with periodic "joints" and patches (patches and "joints" might challenge some of the height sensors; roughness level might cause out-of-range problems; roughness might cause bouncing of mechanical systems; patching might challenge digital systems)
21	483	Medium and long-wave roughness, PCC slab in middle, large deflection mound (very large amplitudes overall; transition from asphalt to PCC might cause bouncing of mechanical systems; color change might challenge optical systems; large mound can cause vehicles to leave ground at high speeds)
22	483	Medium and long-wave roughness, PCC slab in middle, large deflection mound (very large amplitudes overall; transition from asphalt to PCC might cause bouncing of mechanical systems; color change might challenge optical systems; large mound can cause vehicles to leave ground at high speeds)
23	483	Sand-asphalt surface, moderate quality (has no specific features that would challenge systems)
24	483	Sand-asphalt surface, moderate quality (has no specific features that would challenge systems)
26	644	Relatively smooth with eroded PCC texture (open texture might challenge laser and ultrasonic systems)
26	644	Relatively smooth with sand-asphalt surface (has no specific features that would challenge systems)
27	644	Relatively smooth with red-stone asphalt surface (open texture might challenge laser and ultrasonic systems; mottled color might challenge optical systems)

NOTE: Sites 19 and 20 are adjacent lanes of "12 Mile Rd;" sites 21 and 22 are adjacent lanes of "Pontiac Trail;" sites 23 and 24 are adjacent lanes of "Sound Test;" and sites 25, 26, and 27 are adjacent lanes of the acoustic area at the GMPG.

For convenience of data reduction and analysis, each site was divided into sections 161-m (1/10th-mile) long, as shown in the figure. The endpoints of the sections were marked with a "T" on the pavement, while intermediate reference points were marked with small rectangles. The reference marks fell approximately at the left-hand edge of the vehicle for most profilometers. The offset is to prevent any artificial error in case some of the optical sensors are sensitive to painted stripes. On very busy interstate highways, it was not always possible to mark the wheeltracks. Instead, marks were placed at the edge of the pavement at 161-m intervals. On these sites, the operators were requested to center the vehicle in the lane. On the GMPG sites, GMPG survey crews placed reflective tape on the sites at 161-m intervals.

The beginning of each site was marked on the side of the road with a red sign, indicating the site number, and the finish of the site was indicated with a red sign with the letter "F." The beginnings of the sites nearly always coincided with semi-permanent off-road objects, such as mileposts or traffic signs.

Summary of the Meeting

The Ann Arbor Road Profilometer Meeting (RPM) was scheduled to run from September 11 to 13, 1984. Twelve profilometers participated, from eleven organizations. On Tuesday, September 11, the participants arrived and the morning was devoted to orientation activities. The systems were all run in the UMTRI parking lot to familiarize the profilometer operators with the markings used on the public roads. UMTRI staff members indicated when a profilometer was left, right, or exactly on the designated wheeltrack. Some of the systems measure two wheeltrack profiles, while others measure only one. All of the systems were capable of measuring the left-hand profile, and therefore accuracy with the left-hand track was emphasized.

In the afternoon, all of the systems traveled over the public road sites in a caravan so that the drivers could become familiar with the locations of the sites.

On Wednesday morning, the operators made measures on the public road sites at their discretion. In the afternoon, all of the systems traveled to the GMPG. The sites there were clustered in two groups, so the profilometers were also split into two groups. Tests were made continuously for 1 1/2 hours, and then the profilometer groups switched locations for another 1 1/2 hours of testing. The sites 25, 26, and 27 were in one cluster that was

17

particularly convenient for testing, so most of the systems were able to make repeated tests at alternate speeds on these sites.

On Thursday, the operators checked their data and made repeat runs on the public road sites as needed.

Two of the systems made measurements after Thursday, as described in the "Results" section. The FHWA system was operated with infrared (optical) height sensors during the RPM, and was operated a week later with Selcom laser sensors. The Colorado system, which had not yet been delivered to Colorado, experienced problems and made its measurements several months later. The rod and level measures were made several weeks after the RPM. Several of the roughest public road sites were repaired shortly after the RPM, and therefore the FHWA/Selcom system and the Colorado system could not cover all of the public road sites.

Table 4 summarizes the runs that were made by most of the equipment. The table gives a good idea of the range of test speeds used, and the relative incidence of bad data. The Swedish VTI system is not included in the table, as it was unable to measure valid profiles. (The reasons that the measures were not valid are described in the "Results" section.) The Pennsylvania system is not shown because PTI was unable to copy the data onto 9-track tapes for analysis by UMTRI.

Table 5 provides a similar overview, but presents the lengths of the tests for the various sites. These lengths are relevant to some of the analyses applied to the data.

Table 4. Summary of profilometer test speeds (km/h) used during the RPM, including runs that were invalidated.

Site No.	APL mechanical	Colorado ultrasonic	S. Dakota ultrasonic	Mich. DOT optical	Ohio optical	W. Virginia optical	Minnesota optical	Gen. Motors laser	FHWA/Selcom laser	FHWA/IR Infrared
1	50[a]	—	29,56[b],68	—	56[b]	—	48	48	—	64[a]
2	50[a]	—	31,51,55[b],58	—	48,64	48	48	56	48[a]	56
3	50[a]	64[b]	51,56	—	32,40	24[c]	72[b]	24,56[c]	—	40
4	50	64[b]	50,55,74	55[d]	80[b]	32[c]	72[b]	56	80	80
5	50	64[b]	55,56,74	55[d]	64,80	32[c]	72[b]	56	80	80
6	50	64[b]	50,58,74	55[d],82	64,80	56	72	56	80	80
7	50	—	58,74	55[d],82	64,80	48	72	56	80	80
8	50	64[b]	55,58,77	55[d],82	64,72	—	—	56	80	80
9	50	89[b]	69,52[b]	82	80[b]	64	80	80	80	89
10	50	89[b]	72,82[b]	82[d]	80[b]	64	80	80	89	89
11	—	89[b]	82[b],89	82	80[b]	64	80	80	89	89
12	50	89[b]	52,53,90	—	80[b]	—	80	80	89	89
13	50	89[b]	52[b],89	82[b]	80[b]	—	80	80	89	89
14	50	—	53,66,80,89	—	80[b]	56[c]	80	80	89	89
15	50	—	51,63,79	—	64,80	—	64	56[a]	80[a]	80[c]
16	50	—	64,76,54	55,82	80[b]	—	80	80	89	89
17	50	—	77,52,54	82[b]	80[b]	64[c]	80	80	89	89
18	50[a]	—	51,63,76	—	80	56	64	56	80	80
19	18,55,90[a]	—	31,51	55,82	24,48,80	24,48	—	24,56,80	32,56,80[a]	32,56,80[a]
20	18,55,90[a]	—	31,51,79	55,82	24,48,80	24,48	—	24,56,80	32,56[a],80[a]	32,56,80[a]
21	55[a],90[a]	—	31,53,77	55,82	24,48	—	24,48,80	24,56,80	56[a],80[a]	32,56,80[a]
22	18,55[a],90[a]	—	31,53	55,82	24,48	—	24,48,80[c]	24,56,80	32,56,80[a]	32,56,80[a]
23	18,55,90[a]	—	29,53,79	55,82	24,48	24,48	24,48,80	24,80	32,56,80	32,56,80
24	18,55,90[a]	—	31,53,76	55,82	24,48	24	24,48,80	24,56,80	32,56,80[a]	32,56,80
25	18,55,90[a]	—	31,32,53,55,77[b]	55[b],82[b]	24[b],48[b],80[b]	24,48,80	24[b],48[b],80[b]	24,56,80	32[c],56,80	32,56,80
26	18,55,90[a]	—	32[b],53[b],55,77[b],79	55[b],82[b]	24[b],48[b],80[b]	24,48,80	24[b],48[b],80[b]	24,56,80	32,56,80	32,80
27	18,55,90[a]	—	31[b],53[b],80	55[b],82[b]	24,48,80[b]	24,48,80[b]	24[b],48,80[b]	24,56,80	32,56,80	32,56,80[a]

a Problem with digitization
b Additional repeats were made at this speed
c Rejected by UMTRI, based on inspection of plotted profile
d Repeat run made with mechanical follower wheel

Table 5. Maximum and minimum lengths (m) of profile measurements on the different sites.

Site No.	PSD analysis	Rod & Level	APL mechanical	S. Dakota ultrasonic	Mich. DOT optical	Ohio optical	W. Virginia optical	Minnesota optical	Gen. Motors laser	FHWA/Selcom laser	FHWA/IR InfraRed
1	300	-	340	471-479	-	489-492	-	482	465	-	-
2	440	60	-	471-515	-	484-484	484	482	505	424	532
3	-	-	220	326-329	-	327-352	-	318-321	320	-	323
4	1010	-	1050	1116-1121	-	1135-1136	-	1122-1122	1085	1090	800
5	555	-	640	634-642	-	652-655	-	644-648	596	606	636
6	725	-	800	795-797	777-784	814-815	799	804	765	787	792
7	860	-	960	955-959	951-958	972-974	973	965	900	908	951
8	560	-	640	628-640	625-626	653-653	-	-	590	606	628
9	735	-	480	797-797	-	673-814	802	803	786	787	792
10	580	-	800	636-794	637	653-1462	675	804	627	787	792
11	740	-	-	705-794	794	815-818	802	799	782	787	791
12	260	-	316	318-324	-	331-331	-	329	299	302	317
13	760	-	800	795-800	318-776	811-813	-	808	797	787	791
14	440	-	480	475-482	-	483-491	-	482	465	423	473
15	910	-	960	954-959	-	974-976	-	965	-	-	952
16	760	-	800	797-798	795-797	813-813	-	804	800	787	792
17	750	-	800	797-801	792-796	816-817	-	804	805	787	793
18	400	-	-	478-481	-	494	494	482	440	424	474
19	160	160	480-480	471-485	481-484	486-493	476-481	-	447-464	479-479	479-480
20	160	160	480-480	474-482	477-477	486-496	475-476	-	453-478	481	482-499
21	160	160	430	474-483	478-479	487-490	-	483-488	444-464	321	478-481
22	160	160	480	475-481	481-484	487-489	-	482-486	441-479	476-476	479-480
23	160	160	396-480	475-485	487-488	486-490	476-476	484-491	451-471	473-480	473-473
24	160	160	480-481	475-482	357-476	486-488	476	481-485	436-473	477-479	478-482
25	160	160	640-641	641-642	275-638	648-662	635-635	642-648	436-631	636-636	636-639
26	320	160-321	640-641	638-642	579-633	645-655	635-635	643-653	591-631	635-640	635-639
27	320	160-321	640-641	639-643	564-643	647-653	635-635	642-650	599-637	636-640	635-641

ANALYSES

Overview

The use of the name "profilometer" is sometimes controversial, as opinions differ as to what qualifies an instrument as a profilometer. The name has been used in the past for a broad range of instruments that are known to differ markedly in their measurement capability. In one extreme, the name has been used for any instrument that goes over a road and produces a signal theoretically related to profile. In the other extreme, some engineers prefer to reserve the name for an instrument that can replicate, point-by-point, the profile as would be obtained manually with rod and level survey methods. Neither of these extreme views is appropriate, inasmuch as a road roughness profile is a broad and continuous spectrum that cannot be measured completely by any system or method available today.

The concept of a true profile is intuitive and simple: it is the measure that would be obtained in the limit—using rod and level methods, with perfect accuracy in reading the elevations, and taking the elevation measures so close together that profile features are distinguished down to the texture level. Yet, measurements to that level of detail are neither practical nor necessary for any one application. Thus profilometers are designed with the intent of measuring the qualities in the roughness spectrum needed for specific applications. An "application" is defined by an analysis that is applied to the profile, for the purpose of assessing some property of the road surface (roughness, cracking, etc.). Validation of a profilometer for an application is performed most directly by applying the analysis to the profile as measured by the profilometer system in question, and comparing the result to a reference obtained by applying the same analysis to the true profile. If the same results are obtained, the system is validated for that application. If the results do not agree within acceptable limits, the system is not validated as a profilometer for that application, even if the results are highly correlated.

A direct validation is normally difficult to perform, because the true profile is not known. A key phase of the RPM was the acquisition of reference profile measures for all of the sites used. (Details about the reference measures are given in the next section.)

No instrument in the world can measure profile with reasonable accuracy for every possible application. For example, the profiles of hills and valleys, which might be desired for mapping the longitudinal grades of a road over its entire length, are not obtained with

21

any of the instruments that participated in the RPM. At the same time, few of the systems can measure the texture of the surface, as it might be used to compute surface friction properties. Nonetheless, most of the systems can measure the profile features that affect ride quality, and are expected to be valid for some applications, but not for others.

The systems that participated in the RPM were checked for three types of applications that yield a roughness measurement: quarter-car simulation from which the International Roughness Index (IRI) is calculated, Texas root mean square vertical acceleration (RMSVA) analysis from which a Maysmeter calibration index called MO is calculated, and a series of waveband indices obtained from power spectral density (PSD) analyses. (These analyses are described below.) The IRI and MO calculations are typical applications in which a single summary statistic is determined for the road. PSD wavebands provide a broader picture of a profilometer's measurement capability, by showing the range of wavelengths over which an instrument qualifies as a valid profilometer.

The above analyses directly reveal the accuracy of the profilometers in specific applications, but the wavebands are not easily generalized for applications that may assume greater importance in future work. Therefore, the profiles themselves were examined to show qualitatively how the profilometers performed. The profiles were studied using two techniques: (1) they were simply plotted to illustrate how the instruments "see" specific surface features; (2) the power spectral density (PSD) functions were computed and plotted, to show how the instruments "see" different wavelengths. These results identified problems that might exist in using the profilometer for the applications considered. They also indicated the overall performance properties of the profilometers in a more general way, so that the suitability of a particular instrument for future applications could be assessed using these results.

Before describing the particular analysis methods used in this study, it is noted that there are many systems that are said to measure "roughness," when in actuality they measure a response of the vehicle (or other mechanical system) to roughness in the pavement. The physical measures can be related to the roughness through correlation equations. These "response-type systems" do not qualify as profilometers unless they are calibrated independently and do not require a reference instrument to measure the "true" property. That is, a system does not qualify as a profilometer if it is calibrated by running it over some roads and determining a correlation to measurements from other systems. Only analyses that apply specifically to a true profile are considered in this study.

Another category of instruments used for roughness measurement is the profilograph, also called a rolling straightedge. These instruments are sometimes called

profilometers—the CHLOE profilometer, for example—but they are not considered to be true profilometers of the sort that participated in the RPM, because they produce a "profile" which does not match the true profile over any range of wavelengths.

Profile Plots

Direct comparison of profiles from different systems is perhaps the most intuitive method for quickly confirming that a system can measure profile. However, this approach does not always work. Figure 2 illustrates the results that are obtained when this method is tried. At first inspection, it would appear that three profiles were being measured: one by the rod and level, one by the APL trailer, and one by the Ohio and Minnesota systems. Yet, the profiles were all measured on the same site, and the plots show how four different instruments see the same wheeltrack. The striking difference in appearance is caused by the different wavelength content in each of the measurements. Only the rod and level measure includes the longest wavelengths without error. The Ohio and Minnesota profilometers agree very well with each other because they have nearly the same response to different wavelengths. (Both are 690-DNC systems made by K. J. Law, Inc.) The APL trailer sees a shorter range of wavelengths, and shows a different result.

Figure 2 is included to point out that direct plots of profile should be used with care. If all the profiles are processed to filter out the very long wavelengths, then direct comparisons are much better. This was done in the RPM, using a moving average filter. (The details of the moving average filter, used extensively in this study, are provided in appendix B.) Figure 3 shows how the same profile measurements compare when all are filtered using a 10-m moving average. Note that the profiles are again offset for readability and the vertical scale has been increased with the filtered plots such that much finer detail can now be examined. It is easily seen that all of the measures are approximately equivalent, and would suggest that all the instruments qualify as valid profilometers when considering only the shorter wavelengths.

Even when profiles are filtered identically, a direct point-by-point comparison is still not a viable means to quantify accuracy. A major problem is that the profiles measured by different systems cannot be perfectly synchronized. If the longitudinal positions on the road differ by only a few meters, a point-by-point comparison will not be valid. Yet to maintain an acceptable synchronization over the entire length of the measurement requires a precision of fractions of a percent. High-speed systems do not need this accuracy, and cannot achieve it unless special calibration effort is expended. Even with this effort, a point-by-point comparison may not be possible because some of the systems still have a
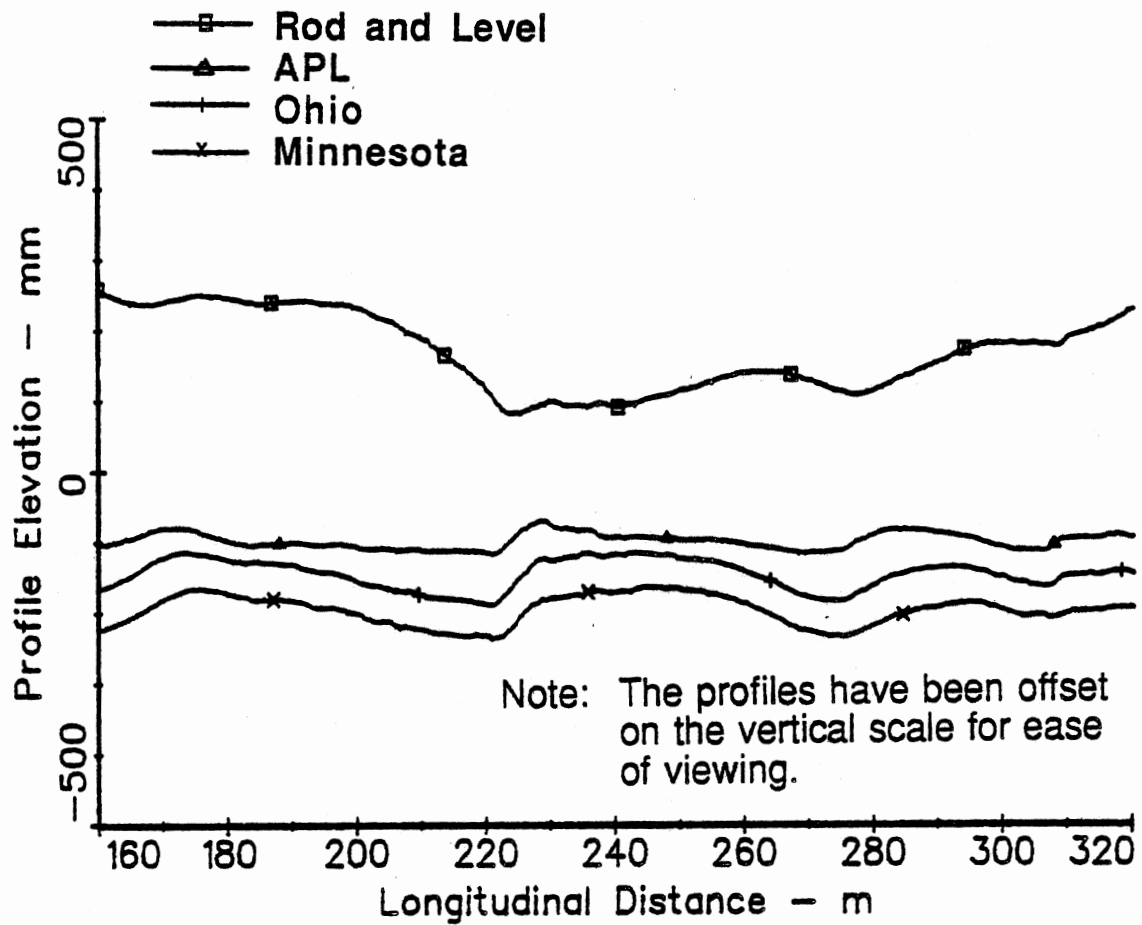
Figure 2. Four measures of a profile from different instruments.

24
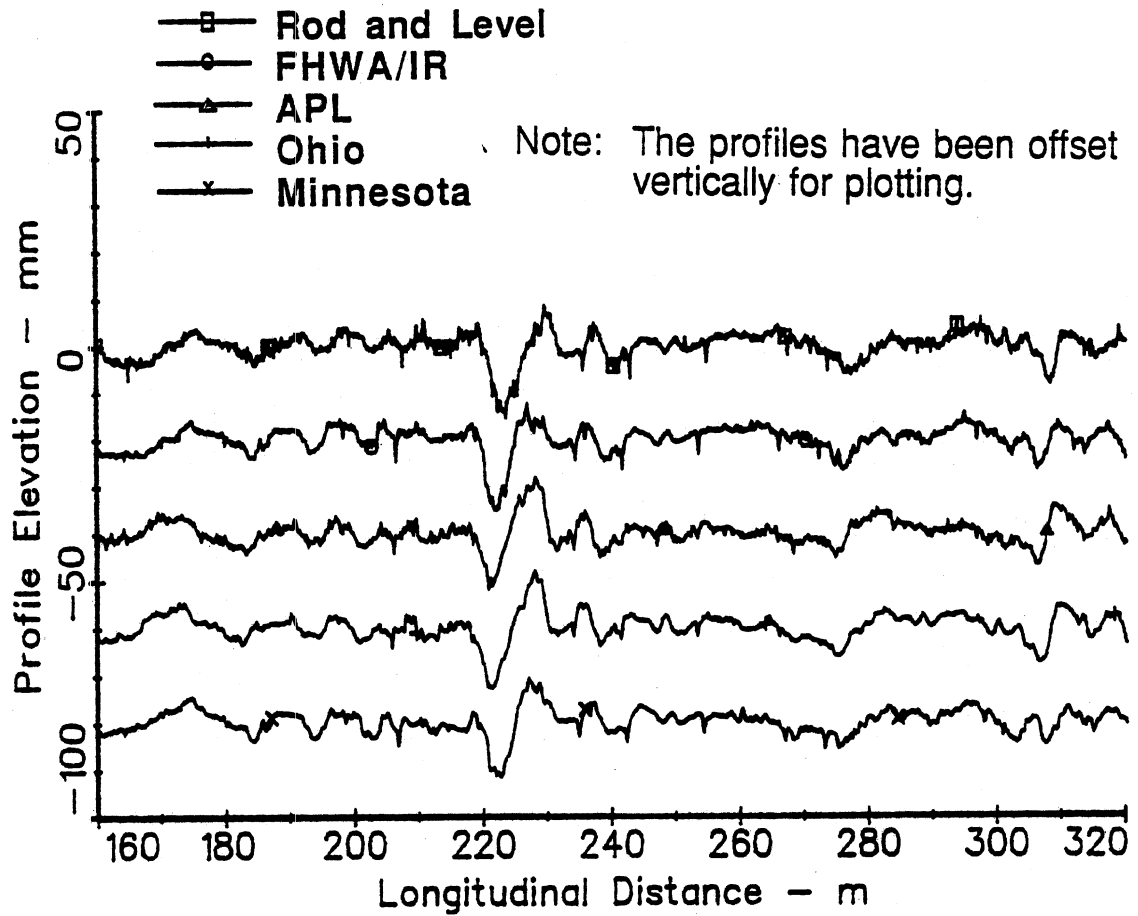
Figure 3. Five measures of a profile, all filtered with a 10-m moving average.

subtle distortion due to phase lag, such that two profiles can be synchronized for long wavelength or for short wavelengths, but not for both at the same time.

The difficulty in comparing profiles directly can be overcome by resorting to statistical methods, even while recognizing that the profile of a road is not random. (A longitudinal road profile is fixed in space and, in the short term, is also fixed in time. Therefore, it is deterministic, not random.) Nevertheless, it does have the appearance of a random signal, and statistical descriptions commonly used for random signals have proven to be useful for characterizing road profile. By analyzing the profile using statistical methods, the very large amounts of information (hundreds or thousands of independent elevation measurements) are reduced to a manageable number of summary statistics. Rather than attempting any quantitative comparisons using the actual profiles (filtered or not), such comparisons will be made on the basis of statistics computed from the profiles.

Measurement of Roughness Indices

Only a small range of applications for profilometers exists at the present time in the United States (although many functionally similar applications have a diversity of names). In the United States, the primary application of profilometers has been the calibration of response-type systems, requiring a roughness index highly correlated with the measures obtained from response-type systems. Two of these were applied to the data collected in the RPM: (1) the International Roughness Index (IRI), obtained from the standardized quarter-car simulation; and (2) the MO statistic developed in Texas, based on the RMSVA analysis. (A third type of index was also applied, and is described in the next sub-section.)

The International Roughness Index (IRI)—Quarter-Car Analysis

For decades, roughness has been characterized by the response elicited from a traversing vehicle. The single-wheeled Bureau of Public Roads (BPR) roughometer was a first attempt to standardize the vehicle by which the measurement is made. In more recent years, various types of roadmeter instruments (Mays meter, PCA meter, Cox meter, NAASRA meter, bump integrator, etc.) have been developed for installation in passenger cars or trailers, as a means to measure a similar type of roughness. Later, with the development of high-speed profilometers, simulations of the BPR roughometer were incorporated into the equipment as means to reduce the measured profile to a summary statistic related to past practice. Simulations of a passenger car have also been developed to replicate the measurements of other roadmeter systems.

26

These vehicle simulations are known as quarter-car simulations because they represent only one quarter of a motor car. Figure 4 shows that the quarter-car consists of a sprung mass, a single unsprung mass, two linear springs, and a linear damper. The engineering equations representing these essential dynamic elements are written and solved when the road displacement (profile) is input at the tire/road contact point. The stroking of the suspension is accumulated, analogous to the measurement obtained from a roadmeter. The final value in "inches/mile" (inches of suspension stroke per mile of travel), "m/km," "counts/mi," or one of many other unitary descriptors is the final measure of roughness.

The dynamic behavior of the BPR Roughometer and the various passenger cars used with roadmeters will differ, and therefore different parameters have been used in the simulation models to describe each system. As a result, different roughness measures were obtained. In the late 1970's, a reference quarter-car simulation (RQCS) was defined as part of an NCHRP research project intended to establish a calibration methodology for the roadmeter vehicles.[9] Today, this model (distinguished by a unique set of vehicle parameters) has been adopted by most practitioners, both in the United States and throughout the world, for calculating a roughness index from a quarter-car simulation. When using the standard set of vehicle parameters, the only variables remaining are the choice of simulation speed, and the choice of whether the simulation is applied for two profiles (a half-car simulation) or one (a quarter-car simulation). The most standardized index is the measure from the simulated roadmeter at a speed of 80 km/h (50 mi/h), for a single wheeltrack. This measure—the reference quarter-car simulation from the NCHRP project, applied to a single wheeltrack, for a simulation speed of 80 km/h—is serving as an International Roughness Index, and has been given the abbreviation IRI.[10, 11]

The plots in figure 5 show the frequency response of the quarter car-analysis. The plot on top shows the response as a function of temporal frequency, as defined by the equations of motion for a quarter-car. The plot on the bottom shows the sensitivity as a function of wavenumber, when the simulation speed has been fixed at 80 km/h (50 mi/h), as specified for the IRI. Wavenumber has units of cycles/length (in this report, cycle/m is used) and is the reciprocal of wavelength. The plot shows that the IRI is primarily sensitive to wavenumbers between 0.04 and 0.7 cycle/m. (These wavenumbers correspond to wavelengths between 1.4 and 25 m.)

The test sites used in the RPM had various lengths, which were all multiples of 161 m (1/10th mile). The IRI numeric was always accumulated over a length of 161 m (1/10th mi), so that all measures would be based on the same measurement length. Therefore, each site included several sections that were measured independently. The total number of test
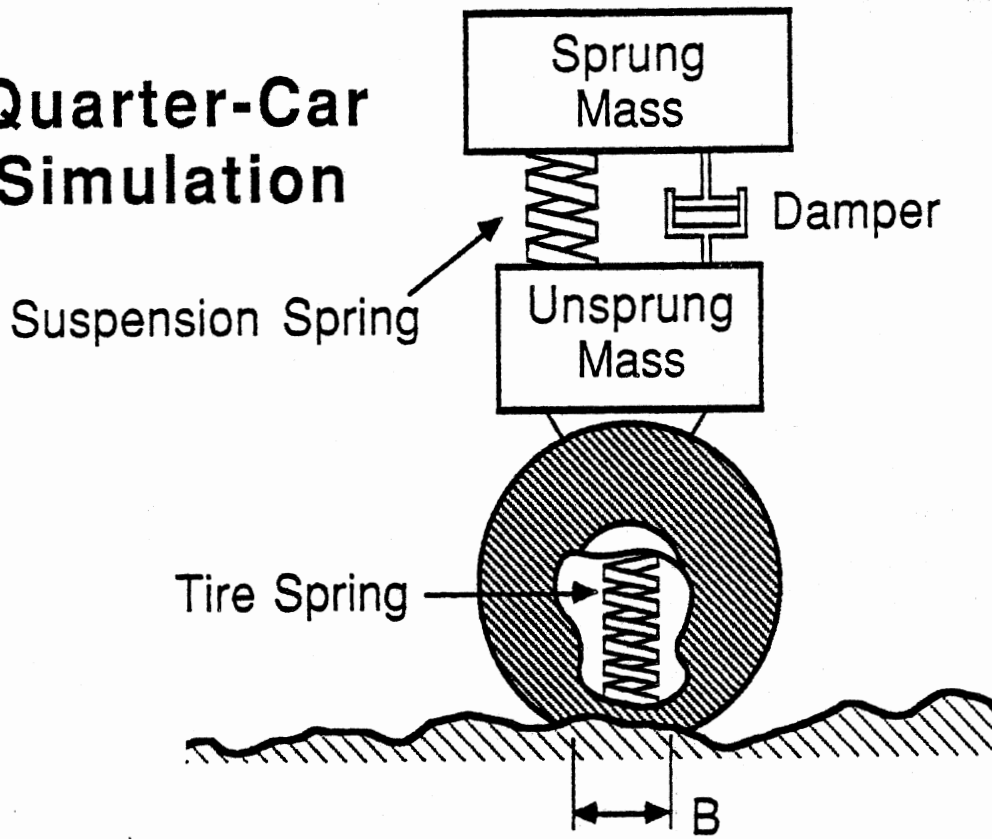
Figure 4. Quarter-car model used as the basis of the international roughness index (IRI).
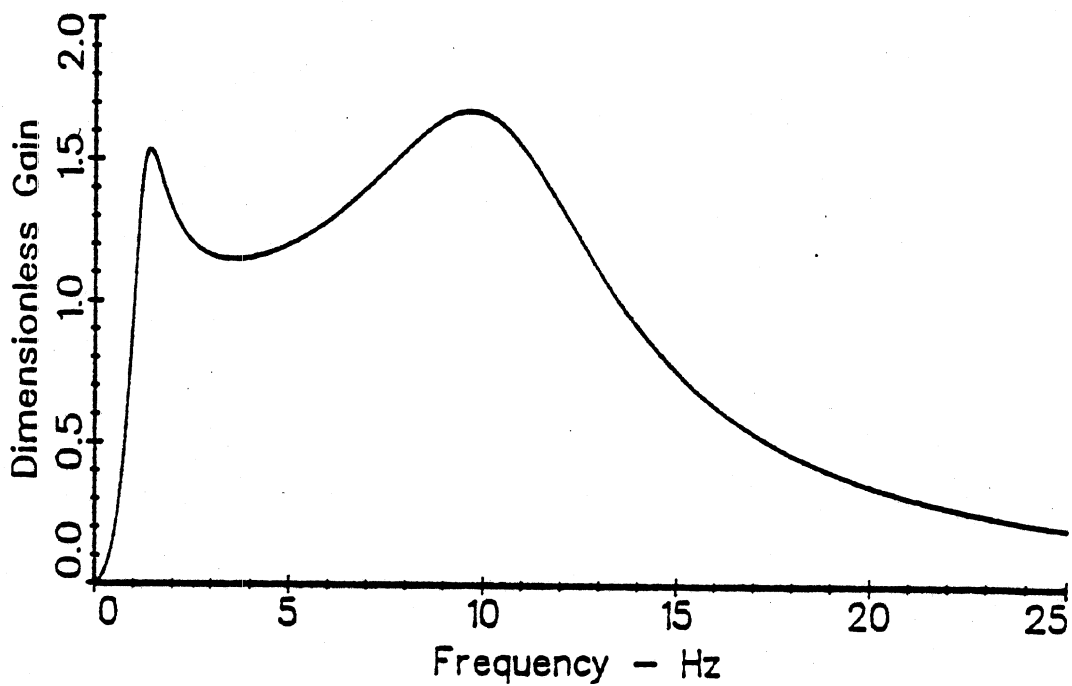
a. Response of the IRI/NCHRP quarter-car in the frequency domain
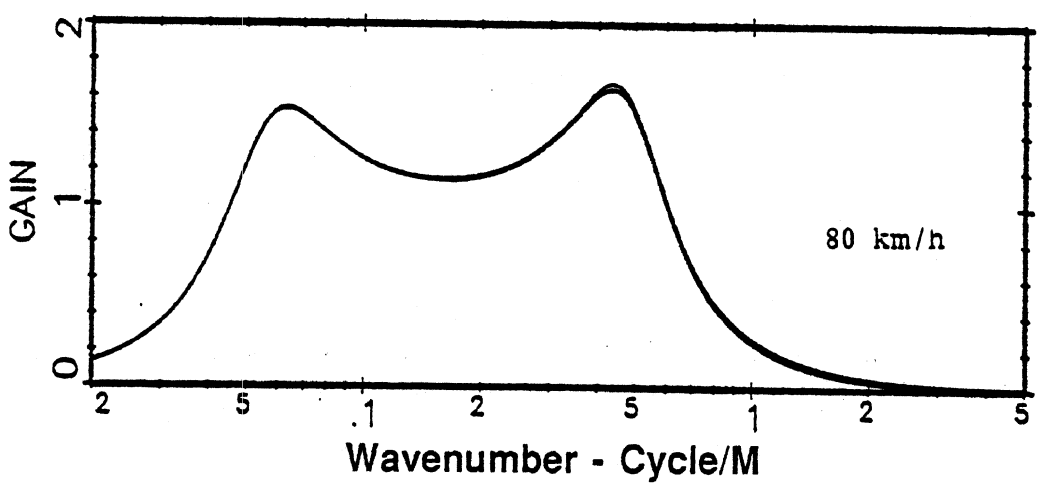
b. Sensitivity of the IRI analysis to wavenumber

Figure 5. Frequency and wavenumber sensitivities of the IRI analysis.

sections measured using the IRI was therefore not 27, but about 90. The first 161-m section of each site was not used, nor was the measure from site 3, the railroad crossing.

Appendix C describes a method used to compute IRI from profile.

MO and RMSVA

A second approach that has been taken to define a quarter-car type of roughness index is to use a simple profile analysis that produces an index correlated to roadmeter systems. The "MO" index, developed in Texas, is a measure of this type. It is determined by first computing two midchord deviations from a profile, each with a different baselength, and combining these via a linear equation.[12] The root-mean-square (RMS) values of the midchord deviations are called "RMSVA," because the equations used sometimes approximate the second derivative of profile—vertical acceleration. Although not widely recognized, the RMSVA analysis actually produces a midchord deviation from a simulated rolling straightedge, as demonstrated in figure 6. Note that the equation for "vertical acceleration" (VA) is simply a re-scaled version of the equation for the midchord deviation (MCD), with the scale factor being $B^2/2$.

The RMSVA analysis acts as a filter with periodically varying sensitivity to profile elevation content, as shown at the top of figure 7. The maximum response occurs at wavenumbers equal to 1/(2•B) (wavelength=2•B) and all odd multiples, and is zero at wavenumbers equal to 1/B (wavelength=B) and all its multiples. Taking a baselength of 4 m as an example, the same maximum output will be obtained for a wavelength of 8 m, 8/3 m, 8/5 m, and so forth. Because the amplitude of the road elevation is greatest at low wavenumbers, most of the measured midchord deviation is associated with the first response peak in the figure (wavenumbers from zero to the baselength)

No single baselength will produce an RMSVA numeric well matched to the wavelengths seen by roadmeter vehicles. Typically, the RMSVA values for at least two baselengths must be combined to obtain a summary roughness numeric that will correlate well with roadmeter measures. In Texas, two baselengths are used to obtain the MO index, which was developed by correlating a variety of RMSVA indices measured with the Texas profilometer with the "inches/mile" measures obtained with response-type systems. The response-type systems were passenger cars and trailers equipped with Mays meters, and the name MO indicates that the numeric is a reference Mays index. MO is defined mathematically as a weighted sum of two RMSVA numerics, using baselengths of 1.2 m and 4.9 m (4 ft and 16 ft). (These are equivalent to midchord deviations for chord lengths of 2.4 m (8 ft) and 9.8 m (32 ft).) The bottom plot in figure 7 shows the sensitivity of the

30

a. Root-mean-square-vertical-acceleration (RMSVA)

Slope $= \Delta y / B$

"VA" $= \Delta Slope / B$
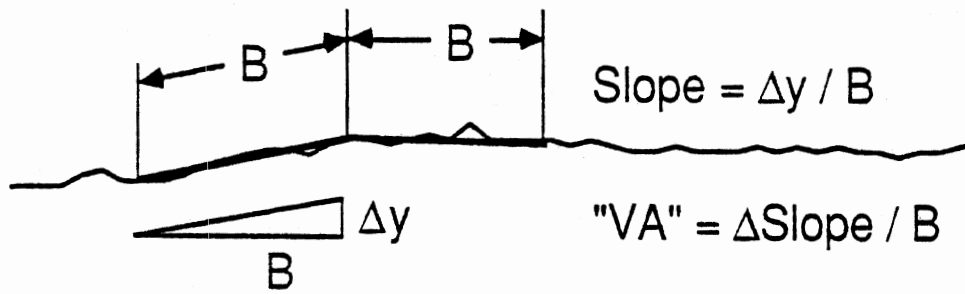
$$VA = [y(x + B) + y(x - B) - 2y(x)] / B^2$$

b. Rolling straightedge

MCD = "Mid-Chord-Deviation"

$$MCD = VA \cdot B^2 / 2$$
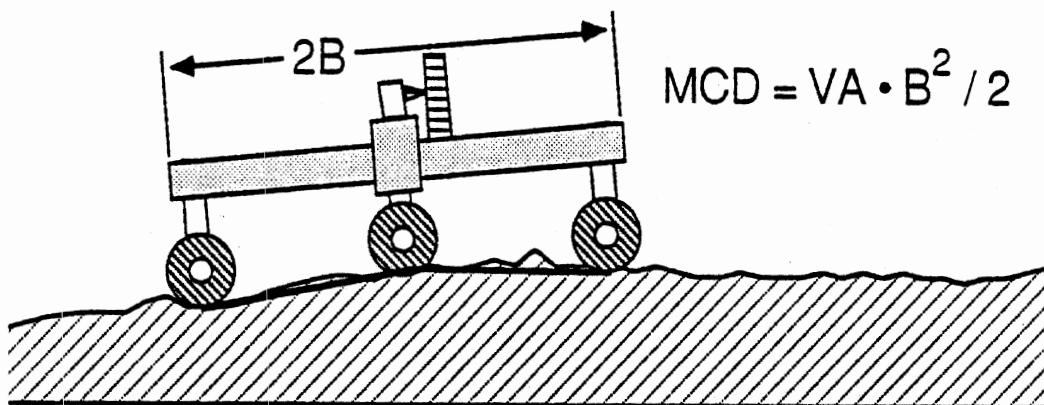
Figure 6. Equivalence between the RMSVA analysis and the rolling straightedge.

31

true vertical acceleration

$VA = [y(x+b) + y(x-b) - 2 y(x)] / b^2$

Wavenumber x b — cycle/baselength
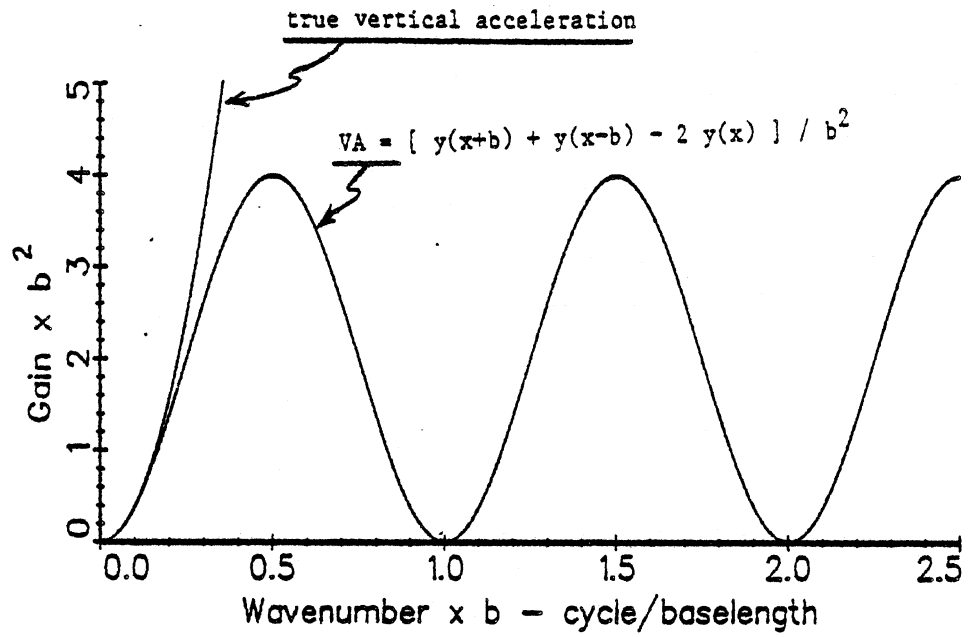
a. Wavenumber response of the RMSVA analysis for a displacement inpi

Wavenumber — cycle/m
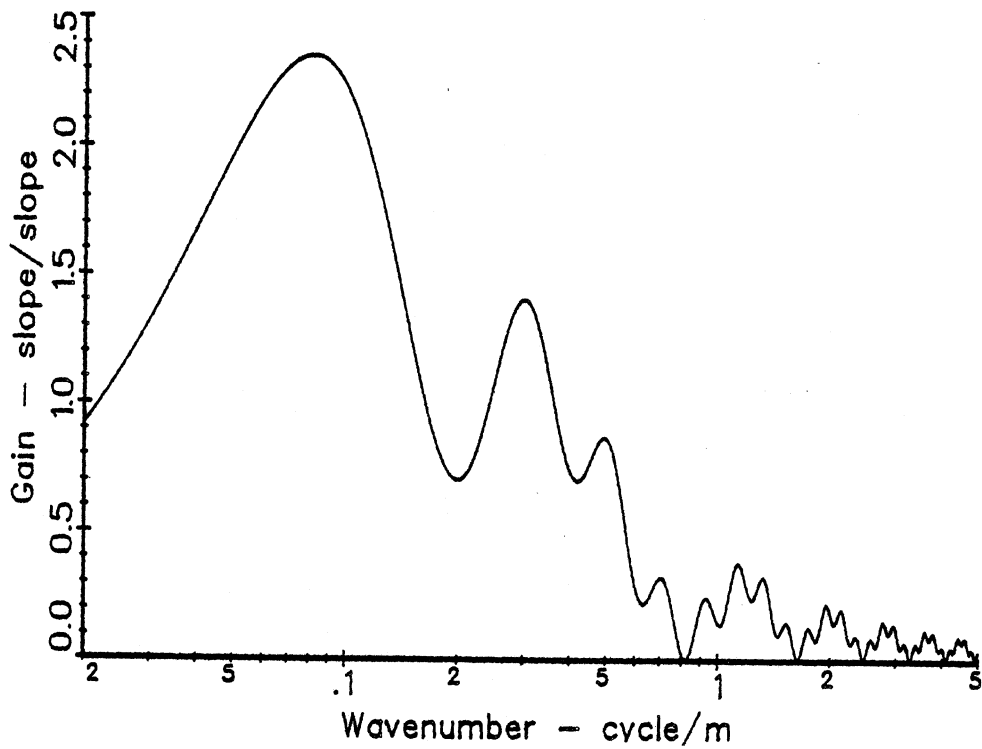
b. Wavenumber response of the M0 analysis for a slope input.

Figure 7. Wavenumber sensitivities of the RMSVA and M0 analyses.

32

MO analysis to wavenumber, based on sinusoidal inputs charactered by slope amplitude. The bottom graphs in figures 5 and 7 can be compared directly (both show the response of a roughness analysis to a slope input), and show that the MO analysis approximates a quarter-car simulation by covering the same range of wavenumbers as the IRI. The MO analysis tends to emphasize the roughness at the lower wavenumbers (longer wavelengths) more so than the IRI, with maximum response at a wavelength of 10 m. Details for computing MO from profile are included in appendix D.

A conceptually similar approach lies behind the QI_r index developed in Brazil.[10, 13] QI_r is a weighted sum of two RMSVA numerics, with baselengths of 1.0 m and 2.5 m.

As described above in the section on the IRI, each test site was divided into 161-m (1/10th-mile) sections. The MO analysis was applied to each of these 161-m sections, and therefore the total number of sections measured was about 90.

Waveband Indices

When correlation with a response-type system is not critical, profile analysis can be designed to provide roughness measures that describes several roughness qualites. Waveband analyses are used in Europe to reduce a road profile to several indices, each summarizing roughness over a different range of wavelengths. (A range of wavelengths or wavenumbers is also called a waveband.) The IRI and MO analyses are actually specialized waveband analyses, each covering the broad bands of wavenumbers shown in figures 5 and 7. In Europe, profiles are commonly processed to produce three indices, summarizing roughness over short-, medium-, and long-wavelengths.[10, 14] In order to characterize the abilities of the profilometers participating in the RPM for measuring profile properties other than IRI and MO, waveband analyses were also performed to separate the roughness into eight wavebands, each covering one octave.

The wavebands are centered (on a log scale) at the wavenumbers corresponding to wavelengths of 0.5, 1.0, 2, 4, 8, 16, 32, and 64 m. Each waveband includes all wavelengths from the $\lambda / 1.4$ to $\lambda \times 1.4$, where λ is the wavelength. The waveband index is then identified as WB(λ). (Although the calculations and plots use spatial frequency—wavenumber—the corresponding wavelengths are used as indices because the wavelength tends to be more familiar.) When the mean square values from all of the wavebands are added, the result is the same total mean-square slope that would be obtained from the original signal. Since units of slope are more common than units of slope squared, the waveband indices were transformed to square roots, yielding RMS slopes.

33

This particular analysis is not in routine use anywhere, but was chosen because it is straightforward and shows the overall capabilities of the equipment more clearly than any analyses that are in widespread use.

Power Spectral Density (PSD) Functions

When the bandwidth used in the waveband analysis is decreased, the mean-square value of the variable also decreases because a smaller fraction of the variance is retained. The amplitude can be normalized by the bandwidth, however, to produce waveband amplitudes that have units of variance/wavenumber. When the bandwidth is reduced to nearly zero, and the number of wavebands increases proportionately, the amplitudes approach a limit that is called the power spectral density (PSD) function. The PSD function for a variable is continuously defined at all wavenumbers, and shows how the variance is distributed over wavenumber. (A more accurate name might be variance spectral density. Early measures of voltages had units of power, leading to the name power spectral density even in applications such as road profile that have nothing to do with power.)

A PSD function always has the units: quantity measured^2/wavenumber. Thus, an elevation profile measured with the units of mm would have corresponding PSD units of mm^2-m/cycle. Although wavelength is more easily visualized than wavenumber, the PSD function is defined as a function of wavenumber because the integral of a PSD function over a band of wavenumbers (waveband) corresponds to the contribution of that band to the total variance. At the limit, the integral over all wavenumbers is equal to the total variance. (In this example, the variance for elevation would have units: mm^2.)

The IRI, RMSVA, and virtually every other roughness numeric ever computed from profiles involve analyses that isolate a band of wavenumbers from the original profile signal. It is therefore helpful to view the variations in profile in terms of wavenumber amplitudes, using the PSD function. This function provides an objective measure of the ability of a profilometer to measure roughness at different wavenumbers.

Figure 8 shows three plots of PSD functions, all of which are computed from the same two measured profiles. (The symbols on the plots are not data points, but are used to identify overlapping lines.) Since road profile is measured as an elevation, it is natural to compute the PSD function directly from that measure. As graph a in figure 8 shows, the PSD is very large at low wavenumbers (long wavelengths), relative to the PSD at higher wavenumbers. In order to show the full range of the PSD, it becomes necessary for the vertical scale to cover many orders of magnitude. The differences in the PSD functions for

34
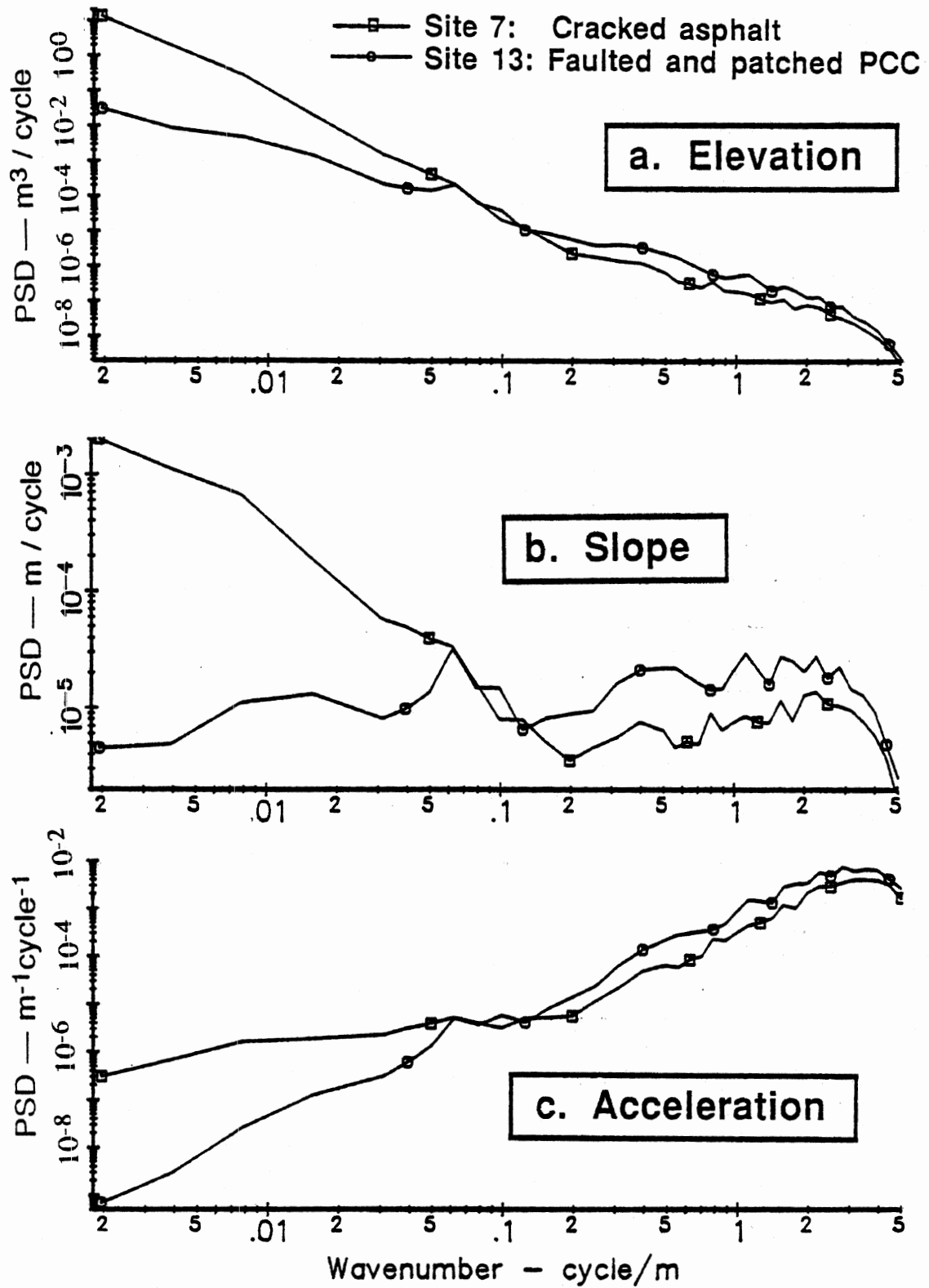
Figure 8. Power spectral density (PSD) functions for two sites.

the two example roads are evident in the low wavenumber range, but differences at high wavenumber are difficult to distinguish accurately.

The PSD function can also be computed for the derivatives of the elevation measurement, i.e., slope and slope derivative (spatial acceleration), as shown by graphs b and c in the figure. As a means for characterizing road profiles, the PSD function of *slope* offers two advantages:

1. The plots can be scaled to show amplitude more precisely. Note that the elevation and acceleration functions cover a wider range of amplitudes (7 to 10 orders of magnitude) compared to 3 orders of magnitude for the slope PSD over the wavenumber range shown.

2. It is easier to visually gauge the importance of different wavenumbers as they contribute to any given roughness index. In the case of elevation PSD's, one must always remember that the amplitudes are much larger at low wavenumbers, and the contribution to a roughness index can be difficult to judge. In contrast, the slope function shows the roughness in a more uniform format. The sensitivity (gain) of an analysis process based on a slope input indicates directly the bands that contribute the most to the summary numeric.

All road PSD functions that follow in this report are presented in terms of profile slope. This contrasts with the standard method for displaying road roughness PSDs presently being considered by the International Organization for Standardization (ISO), ISO/DIS 6806 "Mechanical vibration—Road surface profiles—Reporting measured data." The decision to use slope PSD functions rather than elevation was made because the proposed ISO method does not show the similarities and differences in the profilometers nearly as well as the method used here. Appendix E describes the computational steps followed in preparing the PSD plots.

36

RESULTS

The results obtained with each profilometer system that participated in the RPM are presented in the following sub-sections, which are intended to be more-or-less self contained. Each sub-section includes a brief description of one profilometer design, sufficient to identify the hardware and any unique features that may be relevant to its performance. The sub-section then presents the results obtained from that profilometer from the road profilometer meeting (RPM). To appreciate the findings that are presented, the reader should be familiar with the material in the preceding sections describing the objective of the experiment, and the analysis methods used to obtain the results presented here.

Most of the summary roughness results are provided in tabular form in appendix F.

Reference Profile Measurements

Rod and level measurements of profile were used as the absolute reference against which the other systems were compared. The rod and level measurements were made only on the nine sites at the facilitites of the General Motors Proving Grounds, and on one site on the public roads. Surveys were conducted for a length of 161 m on most sites with some exceptions: only 60 m were included on the public road site to cover the detail of interest, while on two of the GM sites, the measurement lengths were extended to 322 m in order to provide a better reference for long wavelength evaluation.

Special methods were used to obtain very precise measurements. The basic methodology is the same used in Brazil by Queiroz for calibration sites for response-type systems.[13] The wheeltrack was established by placing a surveyor's tape on the road, marked off at 76.2-mm (3-inch) intervals. The base of the rod consisted of a circular pad 76.2 mm (3 inches) in diameter, mounted on a ball pivot. The pad was added to reduce the randomness when taking readings from highly textured surfaces. A precision level with a built-in micrometer (Wild N3) was used for elevation measurements to a nominal accuracy of 0.1 mm (0.004 inches), although a more realistic accuracy figure would probably be around 0.5 mm (0.02 inches), due to the imprecision in placing the rod exactly in the same spot. The level was set up in line with the wheeltrack, to avoid the need for adjusting the aim of the instrument between readings. The elevation/distance values were recorded on log sheets and later entered into a microcomputer for initial processing. This processing

corrected for elevation changes with each repositioning of the level, and plotted the elevation on the screen as the readings were entered. Erroneous entries were quickly identified from the plot and corrected.

The results from the rod and level were used as the reference for the other equipment. Figure 9 gives an overview of how the rod and level compared with several of the profilometers when the IRI and MO roughness indices were calculated from the profiles. In this figure, roughness measures obtained from the profilometers are plotted along the vertical axis against the corresponding measures obtained from the rod and level on the horizontal axis. If any of the rod and level measures were in error, one would expect to see the data points from the profilometers all registering together at a different value, either above or below the line of equality. Instead, the results are generally distributed closely about the line of equality, indicating that the rod and level profiles are the valid reference they are expected to be.

The 17 sites that were not measured by rod and level are also of great interest, because they include a number of features that challenged the various systems. For these sites, some sort of reference measure was also needed. Data from a selection of profilometers were used for this purpose. Based on the comparisons between the profilometers and the rod and level on the nine sites at GMPG, it was possible to determine which of the profilometers were most consistent and accurate. Several of the systems demonstrated high accuracy most of the time, and therefore these systems were compared on the 18 public sites. Based on examination of PSD and profile plots, one of the instruments was selected as the reference for each site. Table 6 summarizes the choice of reference made for each site.

APL Trailer

Hardware Description

The Analyseur de Profil en Long (APL) was developed by the Laboratoire Central des Ponts et Chaussees (LCPC) in France for rapid checking of road unevenness.[2, 14, 15] The APL is a towed trailer, shown in figure 10. The trailer frame acts as a sprung mass supported by a wheel that follows the road surface. An inertial reference is provided by a horizontal pendulum supported on a Bendix-type bearing. The pendulum is centered by a coil spring and damped magnetically. An LVDT displacement transducer is located between the inertial pendulum and the trailing arm of the road wheel, such that its signal is proportional to profile over the frequency range of 0.5 to 20 Hz as the trailer travels along
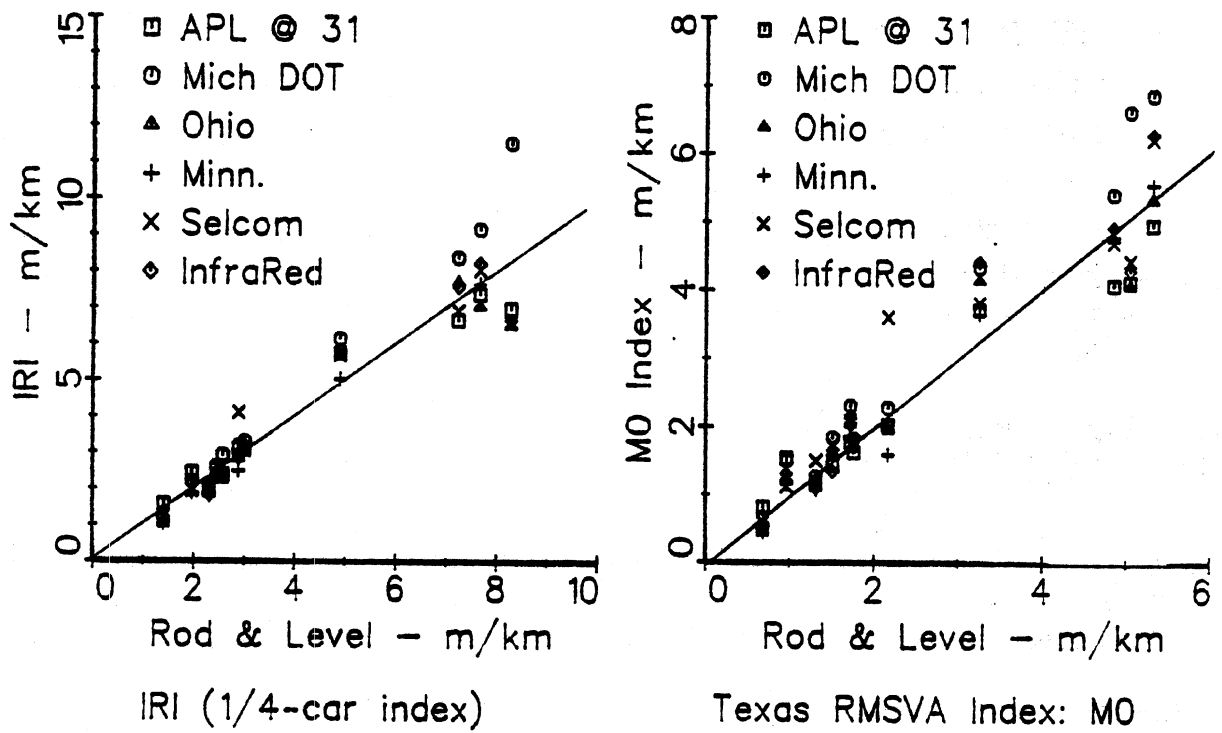
Figure 9. Overview of the agreement between the rod and level reference and
several profilometers.

Table 6. Reference measurements used on public road sites.

Site No.	Reference instrument	Site Description
1	Minnesota	Rough asphalt with cracks and patches
2	Rod & Level	Patched and rolling bituminous, manhole cover
3	—	Railroad crossing
4	FHWA/Selcom	Typical surface treatment
5	FHWA/IR	Typical surface treatment
6	FHWA/IR	Typical asphaltic concrete
7	APL	Both sealed and unsealed asphalt with cracking
8	Ohio	Surface treatment with some corrugations
9	FHWA/IR	Good PCC with lateral grooves
10	FHWA/IR	Good PCC with lateral grooves
11	Minnesota	Good PCC with flush tar-strips
12	FHWA/Selcom	Transition from PCC to smooth blacktop
13	Ohio	PCC with faulting, open joints, patches
14	FHWA/IR	PCC with lateral and longitudinal grooves
15	Ohio	Rough bituminous with cracking and patching
16	Michigan DOT	PCC with open areas at joints
17	FHWA/Selcom	Very smooth bituminous overlay
18	FHWA/IR	Bridge crossing, bituminous to PCC
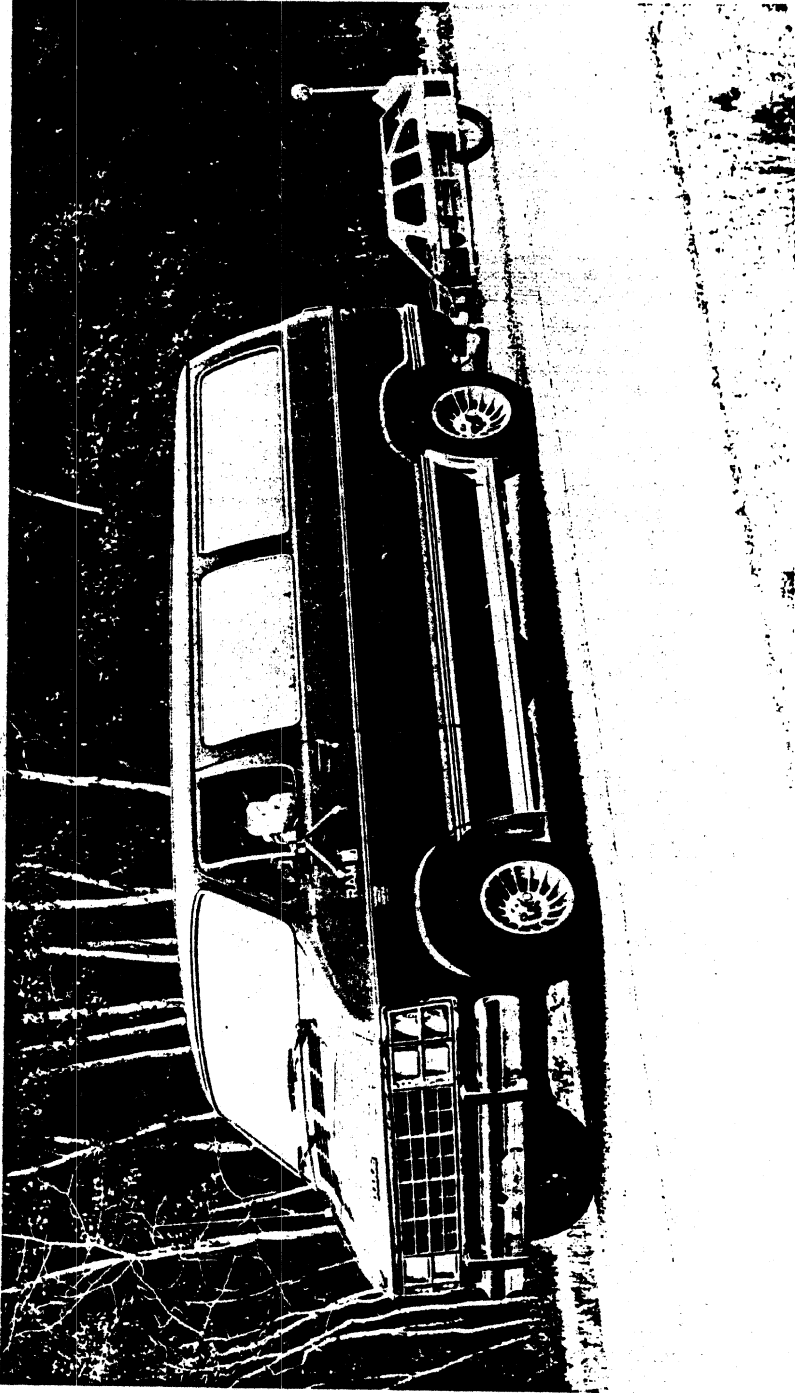
Figure 10. The APL Trailer.

the road. A digital distance transducer on the road wheel measures the distance traveled and the towing speed.

The APL is designed with dynamic properties that make it insensitive to motion inputs at the hitch point. The response of the trailer is calibrated by placing a dynamic shaker under the road wheel and measuring the output for sinusoidal inputs. The mounting locations of the shock absorber and coil spring in the suspension are adjusted to achieve the desired response over the 0.5 to 20 Hz measurement bandwidth. The isolation of the system is also checked by placing the shaker at the hitch point, and verifying that no output occurs.

The APL is used routinely at LCPC in two configurations—the APL 25 and APL 72.[14, 15] The two configurations are distinguished by different testing procedures, data storage equipment, and profile analyses. The APL 25 system runs at 22 km/h and produces an average rectified displacement roughness statistic (CAPL 25 value) for each 25-m section of road. It is commonly used to evaluate new construction, before the road is opened to the public. The APL 72 configuration is used for routine surveying of the road networks. It is towed at 72 km/h, and the profile signal is recorded on magnetic tape. The profiles are analyzed later in the laboratory, using electronic filters to isolate three wavebands covering long, medium, and short wavelengths. A summary index is accumulated for each of the three wavebands for every 200-m section of road traveled. The APL trailer is also used by the Center for Road Research (CRR) in Belgium. At CRR, waveband analyses of the profile are used to determine a coefficient of evenness known as the CP.

Given the objective of the RPM, the APL trailer was not used in either of the two standard configurations. Instead, the instrumentation and other hardware were assembled from various sources. The trailer was shipped from France to Ann Arbor, and arrived several days before the RPM. Some of the instruments normally used with the APL 72 system (power supply, amplifiers, tape recorder) were used to record the APL profile signals. A van was rented, and the participants from LCPC and MAP Sarl purchased a hitch which was modified in the UMTRI shop for towing the trailer. In the laboratory, the tapes were played back through an Apple II computer (owned by UMTRI) with a special card (owned by LCPC) to digitize the profile signals. The digitizer converted the analog profile signal into numerical values with 12-bit resolution (integer range of -2048 to +2047).

As shown in table 4 in the "Experiment" section, the APL trailer was towed at a speed of 50 km/h (31 mi/h) on the public roads. At GMPG, three speeds were used for repeat

runs on all of the sites: 18 km/h, (11 mi/h), 55 km/h (34 mi/h), and 90 km/h (56 mi/h). At the lowest speed of 18 km/h, the recorded signals were digitized at a sample interval of 100 mm. At the other speeds, the sample interval was 250 mm. Once digitized and stored on diskettes, the profiles were transmitted to the mainframe computer for processing.

Profile Plots

Figure 11 shows a representative comparison between the measurements from the APL trailer and the rod and level, when both profiles are filtered with a 10-m moving average. The only notable difference between the rod and level and APL profiles is seen at the 90 km/h (56 mi/h) speed. Visually, it appears that the trailer captures the basic profile shape correctly when towed at 90 km/h, except that the profile appears compressed (i.e., the profile features are all present, but occur closer together than they should). Compression is not evident in profiles at the other speeds. The apparent cause of this problem is a shortcoming in the temporary setup used to digitize the profiles, not in the APL trailer itself. Digital sampling frequencies of 50, 60, and 100 Hz were used at each of the three test speeds. Apparently, the digitizing system was not able to handle the 100 Hz rate required for the 90 km/h tests, with the result that some samples were skipped. The problem was not recognized at the time the data were digitized. It would be solved by either using different hardware to digitize the data, or by selecting a longer sample interval. Given that the profiles obtained at the highest speed are seen to be in error, roughness data computed from the high-speed measures will not be shown below.

At the two lower speeds, the APL and rod and level profiles are visually quite similar. The small differences seen are an expected result of the fact that the trailer is designed to measure profile with correct amplitude over its specified waveband, but not necessarily with the correct phase.

The APL trailer did not experience any problems on those public road sites with surface characteristics selected to challenge the noncontacting systems. The roughest sites were most likely to challenge the APL, in which case bouncing of the follower wheel is a possibility. Unfortunately, the data from the roughest sites could not be used, due again to problems with the temporary digitizing setup. In several cases the range that was set for the digitizer was not adequate, and the signal exceeded the range of the digitizing card (see table 4). Except for the problem in digitizing, roughness did not seem to be a problem with the APL trailer. Site 15 included several large patched areas that could excite follower wheel bounce; but, as figure 12 shows, the profile from the APL matches the profiles from two of the noncontacting systems quite well. From the authors' experience with the APL
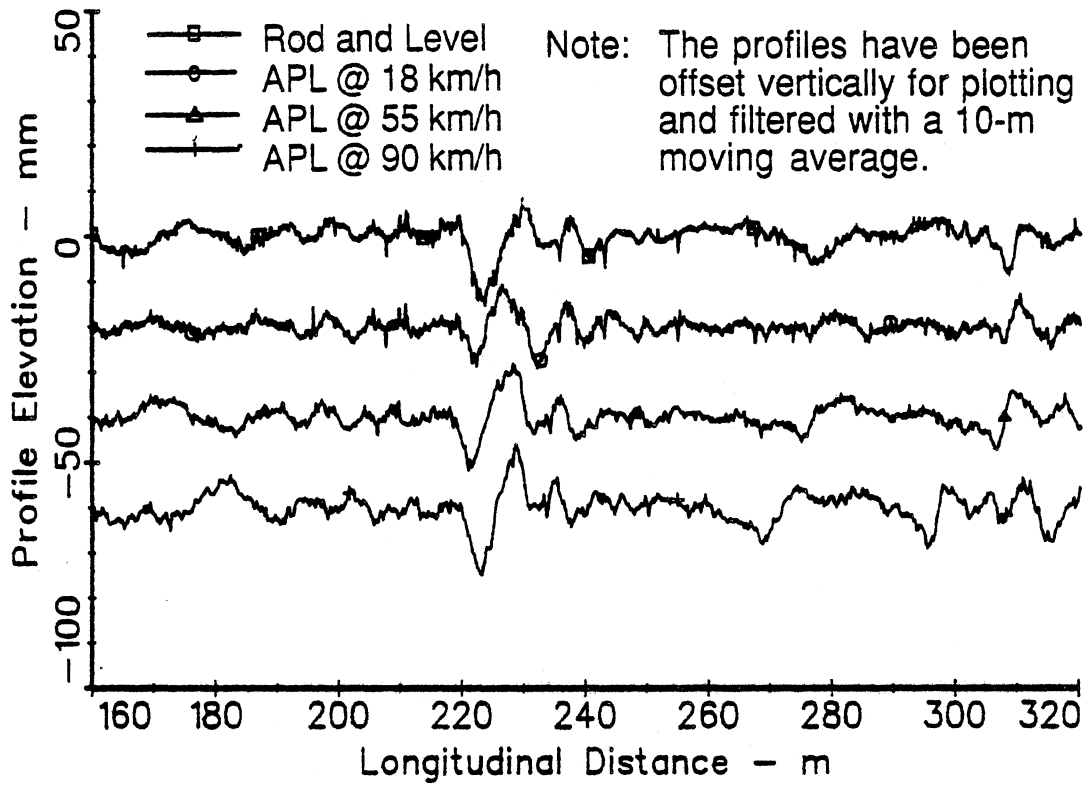
43

Figure 11. Comparison of APL profiles with rod and level on a road with medium roughness.

44
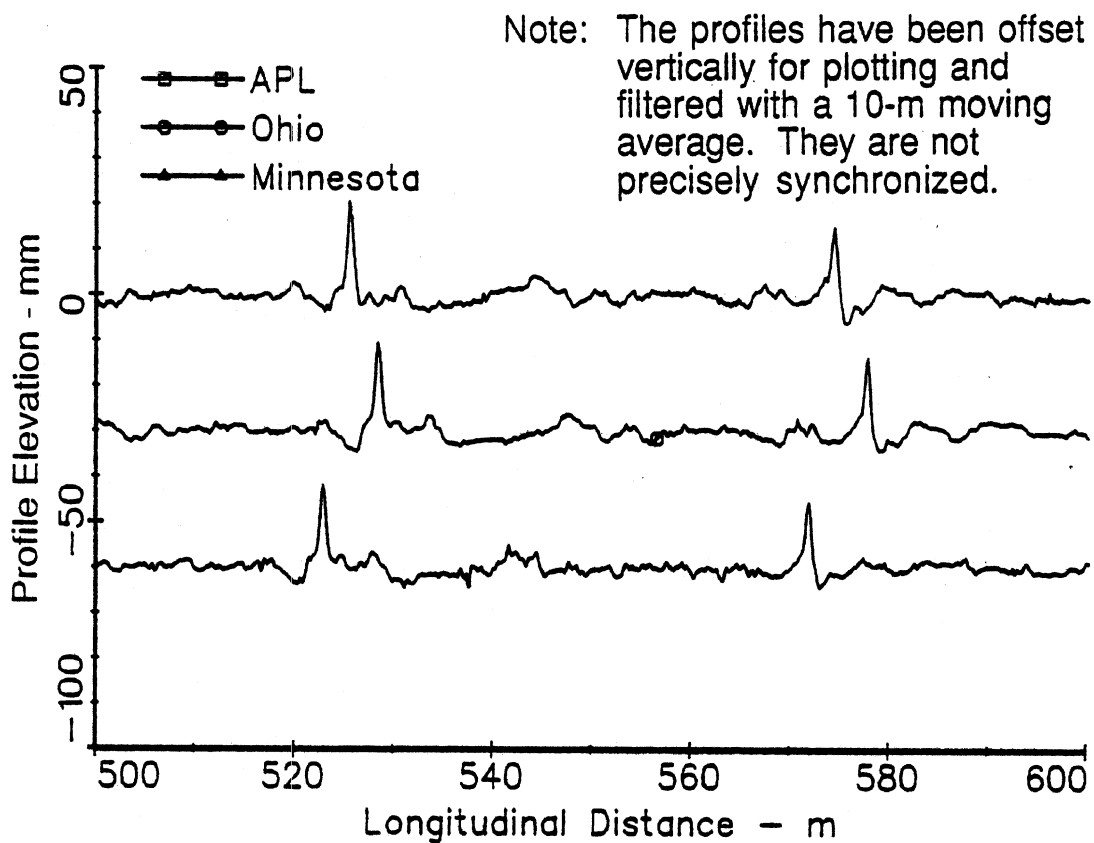
Figure 12. Comparison of profiles from several systems on a rough asphalt road with patching and cracking.

trailer in another study, including unpaved roads that were about twice as rough as the worst in this project, wheel bounce was not a problem in determining roughness statistics.[10] Thus, it is expected that with proper scaling, the trailer can be used for measuring roughness indices for any realistic level of roughness. The other project did not include special events such as the bridge crossing and railroad crossing sites, and it is unfortunate that the data for these sites had to be rejected due to the digitizer problem.

At the other extreme, figure 13 compares the profiles obtained from the APL and several other systems on the smoothest site. The figure does not show any visible influence of extraneous vehicle vibrations in the APL profile.

Additional profiles from the APL trailer are shown in figures 2 and 3.

Measurement of Roughness Indices

Figure 14 shows a comparison of the IRI and MO roughness measures computed from profiles of the APL and the reference. The APL trailer gives consistent results for all of the tests, and visually indicates the type of accuracy that can be expected. The upper plots in the figure show that the APL is quite accurate for measuring IRI for roughness levels less than 5 m/km. On the rougher sites, the APL measures tend to be a little lower than the reference measures.

The ability of the APL to measure IRI was also tested in the International Road Roughness Experiment (IRRE) in Brasilia, Brazil[10]. The test design was similar to that of the RPM, and therefore it may be appropriate to mention those results here, especially since there were some differences in the test conditions and equipment which should be noted. In the Brasilia study, the sites were 320 m in length, rather than the 160 m used to compute IRI in this study. As a result, an identical instrument would be expected to show better accuracy with the longer IRRE sites, since more averaging occurs during measurement. The Brasilia study included unpaved roads, with roughness levels up to 15 m/km IRI. But for the paved roads, the roughness range was greater in the RPM, including both pavements smoother than the smoothest in Brasilia, and pavements rougher than the roughest in Brasilia. The IRRE sites did not include any PCC sections. The accuracy in measuring IRI displayed by the APL in this study is improved over that shown in Brasilia, even though the sites are shorter. This probably reflects the fact that the instrumentation used in the RPM was assembled for the purpose of measuring profile signals for later analysis, whereas the setup in the IRRE was geared towards demonstrating the APL 72 and APL 25 methods used in France.

46
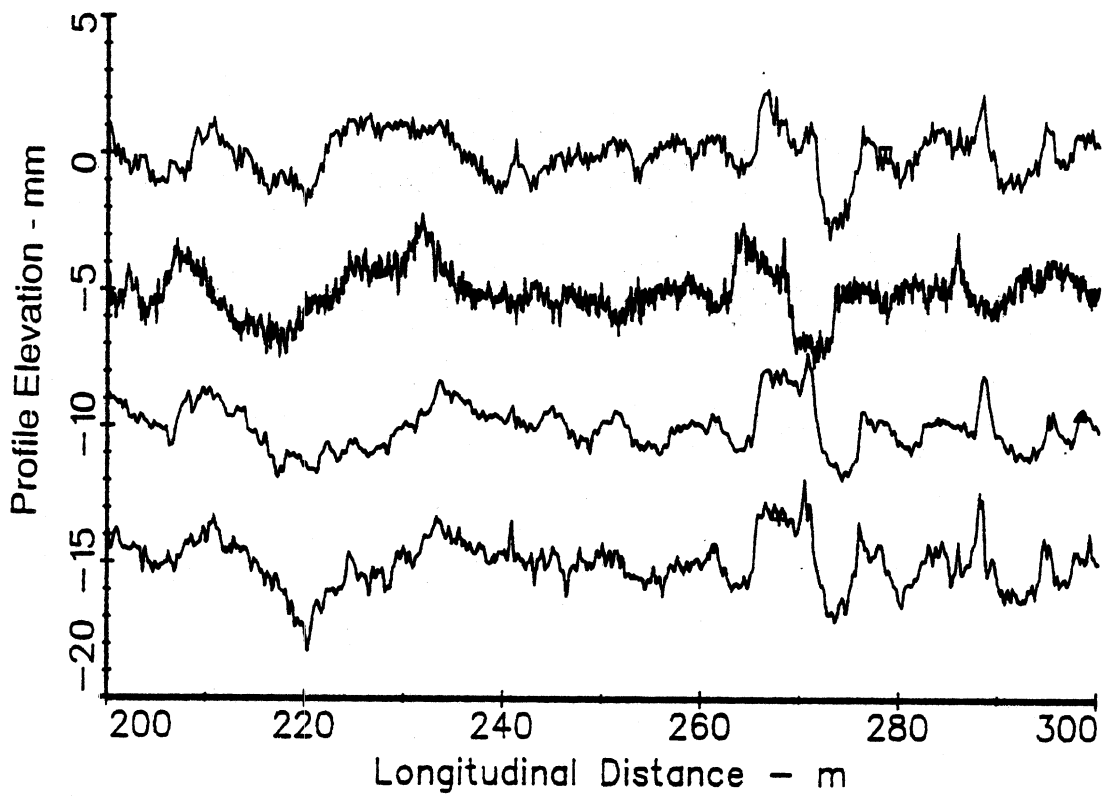
Figure 13. Comparison of several profiles on a very smooth road

GMPG Sites

APL @ 18 km/h
APL @ 50 km/h

IRI — m/km

Rod & Level — m/km

IRI (1/4-car index)

All Road Sites

APL @ 18 km/h
APL @ 50 km/h

IRI — m/km

Reference — m/km

IRI (1/4-car index)

APL @ 18 km/h
APL @ 50 km/h

MO Index — m/km

Rod & Level — m/km

Texas RMSVA Index: MO

APL @ 18 km/h
APL @ 50 km/h

MO Index — m/km

Reference — m/km

Texas RMSVA Index: MO
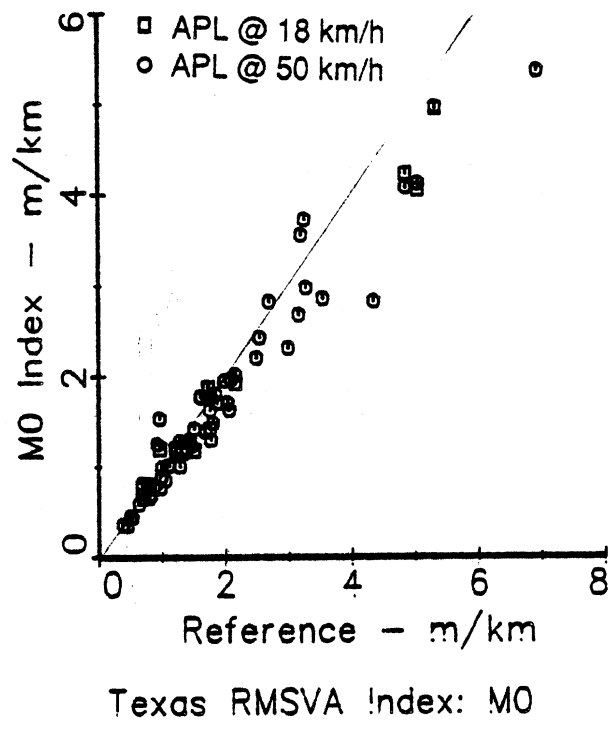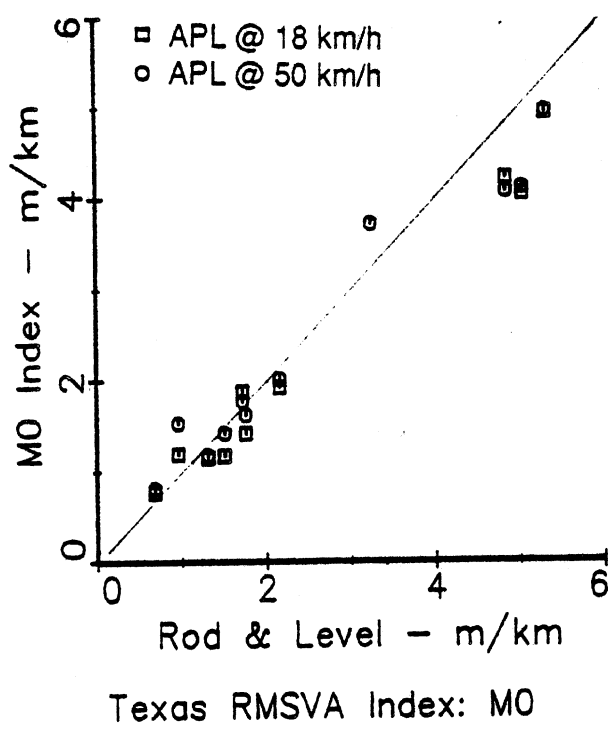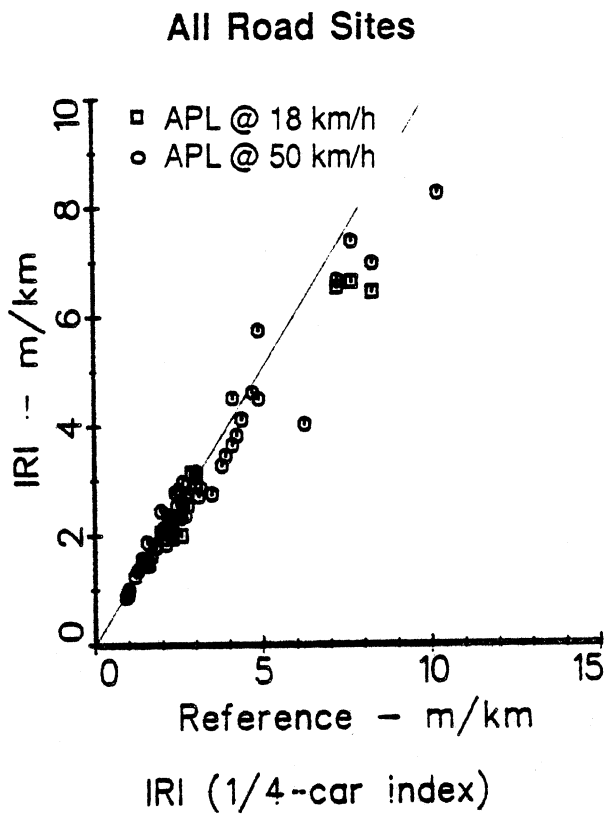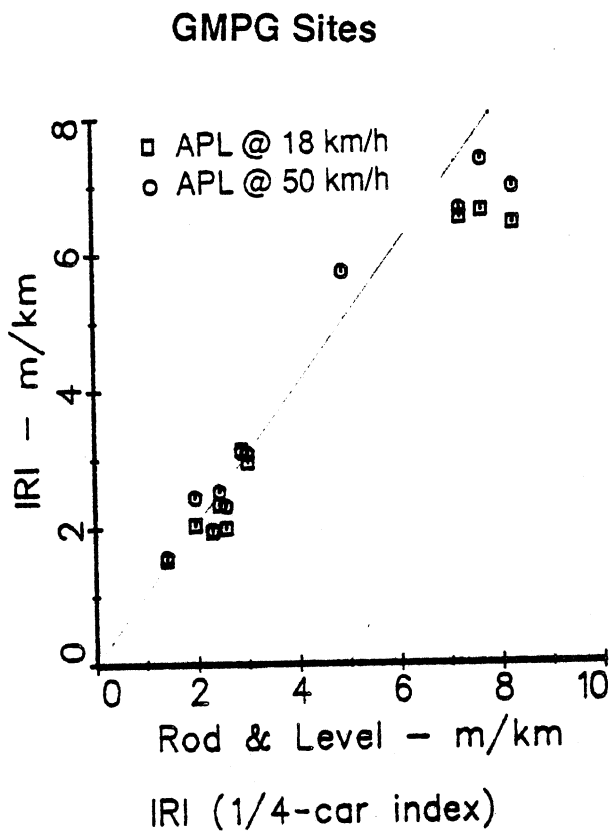
Figure 14. Measurement of IRI and MO with the APL trailer.

48

Good agreement between the APL and the reference is also seen for the MO index in the lower plots in figures 14, although the scatter of the MO on the smoother sites is larger than for the IRI. The MO relationship is slightly biased on the public roads, being lower on the average than the reference.

In the IRRE held in Brazil, it was found that the APL trailer could not accurately measure QI_r, which is an index based on RMSVA and used in Brazil.[10, 13] QI_r and MO are both defined using the RMSVA analysis, but they differ in the baselengths used. QI_r uses baselengths of 1.0 and 2.5 m, whereas MO uses baselengths of 1.22 m (4 ft) and 4.88 m (16 ft). The APL was not valid for measuring QI_r, producing measures of QI_r that were too low. The reason is that the QI_r is influenced by short wavelengths that are not sensed by the APL trailer. (This is particularly true on unpaved roads.) Since the MO analysis includes longer wavelengths, the shortest wavelengths assume less significance and the bias becomes smaller when MO is computed.

Waveband Indices

Figures 15 and 16 summarize the accuracy of the APL for a full range of 1-octave wavebands. For the 64-m waveband, all measures from the APL are low, confirming that the trailer does not fully see the longest wavelengths. The results are closest to the reference when the APL is towed at the higher speeds. Although the 90 km/h data were invalidated due to the digitizing problem, the data points are shown for the 64-m waveband to demonstrate that the ability of the trailer to see long wavelengths is improved by towing it at a higher speed. The eight plots in these two figures show that at a speed of 50 km/h (31 mi/h), the APL gives valid measures for the wavebands covering 2- to 32-m wavelengths, although the 32-m results are perhaps marginal in view of the better accuracy seen for the other wavebands. For a speed of 18 km/h (11 mi/h), the wavebands covering wavelengths longer than 8 m are attenuated. The best accuracy for the speed of 50 km/h (31 mi/h) is for the wavebands centered at 16, 8, and 4 m, while the lower speed measures are best for wavebands centered at 8 and 4 m. For the shorter wavelengths, the APL is less consistent, particularly on the rougher sites where the APL measures are somewhat low. These results help explain why the IRI and MO measures were low on the roughest GMPG sites: the APL was not sensing the full amplitudes of the shortest wavelengths.

Power Spectral Density (PSD) Functions

PSD plots were generated for all of the profiles obtained with the APL trailer and compared with the reference measures. The PSD plots obtained from the 90 km/h tests

49
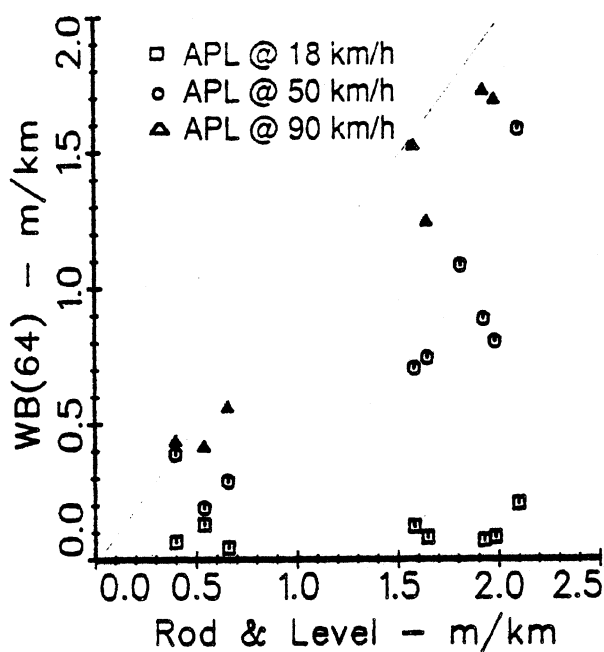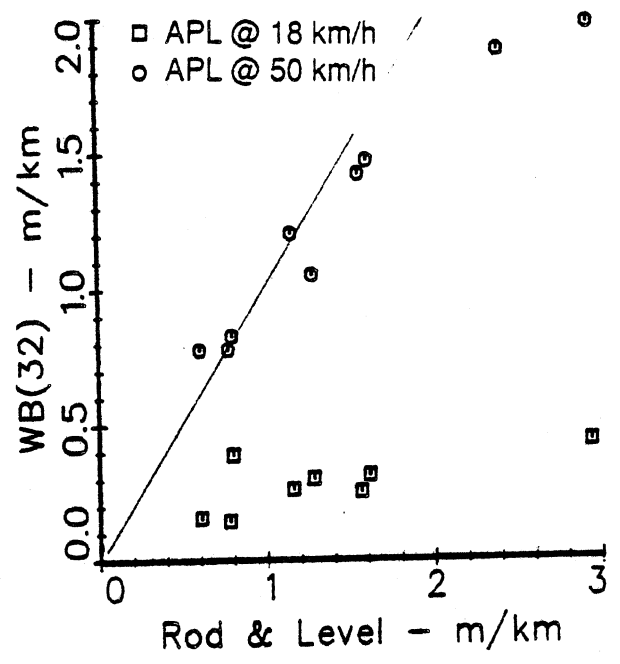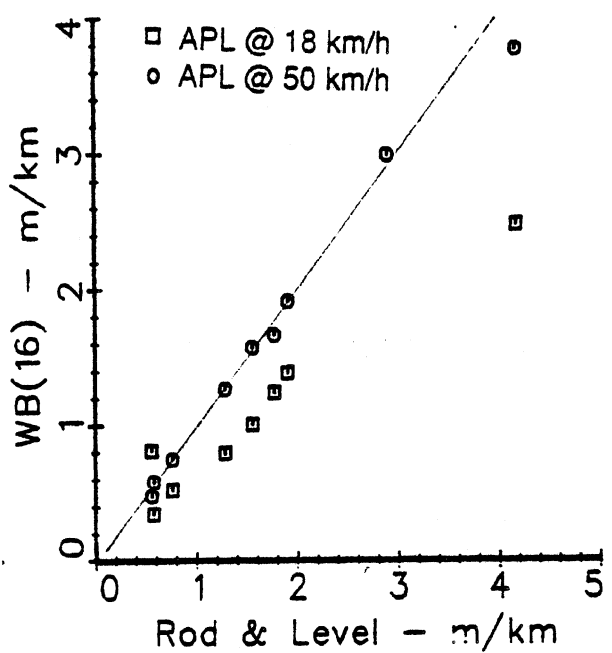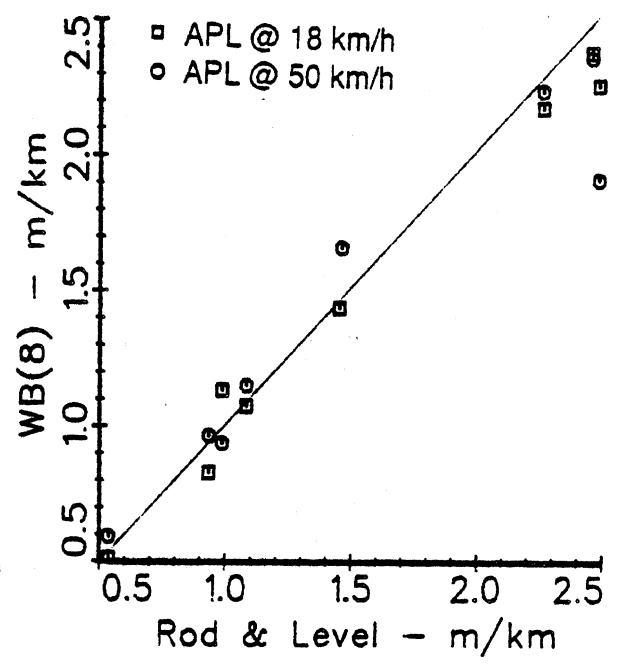
Figure 15. Measurement of waveband indices for the longer wavelengths with the APL trailer.
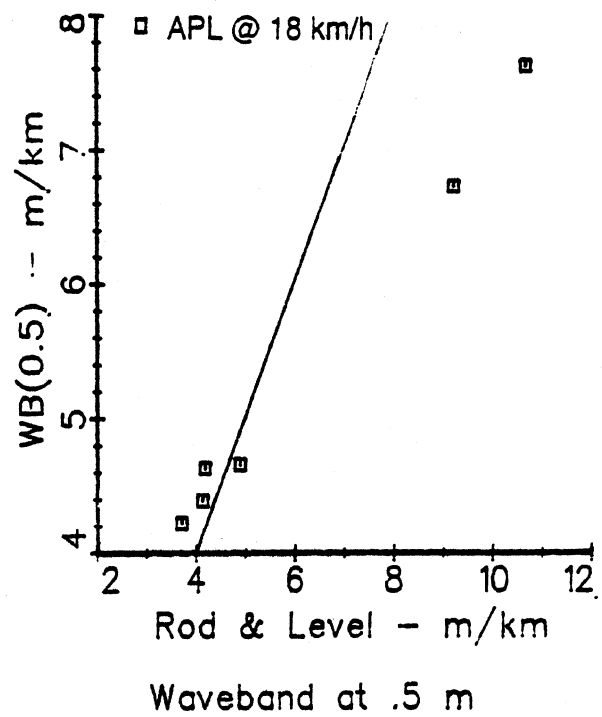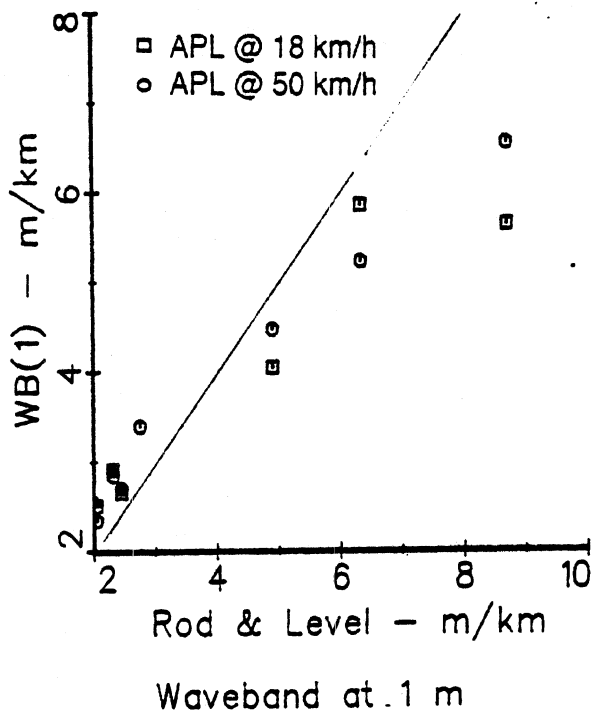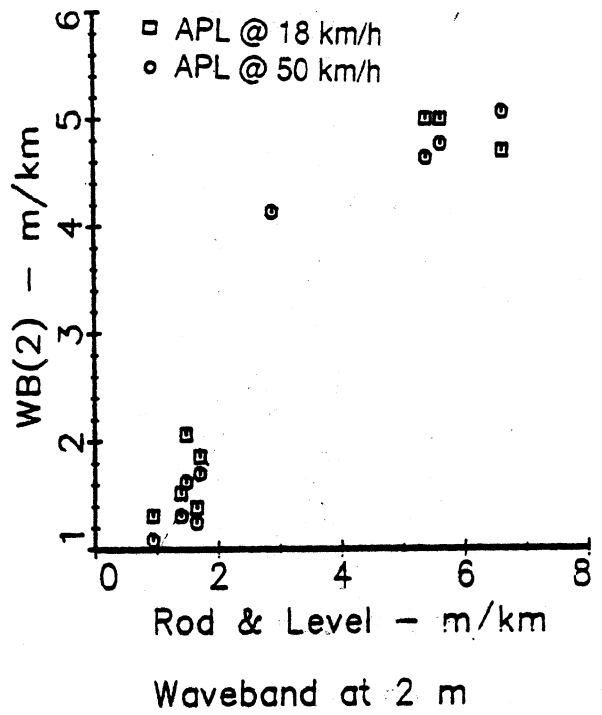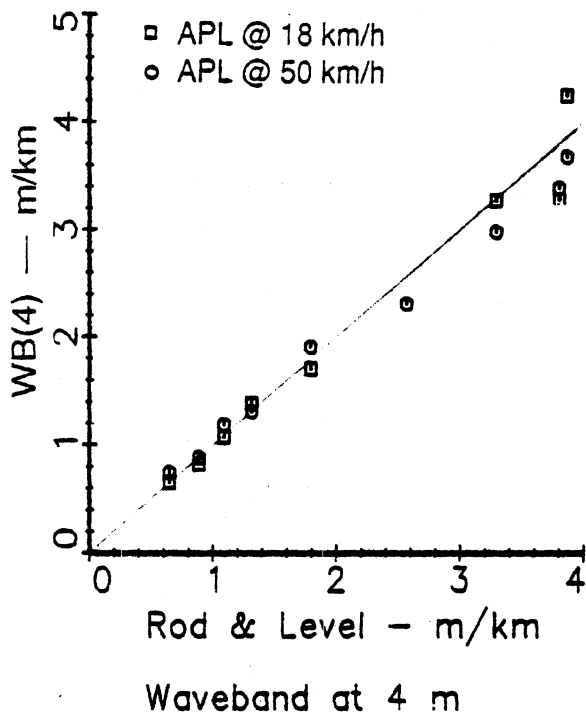
Figure 16. Measurement of waveband indices for the shorter wavelengths
with the APL trailer.

51

were not consistent, as might be expected from the compression problem caused during digitization. All other PSD plots that were computed from valid runs (see table 4) matched the reference within reason. Figure 17 compares the PSDs from the APL with the rod and level reference on a typical site. (The reader is reminded that the PSD plots are offset vertically in the plots for readability.) The lowest wavenumber (longest wavelength) that can be accurately transduced by the APL can be seen very clearly in the figure for each of the three speeds. For the 18-km/h (11-mi/h) speed, the PSD matches the reference above a wavenumber of 0.1 cycle/m. This is a wavelength of 10 m, and corresponds to a frequency of 0.5 Hz. For the 55-km/h (34-mi/h) speed, the PSD matches the reference down to a wavenumber of 0.035 cycle/m, which again corresponds to a frequency of about 0.5 Hz. The APL is claimed to measure profile for wavelengths up to a limit corresponding to 0.5 Hz at the measurement speed, and figure 17 (along with every PSD plot obtained in the RPM) supports this claim.

Figure 18 shows PSD functions for one of the smoothest GMPG sites, and illustrates an effect common with mechanical follower wheels. In all three of the APL plots, there is a peak at a wavenumber of about 0.5 cycle/m. This is first harmonic runout of the follower wheel (circumference equal to two meters). Thus, the spectral peak shown in the APL plots, which is not evident in the rod and level plot, is the result of a component in the APL signal due to the rotating wheel, rather than the profile. There is also a second peak at exactly twice this wavenumber, which is the second harmonic. Harmonics also exist at all multiples of the first, but are usually obscured by the road roughness. The effect of the wheel harmonics can generally be seen only on very smooth surfaces. Although the spectral peak can be very noticeable in PSD plots, particularly when narrower bandwidths are used, the wheel nonuniformities are only a problem if they influence the processed results obtained from the measure. (The methods used to prepare the PSD plots tend to visually diminish these types of spectral peaks. Other methods will result in plots that show the peaks much more spectacularly.) The amount of nonuniformity shown by the APL trailer that participated in the RPM was too small to affect any of the indices considered, as was seen from the direct profile plot in figure 13. However, it could be a problem with other applications.

Conclusion

The APL trailer is a profilometer that is based on a completely different design concept than the GM-type used in all of the other participating instruments. Although the design is different, the results show that it is successful. The APL measure matches the true profile over a band of wavelengths, which correspond to frequencies of 0.5 and 20 Hz at the
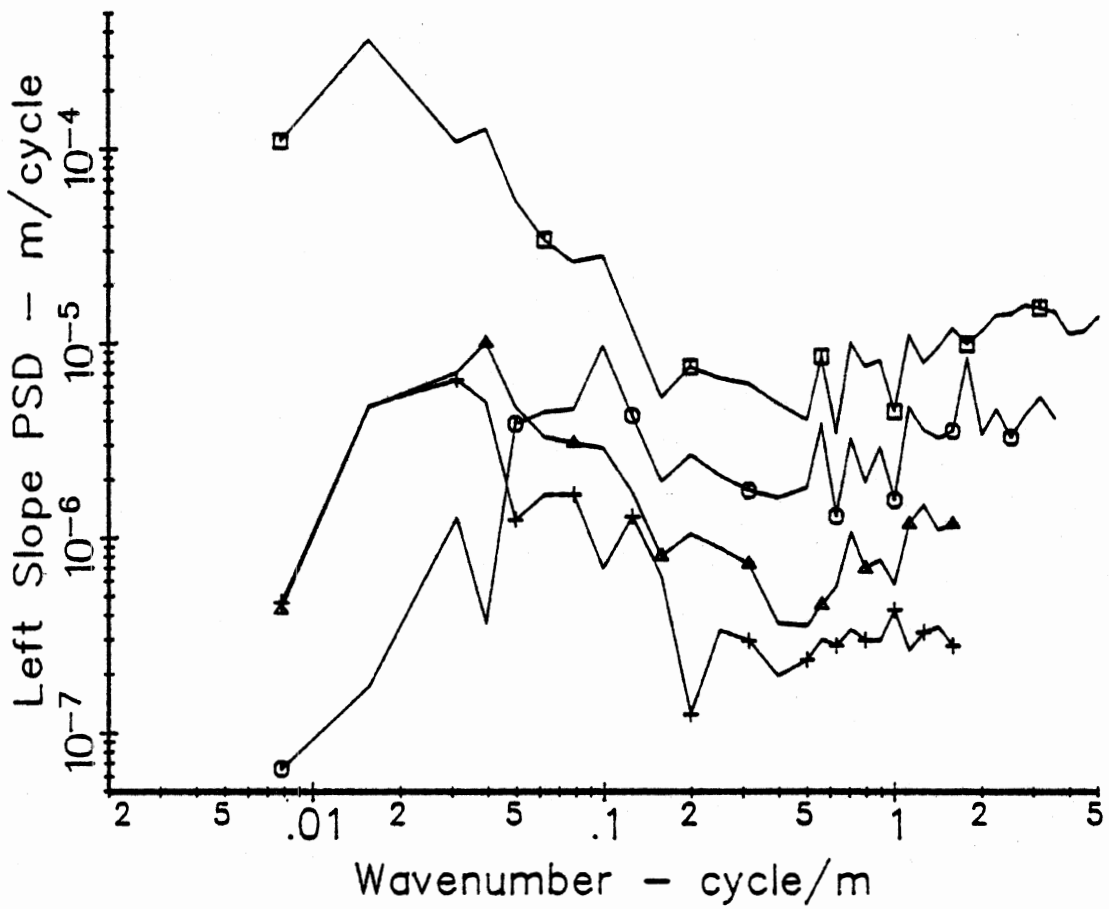
Figure 17. PSD functions from the APL trailer on a moderately rough site.
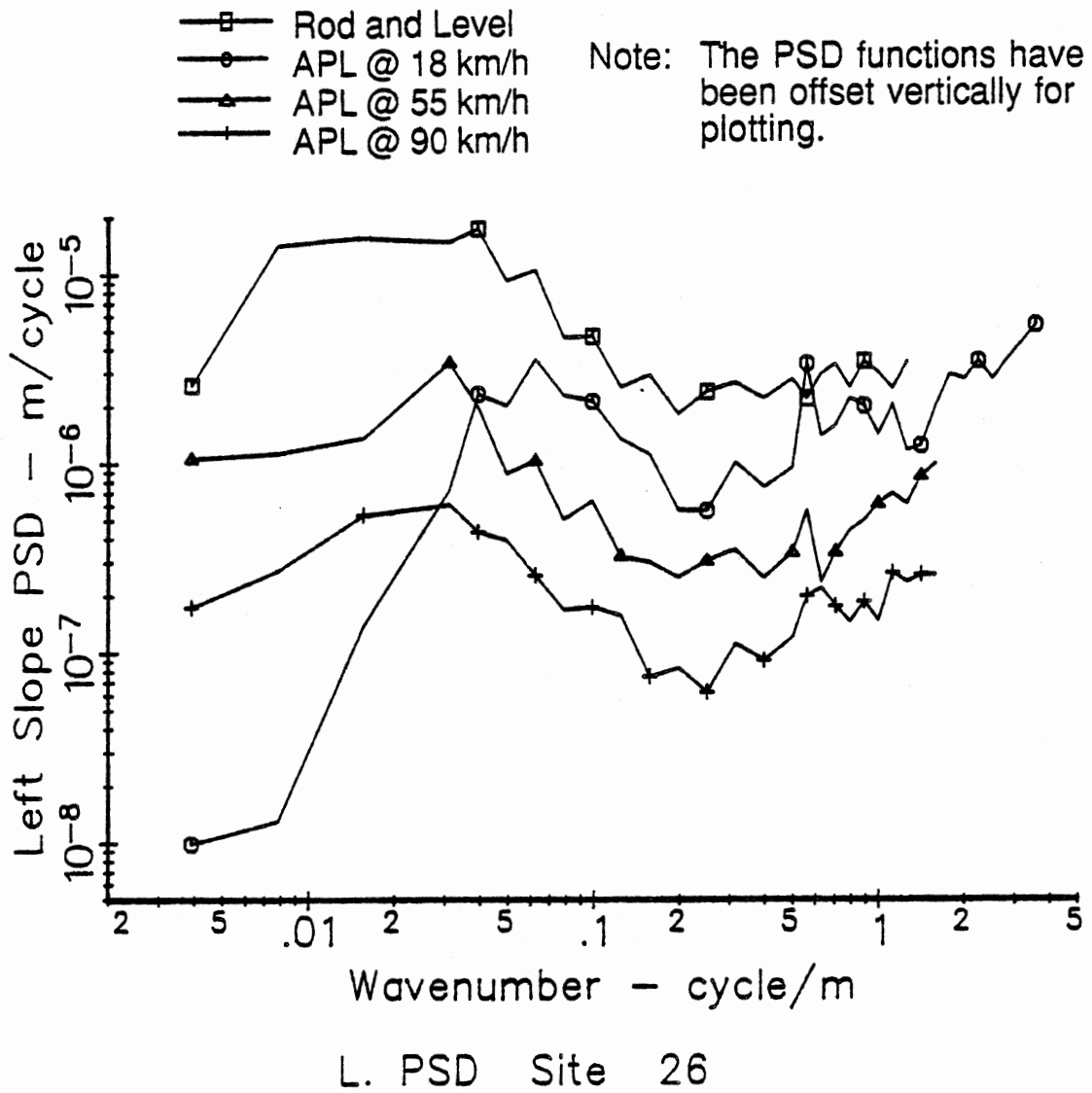
Figure 18. PSD functions from the APL trailer on a smooth site.

measurement speed. That is, it measures longer wavelengths when it is towed at higher speeds. The instrument can be used at its normal measurement speeds to measure the IRI and MO roughness indices with reasonable accuracy. Unlike the early mechanical GM-type profilometers, the APL is also suitable for a full range of roughness, from very smooth to fairly rough. The only problem experienced in the RPM involved the temporary setup used to transfer the data to the UMTRI computer, which precluded the analysis of the measures taken at high speeds and on the very roughest sites.

Colorado (K. J. Law Model 8300 Roughness Surveyor)

Hardware Description

K. J. Law Engineers, Inc. has developed a roughness measurement instrumentation system that can be readily installed in most vehicles. The system is described in the brochure, "Descriptive Specification for the Model 8300 Road Roughness Surveyor," dated 11/83, and available from K. J. Law Engineers, Inc.[16] It is based on the concept of the GM-type inertial profilometer—incorporating an accelerometer, ultrasonic road sensor, speed sensor, and a digital computer. Road profile is calculated during measurement for the purpose of computing any of a number of summary roughness indices, but the profile is not recorded. Thus, profiles were not available for critical analysis as with the other profilometers.

At the time of the RPM, a roughness surveyor (shown in figure 19) was under construction for the Colorado Department of Highways. By a cooperative arrangement between the Colorado DOH and K. J. Law Engineers, Inc., the completed unit participated in the meeting, being operated by staff from K. J. Law Engineers. At the time of the meeting, the system had not yet been delivered, and the RPM was part of its final checkout. The system experienced problems during the RPM, particularly when trying to measure pavement surfaces with open textures that are poor reflectors of ultrasound. Following refinements by the manufacturer, the system was retested in November over most of the public road sites that were used in the RPM. Although a few of the pavement markings from the RPM were gone, most of the sites began at semi-permanent markers (such as mileposts and highway signs) so that retests were made over approximately the same sites.

Tables 2 and 4 in the "Experiment" section indicate the range of surface conditions that were eventually covered with the Colorado system. The sites include asphalt, surface treatment, and PCC. Several of the PCC sites had lateral grooves that produce an open texture that doesn't reflect ultrasound very well. Site 13 was a PCC site with open joints
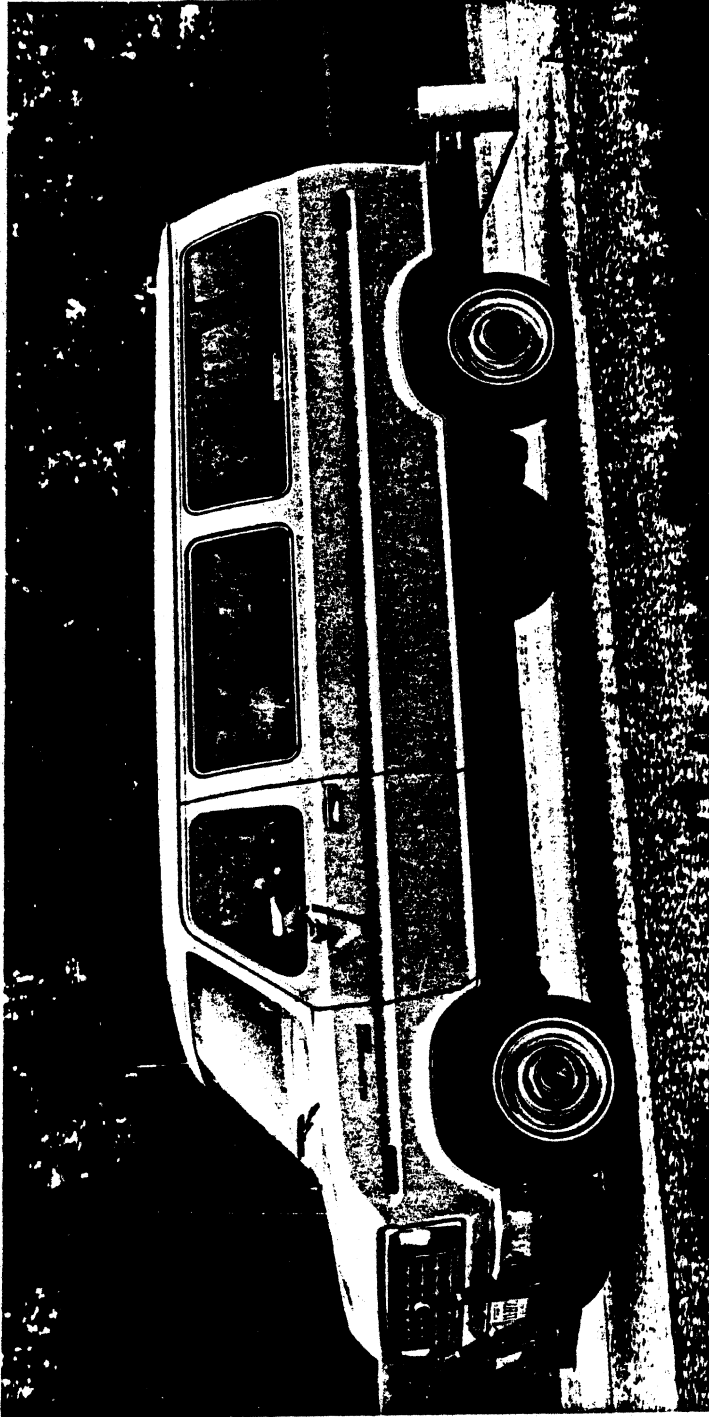
Figure 19. The Colorado roughness surveyor.

that might cause problems with noncontact sensors. These sites were measured successfully by the system, and the results are valid. Site 7 included a portion of asphalt road that had not been coated for several years and therefore had cracks and an open texture. No data were obtained for this site to prove that it could be successfully handled by the 8300 Roughness Surveyor.

Measurement of Roughness Indices

The roughness analysis installed in the Colorado unit is called a Mays meter simulation, and is identical to the IRI. That is, it is a quarter-car simulation, using the parameter values from the NCHRP 228 report[9], computed for a single wheeltrack, and based on a standard speed of 80 km/h (50 mi/h). Although all roughness data with units of slope are presented in this report with units of m/km, it should be noted that the normal units for the Colorado measures are inches/mi. They are converted to m/km by dividing by 63.36 (there are 63,360 inches in a mile). Figure 20 shows how these measures compare with the reference. The graph on the left shows mean values from multiple tests on each 160-m section, while the graph on the right shows the range of values obtained in individual tests. The high roughness levels (greater than 5 m/km) from the RPM are not included in these plots. Several of the roughest sites were at GMPG, and the unit was not retested there after the RPM. The other rough sites, on the public roads, were all repaired to various degrees in the weeks immediately following the RPM and therefore did not have the same profile.

There is a more-or-less constant error level in the measurement that may be due to limitations in the resolution of the ultrasonic sensor. The data indicate that the system is somewhat less accurate on the smoother sites than it is on the rougher sites because the error assumes a proportionately larger role when the road roughness is less. The plots also show that the 8300 Roughness Surveyor is capable of measuring the profile-based IRI, without any significant bias, and with an accuracy that will be acceptable for many uses of the data.

Conclusion

The 8300 Roughness Surveyor proved its ability to measure IRI, a standard roughness index on smooth to moderately-rough roads. Measures obtained from the Model 8300 are compatible with those obtained with other profilometers. The system appeared to have difficulty on some types of surface, however, and therefore its reliability for some road types—particularly rough roads and roads with open textured surfaces—remains to be demonstrated.
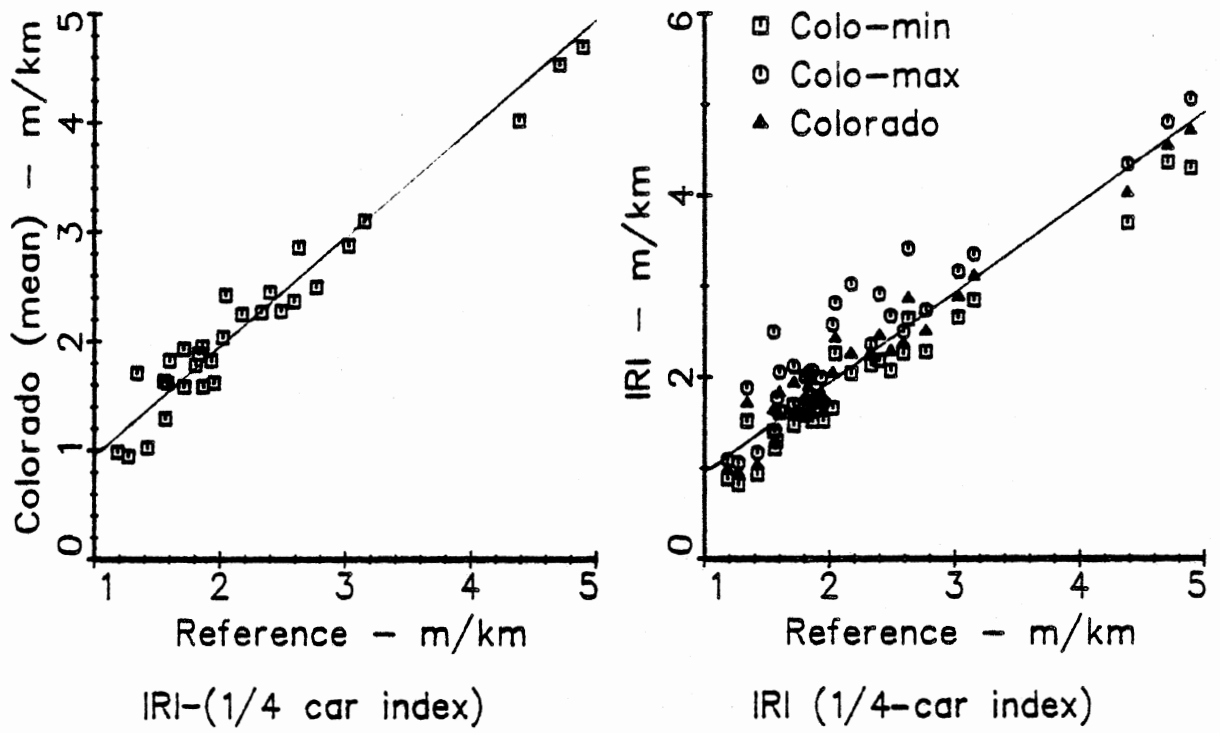
Figure 20. Measurement of IRI with the Colorado roughness surveyor.

FHWA Profilometer: Infrared Version

Hardware Description

The project under which this work was performed originally focused on the design and construction of a profilometer system for the FHWA, capable of measuring both profile and rut depth. A photograph of the profilometer is shown in figure 21. A detailed description of this system is planned as the final report for this project, and therefore only a brief overview is given here. The system follows the GM-type inertial profilometer concept, with the provision that noncontacting sensors are used to measure the height of the vehicle body above the road.

The instrumentation and recording hardware are based on the IBM-PC family of microcomputers. The PC was equipped with an expansion chassis (needed to plug in all of the special function cards used), extra memory (640 kbytes total), a digitizer, a bubble memory (containing the profilometer software), and a 3-M cartridge tape system to record the data. An analog box developed previously at UMTRI contains power supplies and amplifiers for the analog transducers (the height sensors and accelerometers), and also contains antialiasing filters to attenuate high frequencies before the signals are digitized (converted from voltages to numbers).

As with other GM-type profilometers, an accelerometer is attached near each height sensor to obtain the vehicle motions relative to an inertial reference. To measure longitudinal distance, a rotor at the right-front wheel position is sensed by an inductive pickup. The signal from this pickup is used to trigger the digitizing of the signals. In addition, it is fed into a frequency/voltage converter to obtain a continuous speed signal.

At the time of the RPM, the system had just been assembled, and included only the mimimal software needed to acquire data. During testing, the computer memory would fill with data. Then, when the test was completed, the data were transferred to the tape cartridge. Later, the data were transferred from an IBM PC in the office to the mainframe computer, where the numbers were stored on conventional 9-track computer tapes. All processing, including the computation of the profile, was performed on the mainframe computer using the algorithms that will be eventually installed in the onboard computer.

Five signals are measured—two from the noncontacting height sensors in the right- and left-hand wheeltracks, the two corresponding accelerometers, and the speed signal. The
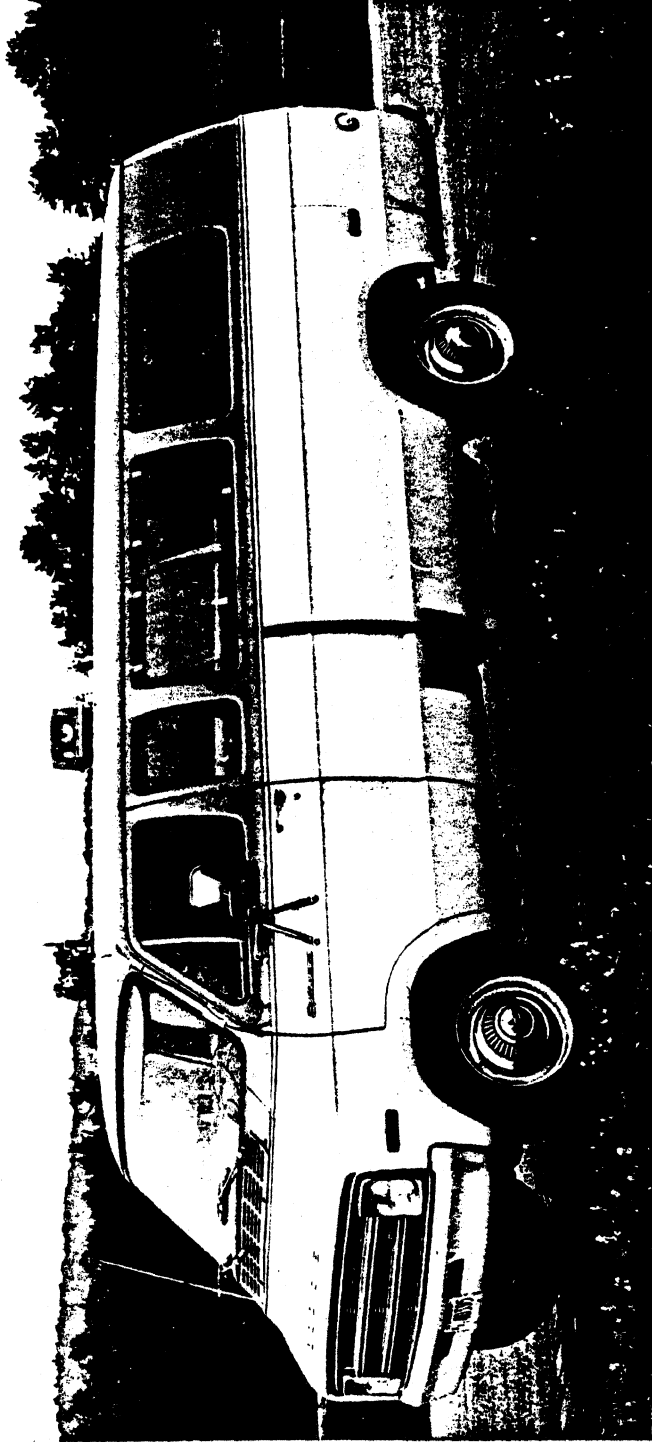
Figure 21. The FHWA profilometer.

signals are sampled at an interval of 76 mm (3 inches), as triggered by the signal from the inductive distance pickup. The antialiasing filters in the analog box are 4-pole Butterworth filters, with a cutoff frequency set by the computer to be 1/3 of the sample frequency (at the intended test speed).

The system senses the vehicle-to-road distance using the infrared (IR) system designed and built by Southwest Research Institute under contract with the FHWA.[8] This sensor, shown in figure 22, projects a circular image approximately 76 mm (3 inches) in diameter onto the road surface, and detects the vehicle height using triangulation. The position of the IR image is detected from both sides of the projected beam, so that variations in the reflectivity of the surface can be cancelled.

Early tests with the IR sensor in the laboratory indicated that its design does not always eliminate sensitivity to surface reflectivity,[7] and therefore efforts were made to acquire an alternative height sensor. Several Selcom laser sensors were obtained, and were also used with the system. The FHWA profilometer was tested on the RPM sites with the IR sensors, which were then removed and replaced with the Selcom sensors. The system was then tested again, in order to obtain a measure of the comparative performance of each. The results obtained with the Selcom sensors are described in the sub-section following this one. In this report, tests of the FHWA system with infrared sensors installed are often identified as "Infrared" or "IR." Tests made with the Selcom sensors are designated "Selcom."

Profile Plots

The FHWA systems were configured with less filtering of long wavelengths than any of the other GM-type profilometers. The good response at the longest wavelengths means that this profilometer provides one of the best matches with rod and level for preparing profile plots with the fullest level of detail. For example, figure 23 shows the comparison with rod and level, when the profiles are filtered with a moving average of 100 m.

Figure 24 shows a comparison of the measures on a site with large amplitudes and color changes, which occur at the joints in a damaged PCC road. Figure 25 shows that the system also did very well in handling the manhole cover on site 2. The system also did well in handling the railroad crossing on site 3 (see figure 45). In both of these cases, the IR sensor was able to detect the combination of a height change and color change as it crossed the metal manhole cover and railroad rails.

61
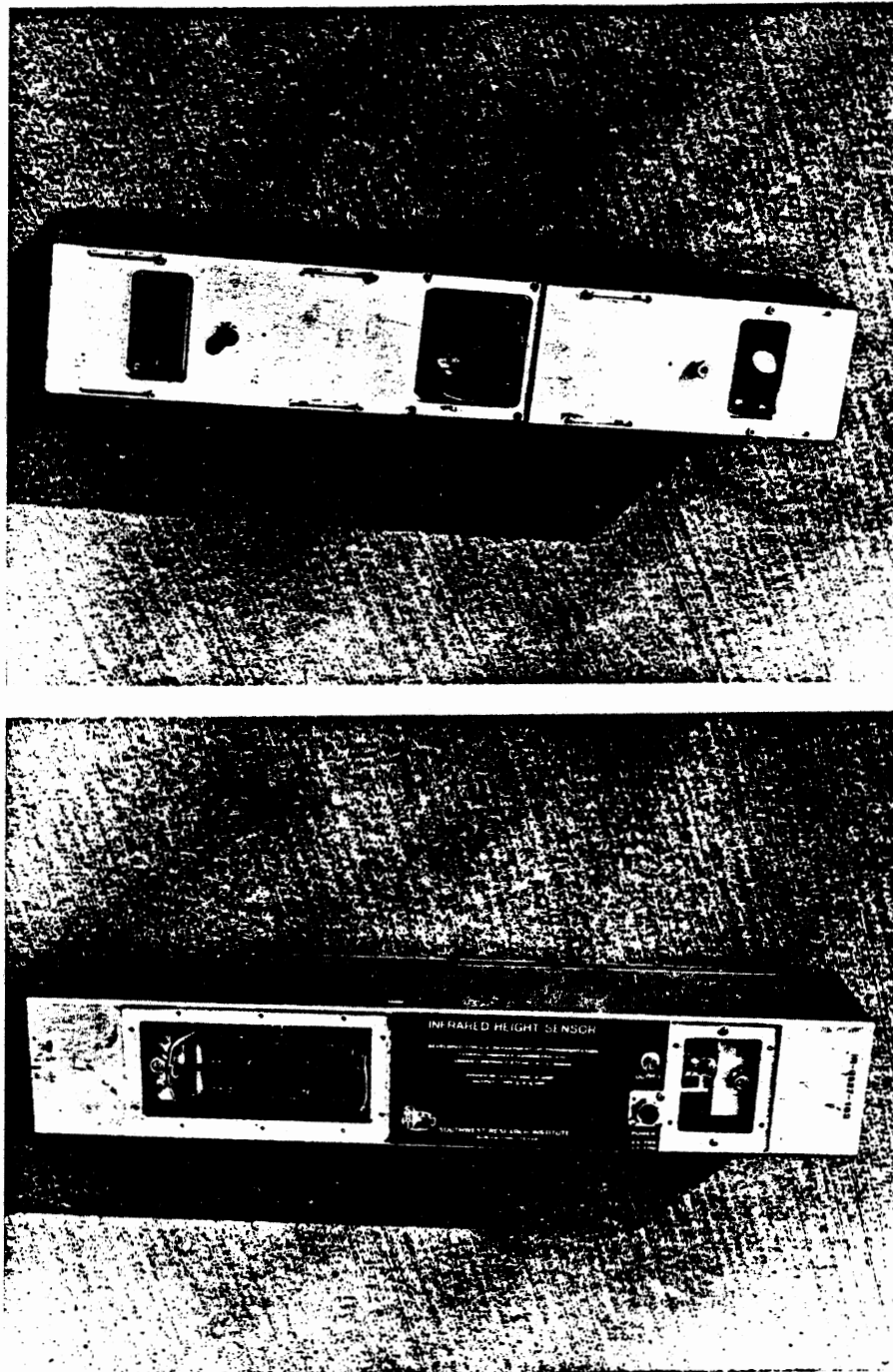
Figure 22. The FHWA infrared height sensor.
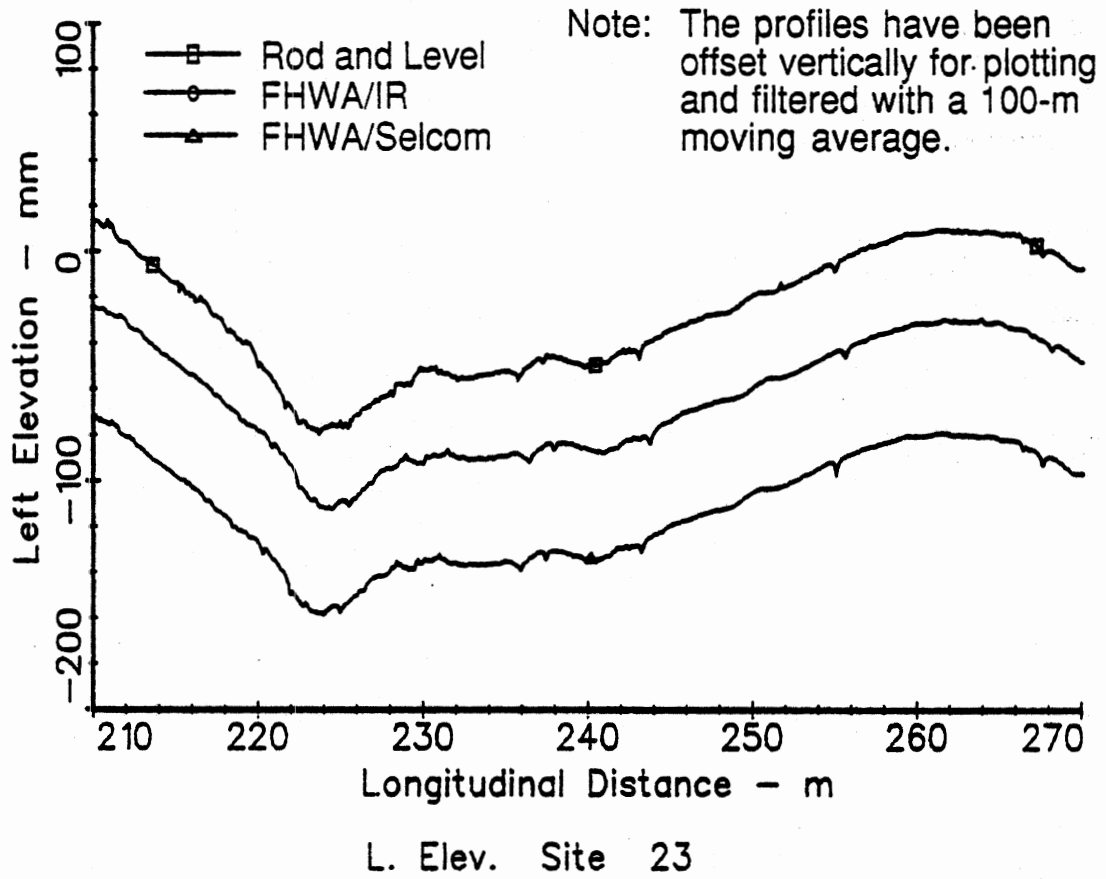
Figure 23. Measures from the FHWA profilometer on a rough road, looking at longer wavelengths.

Note: The profiles have been offset vertically for plotting, and filtered with a 10-m moving average. They are not precisely synchronized.

—□— Ohio
—○— Minnesota
—▲— FHWA/Selcom
—+— FHWA/IR

L. Elev.   Site   16
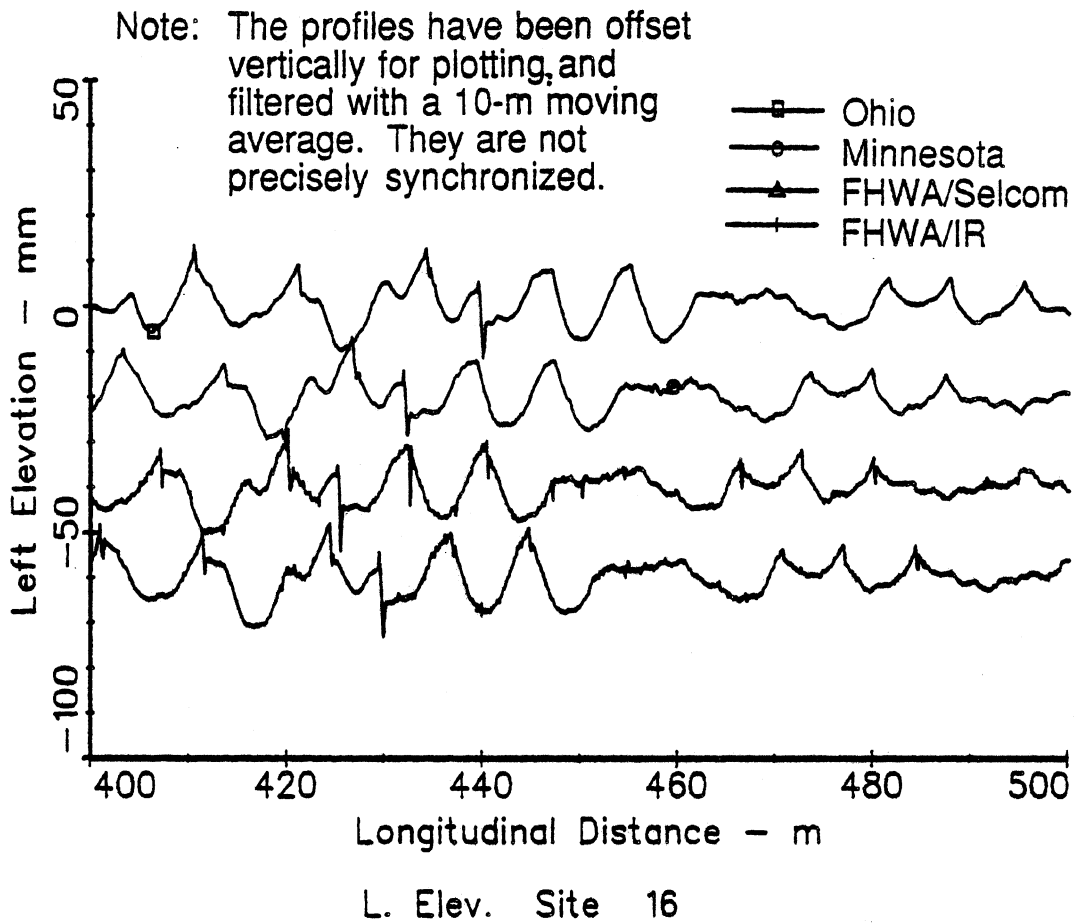
Figure 24. Comparison of several profilometers on a PCC site with open depressions at the joints.

64
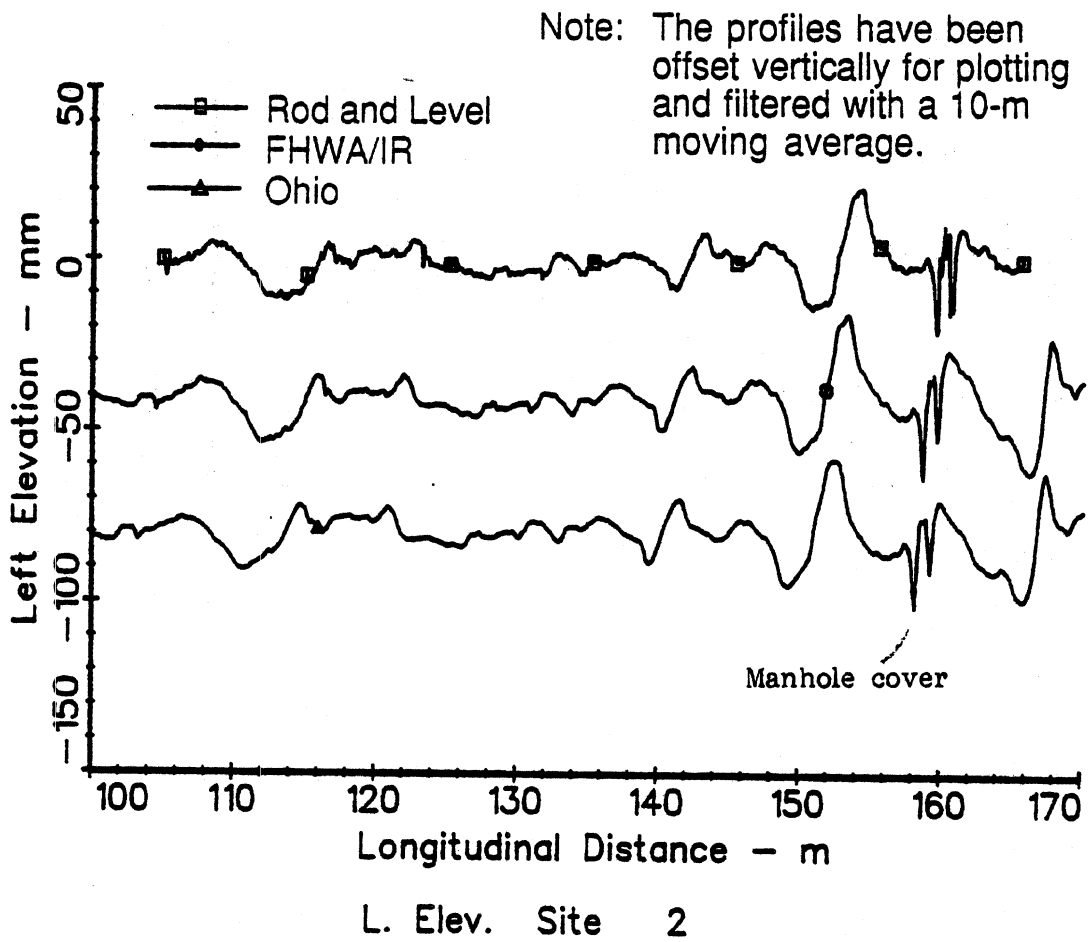
Figure 25. Comparison of several profilometers on a rough site that includes a manhole cover.

On the other hand, the IR system gave erroneous data on one of the roughest sites, site 15. Figure 26 shows how the IR system compared with several other profilometers on this site, when all of the results are similarly filtered with a 10-m moving average. On this site, profile produced from the IR system is in error, due possibly to large amplitudes and the IR nonlinear response, or perhaps due to changes in the reflectiveness of the surface. This site included extensive patching, a condition that is known to challenge the IR sensor. The sensor was evidently unable to measure height correctly when faced with extreme height changes accompanied by coloration changes, as occurs with patching.

As table 4 in the "Experiment" section shows, several of the runs had to be rejected because of a digitizing problem. More specifically, the vehicle accelerations were larger than anticipated with the result that the accelerometer signals saturated the digitizer. This problem is easily fixed by setting a slightly broader digitizing range. However, the IR sensor is known to become nonlinear at higher amplitudes. It is possible that when the digitizer range is properly set, the IR sensor will limit the performance on rougher sites at high speeds. Thus, while the system functioned for roughness levels that did not result in saturation of the accelerometer signals, it should not be inferred that extending the range of the accelerometers will extend the valid roughness range of the overall system.

Additional profile plots from the FHWA/IR system are shown in figures 3, 34, 45, 73, and 74.

Measurement of Roughness Indices

Figure 27 shows how IRI and MO roughness indices determined from the IR system profiles compare with the reference. The IR system gives results that are consistent with the reference for both the IRI and the MO on the GMPG sites (the two graphs on the left-hand side of the figure). On the public road sites (the two graphs on the right-hand side of the figure) there is one obvious outlier for both the IRI and MO. That data point is site 15, discussed earlier and shown in figure 26.

Overall, the IR system measures IRI with high accuracy for roughness levels up to 5 m/km. The few sites with higher roughness levels were measured without any obvious bias, but there is more scatter, meaning that less accuracy is obtained. Similar performance was observed when computing the MO index.
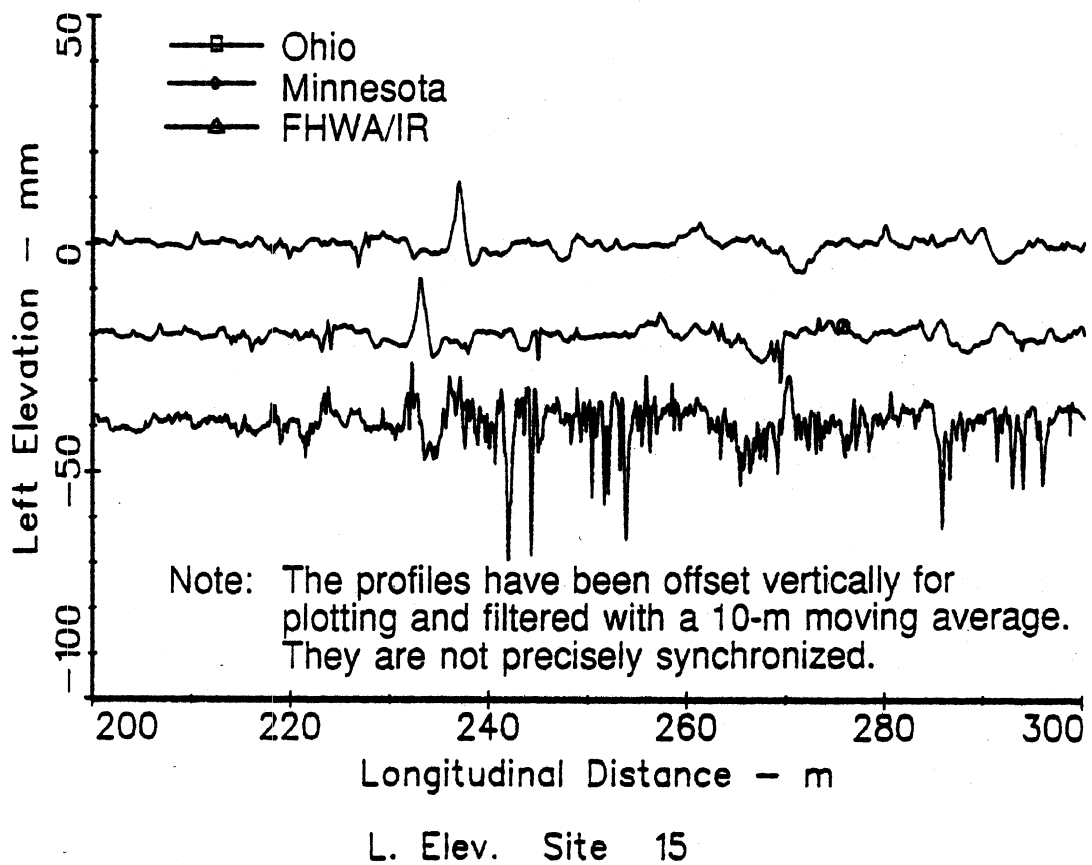
Figure 26. Invalid profile measured with the IR system on a rough, patched surface.

GMPG Sites

□ FHWA/IR @ 32 km/h
o FHWA/IR @ 56 km/h
△ FHWA/IR @ 80 km/h

IRI — m/km

Rod & Level — m/km

All Road Sites

□ FHWA/IR @ 32 km/h
o FHWA/IR @ 56 km/h
△ FHWA/IR @ 80 km/h

Site 15

IRI — m/km

Reference — m/km

□ FHWA/IR @ 32 km/h
o FHWA/IR @ 56 km/h
△ FHWA/IR @ 80 km/h

MO Index — m/km

Rod & Level — m/km

Texas RMSVA Index: MO

□ FHWA/IR @ 32 km/h
o FHWA/IR @ 56 km/h
△ FHWA/IR @ 80 km/h

Site 15

MO Index — m/km

Reference — m/km

Texas RMSVA Index: MO
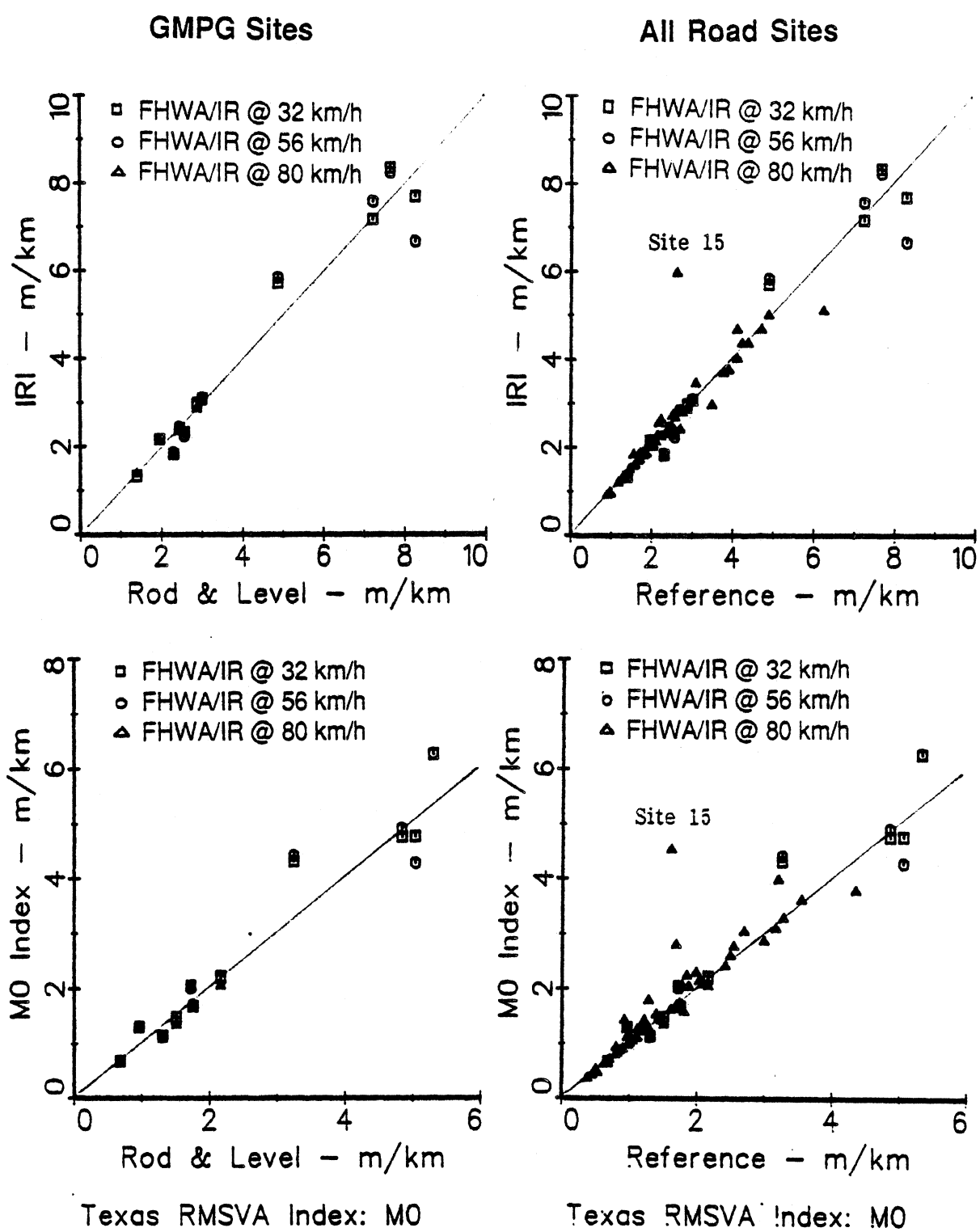
Figure 27. Measurement of IRI and MO with the IR system.

68

Waveband Indices

Figures 28 and 29 summarize the accuracy of the system, at three speeds, for a full range of 1-octave wavebands on the nine GMPG sites. The results for the 64-m waveband show that the IR system overresponds in several tests on the roughest sites, while agreeing fairly well in all other cases. The system shows good agreement on all sites for the wavebands centered at wavelengths of 32, 16, 8, and 4 m. For the wavebands centered at the shorter wavelengths of 2 and 1 m, the measures from the IR system are slightly lower than those from the rod and level on the roughest site, while agreeing well on the others. For the shortest wavelengths, centered at 0.5 m, the IR system is low on the two roughest sites, while agreeing with the rod and level on the others.

Power Spectral Density (PSD) Functions

The PSD plots that were obtained from this system matched those from the rod and level for all of the GMPG sites at all but the longest wavelength. On the rougher sites, the PSD amplitude was usually high for the longest wavelength (over 100 m) when the profilometer was used at the lowest speed of 32 km/h (20 mi/h). Figure 30 shows an example on a rough site, while figure 31 shows an example on a site of medium roughness. At the highest wavenumbers (shortest wavelengths), the effects of the antialiasing filters can be seen, as they cause the rolloff at wavenumbers above 3 cycle/m. Thus, as configured, the system appears to be accurate on all sites down to 1-m wavelengths, and on most of the sites, down to 0.6-m wavelengths. Because of the limited length of the sites at GMPG, it is not possible to ascertain the longest wavelengths that can be measured accurately with the system.

Additional PSD functions from the FHWA/IR system are shown in figures 69, 70, 78, and 79.

Conclusion

This profilometer is still under development, and only parts of the overall system were tested in the RPM, with promising results. The transducers, data acquisition system, and profile computation software proved to work as intended. The IR sensors actually gave results that were better than expected. Although the sensors are known to be sensitive to various factors that cause error, the antialiasing filters used in the data acquisition system seem to mitigate the problem. In most cases, the profiles that were obtained appeared to closely match the true profile for wavelengths covering 0.6 m to 100 m. Measures of IRI
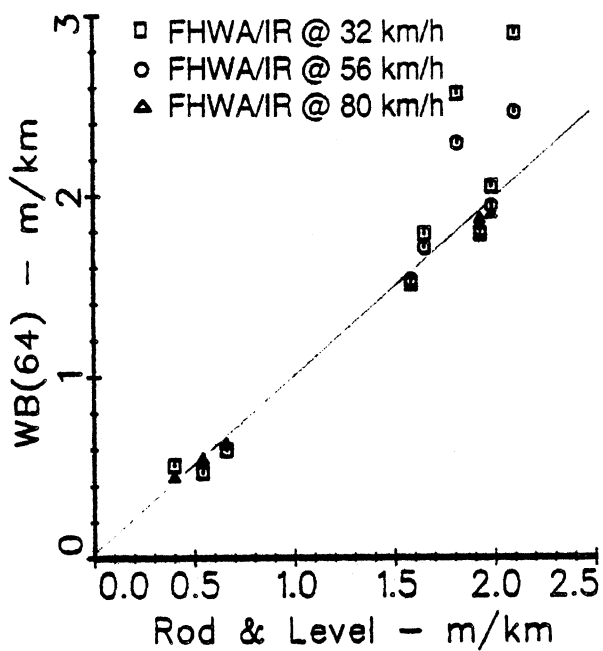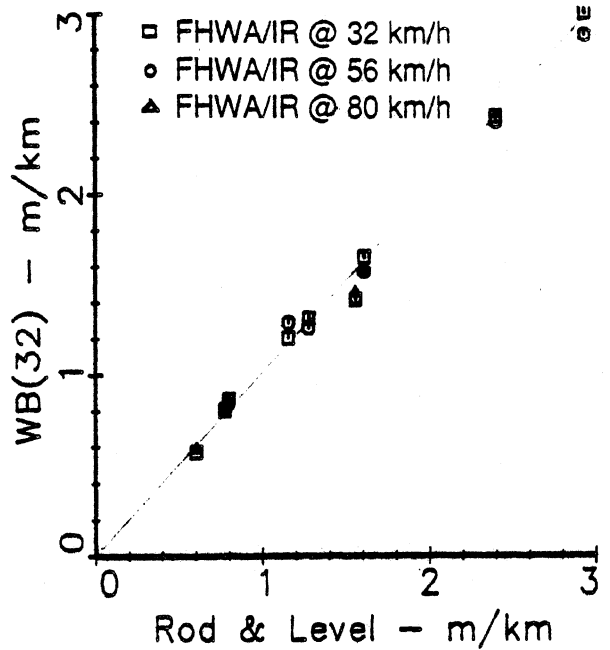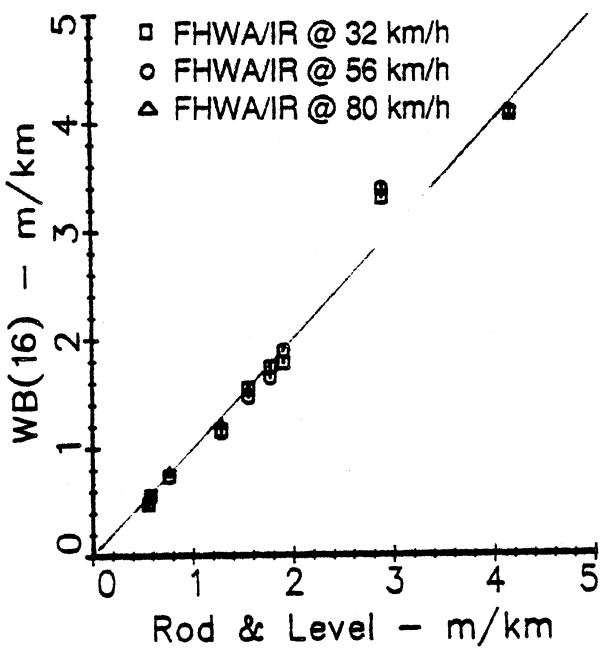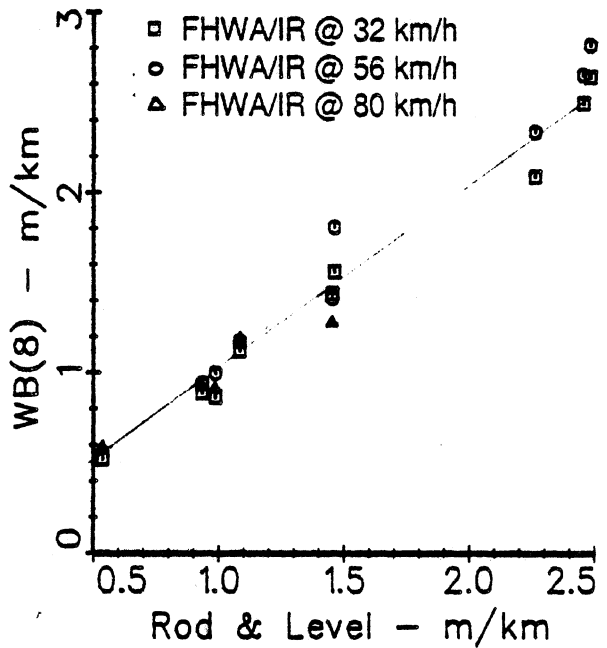
Figure 28. Measurement of waveband indices for the longer wavelengths with the IR system.
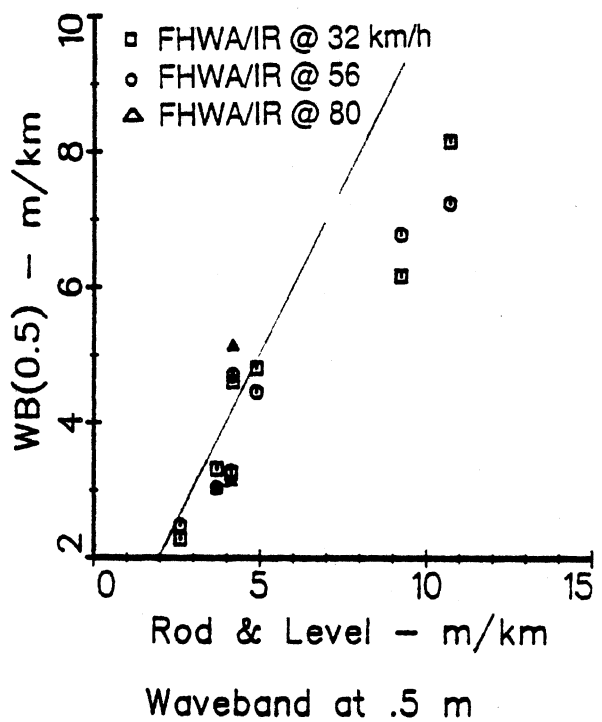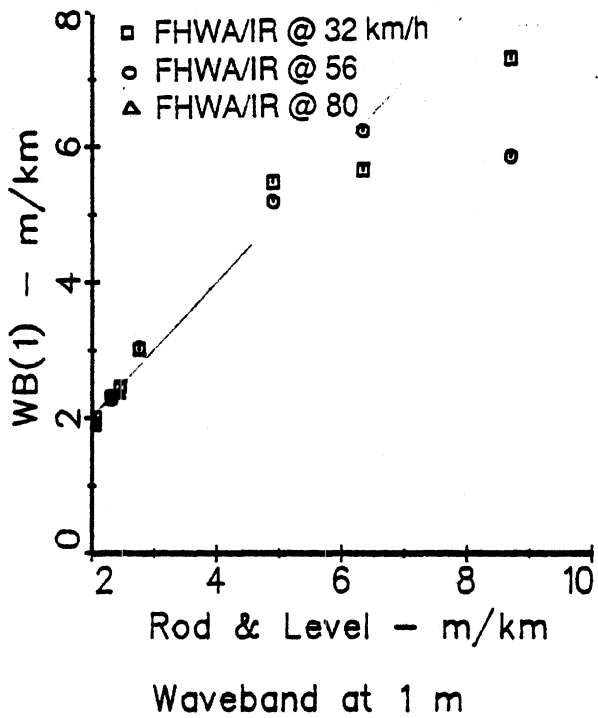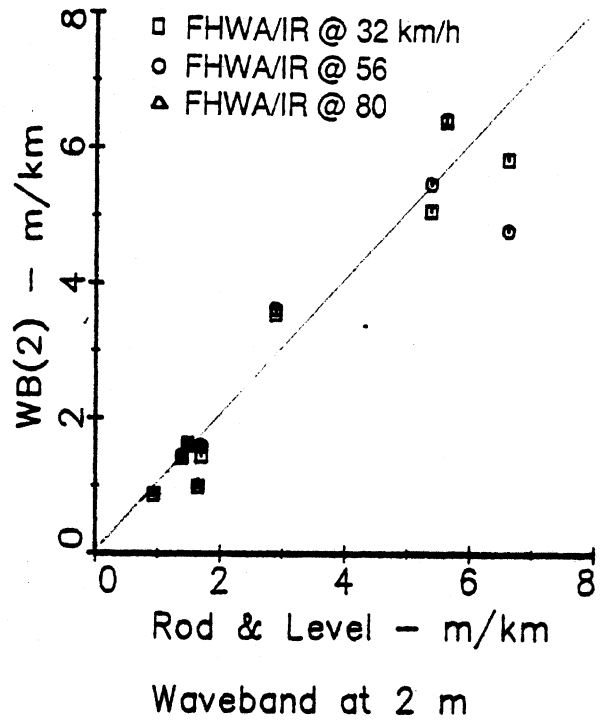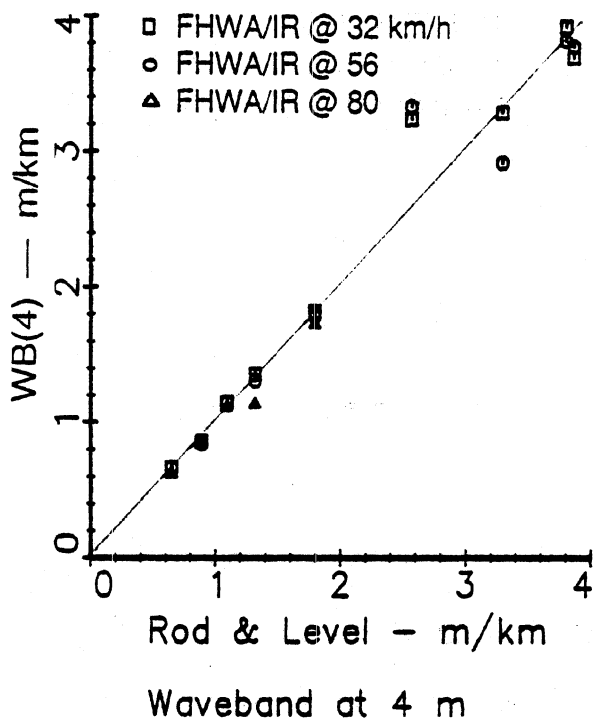
Figure 29. Measurement of waveband indices for the shorter wavelengths with the IR system.
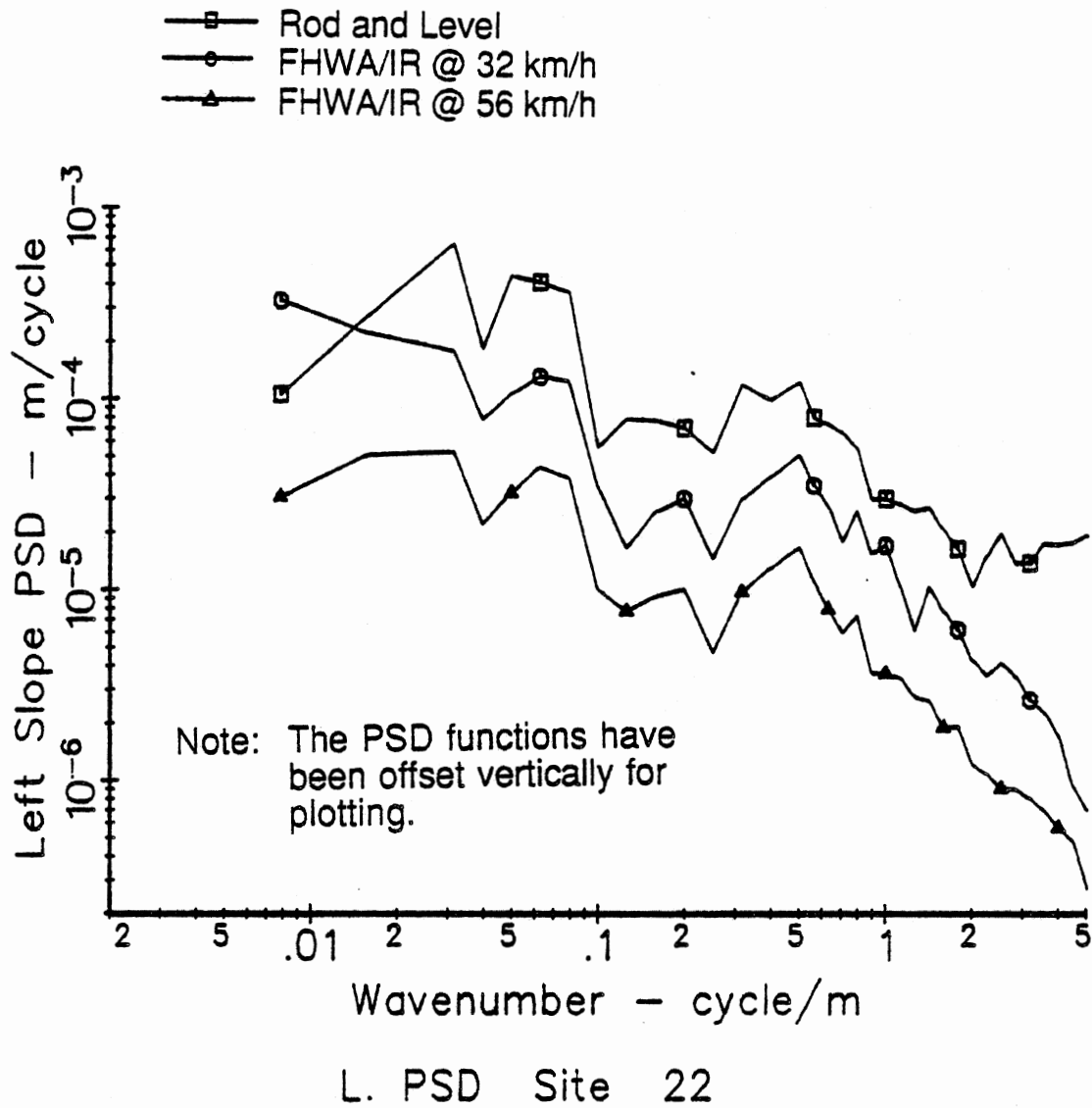
Figure 30. PSD functions from the IR system on a rough site.
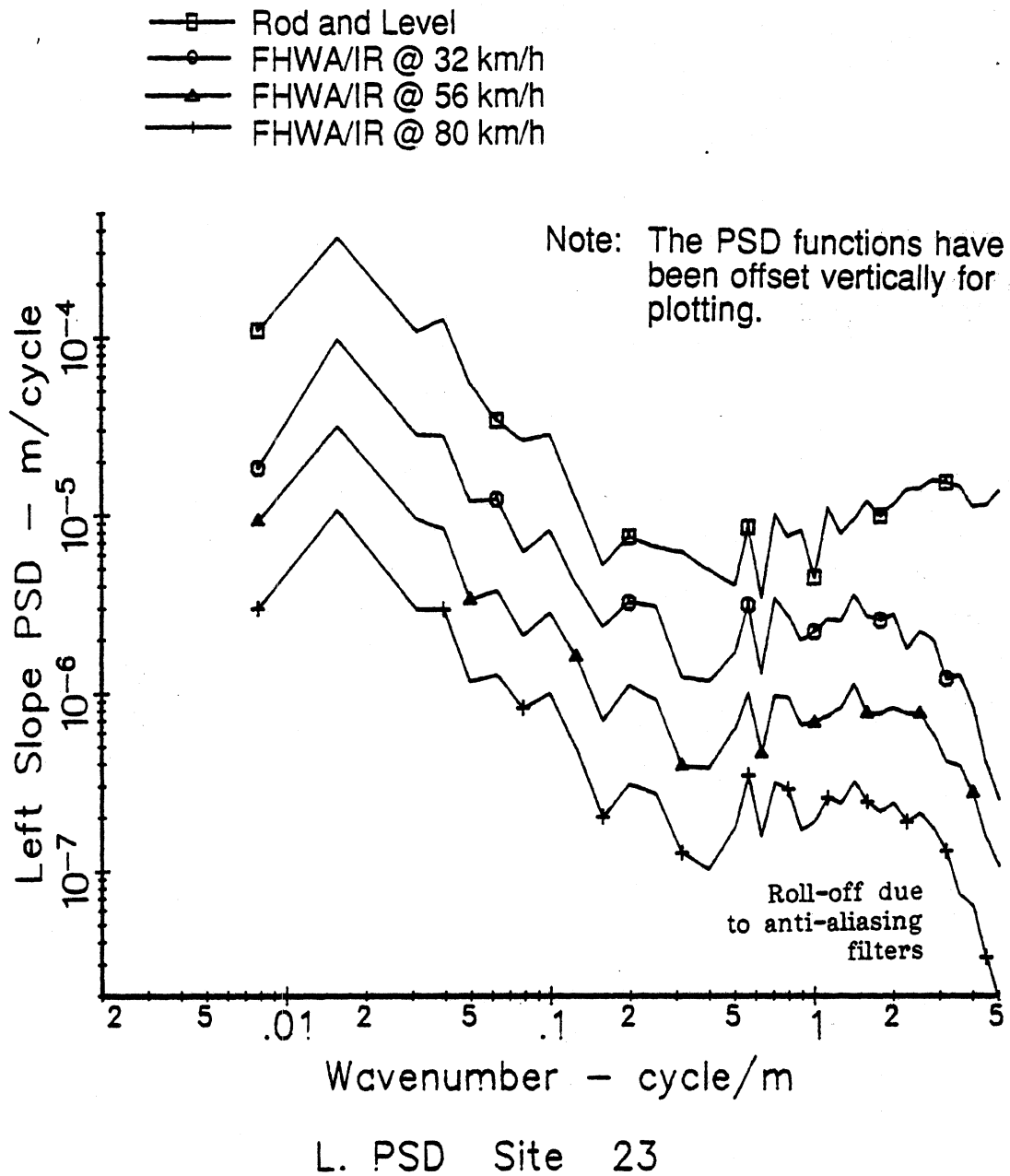
Figure 31. PSD functions from the IR system on a moderately rough site.

and MO closely matched the reference. The measures on the roughest sites were not valid due to a setting in the digitizer which will be corrected in the final version. One of the roughest sites that was measured caused large errors in the IR sensor, which possibly indicates that the sensor cannot be used for some types of surface.

FHWA Profilometer: Selcom Version

Hardware Description ·

The FHWA profilometer being developed by UMTRI was operated in two configurations, using two types of height sensors. The basic system with the infrared (IR) height sensor was described in the preceding subsection. Because of shortcomings in the IR sensors which could affect their adequacy, alternate sensors were obtained for testing. Noncontacting laser sensors marketed by a Swedish company under the name "Selcom" were selected, and units owned by the Federal Aviation Administration (FAA) were obtained on loan. Figure 32 shows one of these sensors. The Selcom works by triangulation, calculating height from the apparant position of a dot-image projected by laser onto the road surface. Tests of the FHWA profilometer with this height sensor are designated "Selcom."

The Selcom sensor consists of two components: (1) a transducer assembly (shown in the figure), which includes the laser, detector, and optics; and (2) a signal conditioning unit, which includes the power supply, digital/analog (D/A) converters, a microprocessor, and assorted filters. Several models are available for both the transducer and conditioning unit. The transducers loaned by FAA have a measuring range of 128 mm (5 inches) and a specified resolution of 0.03 mm. Other models are available with different ranges. The signal conditioner included the basic receiver board, which measures and updates the height digitally at a frequency of 16,000 Hz, and continuously converts these numbers to a voltage, electronically filtered to remove frequencies above 2000 Hz. Other boards are made by Selcom that have additional features. One, the Receiver-Averaging board, includes a feature to detect and reduce the impact of signal dropout. If the dot projected on the surface disappears from view, the signal may go to its limit, producing a large amplitude "glitch" in the indicated height. During this condition, the Receiver-Averaging board holds the last value, whereas the basic receiver board available during this study does not. For profilometer applications the Receiver-Averaging board might be a preferable choice.
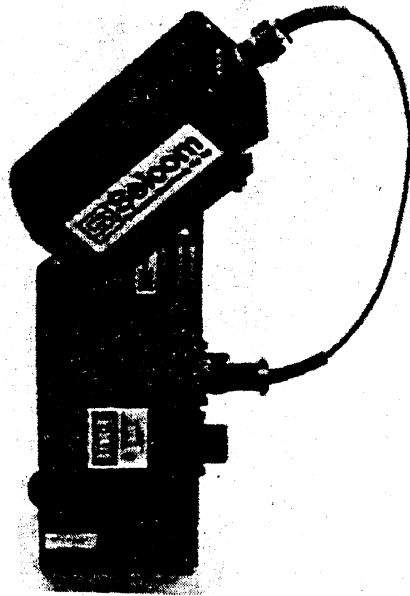
Figure 32. The Selcom laser height sensor.

In the FHWA profilometer, both the IR sensor and the Selcom are treated as generic height sensors, assumed to provide a voltage output that is linearly proportional to height. Thus, the Selcom and IR profilometer systems are identical in every detail other than the height sensors and the calibration data (electrical gains and offsets) associated with the sensors.

Profile Plots

The FHWA systems were configured with less filtering of long wavelengths than any of the other GM-type profilometers. The good response at the longest wavelengths means that this profilometer provides one of the best matches with rod and level for preparing profile plots with the fullest level of detail, as was illustrated in figure 23 in the preceding sub-section. Figure 33 shows that the system also did very well in handling the manhole cover on site 2.

Site 10 was on a highway with a good PCC surface that was textured with lateral grooves. The ability of the Selcom system to measure on the grooved surface is demonstrated in the profiles of figure 34. The figure also illustrates a characteristic of the laser height sensor which should be taken into account when using the sensor to measure profile. The laser image is small enough to detect cracks in the surface. This can be seen in figure 34 by the small downward spikes occurring at intervals in the Selcom profile. These are cracks picked up with the Selcom that were not sensed with all of the other systems. In the case of the Selcom sensor, the measures are made at such a high frequency (16,000 samples/sec) that it is inevitable that the cracks will be picked up. Without antialiasing filters, it would be a hit-or-miss proposition if the reading corresponding to the crack happens to be recorded or skipped. With antialiasing filters, as used in the UMTRI design, texture and small-amplitude cracks will be smoothed away. However, the deep cracks will not be completely eliminated, and will still appear in the profile, as shown in the figure. The implications of having profilometers that respond to cracks are discussed later in the "Conclusions" section of this report.

For the Selcom system, it is possible that the sensitivity to cracks might be eliminated simply by selecting a different configuration for the processing unit, replacing the receiving board installed on the borrowed unit with a Receiving-Averaging board.

Site 24 at the GMPG was found to challenge the Selcom sensor. Figure 35 compares the profile measured with the Selcom system (at three speeds) with the rod and level reference. The Selcom profiles include the true profile shape (as filtered with a 10-m moving average in the figure), but also include an apparent "texture" not present in the
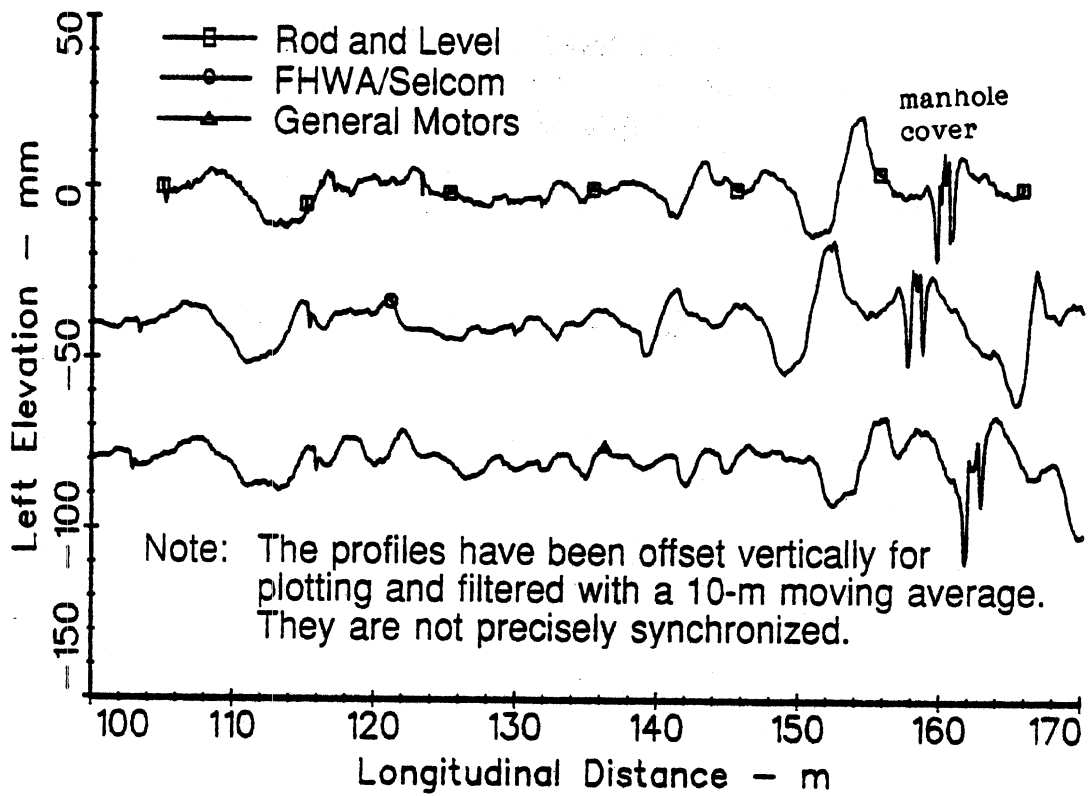
Figure 33. Comparison of two laser profilometers on a rough site that includes a manhole cover.
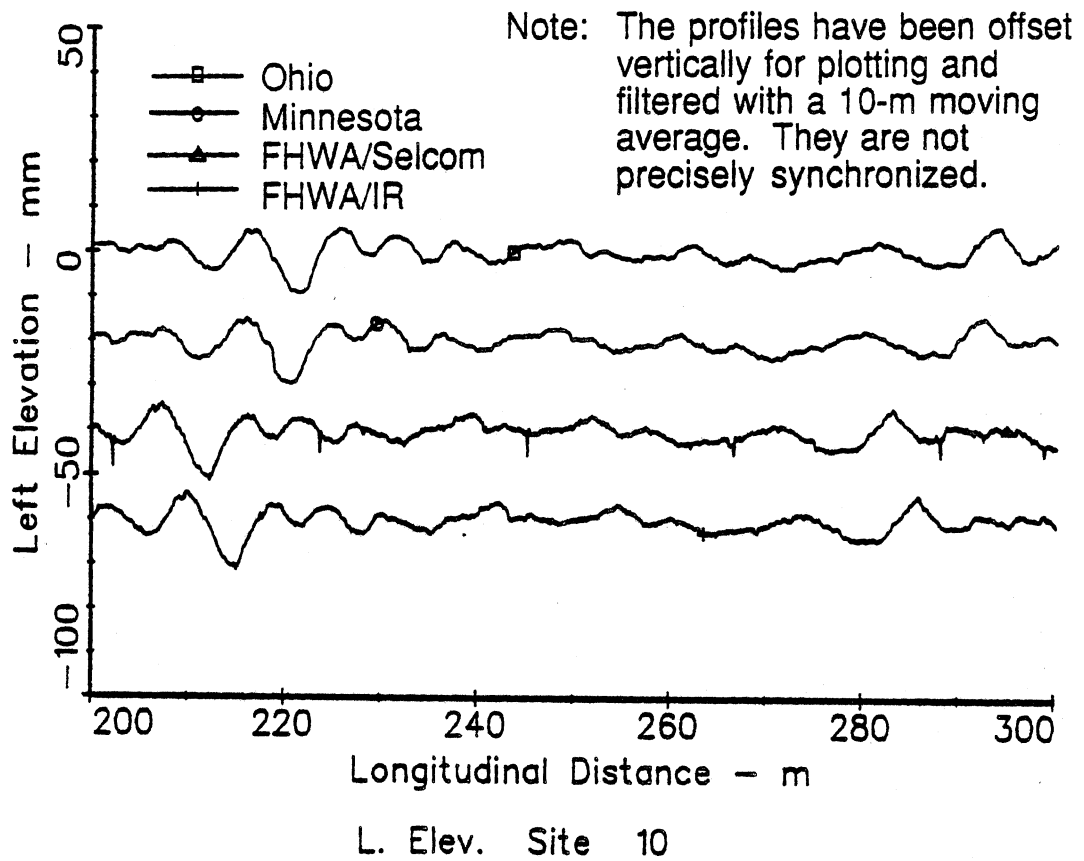
Figure 34. Comparison of several profilometers on a PCC site with lateral grooves.
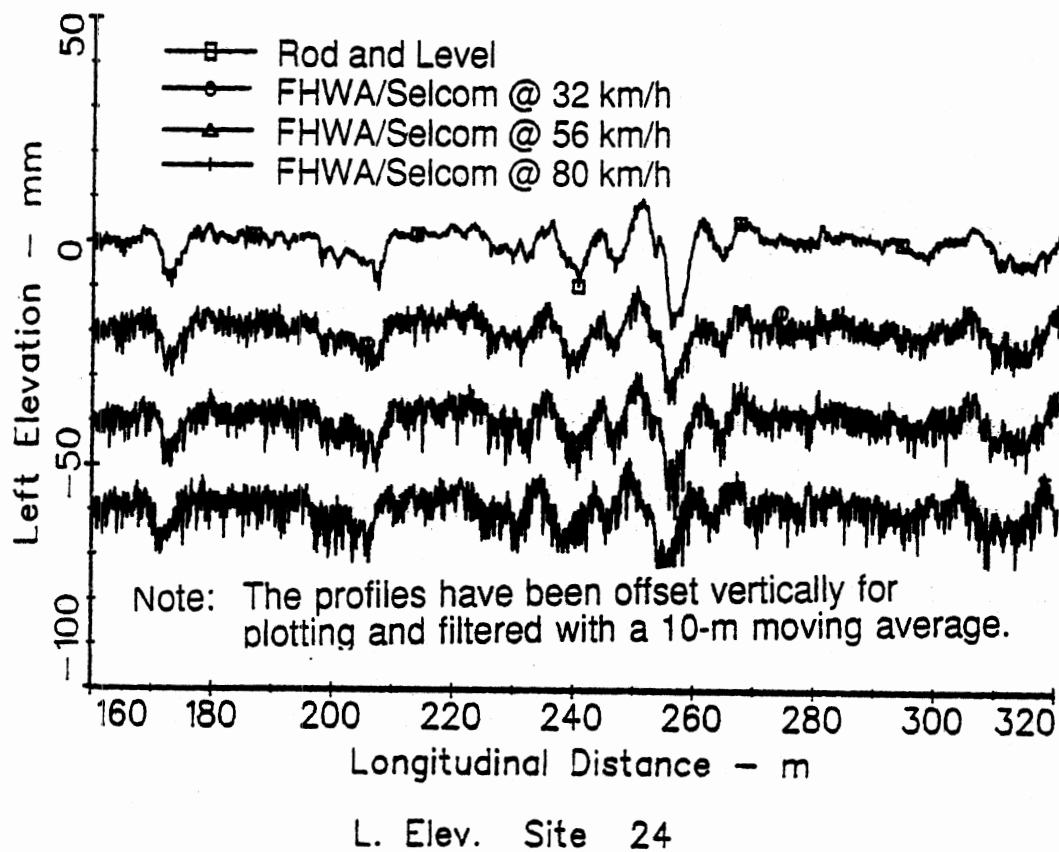
Figure 35. Invalid profile measures from the FHWA/Selcom system on an unusually textured surface.

actual profile. Figure 36 shows a small section of the same site, enlarged to show the character of the "texture" in the Selcom measures. This site was surfaced with an aggregate consisting of white stones, approximately 25 mm in diameter, embedded in black asphalt. Although the site definitely has an unusual texture, the "texture" produced by the Selcom appears to be dominated by some type of measurement error. Since it is relatively small in amplitude and high in frequency, it only affects the roughness measures that include short wavelengths. If the source of the problem is dropout in the signal, there is the possibility that the Selcom averaging board could reduce or eliminate the error.

As table 4 in the "Experiment" section shows, several of the runs had to be rejected because of a digitizing problem. More specifically, the vehicle accelerations were larger than anticipated with the result that the accelerometer signals saturated the digitizer. This problem is easily fixed by setting a slightly broader digitizing range. Unlike the IR sensor, which is known to become nonlinear at higher amplitudes, the Selcom is linear well beyond the range covered in the testing. Thus, it is possible that the valid roughness range of the overall system can be extended by properly setting the digitizer range.

Additional profile plots from the FHWA/Selcom system are shown in figures 23 and 24.

Measurement of Roughness Indices

Figure 37 shows how the IRI and MO roughness measures obtained from the Selcom system compare with the reference. The plots show that the IRI measures from the Selcom system are extremely accurate on most of the sites, but that several of the measurements include a significant error. The site at GMPG that proved troublesome for the Selcom was identified as site 24, described above and shown in figures 35 and 36.

The accuracy obtained with the MO analysis is not as good. The plots show that the measures from the Selcom system are biased, tending to be somewhat higher than the reference on the average. The random error (scatter) is also greater, in general, than for the IRI. Even though it is visible, the bias is small relative to the random error, and therefore it might be acceptable for some uses that might be made of the data.

Waveband Indices

Figures 38 and 39 summarize the accuracy of the system, at three speeds, for a full range of 1-octave wavebands on the nine GMPG sites. For a GM-type of profilometer

Note: The profiles have been offset vertically for plotting and filtered with a 10-m moving average.
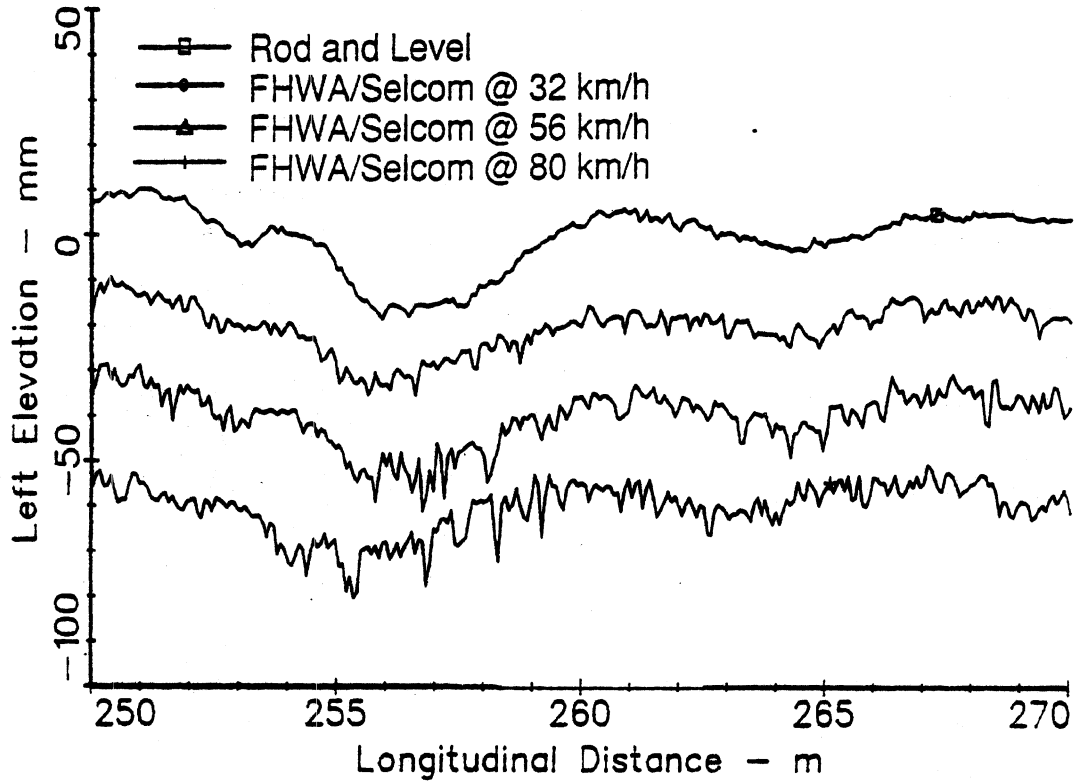
Figure 36. Detailed view of invalid profile measures from the FHWA/Selcom system on an unusually textured surface.

GMPG Sites

- □ FHWA/Sel @ 32 km/h
- ○ FHWA/Sel @ 56 km/h
- ▲ FHWA/Sel @ 80 km/h

Site 24

IRI — m/km

Rod & Level — m/km

IRI (1/4 car index)

All Road Sites

- □ FHWA/Sel @ 32 km/h
- ○ FHWA/Sel @ 56 km/h
- ▲ FHWA/Sel @ 80 km/h

IRI — m/km

Reference — m/km

IRI (1/4 car index)

- □ FHWA/Sel @ 32 km/h
- ○ FHWA/Sel @ 56 km/h
- ▲ FHWA/Sel @ 80 km/h

Site 24

MO Index — m/km

Rod & Level — m/km

Texas RMSVA Index: MO

- □ FHWA/Sel @ 32 km/h
- ○ FHWA/Sel @ 56 km/h
- ▲ FHWA/Sel @ 80 km/h

MO Index — m/km

Reference — m/km

Texas RMSVA Index: MO
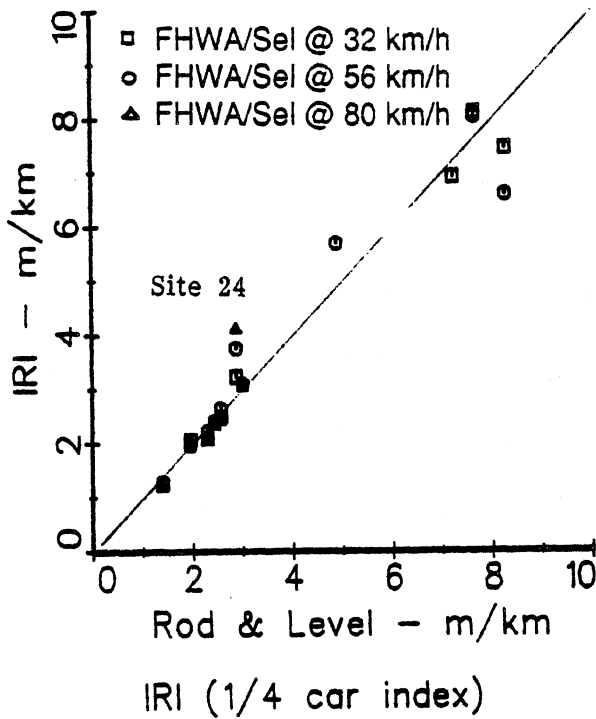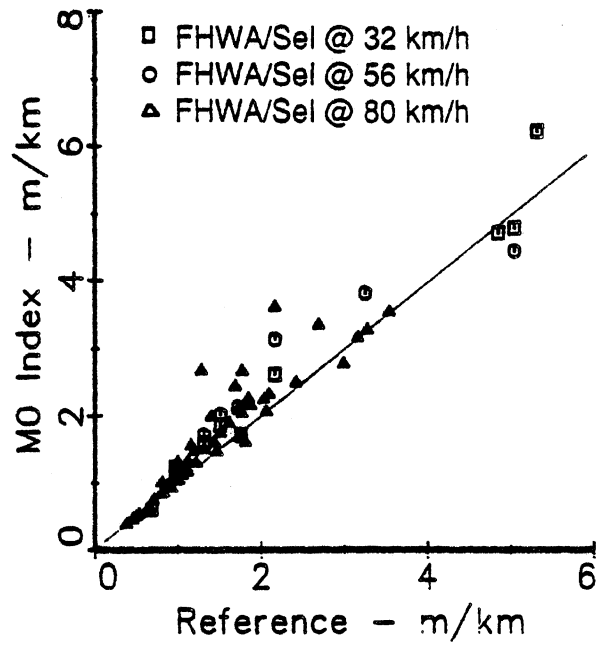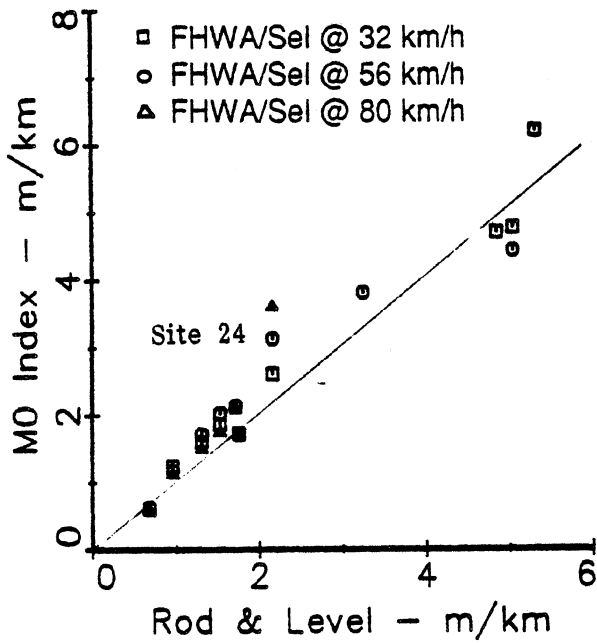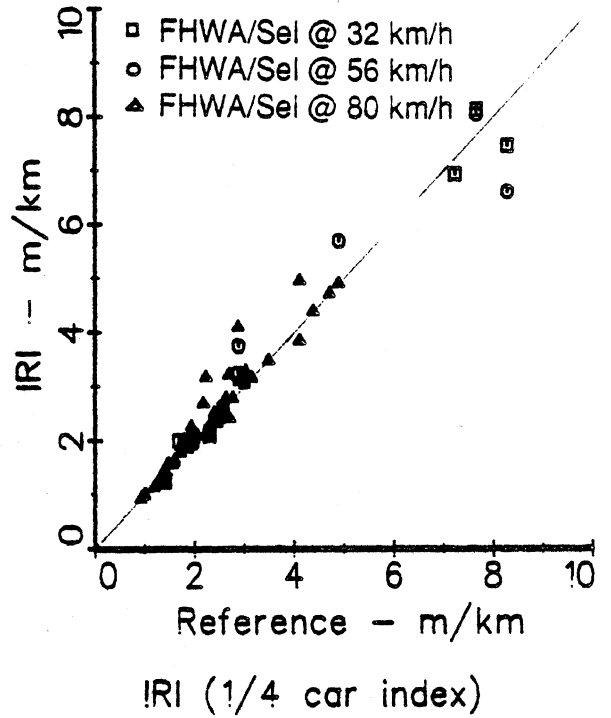
Figure 37. Measurement of IRI and MO with the FHWA/Selcom system.
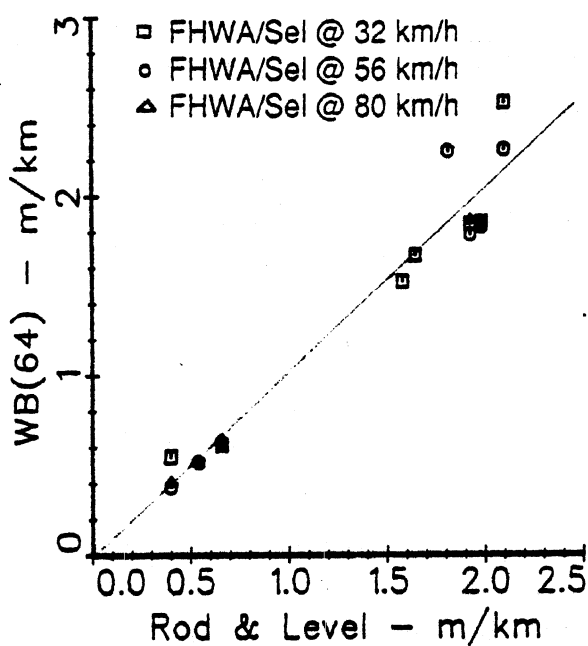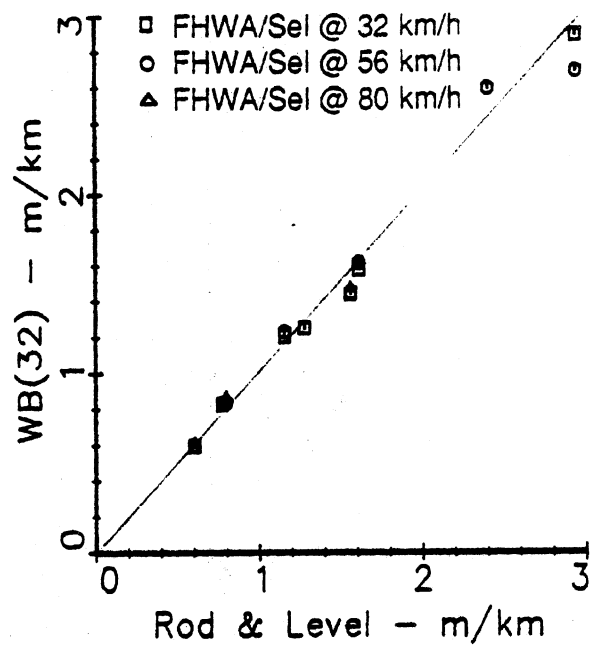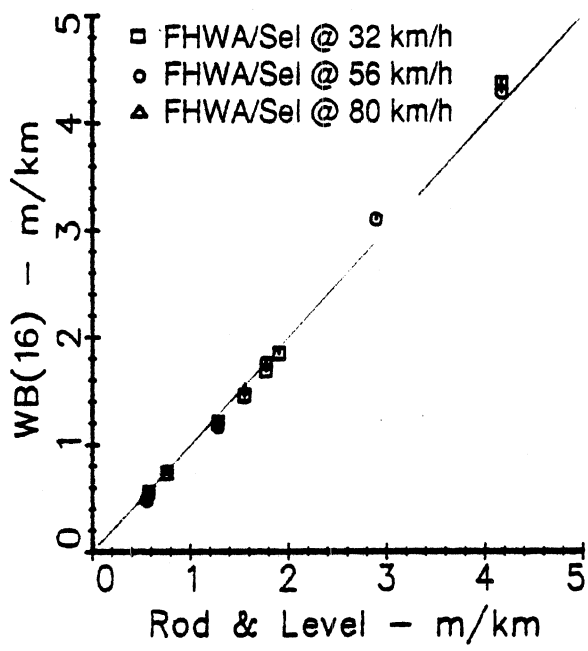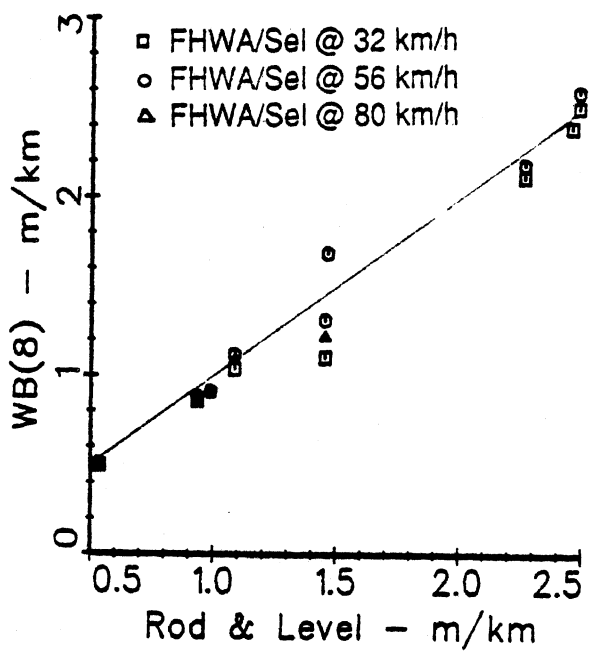
Figure 38. Measurement of waveband indices for the longer wavelengths with the FHWA/Selcom system.
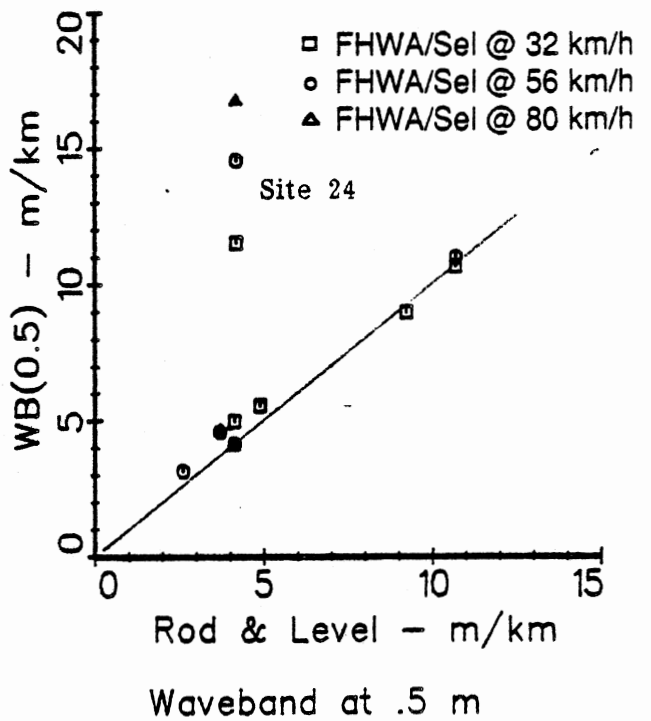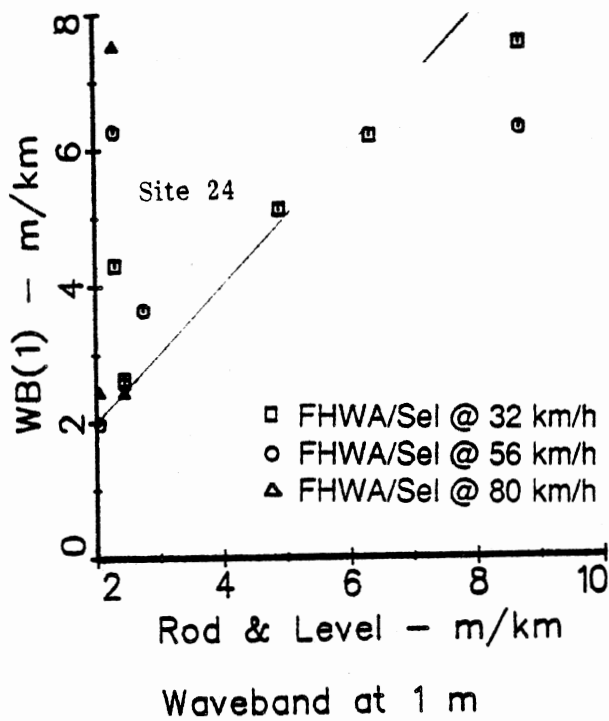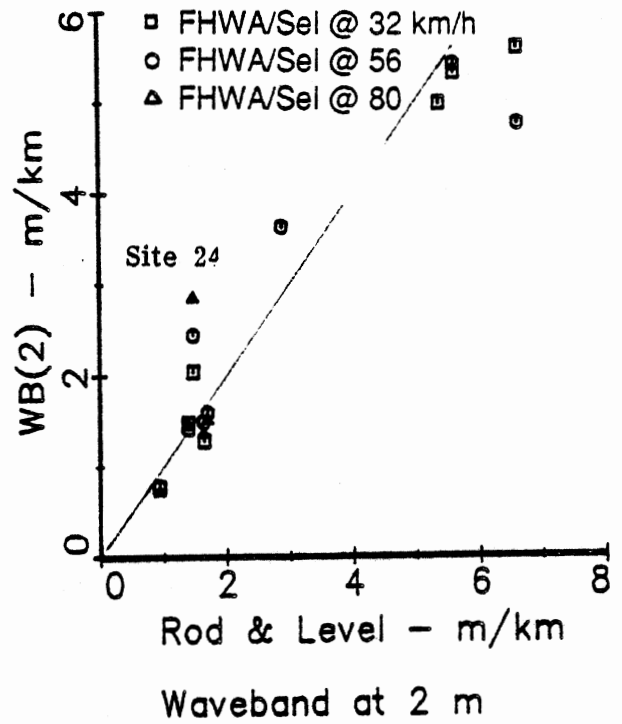
Figure 39. Measurement of waveband indices for the shorter wavelengths with the FHWA/Selcom system.

design, most of the long wavelength data come from the accelerometer signal, whereas the short wavelength data come from the height sensor. Since the IR and Selcom versions of the FHWA profilometer were identical with regard to the accelerometers, data acquisition, and profile computation, they should perform more or less the same for analyses involving the longer wavelengths. Indeed, figures 28 and 38 do show similar performance for the wavebands covering the longer wavelengths, although with slightly less error with the Selcom sensors.

The results for the 64-m waveband show that the Selcom system overresponds in several tests on the roughest sites, while agreeing fairly well in all other cases with the reference. The system shows good accuracy on all sites for the wavebands centered at wavelengths of 32, 16, 8, and 4 m. For the wavebands centered at the shorter wavelengths of 2, 1, and 0.5 m, the measures are accurate on all of the GMPG sites except for site 24 (see figures 35 and 36). The measures for site 24 are too high, with the error depending on both the waveband and the measurement speed. The error is seen to increase for the shorter wavelengths and the higher measurement speeds.

Power Spectral Density (PSD) Functions

The PSD plots that were obtained from this system agreed well with those from the rod and level for all of the GMPG sites at all but the longest wavelength. However, on the rougher sites, the PSD amplitude was usually high for the longest wavelength (over 100 m) when the profilometer was used at the lowest speed of 32 km/h (20 mi/h). Figure 40 shows example PSD plots on a site having moderate roughness. At the highest wavenumbers, up near 5 cycle/m (wavelengths near 0.2 m), the effects of the antialiasing filters can be seen in the attenuation of the PSD amplitude. Thus, as configured, the system appears to be accurate for wavelengths down to about 0.3 m. Because of the limited length of the sites at GMPG, it is not possible to ascertain the longest wavelengths that can be measured accurately with the system.

Additional PSD functions from the FHWA/Selcom system are shown in figures 69 and 70.

Conclusion

This profilometer is still under development, and only parts of the overall system were tested in the RPM, with promising results. The transducers, data acquisition system, and profile computation software proved to work as intended. The borrowed Selcom sensors

Note: The PSD functions have been offset vertically for plotting.
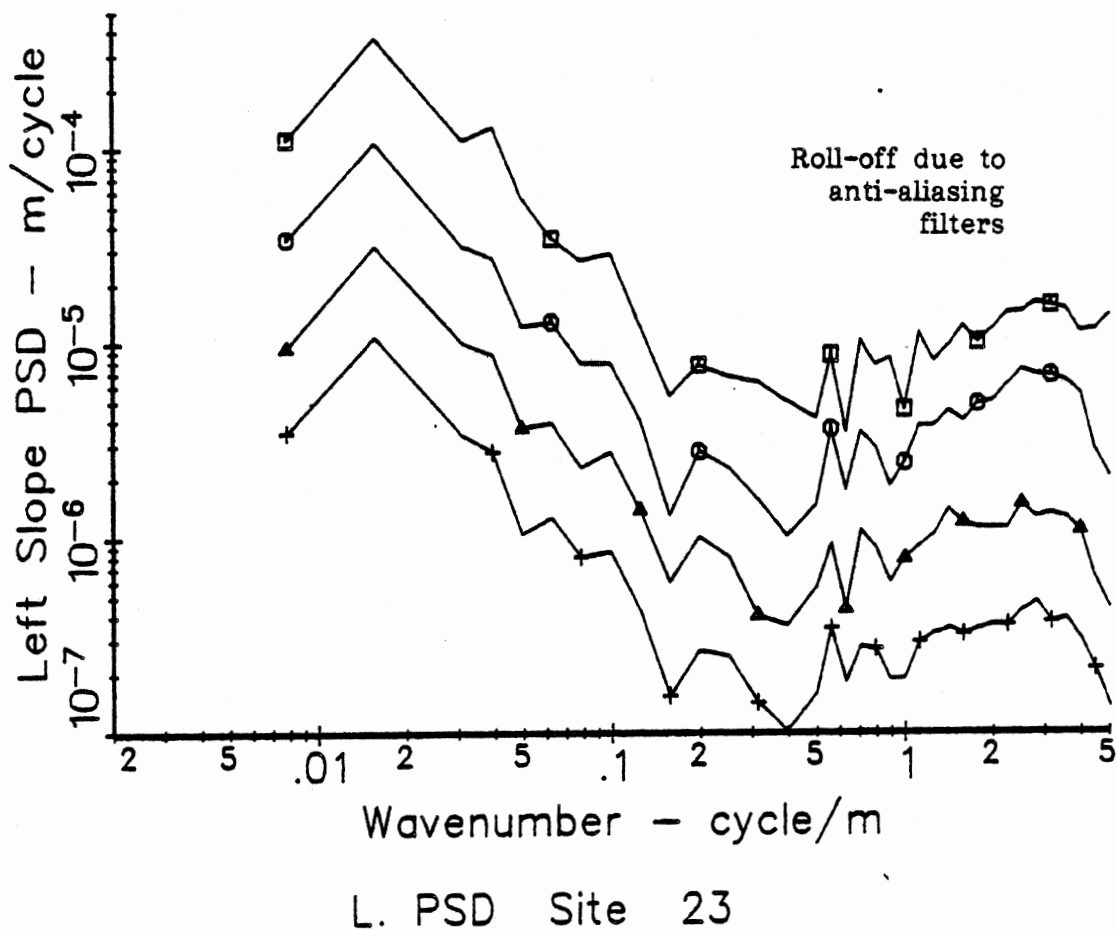
Figure 40. PSD functions from the FHWA/Selcom system on a moderately rough site.

86

were not configured with the Receiving-Averaging board that would be preferred for use in a profilometer, yet the sensors nevertheless performed well on all but one surface. In most cases, the profiles that were obtained appeared to closely match the true profile for wavelengths covering 0.3 m to 100 m. Measures of IRI and MO closely matched the reference. The measures on the roughest sites were not valid due to a setting in the digitizer which will be corrected in the final version. One site with unusual surface properties could not be measured, which indicates that the sensor cannot be used for certain types of surface in the configuration used. It is possible that the problem could be solved by a more appropriate configuration, but this would have to be demonstrated.

GMPG Profilometer

Hardware Description

The General Motors Corporation has long been associated with the concept of a high-speed profilometer starting with the original design by Spangler and Kelly at the General Motors Research Laboratory (GMRL).[1] GM has continued to own and maintain a profilometer since the invention, and all of the profilometers that participated in the RPM are based on the GM design, with the one exception of the APL trailer.

The GM-type profilometer consists of an instrumentation system installed in a vehicle, typically a van, which can be operated at normal highway speeds. The vertical motions of the vehicle body are sensed by an accelerometer, and double integrated to determine the vertical excursions as it travels down the road. The height of the vehicle body above the road is sensed by a road-follower system, and that height is subtracted from the body motion to obtain a profile. The first GM-type profilometer, developed and built by GM Research, used a mechanical follower wheel to sense vehicle height. The profile computations were performed with an analog computer.

The current GM profilometer, which participated in the RPM, was developed in the 1970's to upgrade the concept to use noncontacting height sensors and a digitally based instrumentation system.[17] The profilometer, shown in figure 41, is owned and maintained by the GM Proving Grounds (GMPG). Vehicle height is measured on each side with noncontacting laser height sensors built by the GMPG, and similar in concept to the commercial Selcom sensors. The laser image that is projected onto the pavement has dimensions of 1.5 mm (0.06 in) by 50 mm (2 inches), with the long dimensions oriented transverse to the direction of travel. The signals from the laser height sensors and
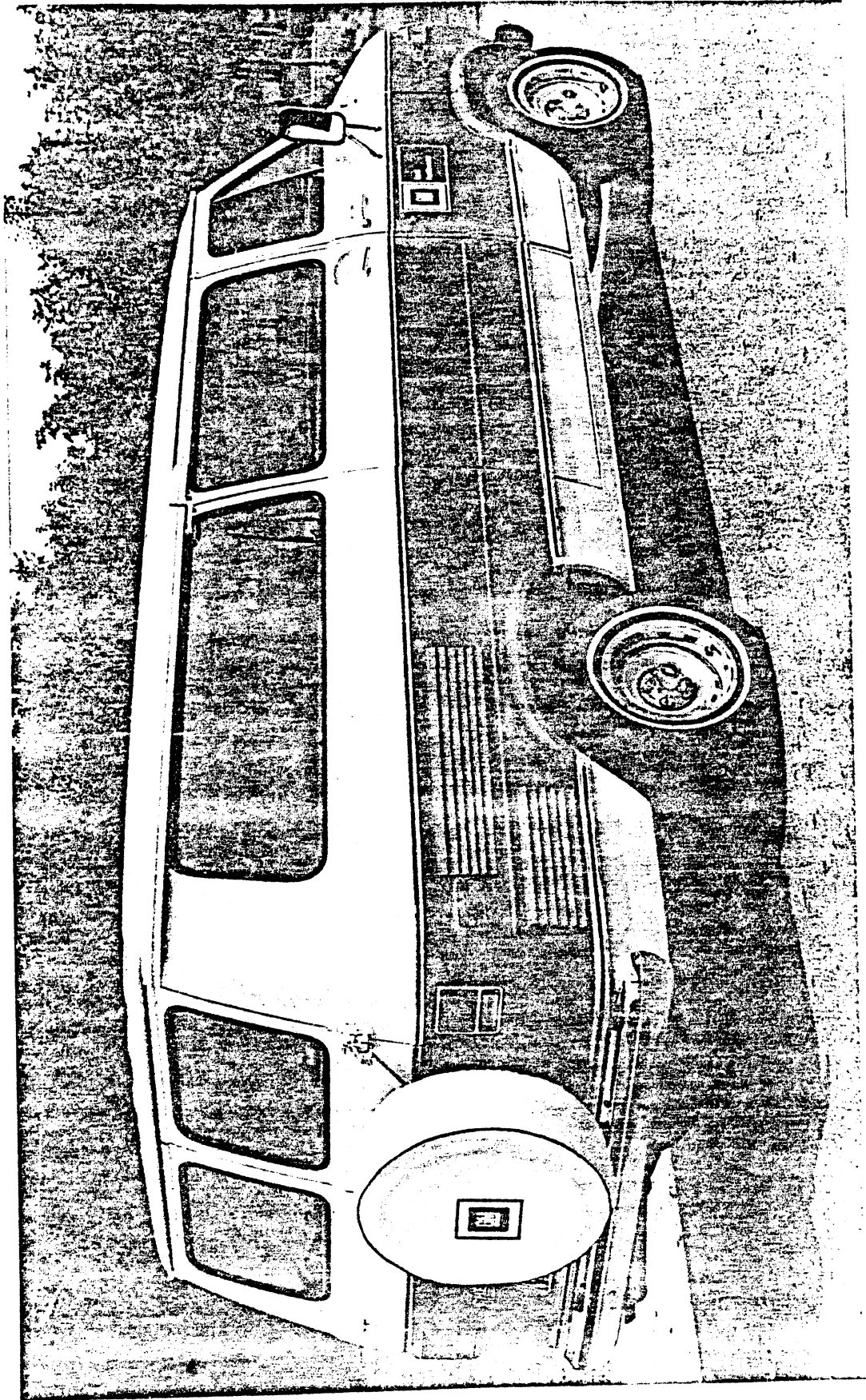
Figure 41. The General Motors Proving Grounds (GMPG) profilometer.

accelerometer are stored in digital form on magnetic tape, but are not processed to compute profile at the time of measurement. The profile computation is performed afterwards on a mainframe computer. A tape with the profiles was prepared by the data-processing staff at GMPG and delivered to UMTRI after the Meeting.

As shown by table 4 in the "Experiment" section, the GMPG system was operated at the three speeds of 24, 56, and 80 km/h (15, 35, and 50 mi/h). Three sample intervals were used: 9.17 mm (109 samples/m), at the speed of 24 km/h; 18.2 mm (55 samples/m) at 56 km/h; and 37.0 mm (27 samples/m) at 80 km/h.

Profile Plots

The profile plots obtained with the GMPG system never compared closely with the reference, even when identical filtering was applied to both measures. Figure 42 shows two plots from the GMPG system together with plots from two of the K.J. Law 690-DNC systems (Minnesota and Ohio) and the rod and level reference. In this figure, all profiles are filtered with a 10-m moving average. The figure shows that the GMPG system replicates some of the features approximately, such as the depression that occurs at a longitudinal distance of 255 m along the horizontal axis, while other features are distorted such that they are not recognizable. Figure 43 shows the measures for the same site when longer wavelengths are included. In this case, the filter was a 50-m moving average. Although the major profile features are replicated in the GMPG measures, there is still visible distortion.

The profile plots did not reveal any failures of the laser height sensor, even though many of the public road sites were selected because they had features that were thought might challenge this type of sensor design. In comparing the plots in figures 42 and 43 with those shown for the FHWA/Selcom system in figures 35 and 36, it can be seen that the texture of site 24 caused a high-frequency noise problem with the Selcom laser sensor, whereas the GMPG sensor performed as it is supposed to. One major difference between the GMPG and Selcom lasers is that the GMPG profilometer projects a wide image onto the surface, to make it less sensitive to small texture effects. Figure 44 shows the profile measured for a PCC site with lateral grooves. The GMPG system did not pick up extraneous noise due to the grooves, but, as with the other profiles, the basic profile shape only approximately matches the other systems.

This system was the only profilometer that proved capable of capturing the fine details of the railroad crossing on site 3, as shown in figure 45. Figure 33 also showed that the
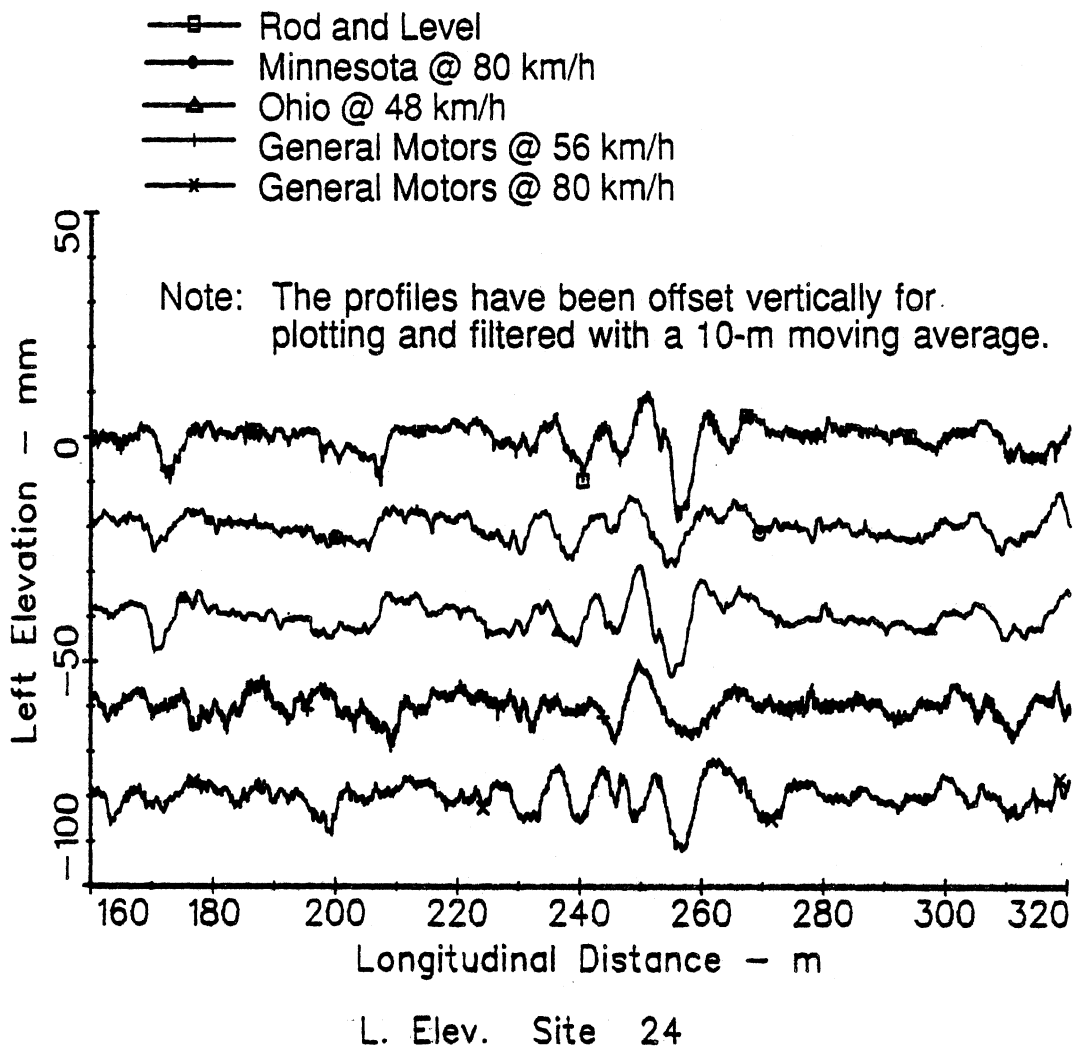
Figure 42. Profiles from the GMPG profilometer on a moderately rough site, looking at shorter wavelengths.
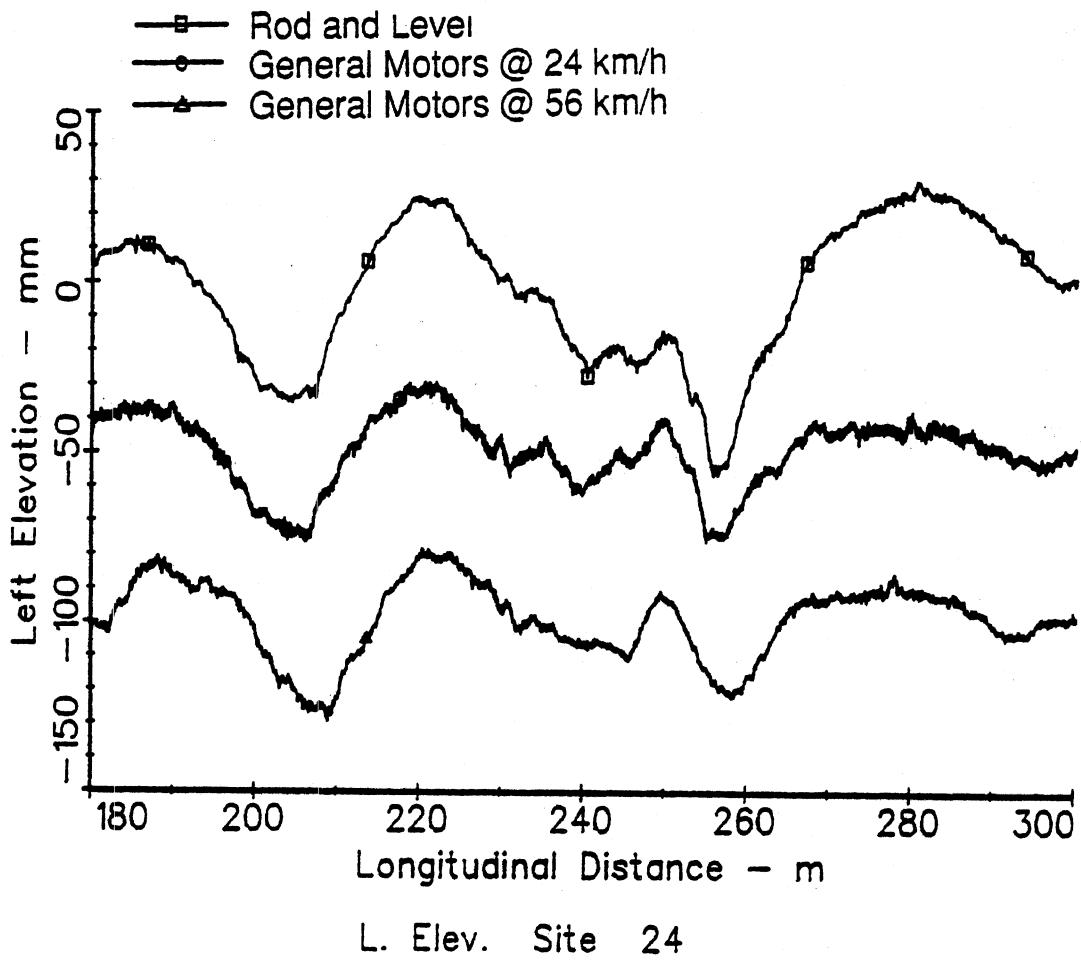
Figure 43. Profiles from the GMPG profilometer on a moderately rough site, looking at longer wavelengths.
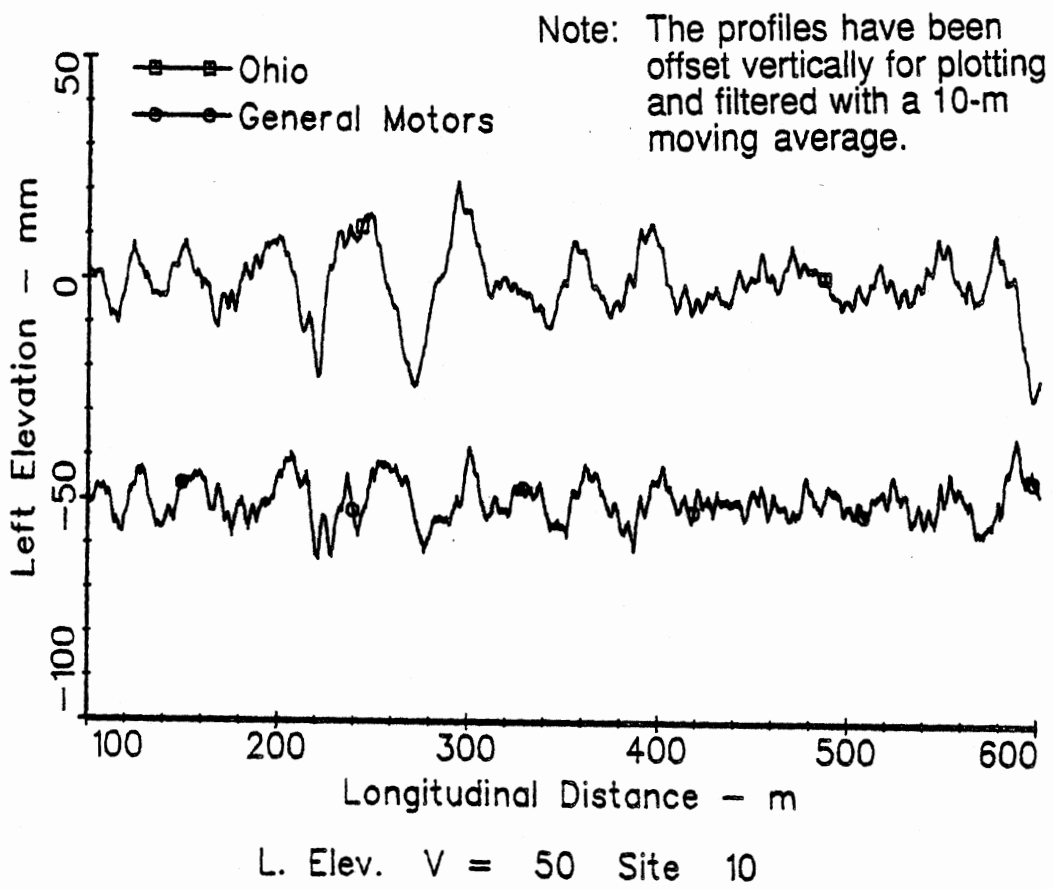
Figure 44. Comparison of two profilometers on a PCC site with lateral grooves.

92
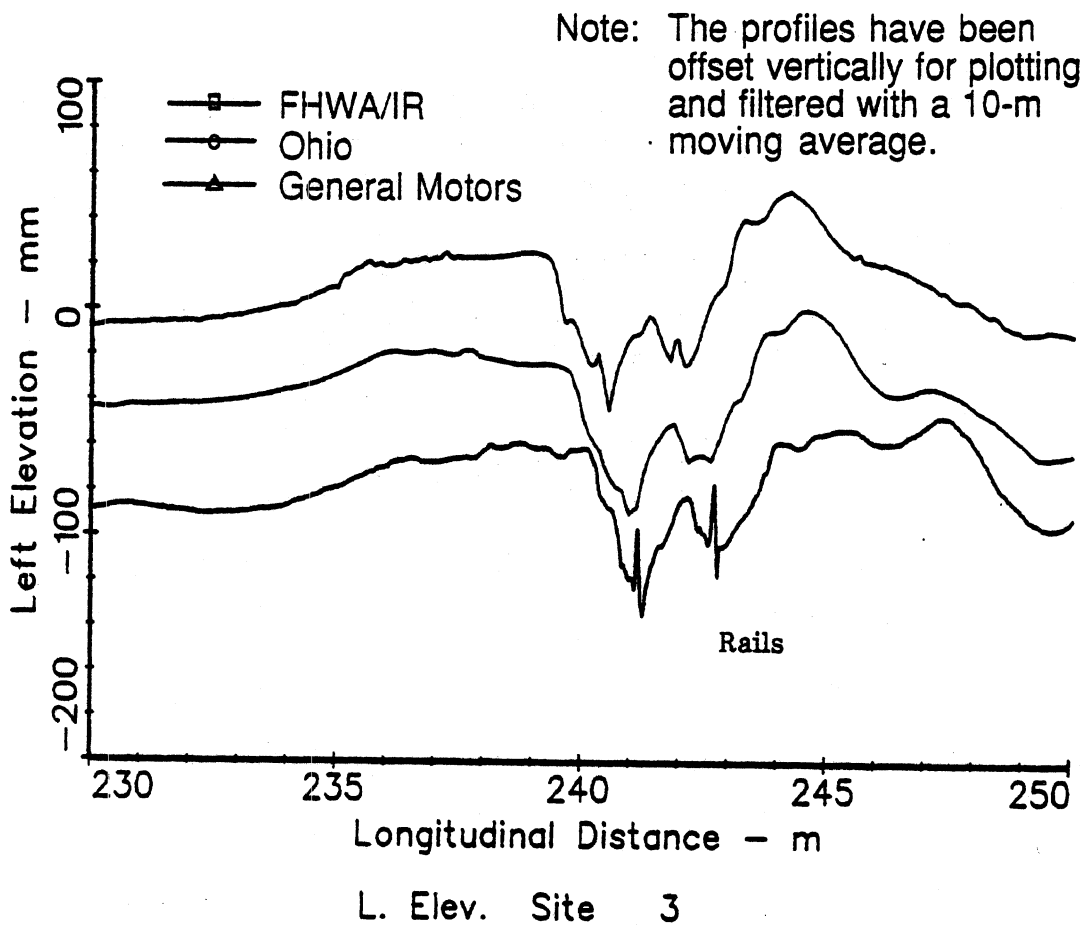
Figure 45. Comparison of several profilometers on a railroad crossing.

system picks up the details of the manhole cover, although the overall profile shape is distorted.

The GMPG profilometer is capable of detecting cracks in the pavement. Although some are smoothed by the antialiasing filters used when digitizing the data, the larger cracks are not eliminated. The implications of this are discussed in the "Conclusions" section of the report.

Many of the measures from this system did not start at the intended location. The starting position often differed by more than 50 m. Because the profiles did not visibly match the profiles from the other systems very well, it proved tedious and difficult to determine exactly where the GMPG measures began. Most of the profile data were not adjusted to correct for the error in starting location, and therefore the analyses performed with the GMPG profiles do not always cover exactly the same piece of road as measured by the other systems.

An additional profile plot from the GMPG profilometer is shown in figure 33.

Measurement of Roughness Indices

Figure 46 shows how the IRI and MO roughness indices computed from the GMPG profilometer compare with the reference. The data in the figure show that the system can measure both statistics without bias and with reasonable accuracy on most of the sites, but that very high measures of both statistics were obtained on one of the sites (site 21). The PSD functions for this site, that will be shown later, show that the profilometer over-responds to a particular waveband.

Waveband Indices

Figures 47 and 48 show how accurately the GMPG system measures RMS slope over 1-octave wavebands. For the wavebands centered at the longer wavelengths of 64 m and 32 m (see the top two plots in figure 47), the measures from the GMPG system tend to be too low. For the wavebands centered at 16 m, the measures from the GMPG match the rod and level reference quite well. For a GM-type of profilometer design, the response for all of these wavelengths originates almost completely from the accelerometer signal, and therefore the difference in the results for these wavebands is caused by the processing method used to handle the accelerometer measures. The figures show that, for the wavebands centered at wavelengths ranging from 0.5 to 16 m, the RMS slope measures

GMPG Sites

All Road Sites
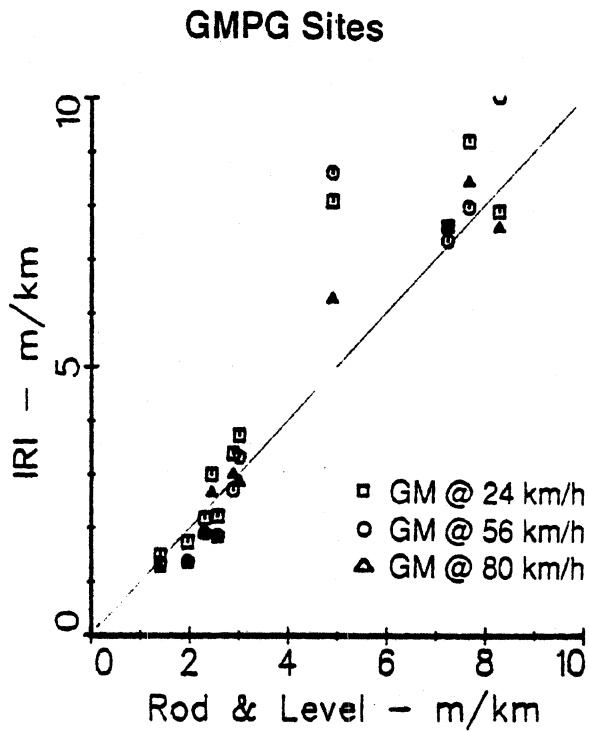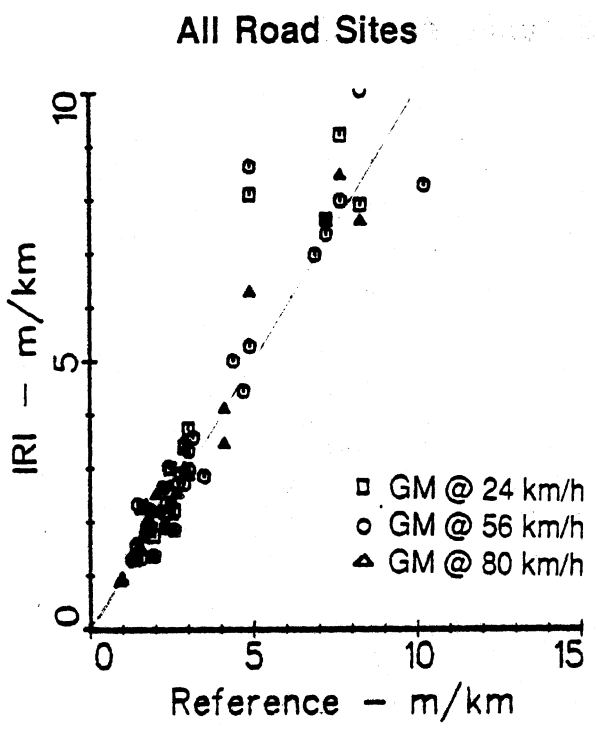
IRI (1/4 car index)

IRI (1/4 car index)
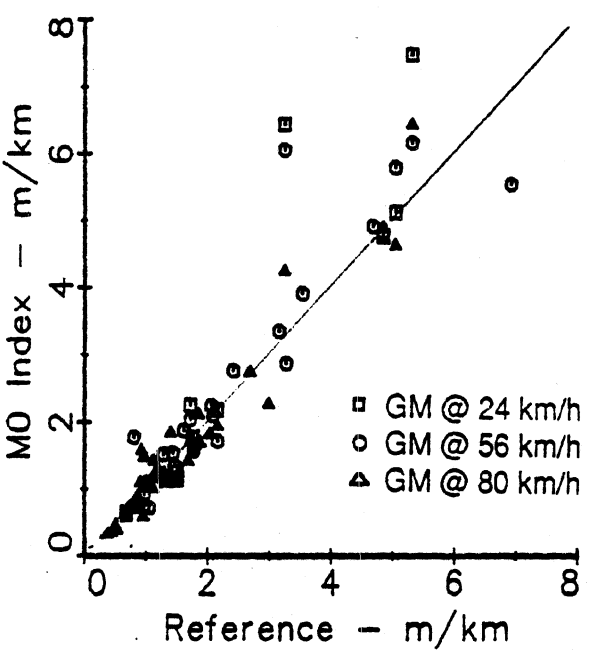
Texas RMSVA Index: MO
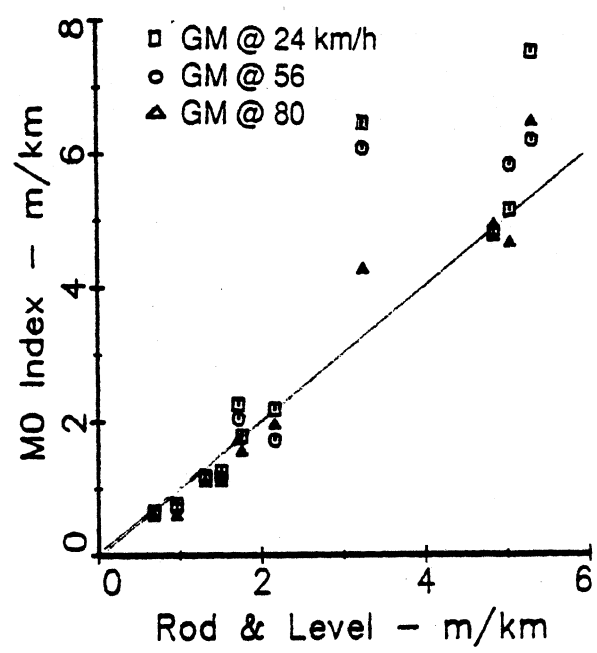
Texas RMSVA Index: MO

Figure 46. Measurement of IRI and MO with the GMPG profilometer.

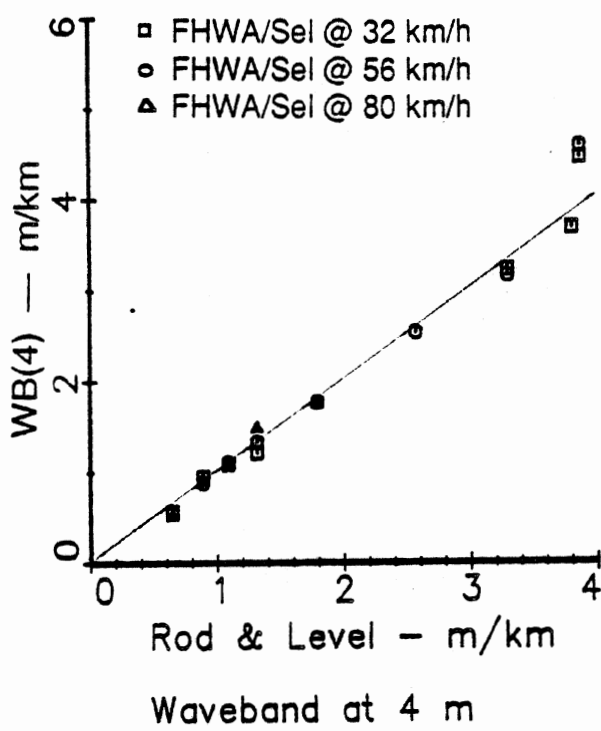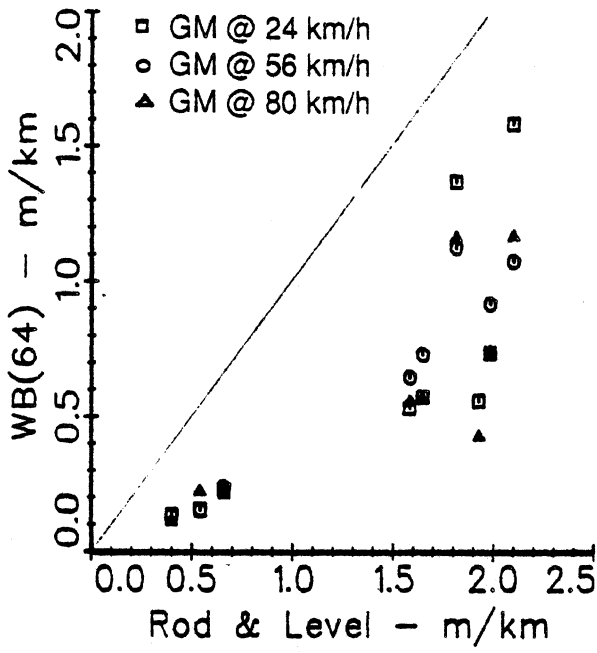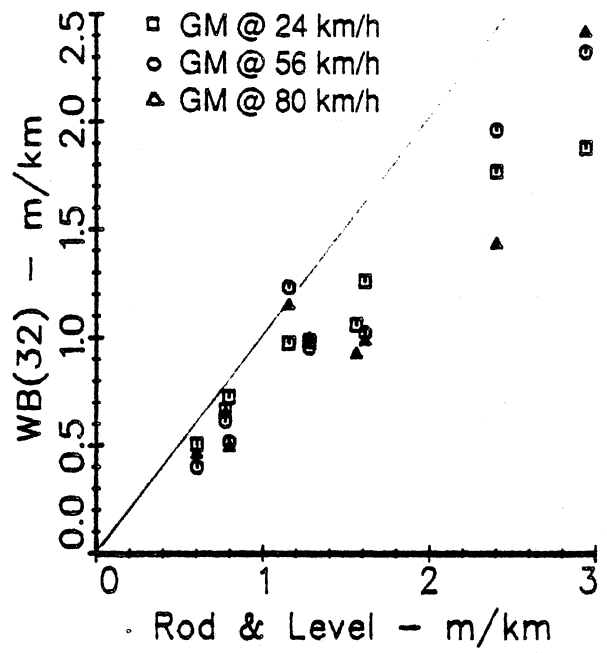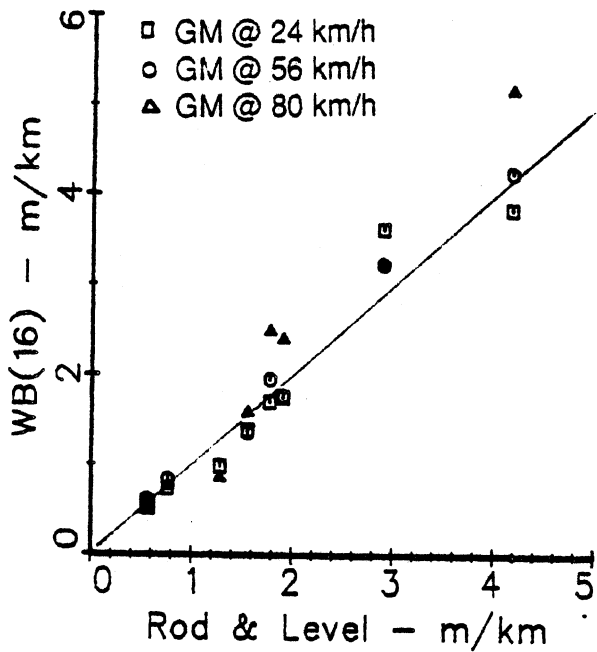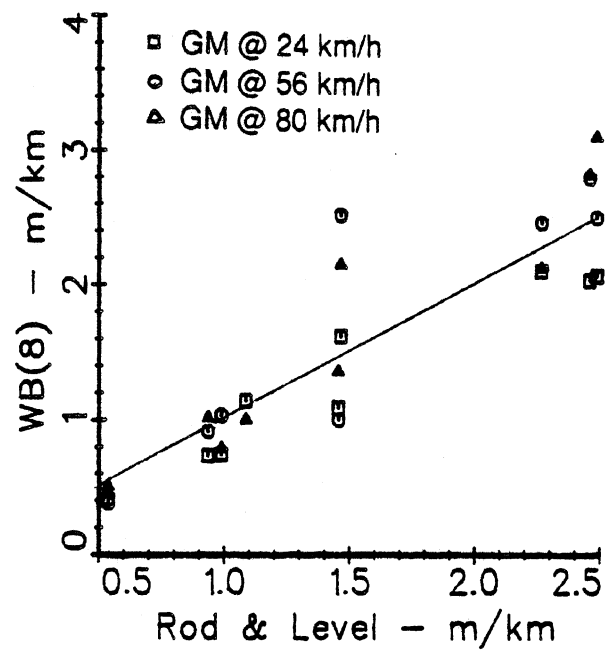Figure 47. Measurement of waveband indices for the longer wavelengths with the GMPG profilometer.
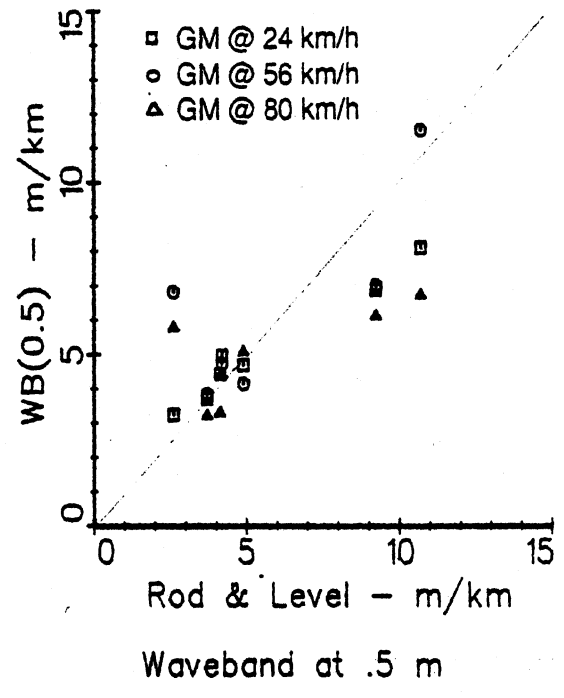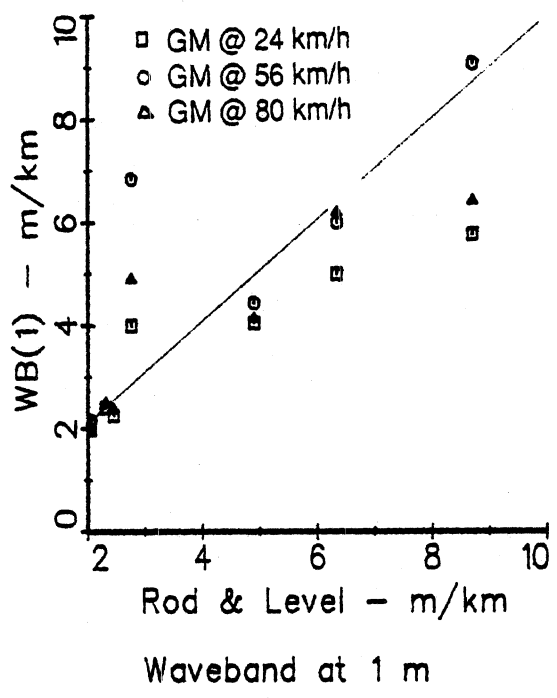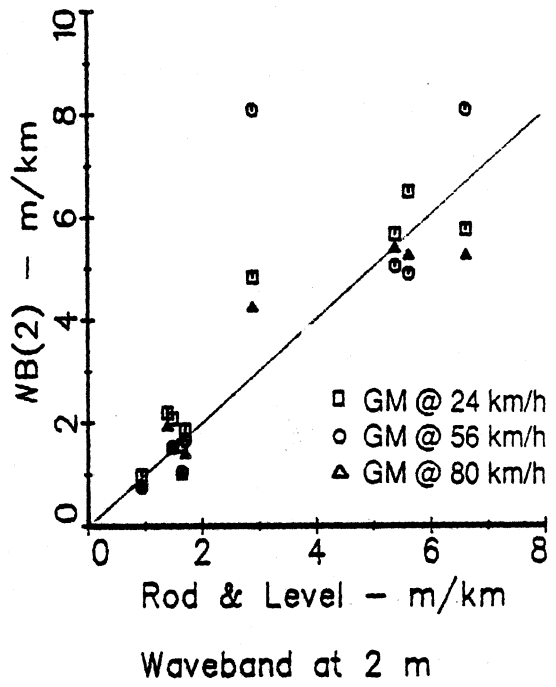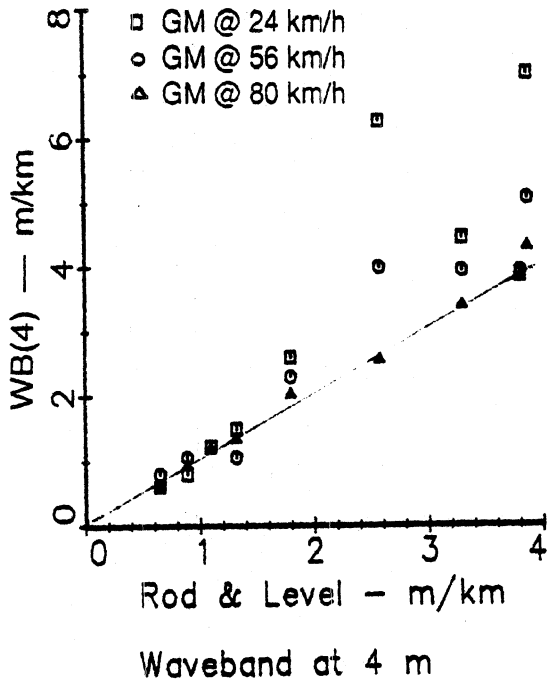
Figure 48. Measurement of waveband indices for the shorter wavelengths with the GMPG profilometer.

from the GMPG system approximately match the rod and level for most of the sites. For all of these wavebands except the 16 m, there are a few measures that show substantial error, usually by being much higher than the true value. The waveband measures that are in error are not common on a single site; thus, the profile measures on a particular site might be accurate for some wavebands but may be too high for others.

Power Spectral Density (PSD) Functions

The PSD plots from the GMPG sites indicate that the GMPG profilometer usually attenuates wavelengths longer than 30 m, and measures wavelengths down to a limit that is determined by the measurement speed. At 80 km/h (50 mi/h), wavelengths are measured without attenuation down to 0.5 m; at 56 km/h (35 mi/h), wavelengths are measured down to 0.3 m; and at 24 km/h (15 mi/h), wavelengths are measured at least to the limit of 0.2 m (the upper limit of wavenumber at 5 cycle/m used in the plots). Figure 49 shows the PSD functions for site 24, which was also the source of the data shown in figures 42 and 43. Over the wavenumber range of 0.05 to 2.0 cycle/m, the PSD from the 80-km/h run closely matches the rod and level. Yet, figures 42 and 43 show that the profile is fairly distorted. The PSD functions show that the correct amplitudes are measured over the entire waveband visible in the filtered profile plot, but they do not give any information about the phase relationships between the different wavelengths. One possible explanation for the difference in the GMPG profile plots is phase distortion in the computed profile.

Figure 49 also shows that the measure made at 24 km/h has amplitudes that are too high at the wavenumbers between 0.3 and 0.8 cycle/m (wavelengths between 1.2 and 3 m). At the same time, the amplitudes are somewhat low over the wavenumber range of 0.07 to 0.2 cycle/m (wavelengths between 5 and 14 m). Most of the PSD functions that were obtained were in error over some of the wavenumbers, sometimes being high and sometimes being low.

Figure 50 shows the PSD functions from the GMPG profilometer and the rod and level for one of the rougher sites (site 19). The agreement with the rod and level is typical for this system, and apparently unaffected by the high roughness level.

Figure 51 shows PSD functions from the GMPG profilometer that include a large error in amplitude at wavenumbers near 0.5 cycle/m (2-m wavelength). The runs made at 24 and 56 km/h (15 and 35 mi/h) show a large spectral peak, which is not seen in the rod and level reference, nor in the GMPG measurement made at 80 km/h (50 mi/h). In addition to the peak, the plots for 24 and 56 km/h also show erroneously high amplitudes for all wavenumbers greater than 0.1 cycle/m (wavelengths less than 10 m). The "outlier" data

Note: The PSD functions have been offset vertically for plotting.
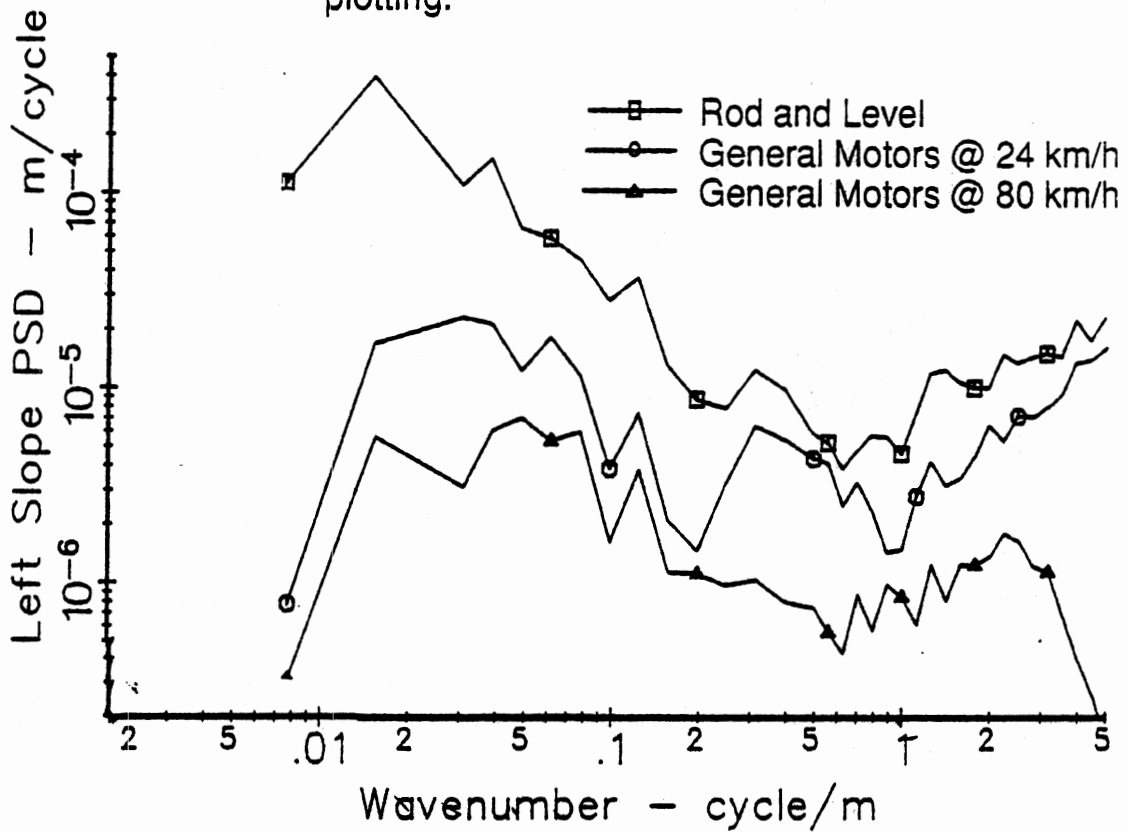
Figure 49. Typical PSD functions from the GMPG profilometer on a moderately rough site.
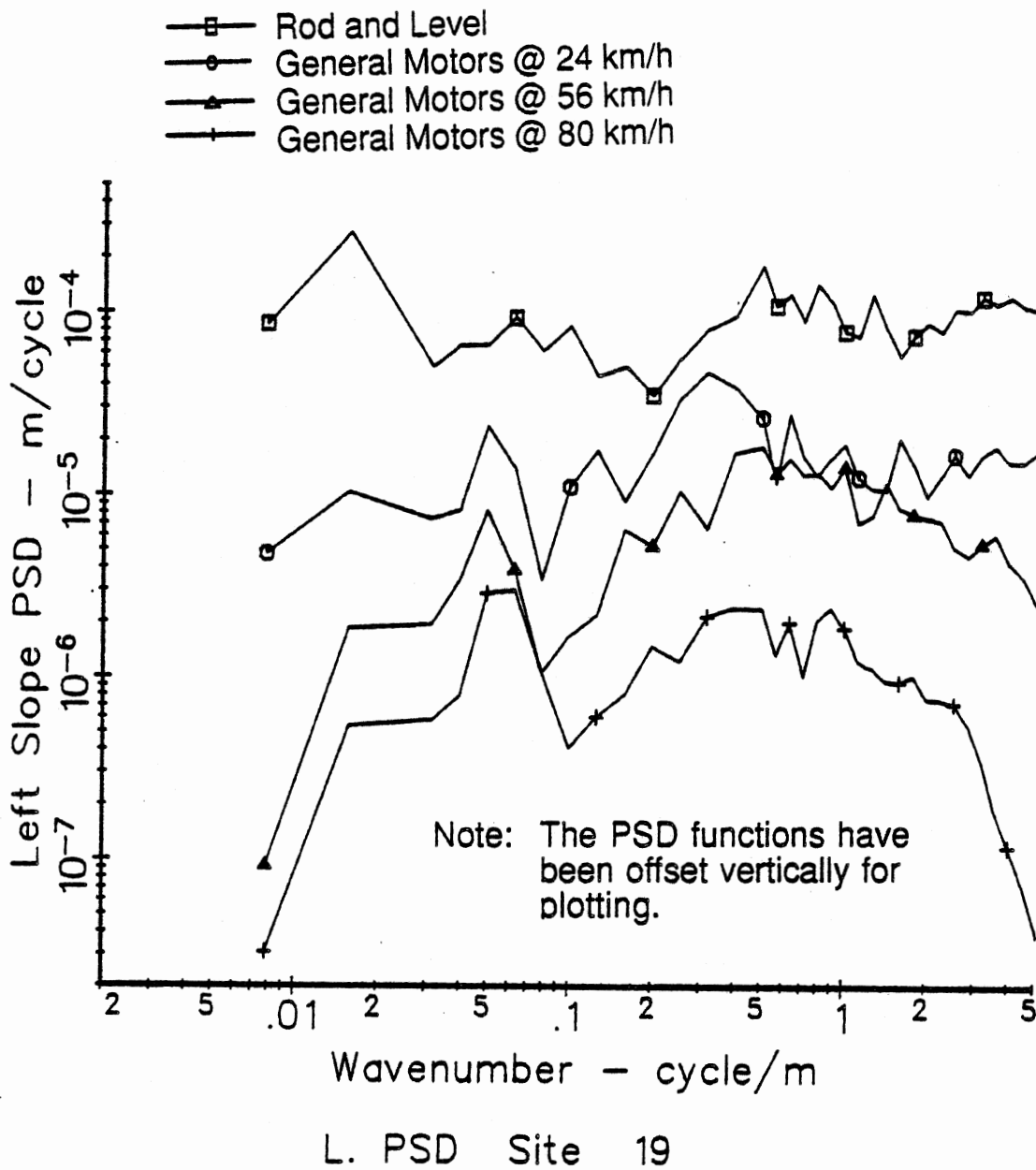
Figure 50. Typical PSD functions from the GMPG profilometer on a rough site.
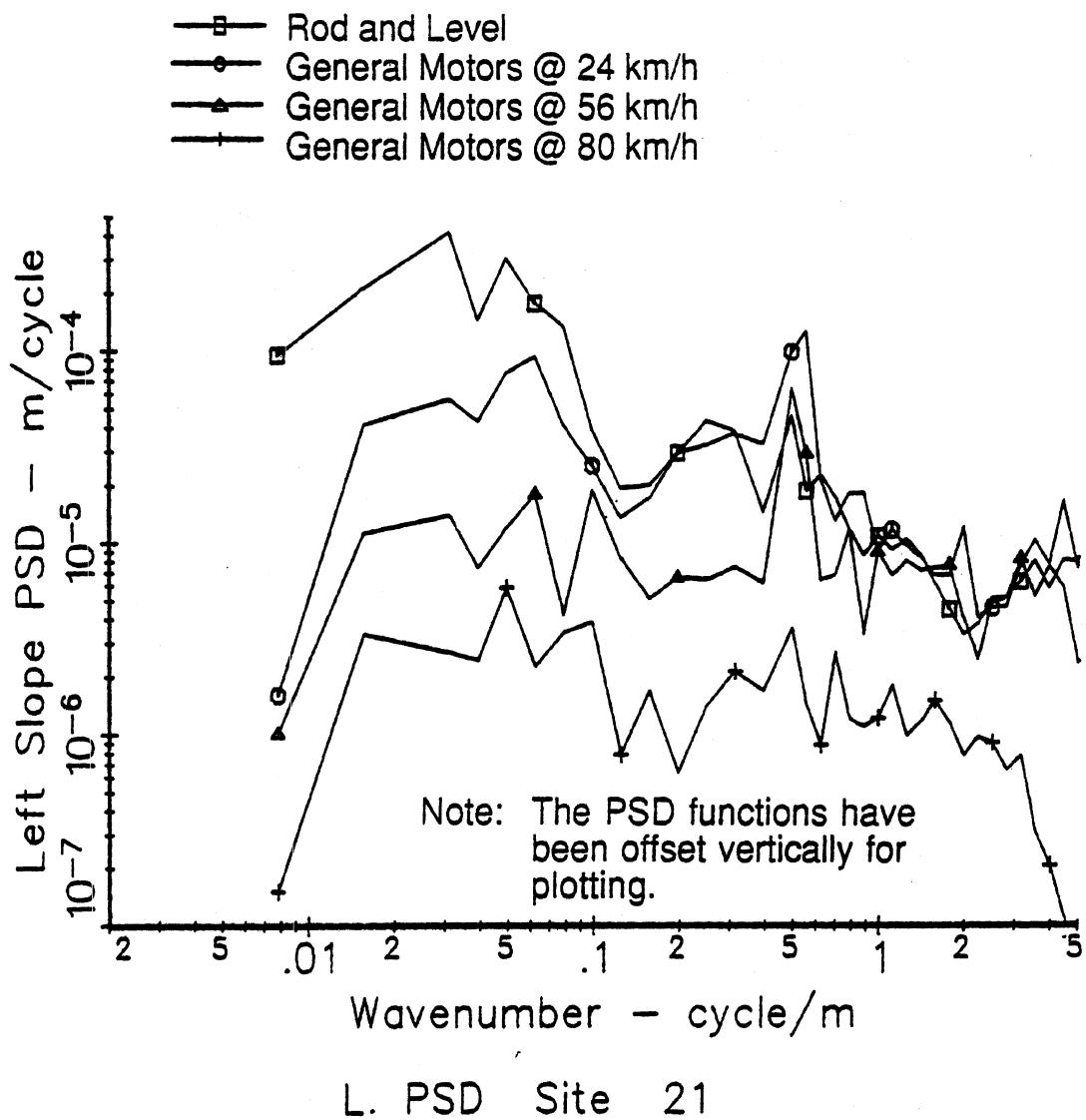
Figure 51. PSD functions from the GMPG profilometer on a rough site that show a measurement error.

points shown in figure 46 for the IRI and MO analyses are the measures made on this site (site 21). Also, the scatter plots in figure 48 show that the measures on this site were also outliers for the wavebands covering the shorter wavelengths.

Overall, the PSD plots show that the GMPG system responds to wavelengths up to 30 m most of the time, but that the measures are not always accurate at all wavelengths. No systematic sources of error were identified that can be related to certain wavelengths.

Conclusion

The profiles obtained with the GMPG profilometer approximately matched the true profile, yet the agreement was not as close as seen with other profilometers based on the same GM-type design. The system sees wavelengths up to 30 m long, which is adequate for most applications involving summary roughness indices. The limitations seem to be caused by software, rather than hardware. The noncontacting laser height sensors appeared to work flawlessly on all types of surfaces, and the high sampling rate of the system allows measurement of extremely detailed profiles. The distortion seen in the profile measures might be caused by the method used to compute profile from the transducer signals, or perhaps from an error in the setting of an electronic component in the data acquisition system. Summary roughness indices computed from profile generally match the reference fairly well, indicating that the overall amplitude response of the system is correct.

K. J. Law 690-DNC: the Minnesota, Ohio, and West Virginia Profilometers

Hardware Description

K. J. Law Engineers, Inc. (23660 Research Drive, Farmington Hills, MI 48024) manufactures a commercially-available, inertial-type profilometer. The original GM-type inertial profilometer design has been refined and improved over the years by K. J. Law Engineers, Inc., with the major improvements being the conversion to a digital instrumentation system, a noncontacting road sensor, and a digital, spatial-based processing method for computing the measured profile. The processing method—which is patented—produces profile measurements that are independent of measuring speed and changes in speed during measurement.[18]

102

The model that includes these improvements is designated the model 690-DNC (where DNC indicates digital, noncontacting). The noncontacting sensor in the 690-DNC measures the height of the vehicle above the road surface by detecting the position of a projected image of light and using triangulation. The image is a slit, nominally 6-mm by 150-mm at the road surface, with the longer dimension oriented in the transverse direction. The profile is computed during measurement, using a DEC PDP 11 minicomputer. Normally, the signals from the accelerometers and height sensors are sampled approximately every 25 mm (1 inch) to perform profile and roughness calculations. The profiles are smoothed with a 305 mm (1.0 ft) moving average and decimated for storing the profile on 9-track computer tape at an interval of 152 mm (0.5 ft). The smoothing is performed to prevent aliasing during the decimation. The 9-track tapes use standard DEC file formats, and can be read with any computer using the standard 9-track drives. The Law 690-DNC inertial profilometer system meets the requirements for ASTM Designation E 950, and has been purchased by FHWA for use in calibration of response-type ride meters. This profilometer will reside at the United States National Bureau of Standards, and is scheduled to be available to perform calibrations for State agencies beginning in the summer of 1986.

Three Law 690-DNC profilometers participated in the RPM. They are owned and operated by the Ohio Department of Transportation, the Minnesota Department of Transportation, and the West Virginia Department of Transportation. Photographs of these units are shown in figures 52, 53, and 54. All three of these systems were functionally identical, although there are minor differences in the hardware. The tapes were submitted to UMTRI by all three of the crews at the end of the RPM.

The Ohio system was distinguished in the RPM by being the only profilometer to obtain valid measures in 100% of its runs, which included every site. As table 4 in the "Experiment" section shows, repeated runs were made on most of the public road sites.

The crew from Minnesota typically ran their profilometer continuously, combining test sites to avoid initializing the computer for individual files. The files containing multiple runs were separated at UMTRI into a standard format for analysis. Tests for several sites were not submitted, as indicated by table 4.

Table 4 also shows that the West Virginia system was not able to provide measures on all of the sites. The system experienced computer problems during the RPM, and a number of runs were invalidated by the operators. As indicated in the table, several runs that were submitted were later rejected by UMTRI, based on inspection of the plotted profiles. The plotted profiles also indicated that the distance interval between samples was not correct.
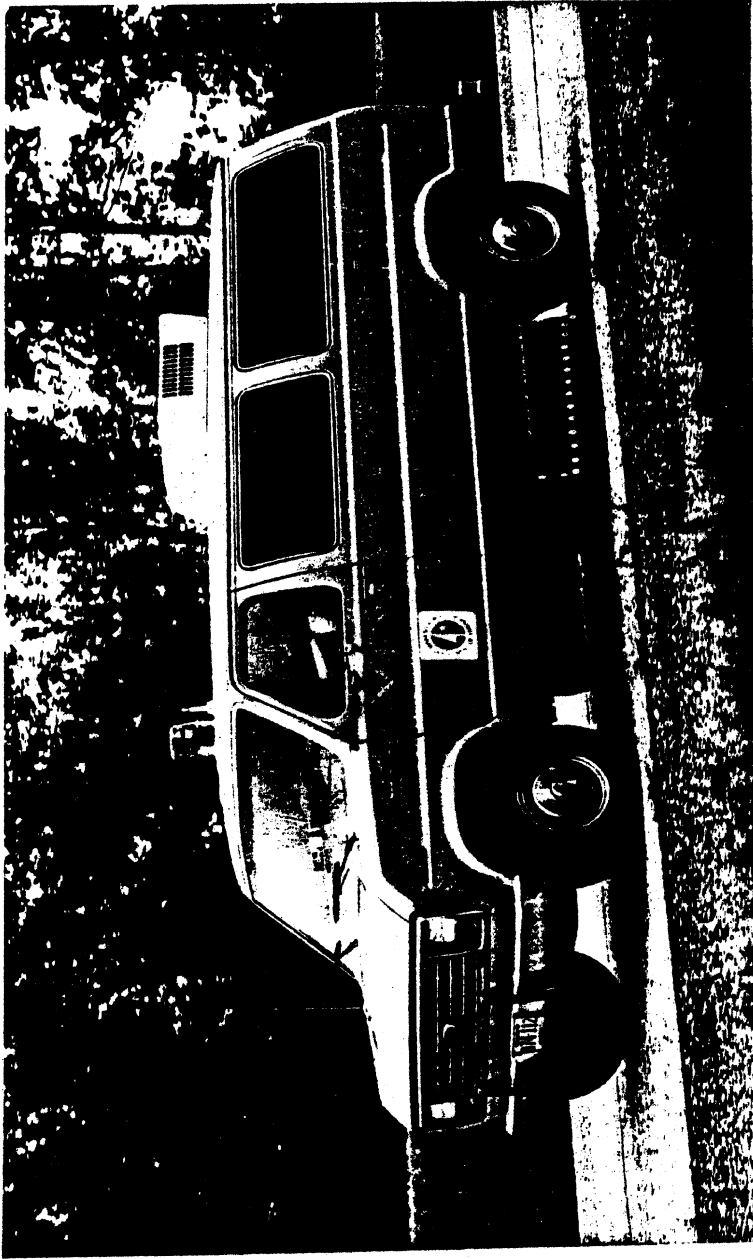
Figure 52. The Minnesota profilometer.
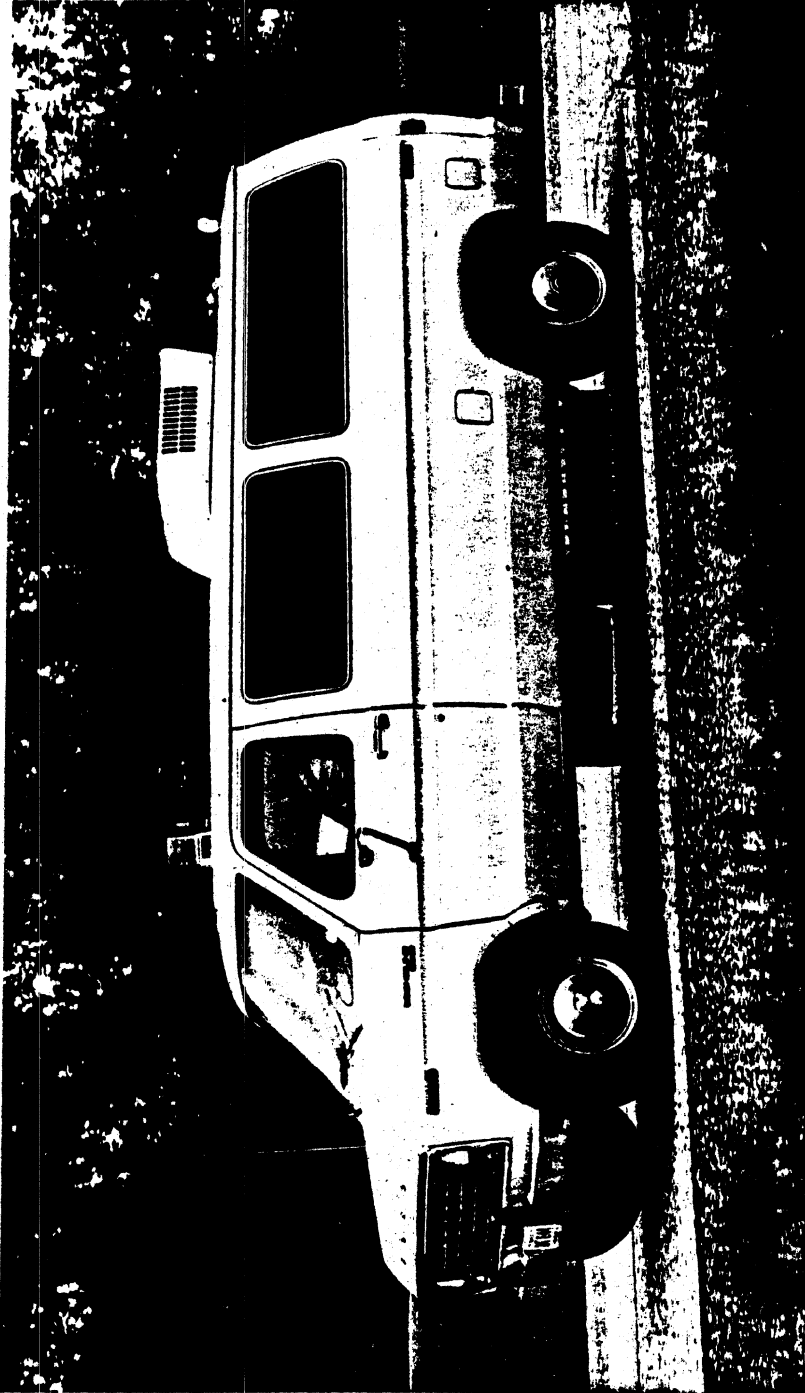
Figure 53. The Ohio profilometer.
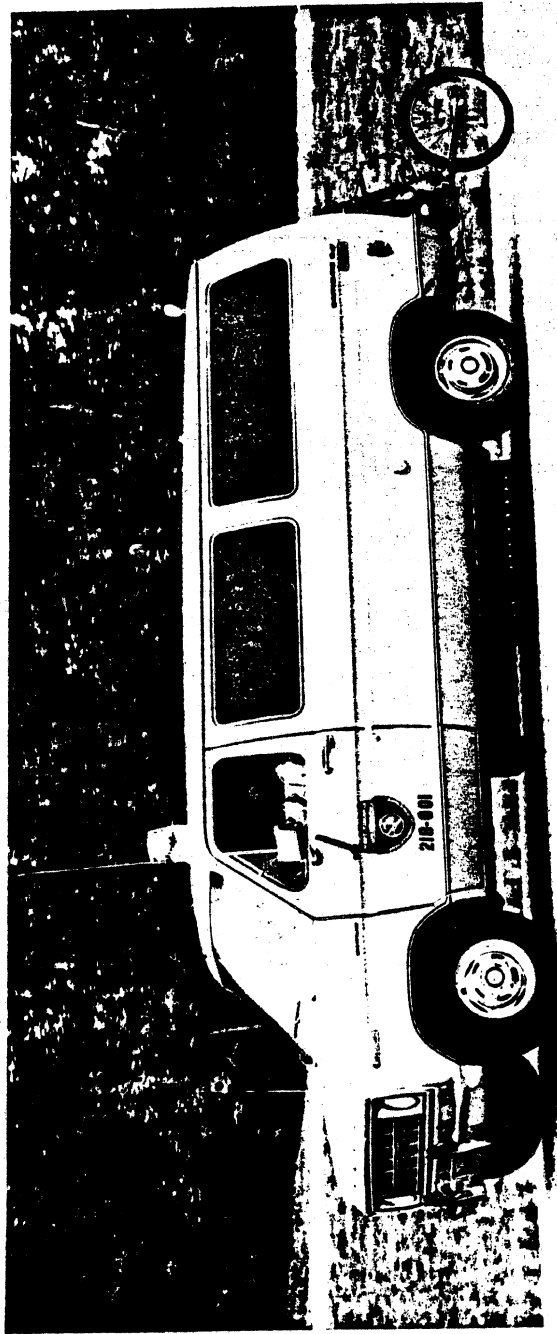
Figure 54. The West Virginia profilometer.

Instead of the specified 152.4 mm, the actual step size was about 150.0 mm, indicating an error in calibration. All of the analyses were performed using the 150-mm step size, to avoid problems in aligning profiles.

Profile Plots

All of the 690-DNC systems have identical responses to long wavelengths, which are determined by the software used to compute profile. The software includes a variable high-pass spatial filter, which was set to 91.4 m (300 ft) for the three 690-DNC systems participating in the RPM. When the different systems are used with the same filter setting, almost identical profiles are obtained from the systems at any speed between 24 and 80 km/h (15 and 50 mi/h). Figure 55 shows nine measures of the same profile, made with the three systems at three speeds. Two of the measures made at 24 km/h differ slightly from the others, but overall the agreement is quite good. When considering only the measures made at the higher speeds of 48 and 80 km/h, the agreement is almost perfect, using simple plots as the means for comparison. As shown earlier in figure 2, the profiles from the 690-DNC do not match the true profile, due to the filtering built into the profile computation. However, when identical filtering is applied to the true profile and the 690-DNC profiles, as was done in figure 3, then excellent agreement is obtained.

Figure 56 shows the good agreement obtained between the 690-DNC systems and the rod and level reference when the profiles are all filtered identically. Other examples of profiles measured with the 690-DNC systems have been shown in other sections. Figure 25 shows the agreement between the Ohio system and the rod and level for capturing the profile features on a public road that include large deviations and a manhole cover. Figure 45 shows how the Ohio system recorded a railroad track crossing. Figure 26 shows how two of the 690-DNC systems provided a reproducible profile on a site with highly variable surface properties, due to extensive cracking and patching. Other examples are shown in figures 2, 3, 12, 13, 34, 42, 44, 73, and 74.

As mentioned earlier, the West Virginia unit experienced problems during the RPM. The operators were not able to provide valid measures for all of the sites, and further, some of the measures submitted were found to be invalid by UMTRI. These runs were indicated in table 4 in the "Experiment" section. Figure 57 shows a representative trace from the West Virginia system that was in error, along with two valid measures of the same profile. The signal from the West Virginia system is typical of the output obtained with a GM-type profilometer when the height sensor has been disconnected. Thus, it is possible that a problem related to the height sensor was the cause for the invalid runs indicated in the table.
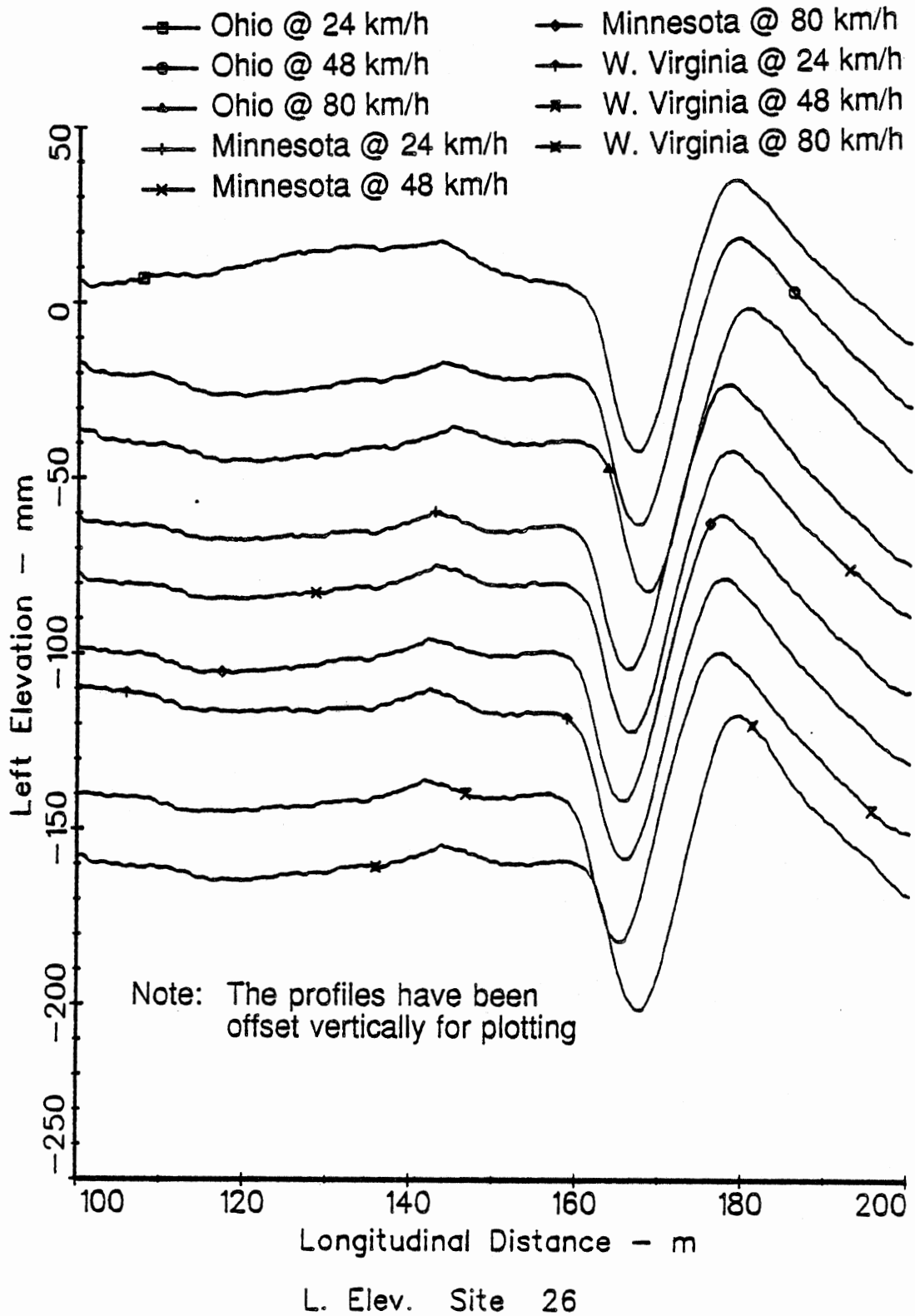
Figure 55. Example of the repeatability of the K. J. Law 690 DNC.

108
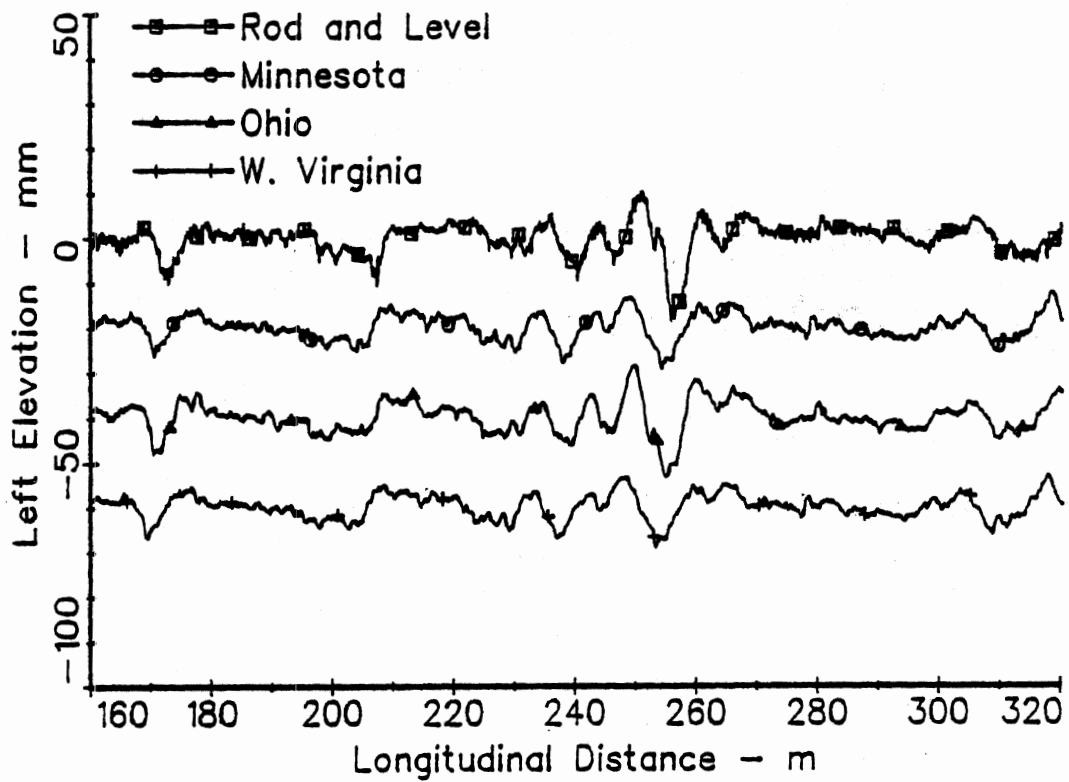
Figure 56. Profiles from K. J. Law 690 DNC systems on a moderately rough road.
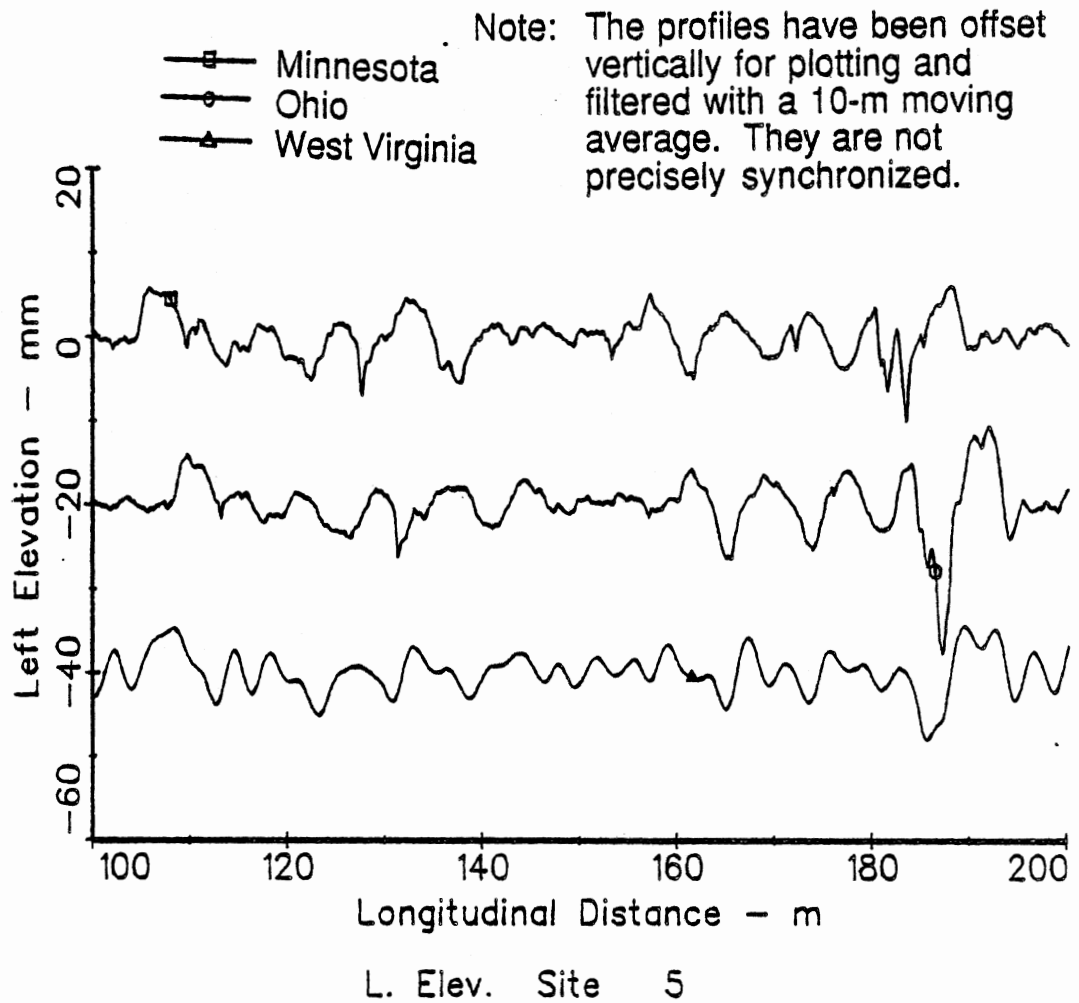
Figure 57. Example of the measurement error exhibited in some of the West Virginia measurements.

Measurement of Roughness Indices

Figures 58 through 60 show how the three 690-DNC systems performed at measuring the IRI and MO roughness indices. The top two plots in each figure compare the IRI measures from the profilometers with the reference, while the bottom two plots compare the MO measures.

The Minnesota system provided accurate measures of IRI on all of the GMPG sites that were released to UMTRI. Overall, only one of the data points showed a significant error.

The Ohio system proved to be very accurate for measuring IRI for all of the smoother sites, having roughness levels under 5 m/km. On the rougher sites, the measures are slightly low compared with the reference, and exhibit more scatter.

The measures from the West Virginia system were slightly biased, being too low. This effect could be caused by the error in the sample interval, as described earlier in this section. The bias is about the same in magnitude as the random error (scatter), and might be considered negligible for some uses of the data. As mentioned earlier, several of the runs submitted were judged to be erroneous by UMTRI, based on plots of the profiles (see table 4). There was one additional run at the GMPG which evidently should have also been omitted. This run appears as an outlier in all of the plots involving summary statistics.

The results for the MO analysis are similar to the results from the IRI analysis, although less accuracy (as seen by more scatter) is obtained in every case.

Waveband Indices

The accuracy of the 690-DNC profilometers over a full range of 1-octave wavebands is presented in figures 61 through 66. The results from the three profilometers are seen to be essentially the same, with the exception of a bad run inadvertently included in the West Virginia data. The systems show the best accuracy for the wavebands centered at wavelengths of 32, 16, 8, 4, and 2 m. For the waveband centered at the 64-m wavelength, the systems do not show significant bias, but exhibit more random error (scatter) than for the shorter wavelengths. For the waveband centered at the 1-m wavelength, the profilometers tend to measure too low, particularly on the rougher sites. In all of the results, the measurement speed does not appear to be a factor in the accuracy.

GMPG Sites

All Road Sites

IRI (1/4 car index)

IRI (1/4 car index)

Texas RMSVA Index: MO
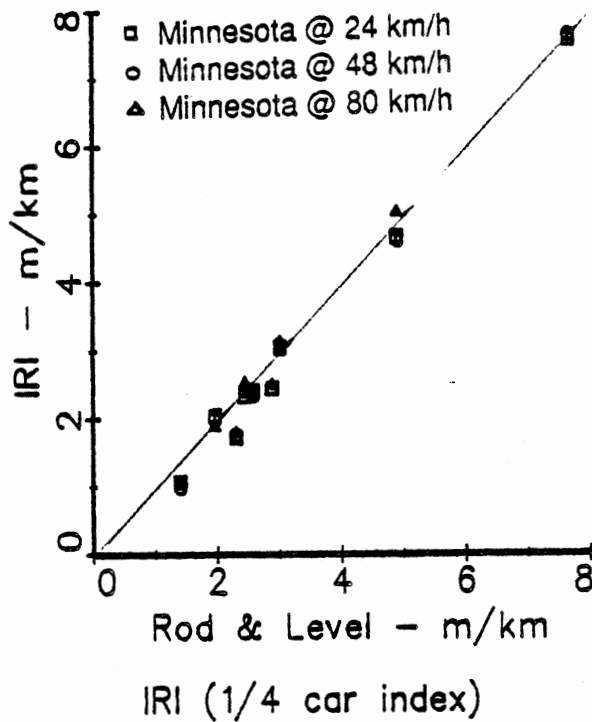
Texas RMSVA Index: MO
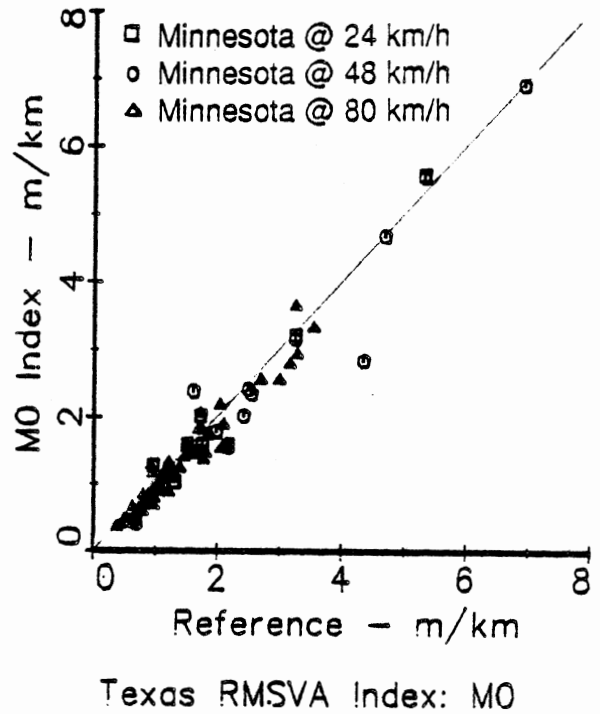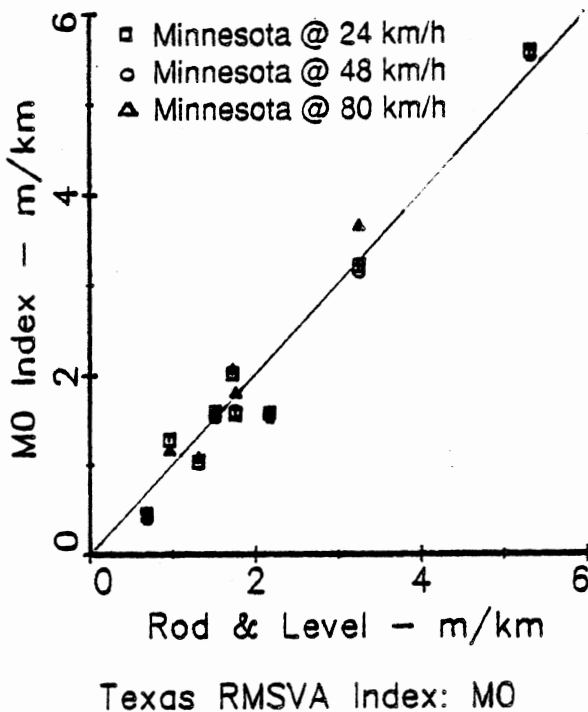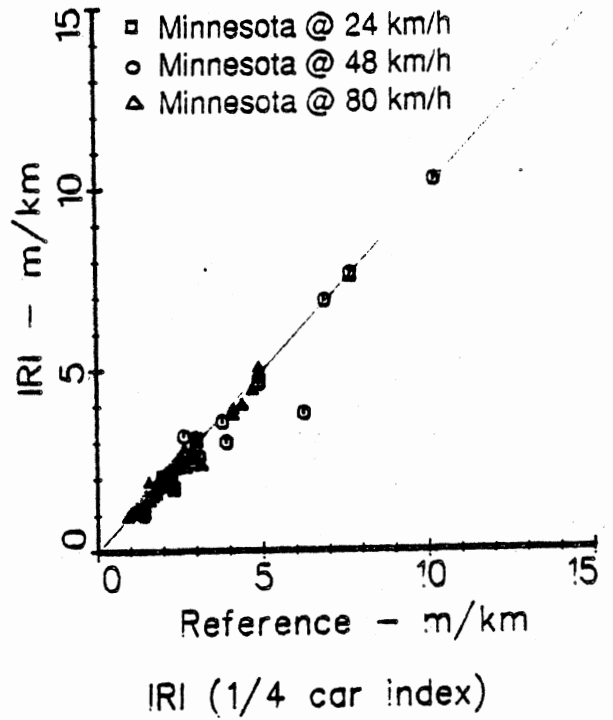
Figure 58. Measurement of IRI and MO with the Minnesota profilometer.

Figure 59. Measurement of IRI and MO with the Ohio profilometer.

GMPG Sites
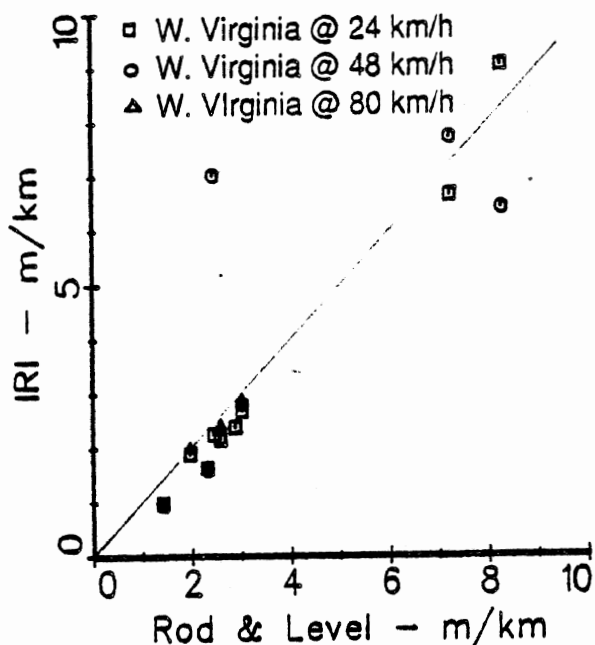
IRI (1/4 car index)

All Road Sites
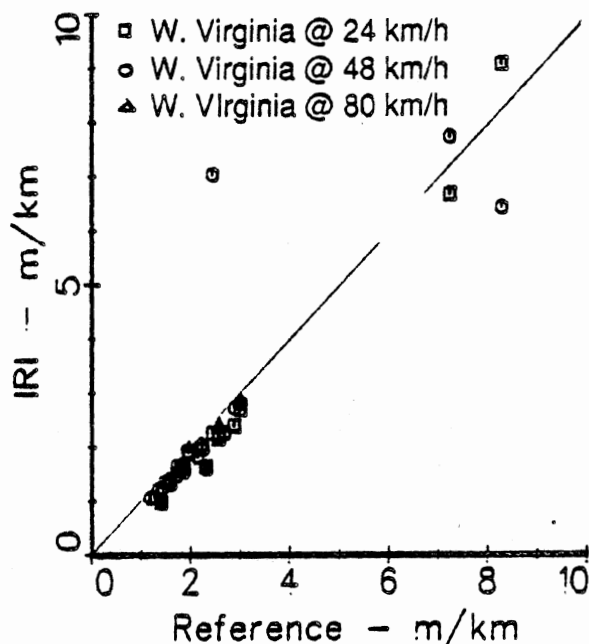
IRI (1/4 car index)
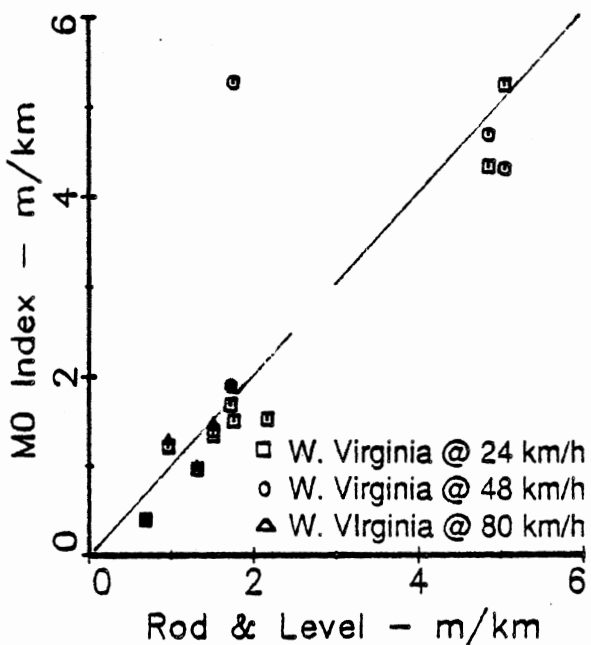
Texas RMSVA Index: MO
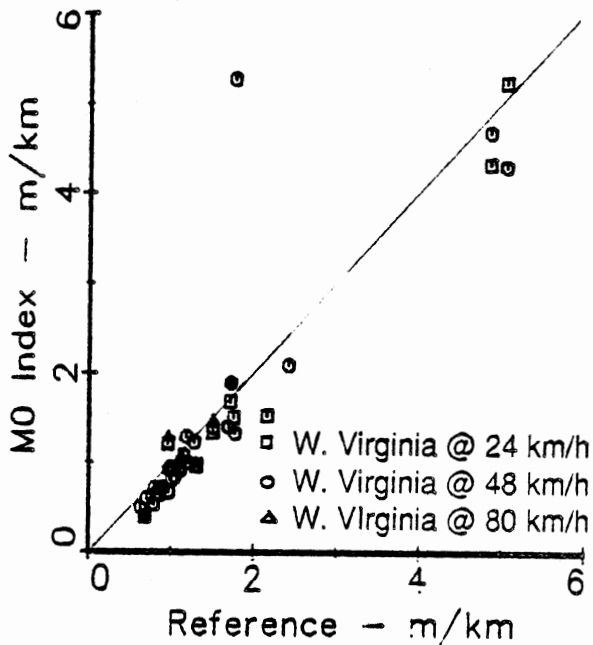
Texas RMSVA Index: MO

Figure 60. Measurement of IRI and MO with the West Virginia
profilometer.

114
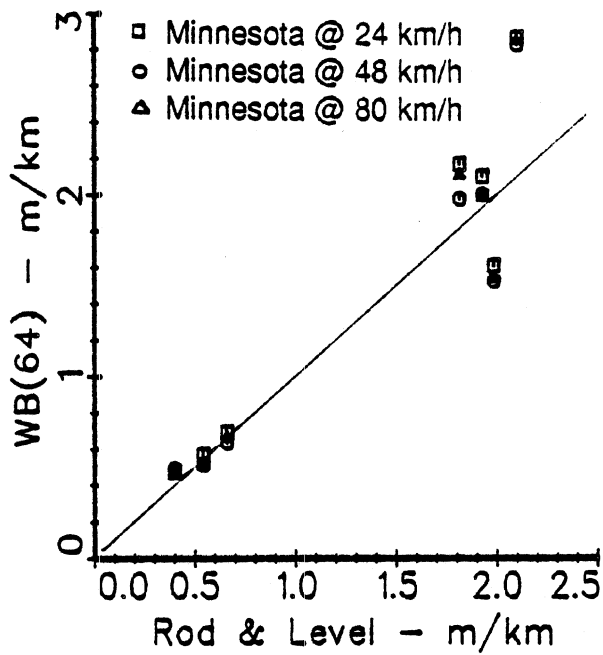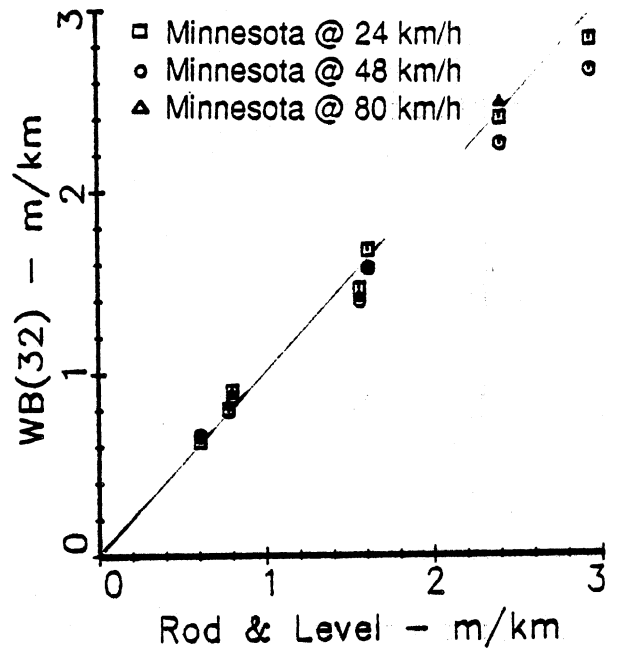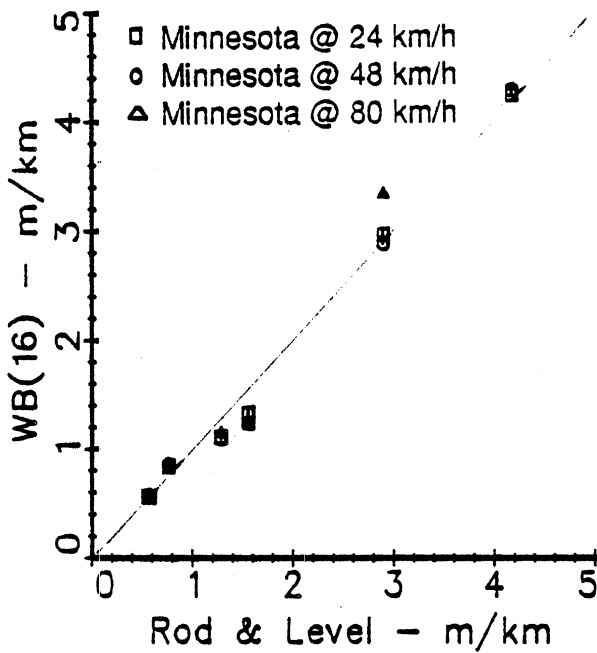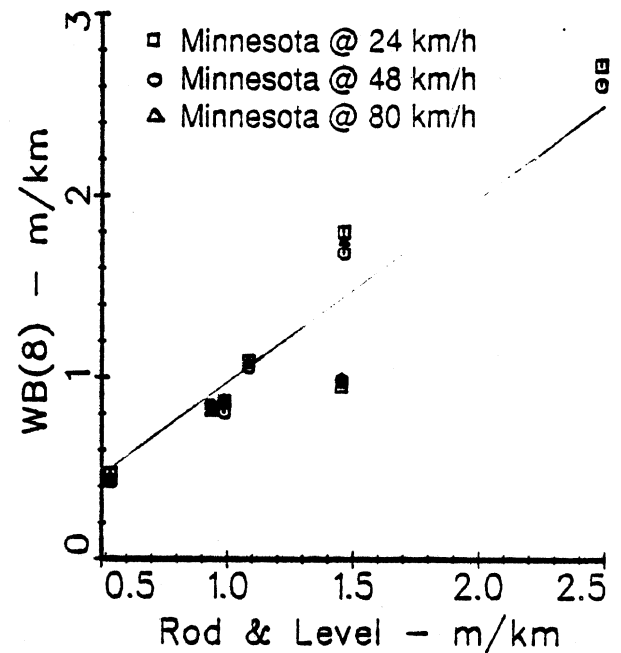
Figure 61. Measurement of waveband indices for the longer wavelengths with the Minnesota profilometer.
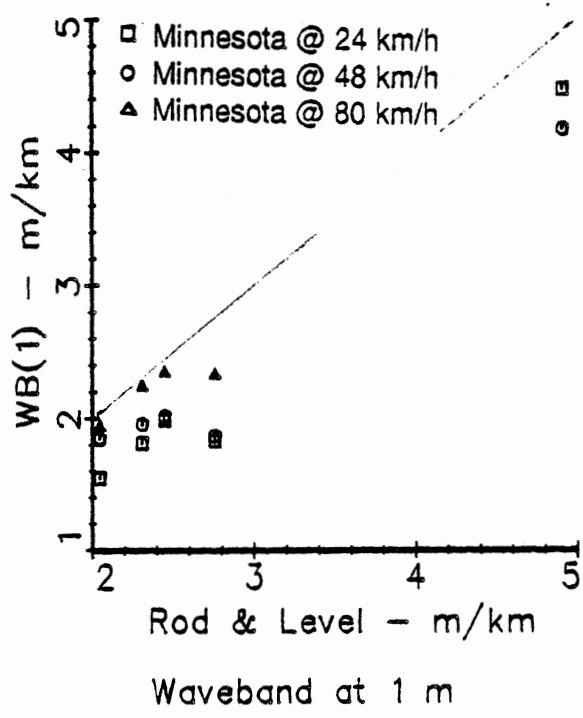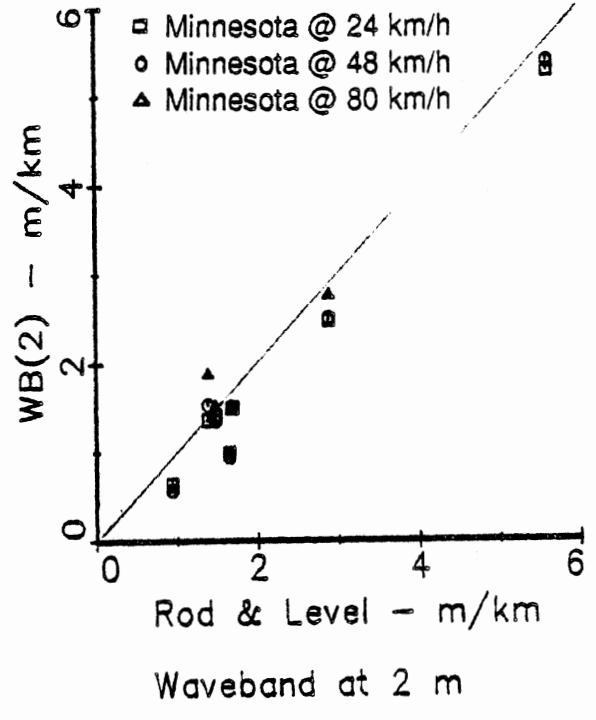
Figure 62. Measurement of waveband indices for the shorter wavelengths with the Minnesota profilometer.

116
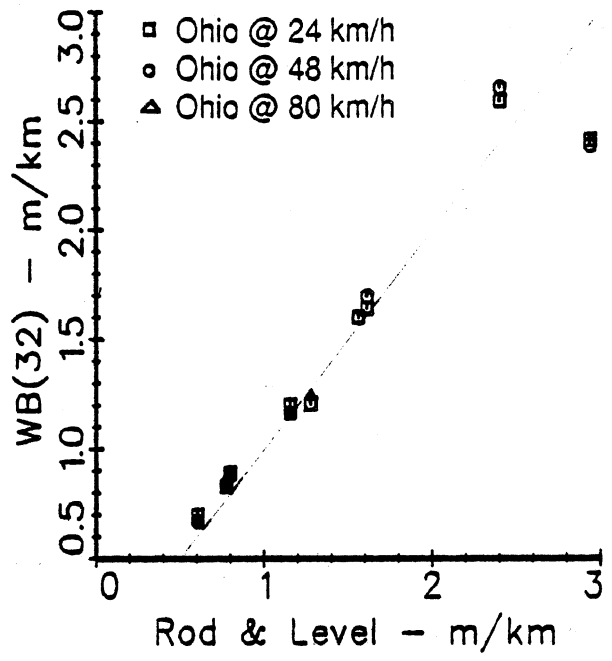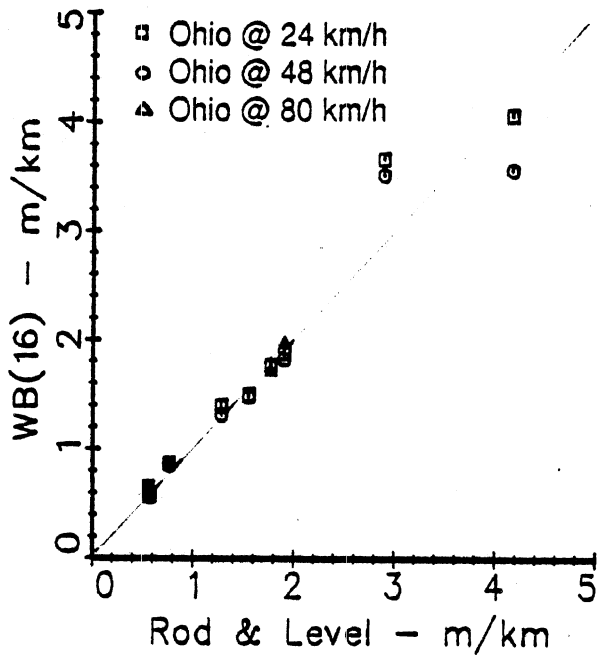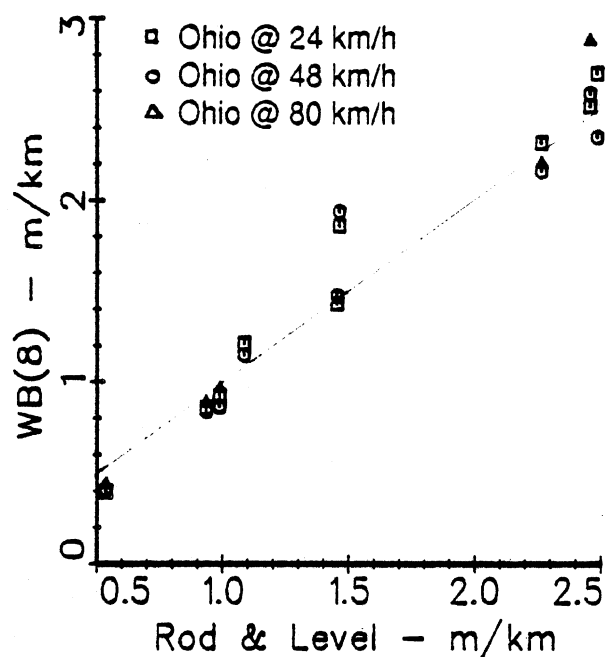
Figure 63. Measurement of waveband indices for the longer wavelengths with the Ohio profilometer.

117
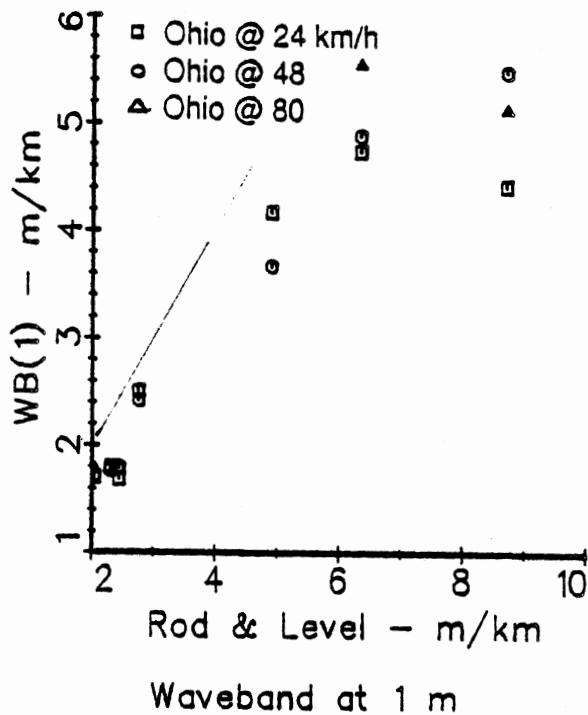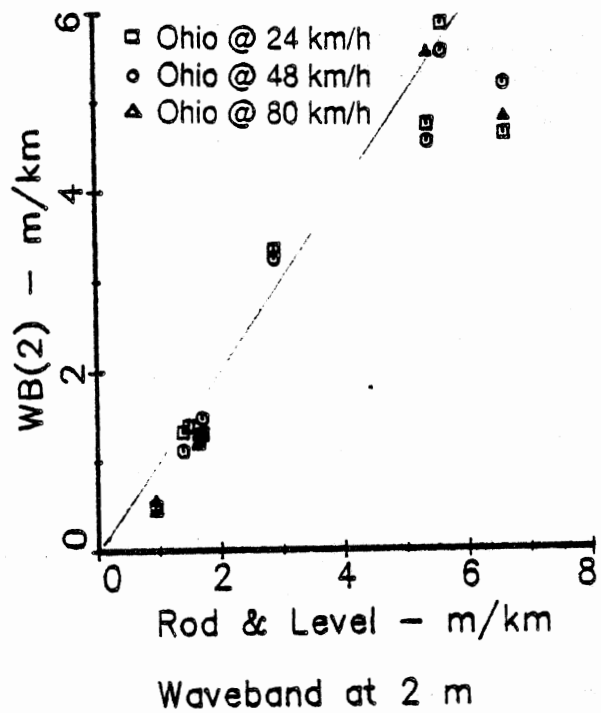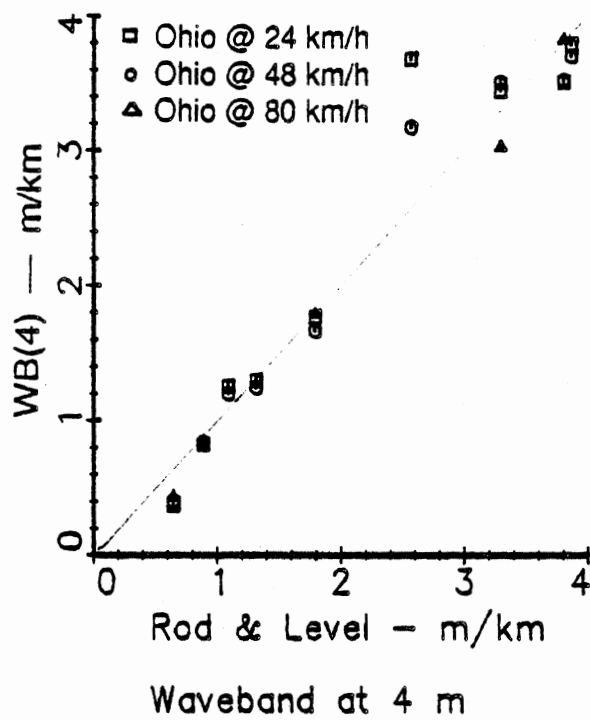
Figure 64. Measurement of waveband indices for the shorter wavelengths with the Ohio profilometer.
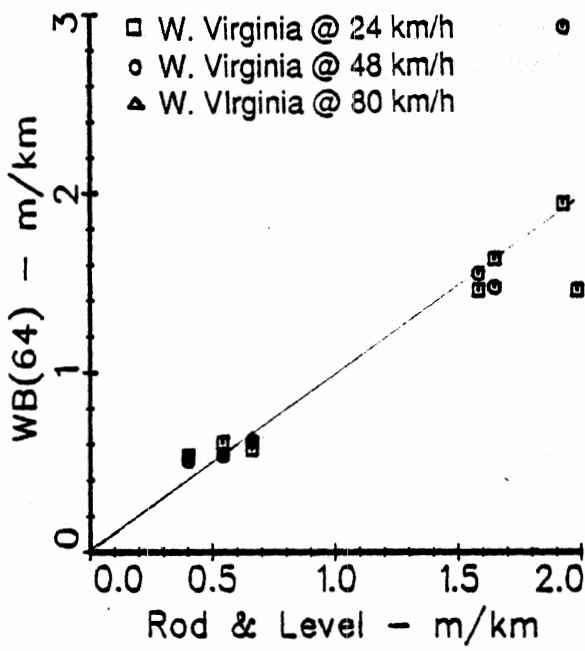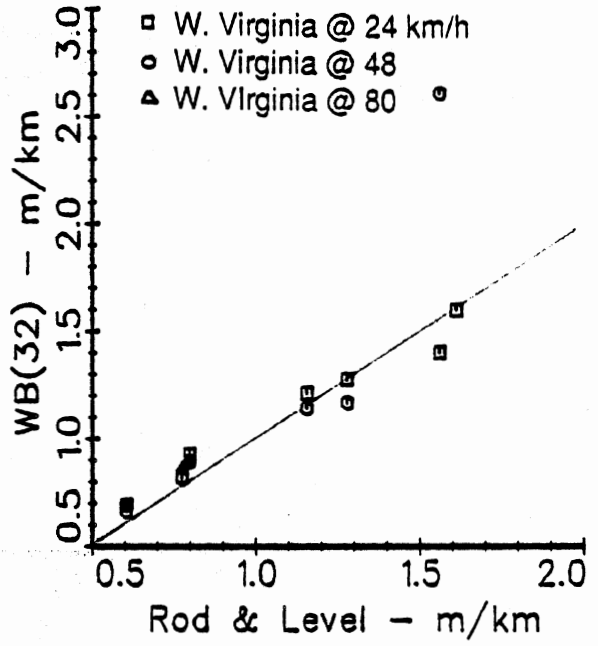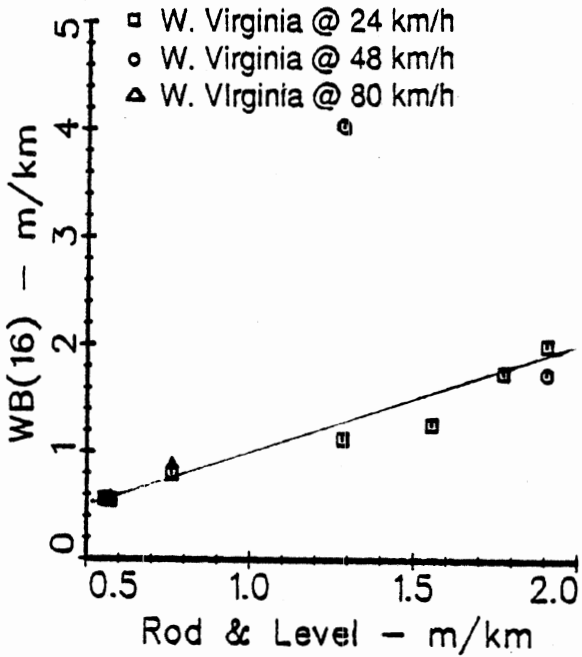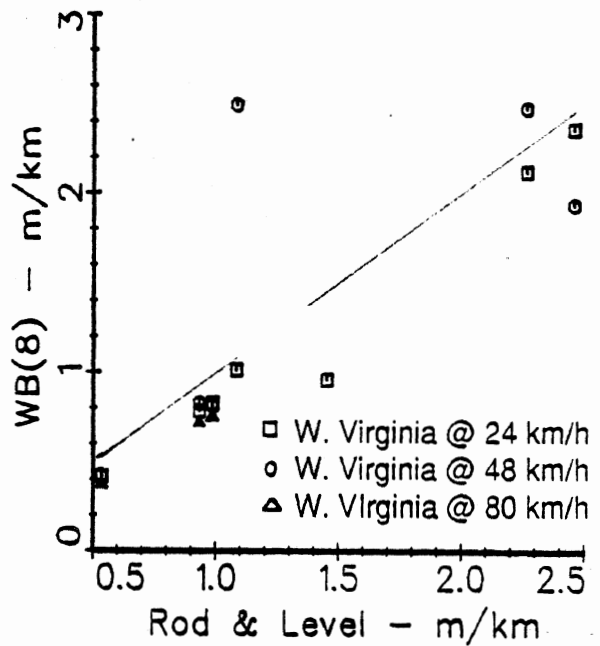
Figure 65. Measurement of waveband indices for the longer wavelengths with the West Virginia profilometer.
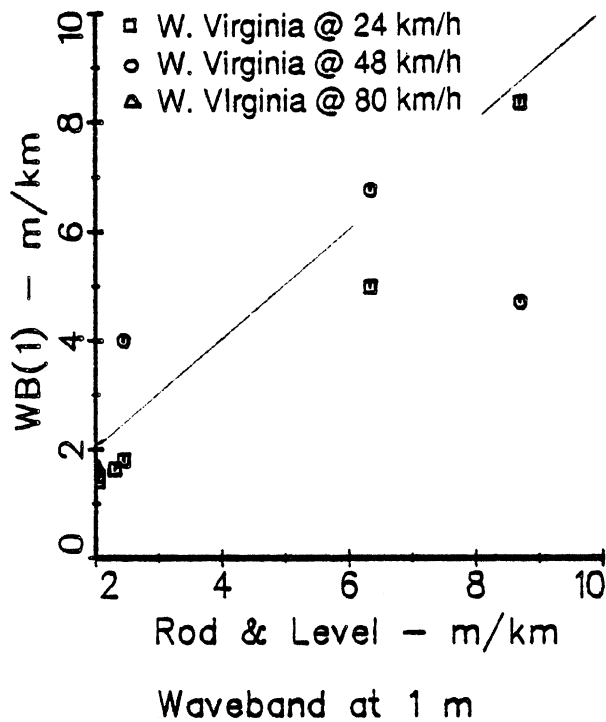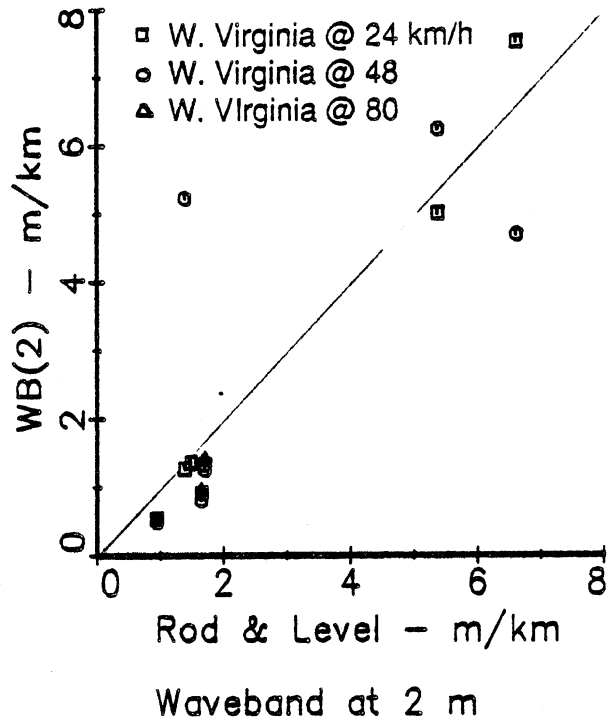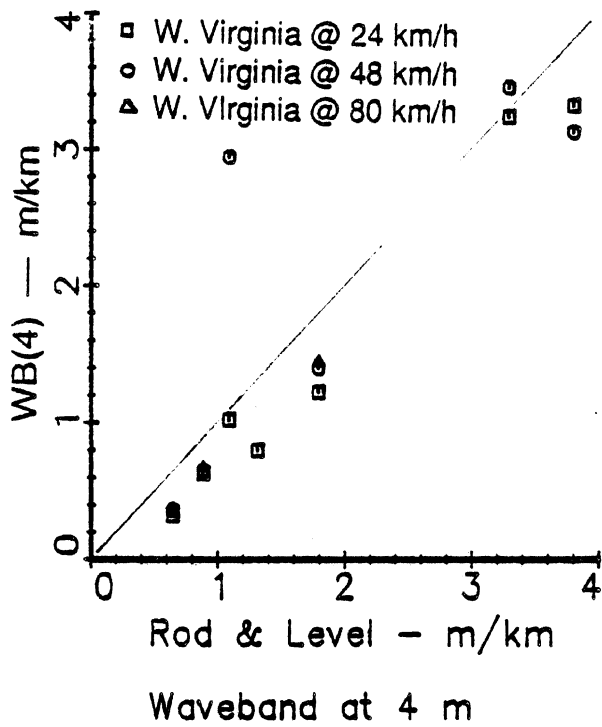
Figure 66. Measurement of waveband indices for the shorter wavelengths with the West Virginia profilometer.

Power Spectral Density (PSD) Functions

The PSD plots from the 690-DNC systems generally matched those from the rod and level over wavelengths from 3 m to approximately 64 m. Because of the limited length of the sections measured with rod and level, it is not possible to determine the longest wavelengths that can actually be measured with the 690-DNC systems with a reasonable level of accuracy. (Most of the sites were only measured over 160-m length with rod and level.) Figure 67 shows the results on one of the two sites that was surveyed for the longer length of 320 m. The figure shows several representative characteristics about the 690-DNC systems. First, the PSD functions obtained at different speeds are very similar, indicating that the system is independent of measuring speed, as it is designed to be. Second, the response at the longest wavelengths (determined by filtering included in the profilometer software) are generally consistent, except at the lowest speed of 24 km/h (15 mi/h), which differs slightly. For wavenumbers ranging from 0.016 to 0.3 cycle/m (wavelengths from about 3 m to 64 m), the PSD functions from the 690-DNC systems closely match the reference rod and level. In the figure, the attenuation of the highest wavenumbers is due to the moving-average smoothing filter that is applied to the profile before it is stored on tape. Figure 68 shows PSD functions on one of the roughest sites of the RPM. In this example, there is very good agreement with the rod and level for wavenumbers less than 0.5 cycle/m (wavelengths longer than 2 m). The attenuation of the short wavelengths due to the 305-mm (1-ft) moving average can be seen clearly.

Two examples from the public road sites are also shown. Figure 69 shows how the PSD functions compare from five of the profilometers on a site that was selected to challenge the systems that use optical height sensors. The entire length of this public road site was used to compute the PSD functions, and therefore more averaging occurred in the processing than for the shorter GMPG sites. As a result, random test variables have less effect, on the average, and better agreement between similar profilometers is usually obtained. In figure 69, all five systems show close agreement over the wavenumber range of 0.04 to 0.5 cycle/m (wavelengths of 2 to 25 m), and the four GM-type profilometers show agreement for wavenumbers down to .016 cycle/m (64-m wavelength). (The APL is limited to wavelengths of 32-m in the figure.) The two 690-DNC systems (Ohio and Minnesota) show the reduced response at low wavenumbers (long wavelengths) caused by the filters built into the system software. Evaluation of the response of the profilometers for high wavenumbers (short wavelengths) is difficult, because all of the systems differ. Nonetheless, the effects of the antialiasing filters can be seen on the two 690-DNC systems, which show a steep rolloff for wavenumbers higher than 1.5 cycle/m.

121
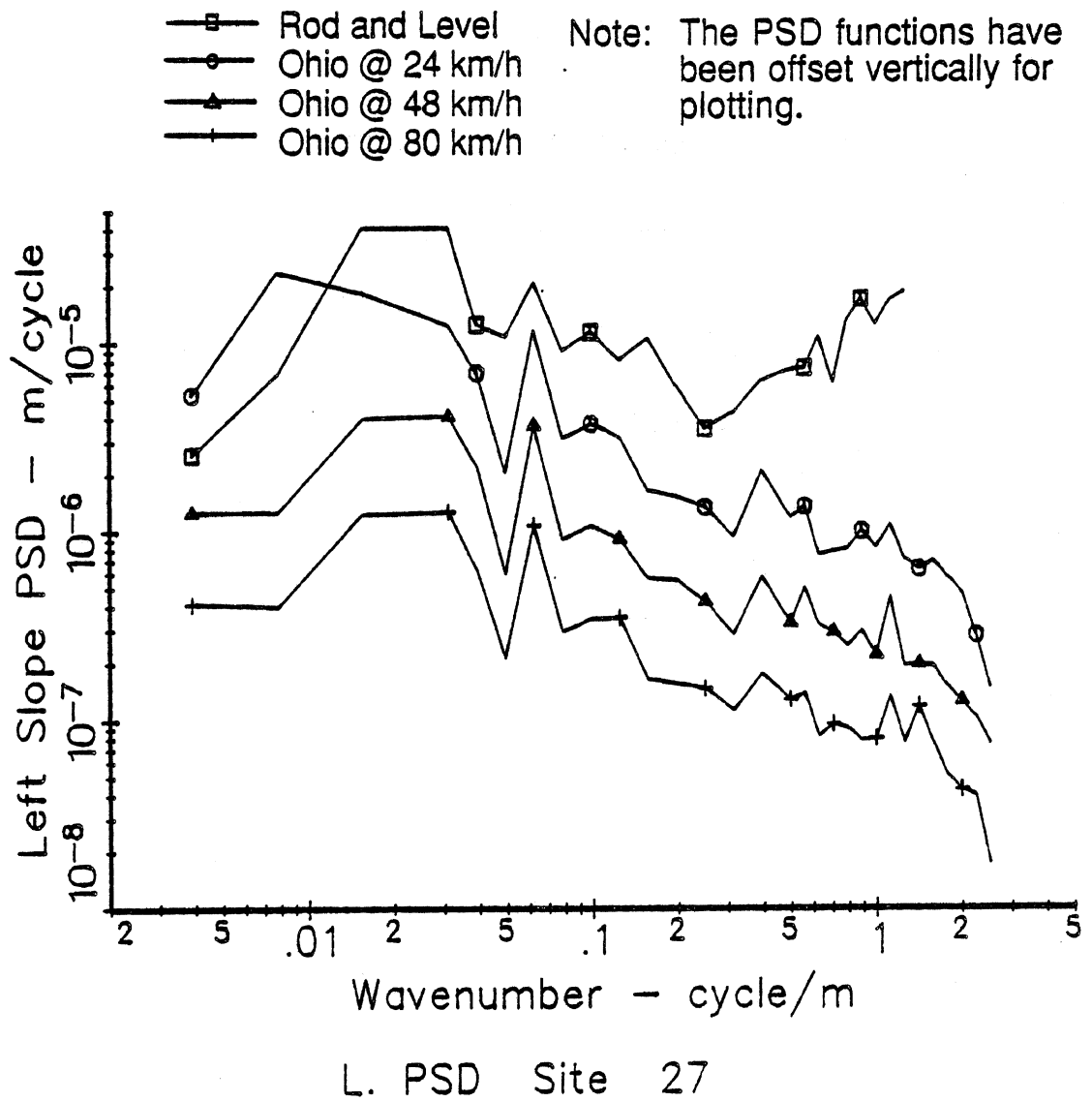
Figure 67. PSD functions from the Ohio profilometer on a smooth site.
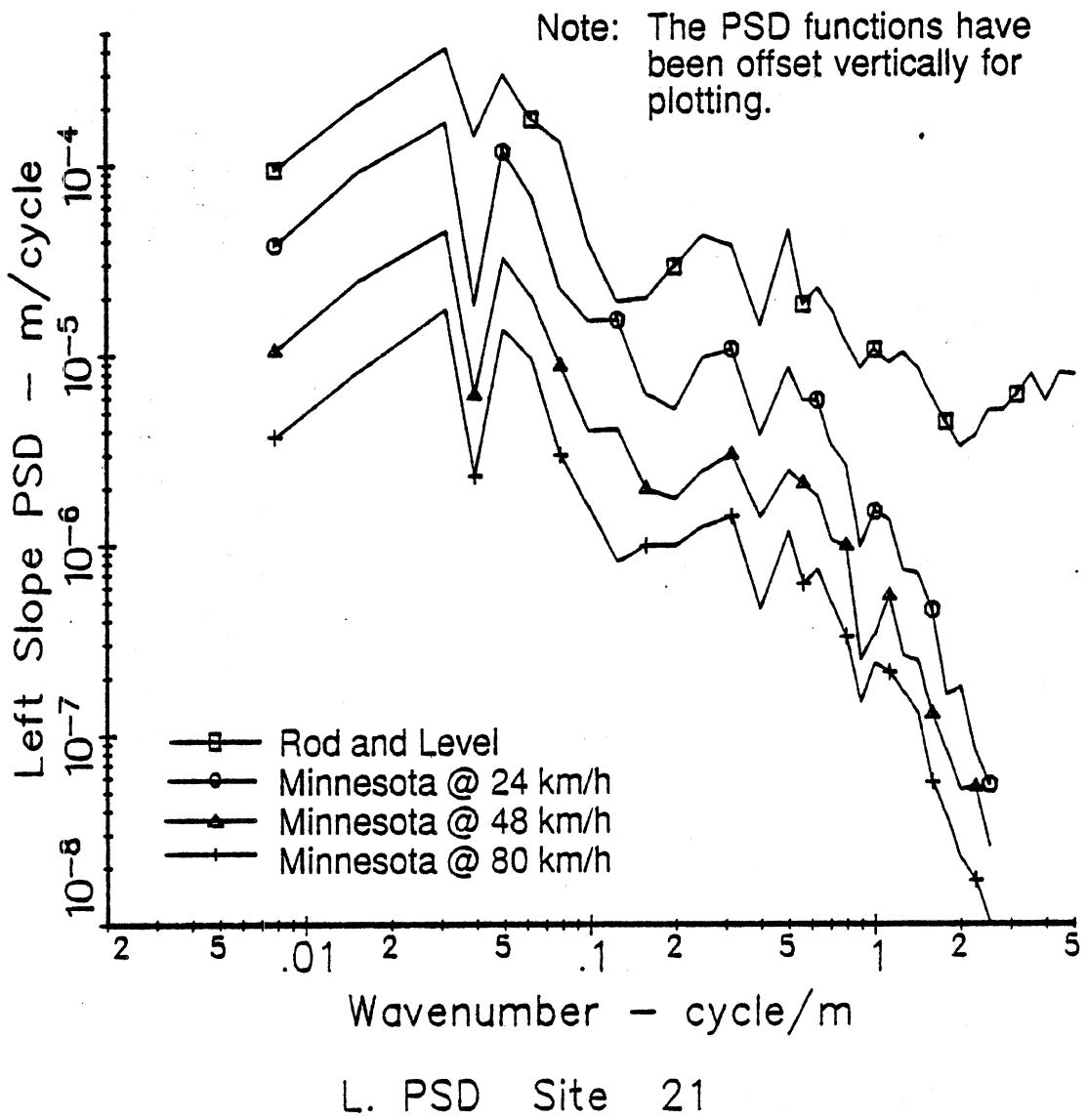
Figure 68. PSD functions from the Minnesota profilometer on a rough site.
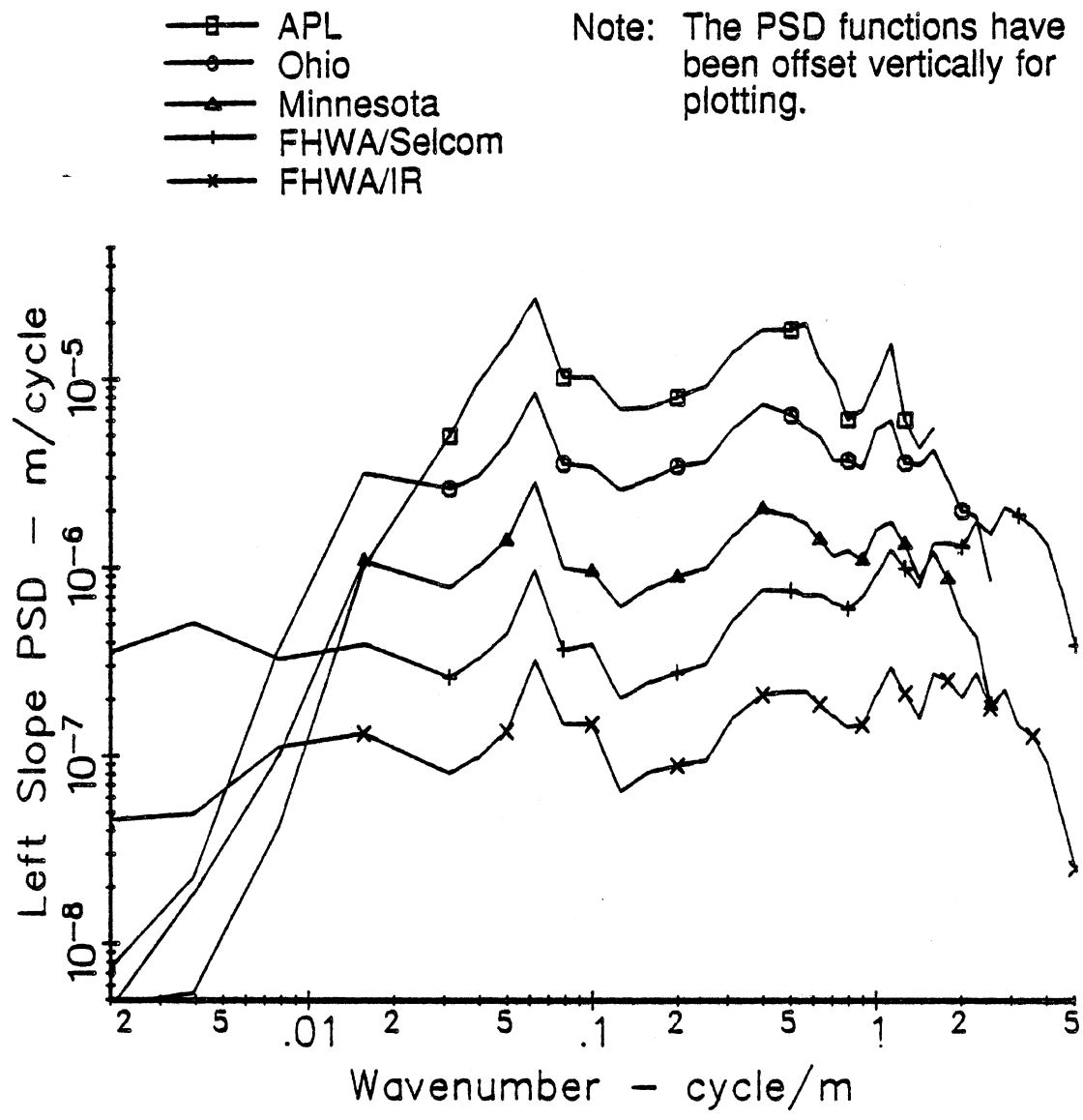
Figure 69. PSD functions from several profilometers on a PCC site with faulting, open joints, and patching.

Figure 70 shows the PSD functions for six of the profilometers on the smoothest site of the RPM. On a smooth site such as this one, any additional components in the profile signal will assume a greater importance. Periodic sources of error are most apparent in plots of PSD functions, where they appear as peaks in the spectrum. Three of the PSD functions in figure 70 show such peaks. The Ohio system shows a peak at 1.4 cycle/m. The periodic error in the Ohio profiles occurs on several of the smoothest sites, and only at the highest speed of 80 km/h (50 mi/h). Although periodic errors are clearly visible in the PSD plots, they do not necessarily have a large enough amplitude to cause error when roughness indices are calculated. (The APL trailer shows a peak at 0.5, and a larger peak at 1.0 cycle/m, which are probably caused by nonuniformities in the tire/wheel assembly of the APL trailer. The Michigan DOT system shows a noticeable peak at 4 cycle/m, and another smaller one at 1.4 cycle/m.) None of the peaks in the PSD functions from the 690-DNC systems were large enough to cause any noticeable error in the roughness indices considered in this project.

Additional PSD functions from the 690-DNC profilometers are shown in figures 78 and 79.

Conclusion

The 690-DNC was able to measure profile accurately and reliably on all of the test sites included in the RPM. The experiment and analyses were designed to cover wavelengths up to 100 m, and the 690-DNC measures had good fidelity up to that limit. The system software attenuates wavelengths shorter than 2 m. Although the hardware is surely capable of accurately measuring shorter wavelengths, the ability of the system to measure shorter wavelengths cannot be demonstrated unless the software is modified. The existing wavelength range is sufficient for accurate measurement of IRI and MO on all sites. The Ohio profilometer was the only system in the RPM that obtained valid measurements for 100% of the runs that were submitted, proving that the system can be used with a high reliability. Some of the runs turned in for the other two 690-DNC systems included invalid runs, however, indicating that some sources of error can go undetected in routine use.
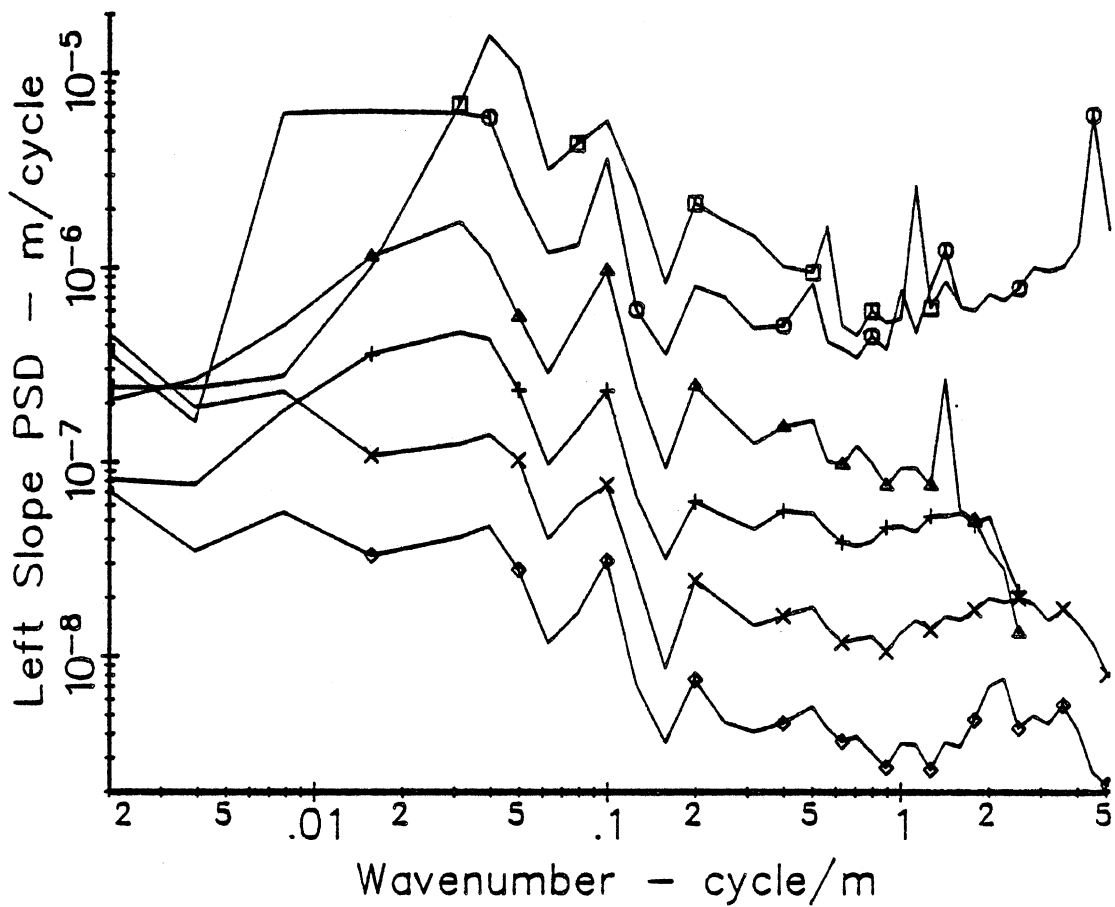
Figure 70. PSD functions from several profilometers on the smoothest site included in the experiment.

Michigan DOT Profilometer

Hardware Description

The Michigan Department of Transportation (MDOT) owns and operates a GM-type inertial profilometer that was originally built in-house in the 1960's. Over the years it has been refined and improved, with the main improvement being the replacement of the mechanical follower wheels with noncontacting optical height sensors, also designed and built in-house. As configured for the RPM, the MDOT profilometer relied on the optical noncontact sensors, although some additional tests were performed with road-follower wheels. The system is shown in figure 71.

The raw transducer signals (speed, distance to road, and vertical acceleration) were recorded in the profilometer on an FM analog magnetic tape recorder. These data were played back and processed in the MDOT laboratory to produce profiles that were subsequently provided to UMTRI on digital 9-track tapes. During the RPM, the profilometer was not able to measure both wheeltracks simultaneously, and therefore each run produced a measure for a single wheeltrack. The profilometer also has the capability of computing profile during measurement; during the RPM, however, all profile computations were performed afterwards in the laboratory.

As indicated by table 4 in the "Experiment" section, not all of the sites were included in the MDOT measurements. Originally, MDOT planned to provide several tapes, with the profiles on each corresponding to different ranges of wavelengths. The first tape sent was processed to include the longest wavelengths possible, up to 91-m (300-ft) wavelengths. Some runs, not indicated in the table, could not be processed at MDOT to include the 91-m wavelengths, although they were probably valid runs for many applications. Unfortunately, due to a misunderstanding between the staff at UMTRI and MDOT, these profiles were never requested by UMTRI, and they were therefore not included in the UMTRI analyses.

Many of the sites were only measured in the right-hand wheeltrack with the MDOT profilometer. This presented a problem in the analyses, because all of the comparisons with the other equipment were made on the basis of the measures in the left-hand wheeltrack. All of the rod and level profiles were obtained in the left-hand wheeltrack, so that comparison of the MDOT system with the static reference was possible on only one site. The FHWA/IR profilometer and the Ohio profilometer were both shown to be reliable

127
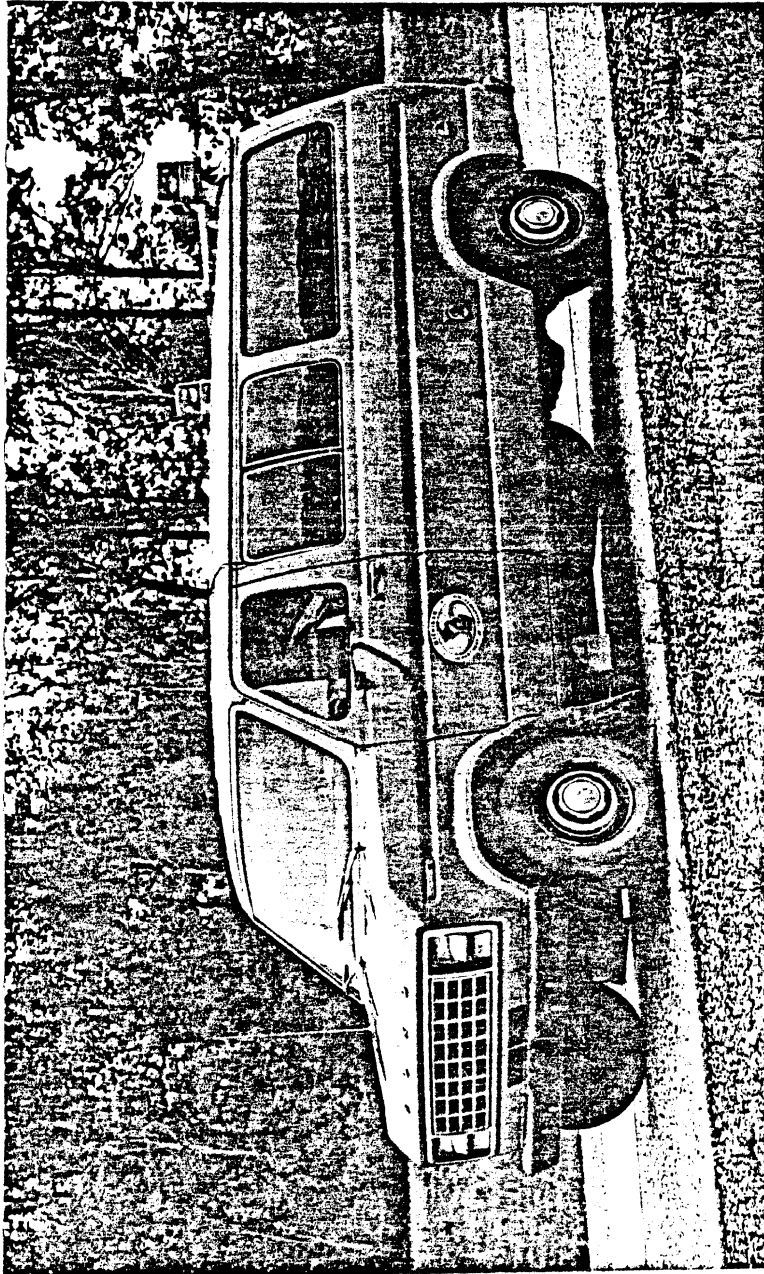
Figure 71. The Michigan DOT profilometer.

and accurate (see the corresponding sub-sections for the descriptions of these instruments), and both of these systems made measures in both the left- and right-hand wheeltracks. Therefore, these two systems were used as references for the MDOT profilometer.

In the course of examining some of the profiles, it was noticed that a few of the MDOT profiles that had been identified as the right-hand wheeltrack were actually measured in the left-hand wheeltrack. As a result, some of the comparisons probably show errors due to improper identification of the runs, rather than the instrument itself.

Profile Plots

Figure 72 compares the profile as measured with the MDOT profilometer with the profile as measured with the rod and level. Most of the time, the repeatability of the MDOT system was very good, yet the agreement with other profilometers was not as close. For example, the agreement between the MDOT measures and the rod and level is not as close as the agreement shown in figure 2 for several of the other systems. Figure 73 shows one of the more extreme cases in which repeat runs made with the MDOT system agreed closely, while measures made with other systems matched each other but not MDOT. This particular figure shows two kinds of difference between MDOT and the other measures: (1) profile features are recognizable, but distorted; and (2) the MDOT system responds as if there are deep cracks in the pavement surface, while the other systems do not. An example of the first type of difference is seen in the bumps at 200 m along the horizontal axis. The FHWA and Ohio profilometers see these features one way, but the MDOT profilometer sees them another way. The second type of difference appears at 144 m along the horizontal axis, where the MDOT profiles include a large crack that is not included in the Ohio and FHWA measures. Figure 74 shows a closer view of these profiles. All four of the profiles show a depression at 144 m, but the magnitude of the depression is 10 to 15 mm for the Ohio and FHWA systems, and over 50 mm for one of the MDOT measures. One possibility is that the MDOT system experiences a measurement error, triggered by a surface feature. Another possibility is that the MDOT system can see cracks in more detail than the other systems, and correctly records their full amplitudes. Unfortunately, since only a few of the systems made measures of the right-hand wheeltracks, it is difficult to determine the cause of this discrepancy.

Assuming for a moment that the MDOT system is not in error, but does see cracks that other profilometers do not, there is a question about how cracks affect roughness measurements. Several of the profilometers were able to detect cracks, and the implications of this are discussed in the "Conclusions" section.

129
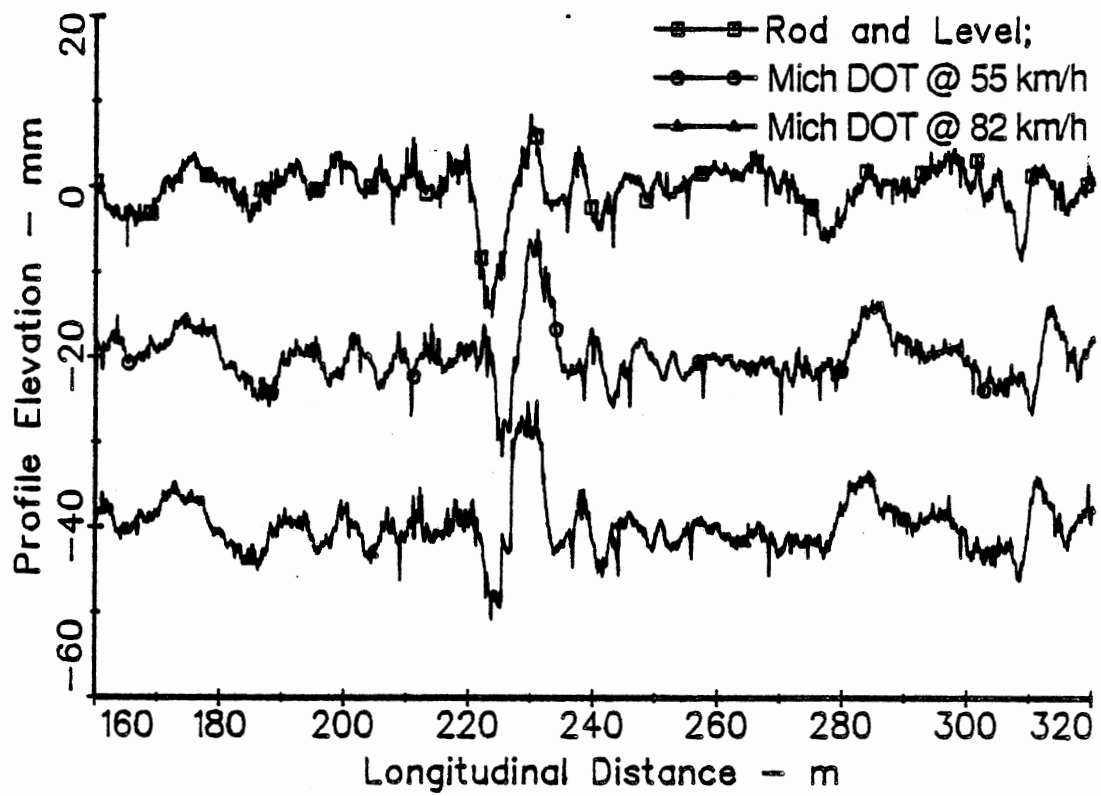
Figure 72. Measures from the Michigan DOT profilometer on a moderately rough road.
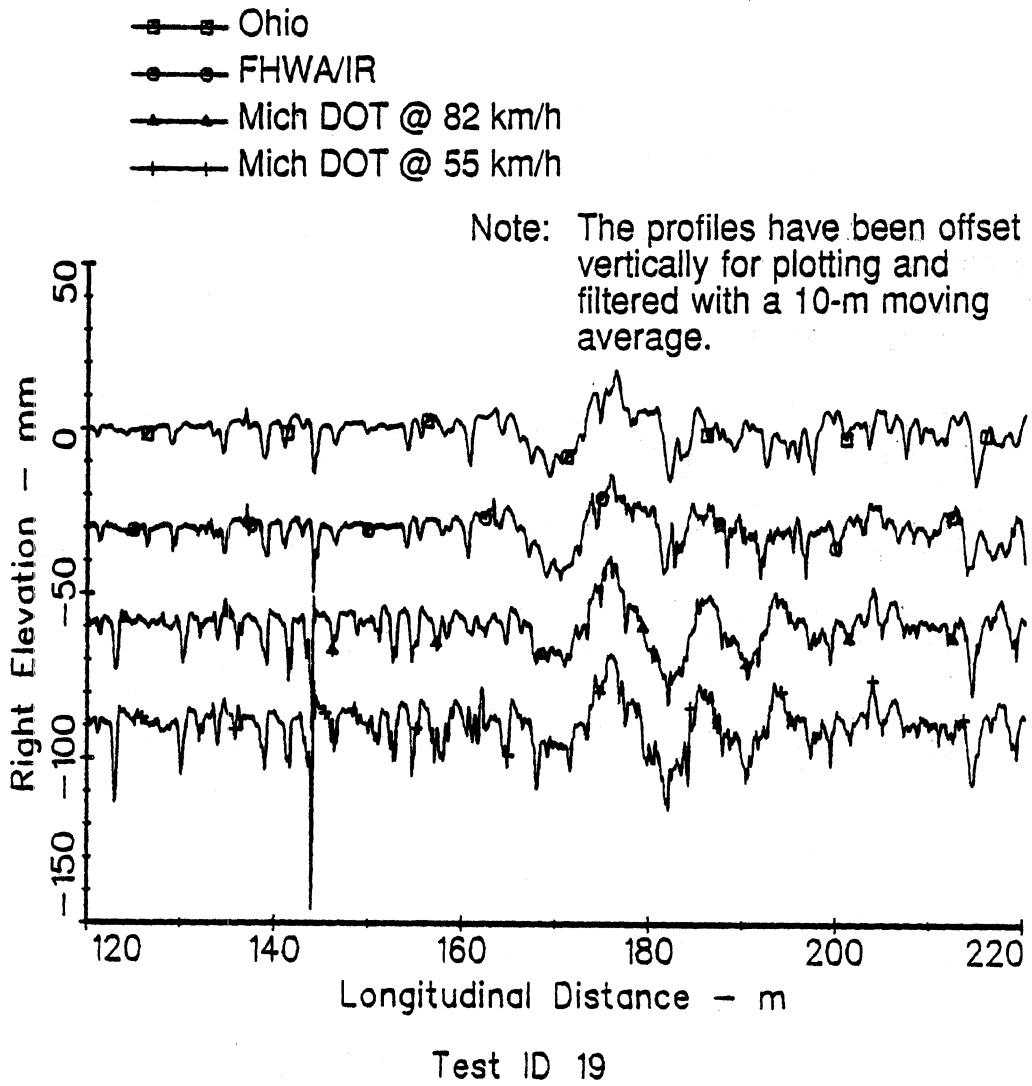
Figure 73. Comparison of several profilometers on a rough, patched surface.

131
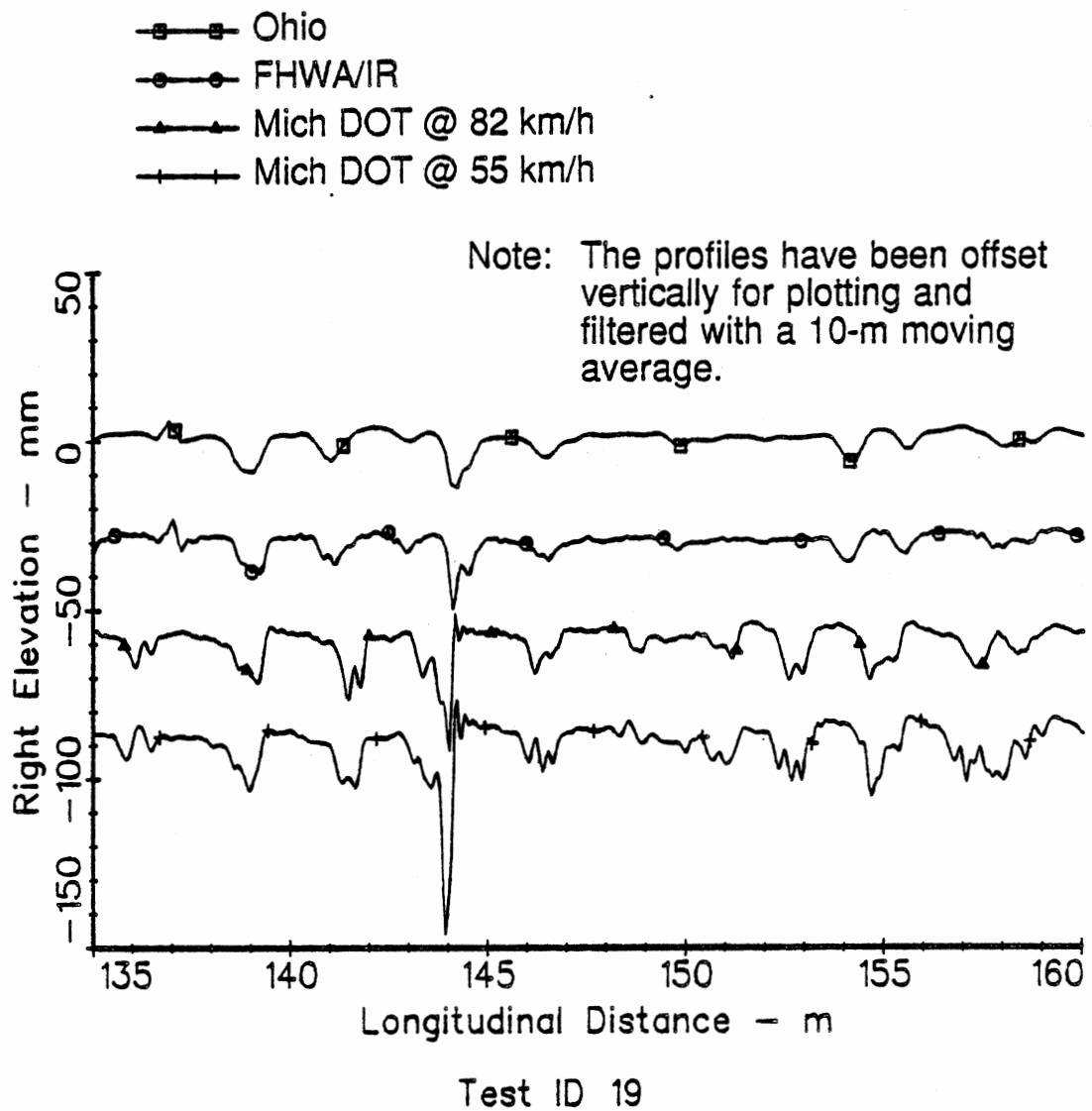
Figure 74. Close view of "crack" as seen by several profilometers.

An additional profile plot from the MDOT system is shown in figure 13.

Measurement of Roughness Indices

Figure 75 summarizes the ability of the Michigan DOT system to measure the IRI and MO roughness measures, as compared with the Ohio and FHWA/IR profilometers. The MDOT measures of IRI agree well for most of the sites, but on some, the MDOT results are higher than for the other profilometers. The measures of MO are nearly all too high, and there is greater scatter than when measuring IRI. As noted earlier, some of the MDOT profiles appeared to be labelled incorrectly, with regards to which wheeltrack was measured. This means that some of the scatter shown is possibly not the fault of the instrument.

Waveband Indices

The accuracy of the MDOT system over a full range of 1-octave wavebands is demonstrated in figures 76 and 77. For these plots, the reference is the FHWA/IR system, which closely matched the rod and level reference (see figures 28 and 29 for the validation using the left-hand wheeltrack). The results for the waveband centered at a 64-m wavelength show that a few of the measures on the roughest sites were quite a bit too high, while the others more-or-less agree with the reference. For the other wavebands, the measures from the MDOT system agree better with the reference, although they are typically higher on the average. On the smoother sites, good accuracy is shown for the wavebands centered at wavelengths of 16, 8, and 4 m/cycle. For the wavebands centered at shorter wavelengths, there is more scatter, with the scatter generally increasing as the center-wavelength decreases. As noted earlier, some of the MDOT profiles appeared to be labelled incorrectly, with regards to which wheeltrack was measured. This means that some of the scatter shown is possibly not the fault of the instrument.

Power Spectral Density Functions

Figure 78 compares PSD functions from the MDOT, Ohio, and FHWA/IR profilometers and show close agreement for wavenumbers between 0.02 and 0.5 cycle/m (wavelengths from 50 m down to 2 m). For the longer wavelengths, the differences in PSD amplitude are due mainly to the high-pass filters used by the different profilometers when computing profile. The MDOT and Ohio profilometers use similar filters set to attenuate wavelengths longer than 91 m (300 ft), whereas the FHWA profilometer was run

133
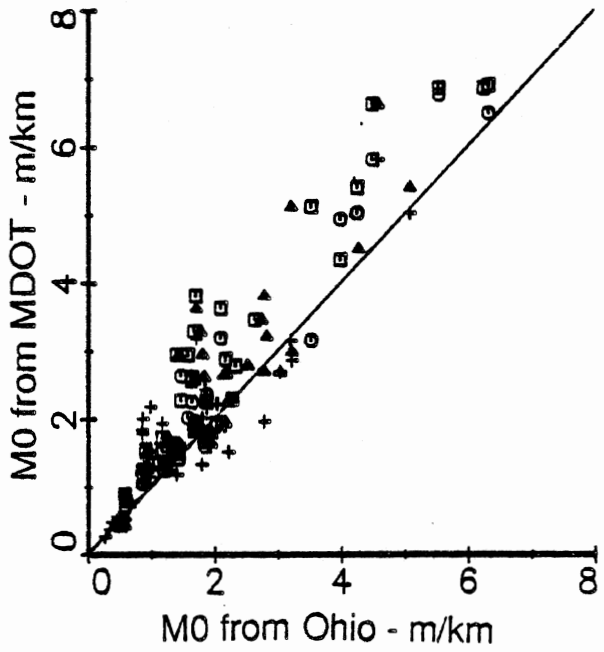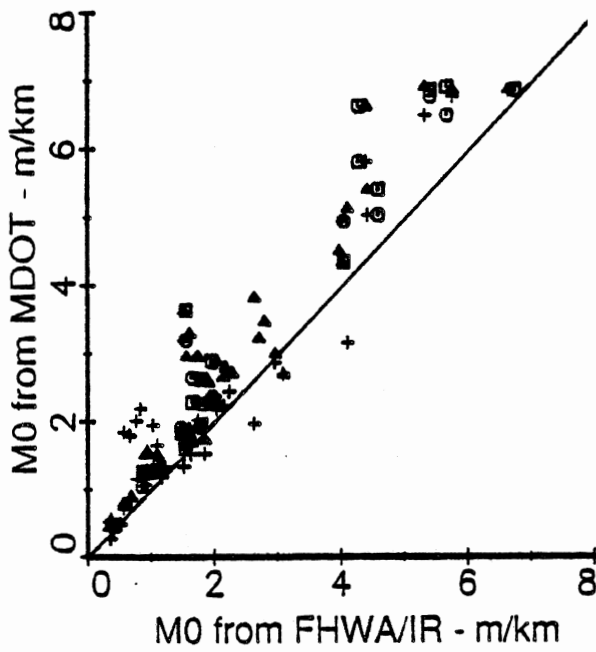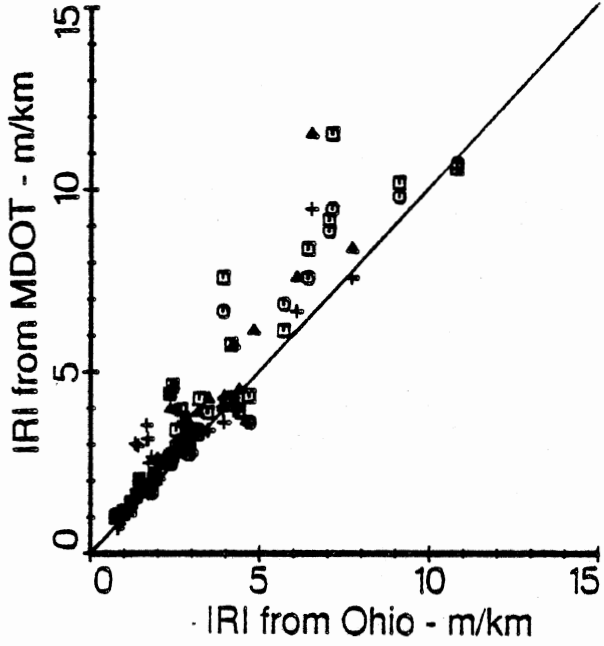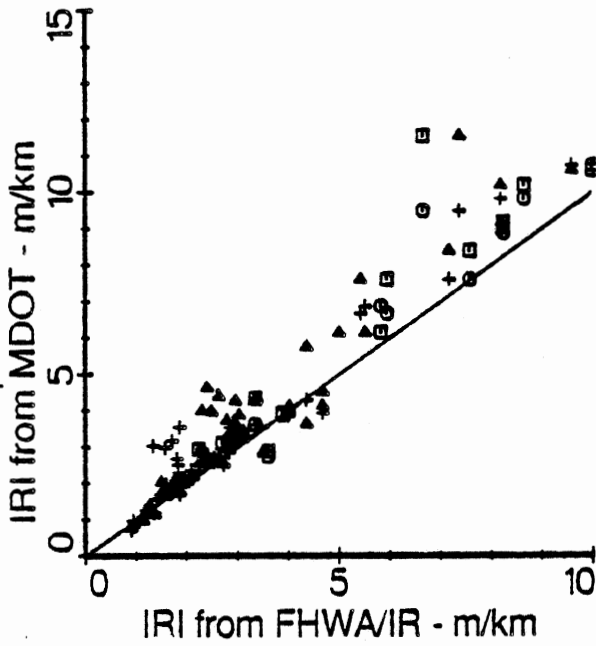
Figure 75. Measurement of IRI and MO with the Michigan DOT
profilometer.

134
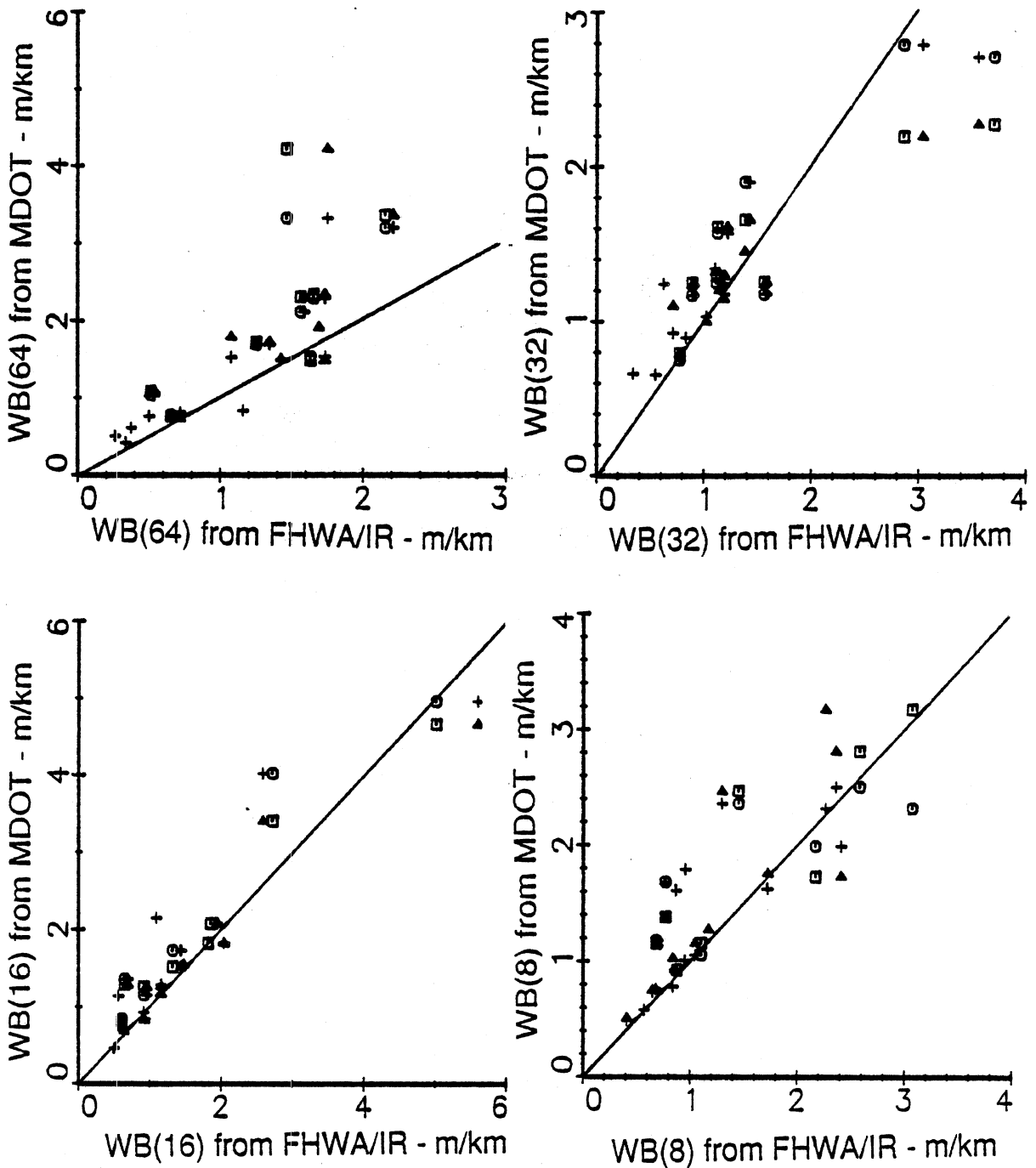
Figure 76. Measurement of waveband indices for the longer wavelengths
with the Michigan DOT profilometer.
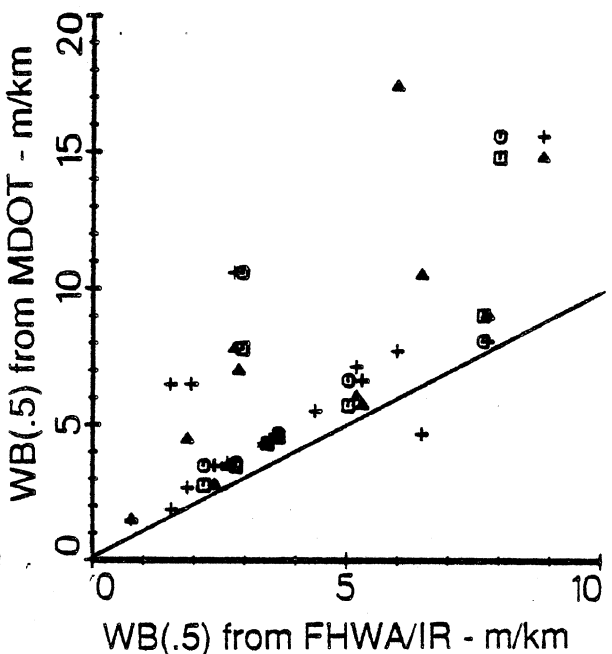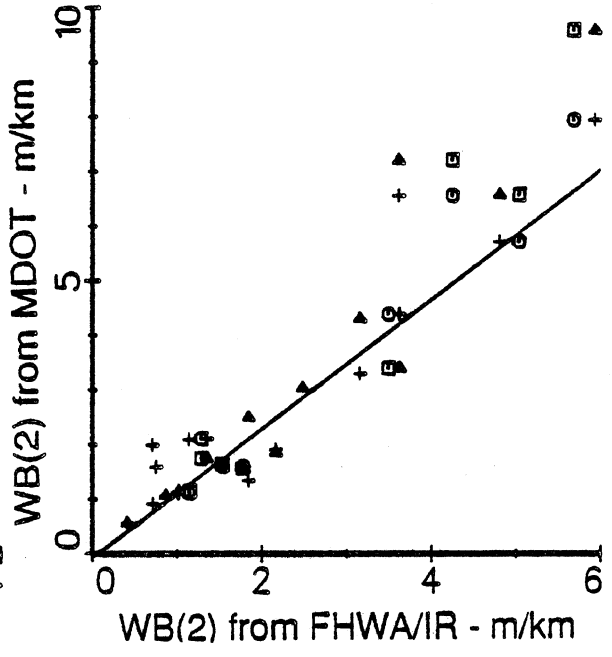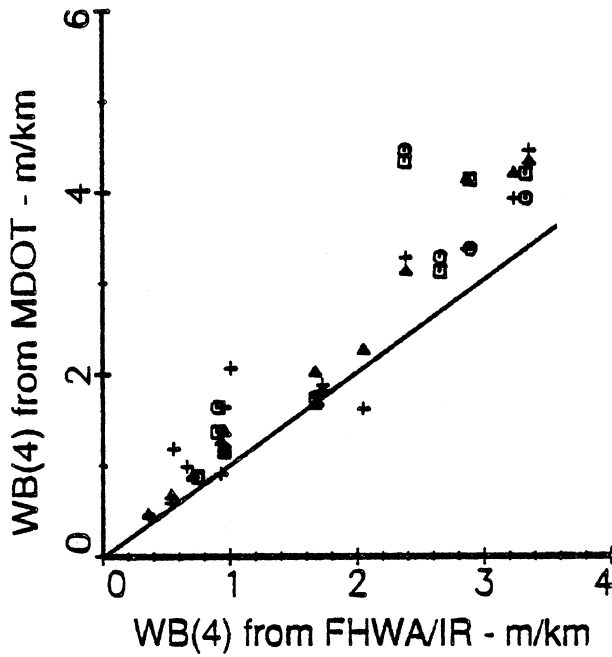
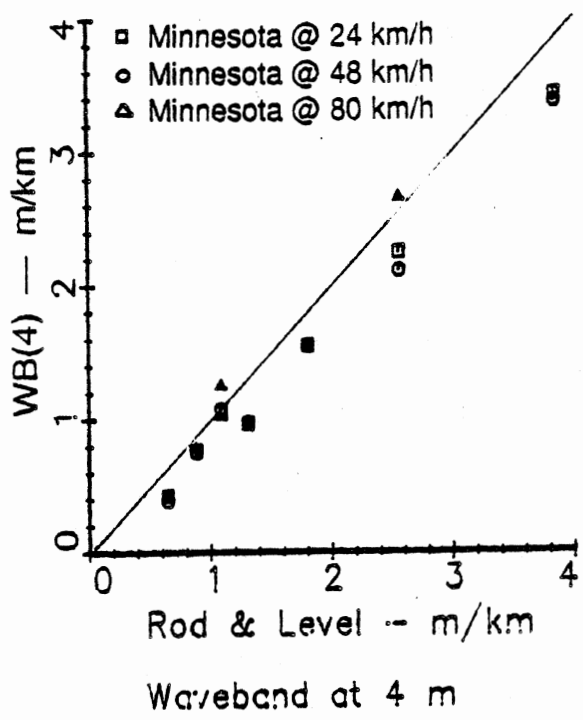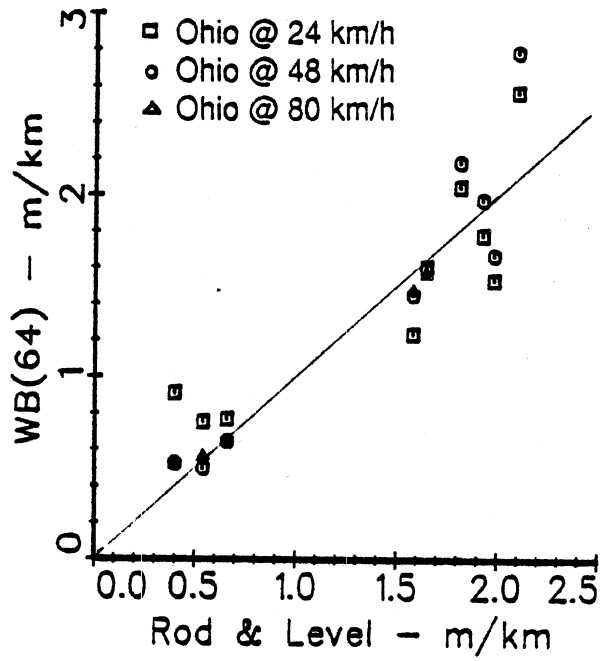Figure 77. Measurement of waveband indices for the shorter wavelengths with the Michigan DOT profilometer.

Note: The PSD functions have been offset vertically for plotting.
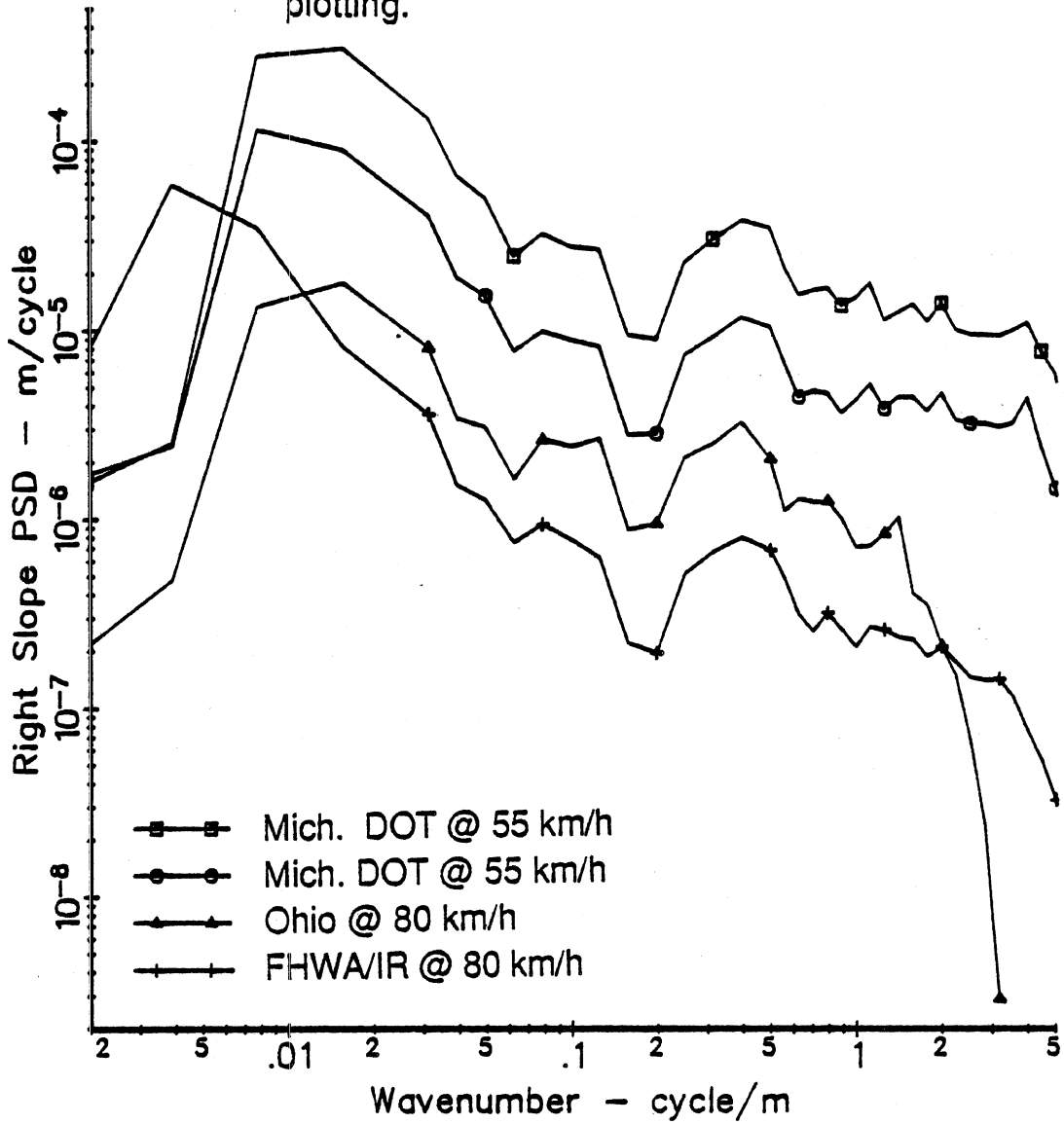
Test ID 5.

Figure 78. PSD functions from several profilometers on a long, moderately rough site.

137

with no attenuation of these wavelengths. At the highest wavenumbers—above 0.5 cycle/m—the rapid rolloff seen for the Ohio measure is due to the antialiasing filter employed with that system. The MDOT and FHWA instruments, which use different antialiasing filters, show close agreement for wavenumbers up to 0.8 cycle/m.

Figure 79 shows the PSD functions for the profiles shown in figures 73 and 74, and reveals how the cracks in the road appear at different wavenumbers. There is not much influence for wavenumbers less than 0.4 cycle/m, but for higher wavenumbers, the PSD functions from the MDOT profilometer are much too high.

The PSD plots all show a rolloff above 4 cycle/m—the result of antialiasing filters used when the analog profile signal was digitized in the laboratory.

Additional PSD functions from the MDOT system are shown in figures 70 and 81.

The Mechanical Follower-Wheel

In the earlier years of the GM-type profilometer, vehicle height was always measured with a mechanical follower-wheel. Several runs were made with the MDOT profilometer using one of the original follower-wheels instead of the optical sensor now used. Figure 80 compares the profile measures obtained using the different height sensors, and shows that the profile measurement from the mechanical system includes a high-frequency noise component added to the underlying profile shape. Figure 81 shows the corresponding PSD functions, and indicates rather clearly that the mechanical vibration of the follower-wheel leads to measurement error for wavenumbers above 1-cycle/m (wavelengths shorter than 1-m/cycle). Figure 80 also shows several spots where the follower-wheel bounced, resulting in measurement errors that indicate non-existant bumps at 315 m, 328 m, and 372 m along the horizontal axis.

Conclusion

The MDOT system is capable of measuring profile accurately over a broad range of wavelengths extending to 91 m (300 ft). Some of the runs were not as accurate, however, and not all of the test conditions were covered by the data submitted. Most of the profiles were measured only in the right-hand wheeltrack, so that validation of the system against the rod and level measures was not possible. It appears that some of the runs were not made in the same wheeltrack location as used by the other systems, because some of the MDOT profiles were reproduced quite well in repeat runs by MDOT, but did not match the

Note: The PSD functions have been offset vertically for plotting.
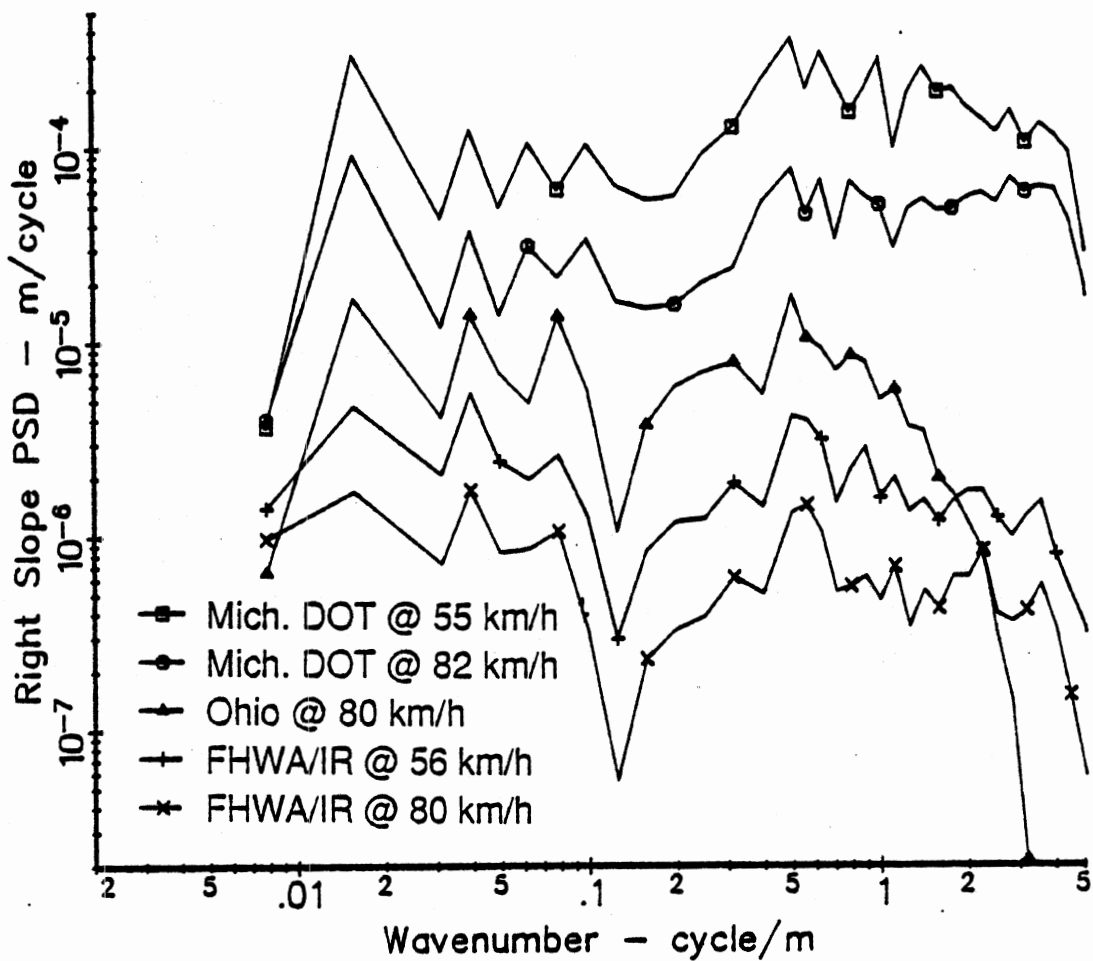
Figure 79. PSD functions from several profilometers on a rough, patched surface.
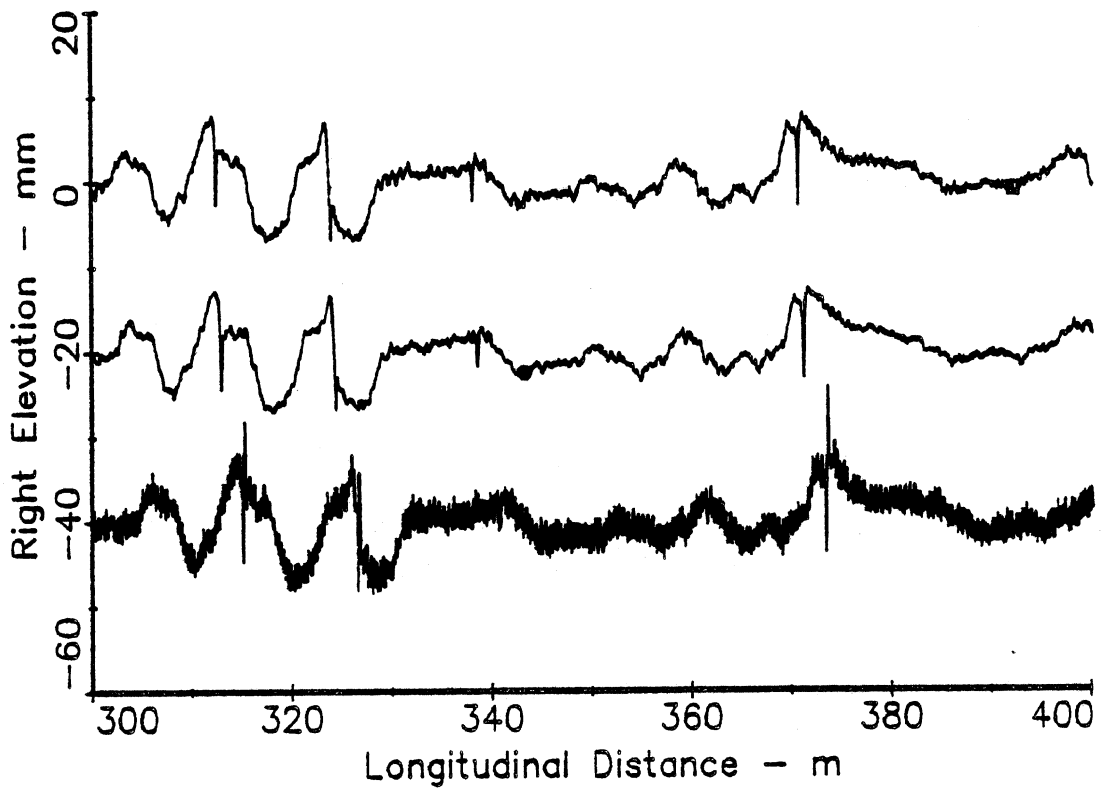
Figure 80. Comparison of profiles measured using the mechanical and optical height sensors of the Michigan DOT profilometer.
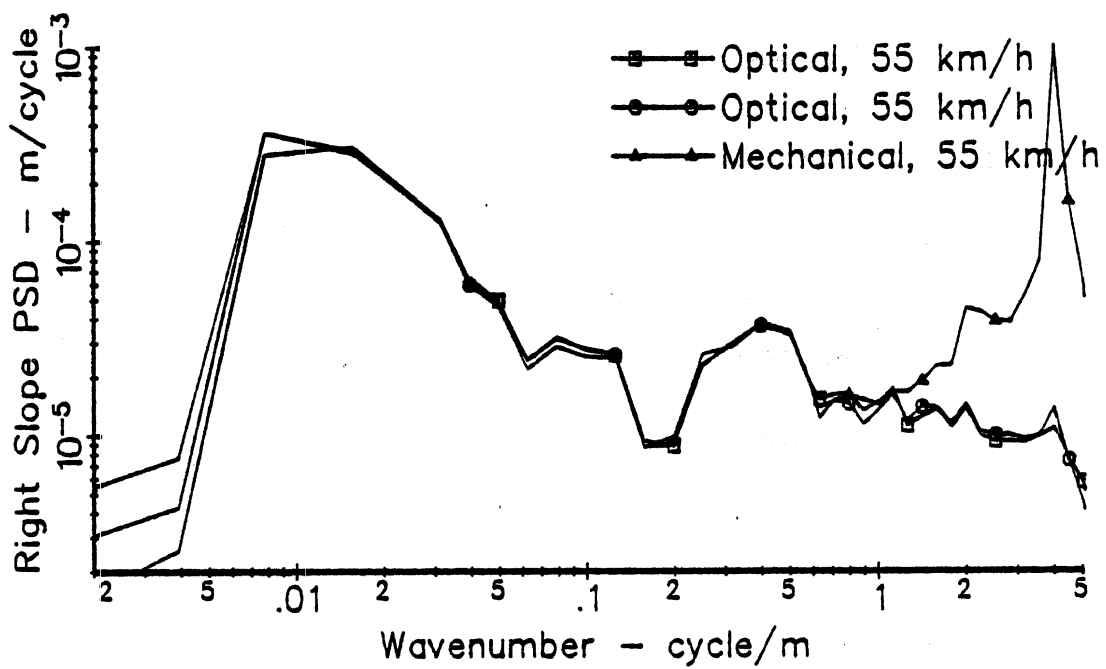
Figure 81. Comparison of PSD functions from the mechanical and optical
height sensors of the Michigan DOT profilometer.

profile measures from the other systems. Many of the sites selected to challenge the noncontacting sensors were not analyzed and thus the ability of the system to handle these conditions could not be demonstrated.

Several runs were made with a mechanical follower-wheel, used on the early GM-type profilometers. The results showed measurement error due to mechanical vibration of the assembly, which is eliminated when the noncontacting sensor is used.

Pennsylvania Profilometer

The Pennsylvania Transportation Institute (PTI) currently maintains and operates a K. J. Law model 690 Surface Dynamics Profilometer owned by the State of Pennsylvania. This is a GM-type inertial profilometer closely following the original GM design, using mechanical follower-wheels and analog data processing. A photograph of the unit is shown in figure 82. PTI has been exploring various noncontacting height sensors to measure the distance between the vehicle body and ground, but for the RPM, the system used the regular follower-wheels (visible in figure 82), in order to provide a link with profilometers of the past. The original 690 system included an analog computer that produced profile during measurement, and a tape recorder to store that profile signal. In the PTI system, the unprocessed transducer signals (distance pulses, vehicle height, and vertical acceleration) are normally stored directly on the tape recorder. These signals are later digitized in the laboratory, and processed to obtain quarter-car roughness measures without actually computing the profile.[19]

Although PTI does not routinely obtain profiles, there was interest in the quality of the profiles that can be obtained using the accelerometer and height signals from this type of system, because a great deal of profile data have been collected with these systems in the past. Similar 690 systems are also owned by the States of Kentucky and Texas, and by the government of Brazil. The Michigan DOT system was also operated on a few sites using a similar mechanical follower-wheel, and representative results were shown in the preceding sub-section.

The Pennsylvania profilometer was not operated on all of the test sites. It was used only on the smoother public road sites covering roughness levels between 1 and 5 m/km on the IRI scale, because of the tendency for the follower-wheel system to break on rough surfaces. The system broke during testing at the GMPG on one of the smooth sites, and it was not taken to the rougher test area. Unfortunately, PTI was not able to provide UMTRI with a standard 9-track computer tape with the measured data, and therefore no results could be included in this report.
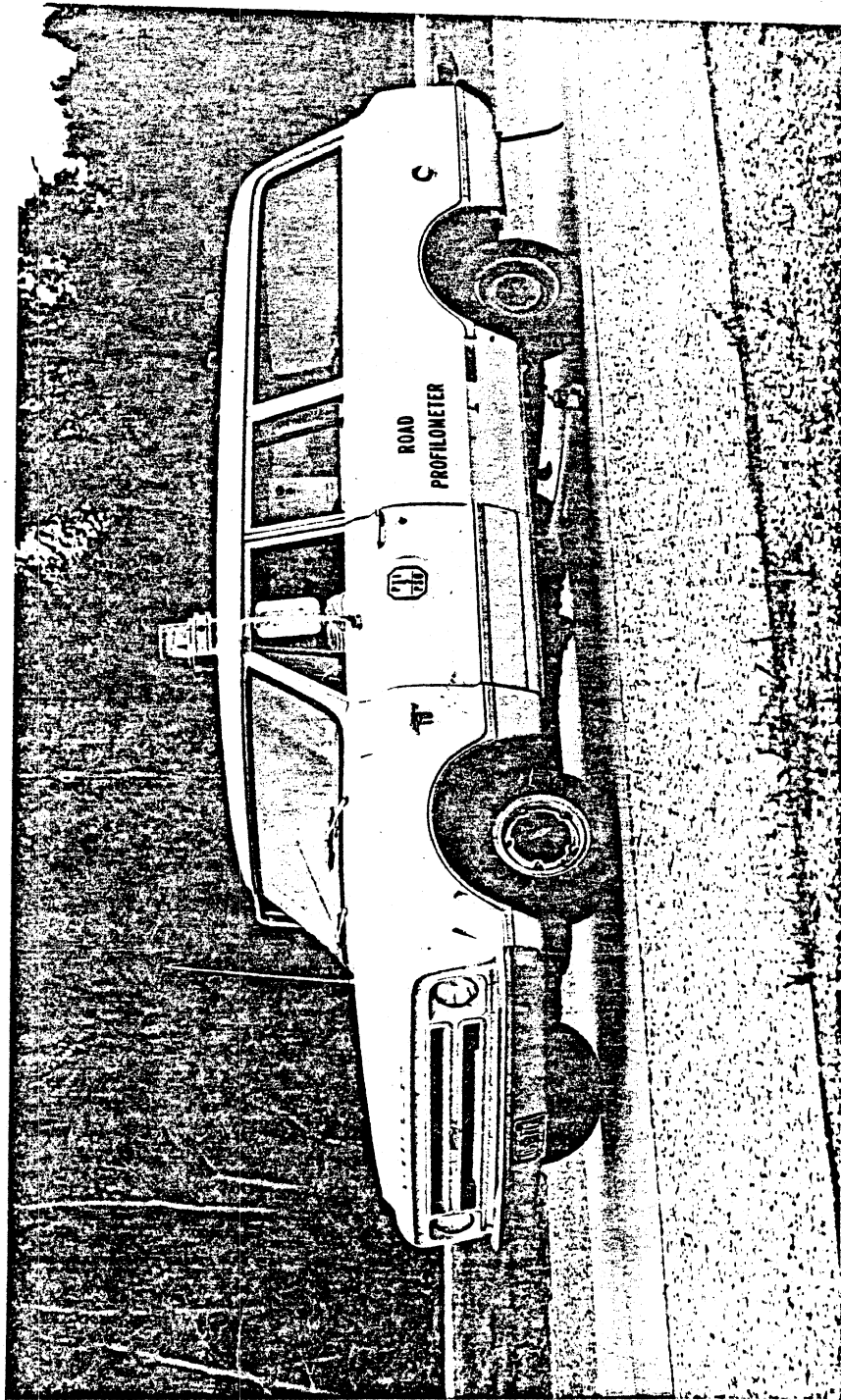
Figure 82. The Pennsylvania profilometer.

143

South Dakota Profilometer

Hardware Description

The South Dakota Department of Transportation (SDDOT) designed and built its own GM-type profilometer system in 1981.[4] The profilometer consists of a portable instrumentation package that can be mounted in a passenger car, and powered with an inverter from the electrical system of the car. Figure 83 shows the profilometer as it appeared during the RPM. The system is based on a DEC PDP-11 minicomputer, which controls the testing and performs the profile computations. An ultrasonic road sensor (an instrument grade version of the Polaroid ultrasonic device used for autofocusing in cameras) is mounted on the front bumper along with a vertical accelerometer. The computer, disk drive, and electronic signal conditioners are placed in the back seat of an ordinary sedan passenger car. The system is controlled by an operator sitting in the front passenger seat, using a laptop keyboard with a liquid crystal display.

The South Dakota system uses a unique method for computing the profile. The accelerometer signal is sampled at constant intervals of time (controlled by a clock in the computer), and is double-integrated numerically to update the absolute height of the vehicle at each time step. This method of computing vehicle height does not require measurement of the vehicle travel speed. Distance to the road, measured by the ultrasonic height sensor, is sampled at regular intervals along the road, as specified by the operator and detected with a wheel pulser. At each sampling position, the relative vehicle height (as measured with the ultrasonic sensor) is subtracted from the most recent value of the absolute vehicle height to obtain the profile elevation. The profile elevation values are recorded during measurement on floppy disk.

The profile signals on the floppy disks that were obtained during the RPM were transferred to 9-track tape in South Dakota several weeks after the experiment, and the tapes were sent to UMTRI. As table 4 in the "Experiment" section shows, the South Dakota system made repeat measurements on all 27 of the test sites. There is no standard speed used with the system, as it is designed to operate at prevailing traffic speeds. On most of the public road sites, the measures were made at typical speeds. On the GMPG sites, some of the repeat runs were also made at lower speeds.

The profile signal is normally sampled at a 305-mm (1.0-ft) interval. The ultrasonic transducer limits the sample frequency, because new measures cannot be made until the

144
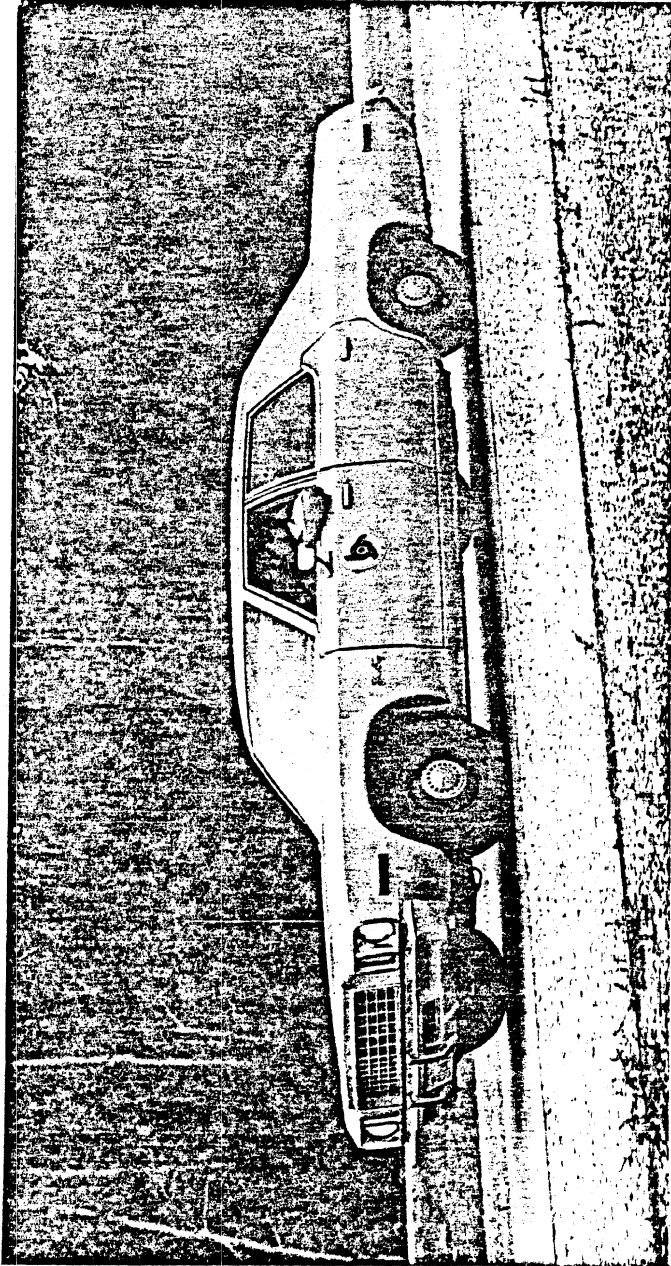
Figure 83. The South Dakota profilometer.

145

echos from the previous measure have dissipated. Because the limit is based on a time interval, a shorter sample distance can be used when the measuring speed is reduced. Thus, some of the lower speed tests were recorded using shorter intervals of 152 mm (0.5 ft) or 76 mm (0.25 ft). To save disk space, the profile is stored by recording the changes in elevation at each sample, rather than the total elevation. (Because the changes in elevation are small over the sample interval, even if the elevation values are large, fewer digits are needed to store the profile using this method.) The original profile can be reconstructed later by serial addition of the differences. The profiles were recorded on disk with a resolution of 3.0 mm (0.01 ft)—approximately the resolution of the ultrasonic sensor.

As with the other GM-type profilometers, the South Dakota system uses a filter to remove the longest wavelengths. For the RPM, the filter was set to remove wavelengths longer than 305 m (1000 ft).

As a result of the RPM, an error in the software of the profilometer was discovered by SDDOT and corrected. Therefore, the results obtained in the RPM may not apply to the current system. Even with the software error, the South Dakota system showed capabilities as a profilometer and the findings are relevant until the system is tested again in South Dakota. Thus, the results of the RPM are presented below, with the qualification that the system has been since modified.

Profile Plots

Many of the profile measurements on a given site by the South Dakota system are nearly identical in appearance when plotted, despite different measurement speeds. Figure 84 shows an example of the close agreement between three runs made over the same site at different speeds. Comparisons of data from the profilometer and the rod and level showed that the South Dakota profilometer can capture the profile shape correctly, regardless of speed, on surfaces with high or medium roughness. Figure 85 shows an example of the agreement that can be obtained.

However, the results of the RPM revealed that the unit would not produce the correct profiles under all conditions. Careful examination of the RPM data by SDDOT staff revealed that there were two separate problems with the system. One potential problem involved an error in the initialization of the profile computation, which occasionally causes the beginning of the profile to include a transient error in addition to the correct profile, as shown in the bottom trace in figure 86. This behavior only influences the longest wavelengths included in the profile, and only at the beginning of the run. It has little or no

146
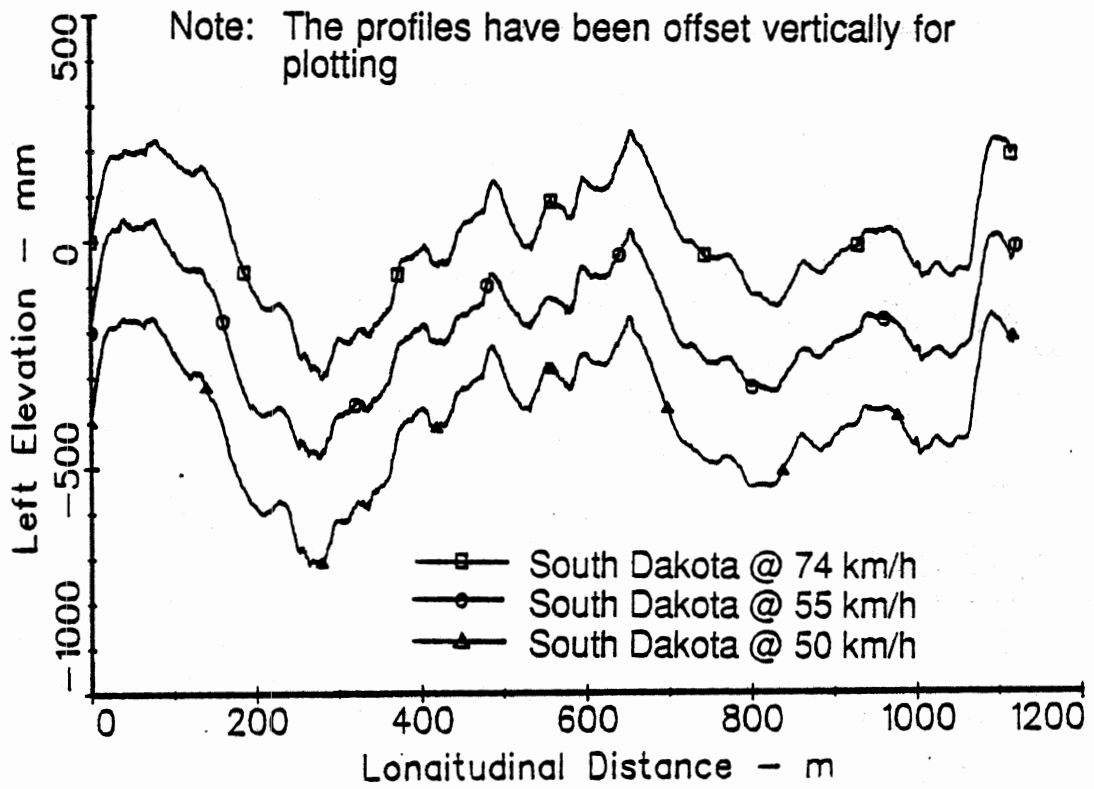
Figure 84. Repeatability of the South Dakota profilometer.

Note: The profiles have been offset vertically for plotting and filtered with a 10-m moving average. They are not precisely synchronized.
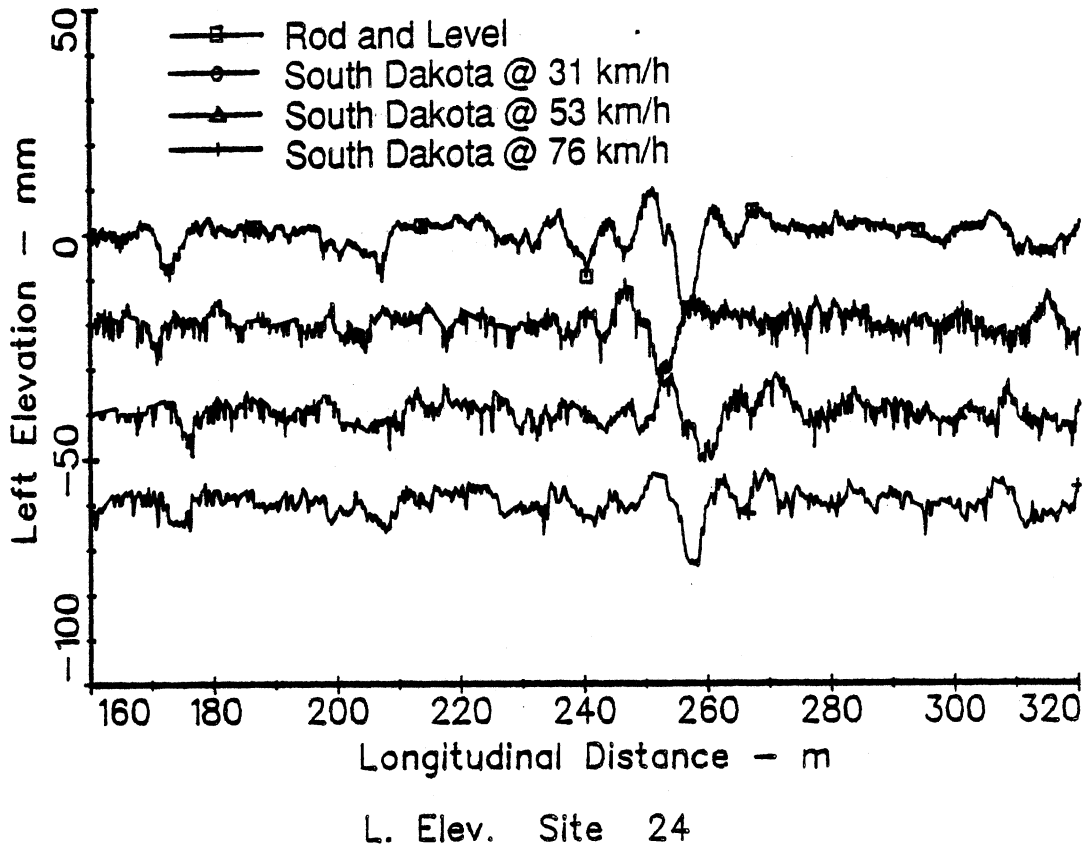
Figure 85. Measures from the South Dakota profilometer on a moderately rough road.
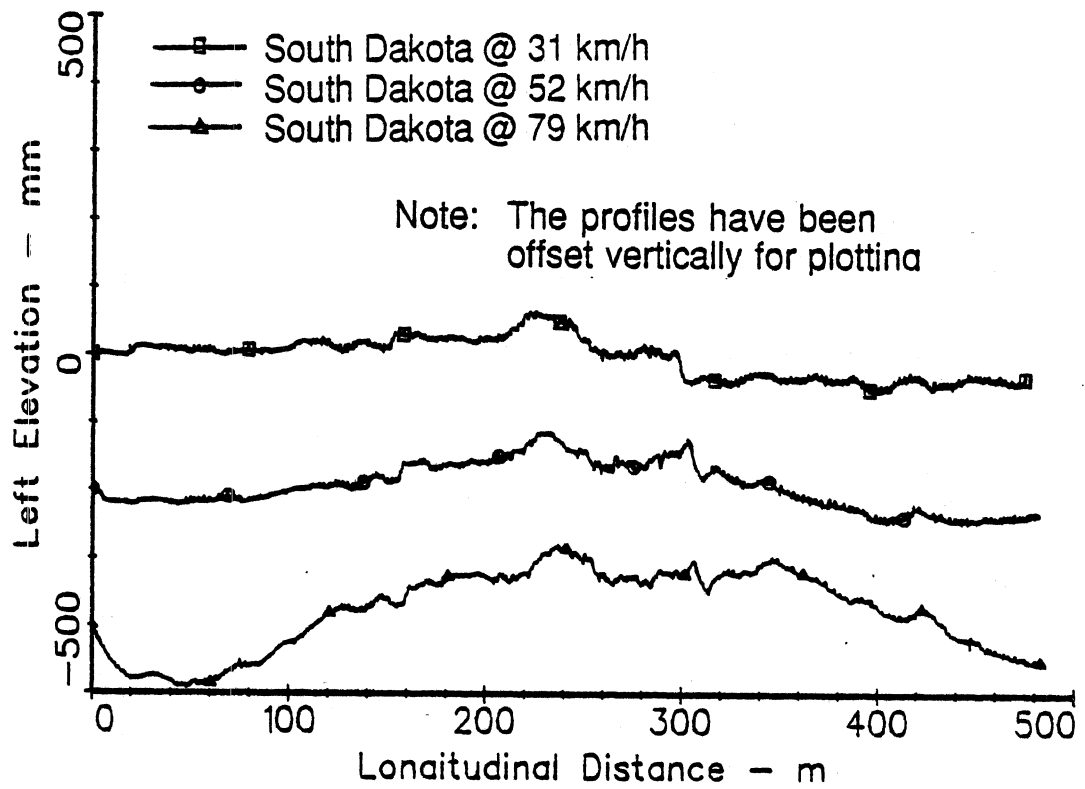
Figure 86. An example of the initialization problem with the South Dakota profilometer.

149

affect on most summary roughness indices, such as the IRI. This peculiarity was known by the staff at SDDOT, but was not considered to be a serious problem because the profilometer is normally started before reaching a test area so that initialization effects can settle out.

The second problem, discovered after the RPM, was caused by a simple error in the way the profile is stored on disk. As mentioned earlier, the profile is recorded as a series of differences in elevation from one sample point to the next. The profile values were truncated to a convenient resolution of 3 mm (0.01 ft) before storage. The truncation operation is supposed to be applied to the absolute elevation values *before* the differences are computed; however, an error was made in the software and the truncation occurred *after* the differences were computed. The software has been corrected, and SDDOT plans to validate the profilometer against a static profile measured in South Dakota.

The consequence of this problem is that the measured amplitudes of the profile are always lower than they should be, with the effect becoming more profound when the difference amplitudes are small. The profiles shown in figure 87 were measured on one of the smoothest sites, such that the changes in elevation were often truncated to zero. Even when the changes were not completely eliminated, they were reduced by the truncation with the effect of reducing profile amplitudes. The loss becomes less evident as the surface roughness increases, as was seen in figures 84 and 85. Figure 88 shows how the same problem affects measures made using a short sample interval. As the interval is made shorter at lowered speeds, the differences in elevation between adjacent points become smaller, and therefore the truncation error becomes more significant. At the two higher measurement speeds used for this figure, the profilometer measures match the true profile overall, although details of the manhole cover at 154-m along the horizontal axis are lost due to a long sample interval of 305 mm (1.0 ft). At the lowest speed of 31 km/h (19 mi/h) the sampling interval was reduced to 76 mm (0.25 ft) such that the manhole cover becomes better defined. However, the profile elevation is noticeably attenuated by the truncation error.

Measurement of Roughness Indices

Figure 89 shows how the IRI and MO roughness indices computed from the South Dakota profile compared with the reference during the RPM. The scatter plots show that the system can measure the IRI and MO statistics best for roads having roughness levels from 2 to 5 m/km on the IRI scale. On the roughest sites at GMPG, the measures from the South Dakota system tend to be lower than the reference values. The measures from the

150
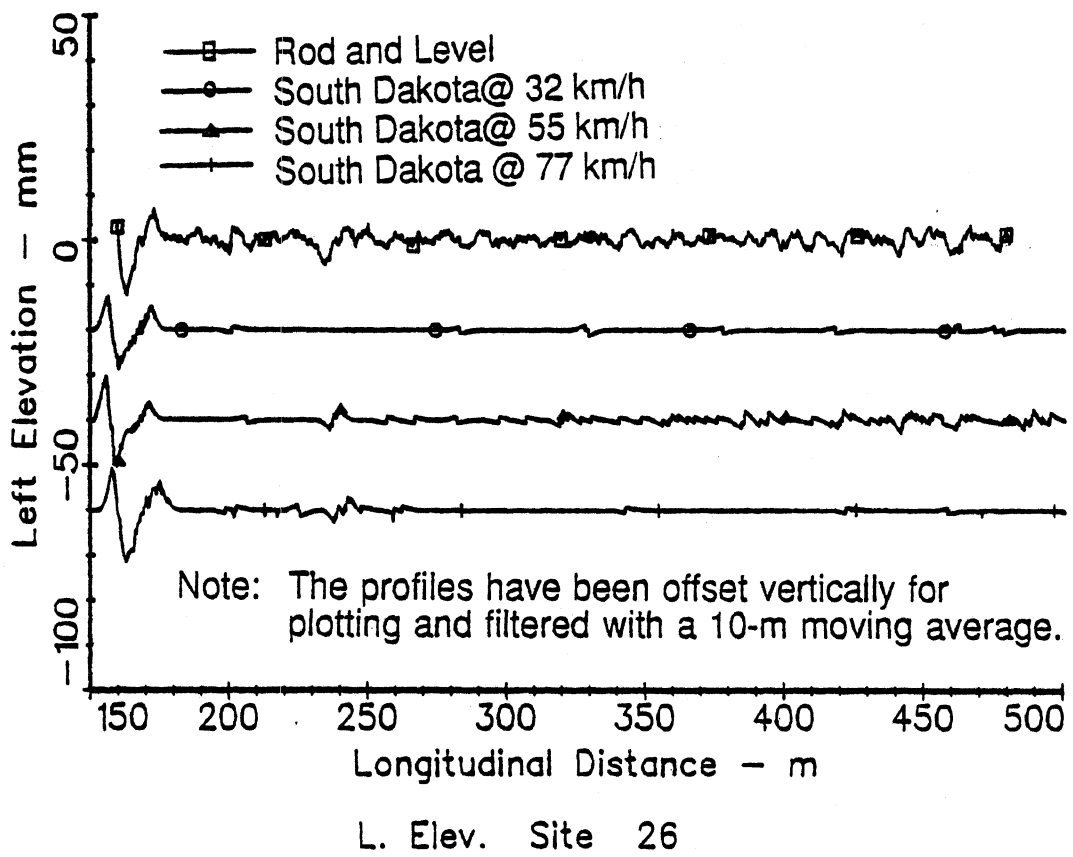
Figure 87. An example of the truncation problem with the South Dakota profilometer on a smooth site.

151
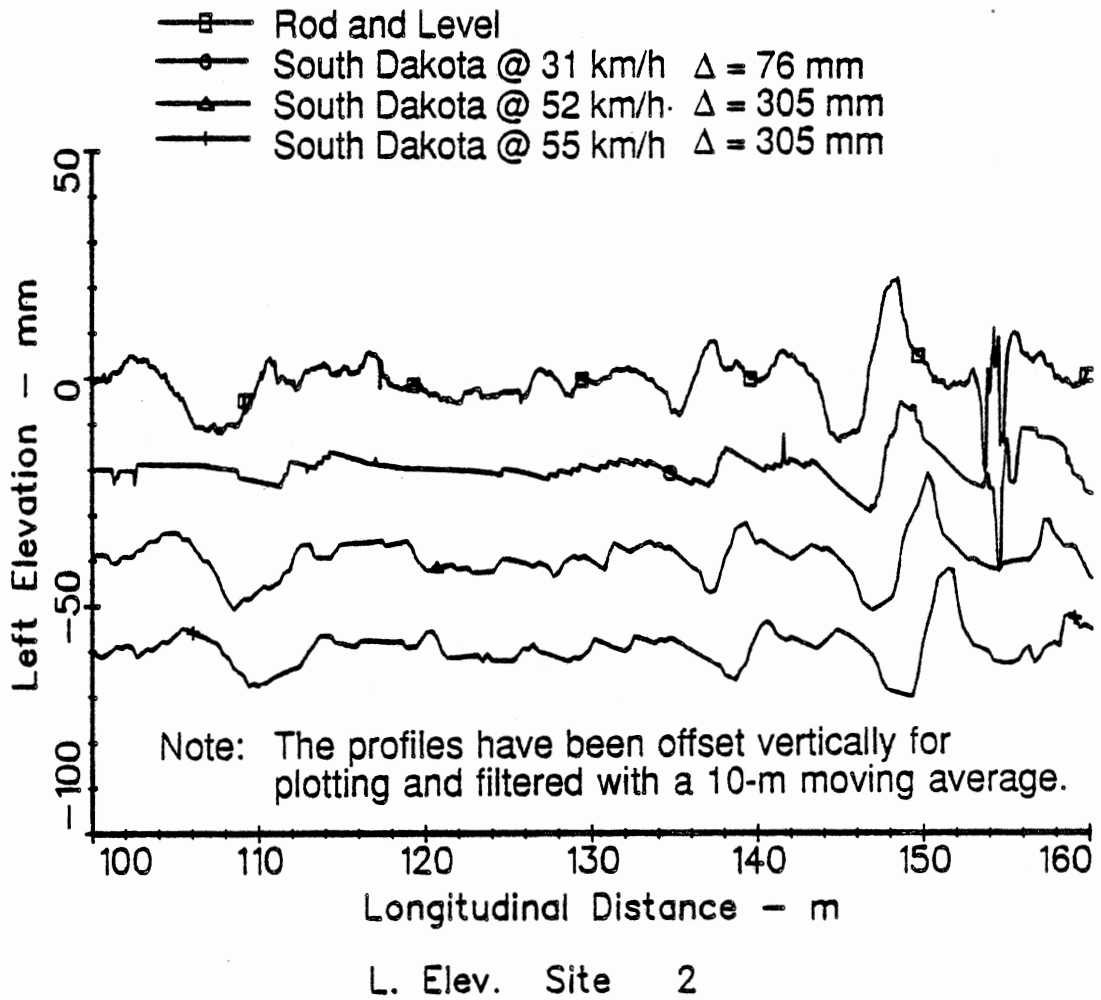
Figure 88. An example of the truncation problem with the South Dakota profilometer using a short sample interval.

GMPG Sites
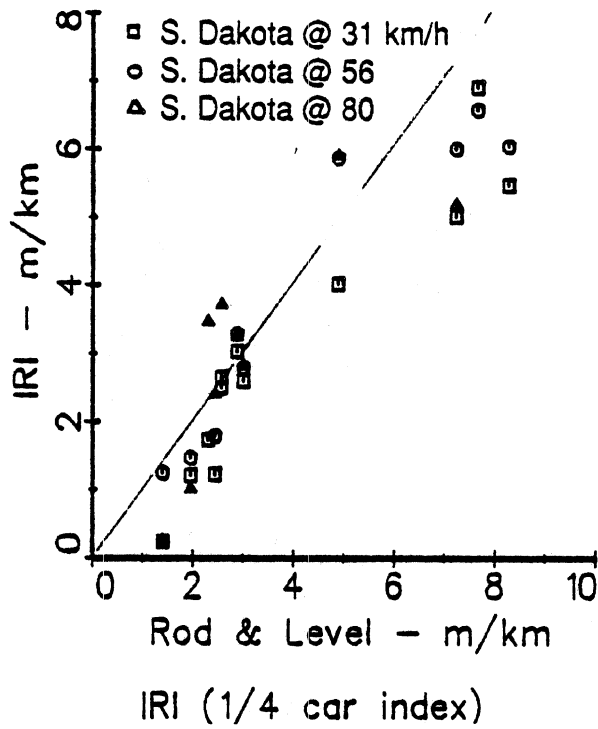
All Road Sites
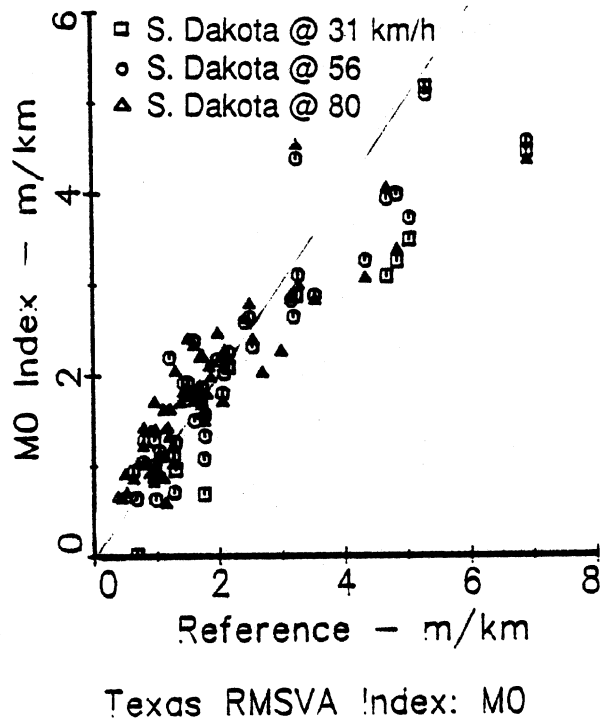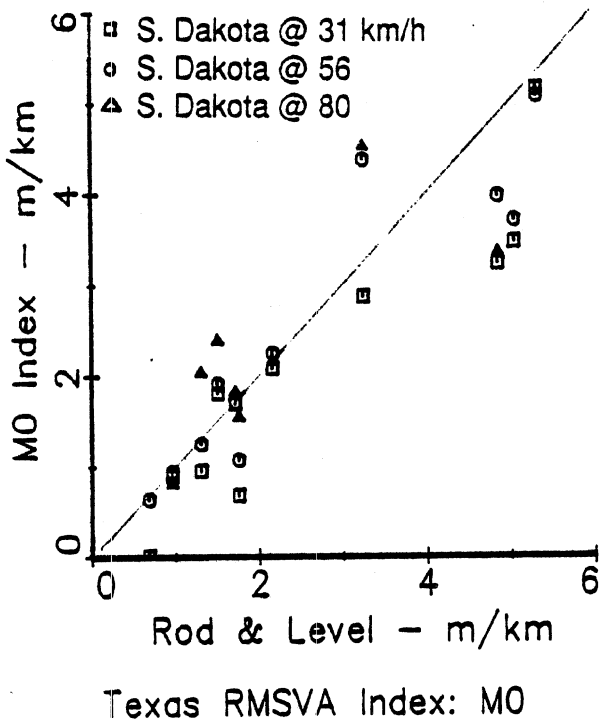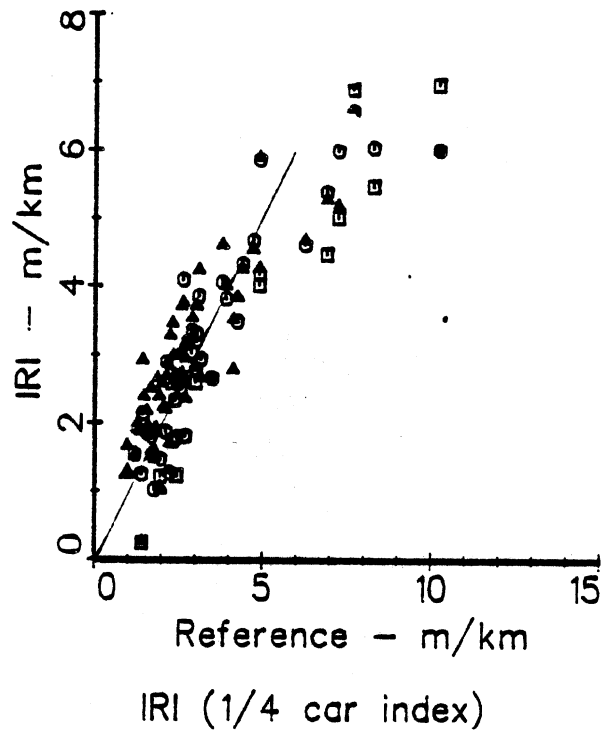
Figure 89. Measurement of IRI and MO with the South Dakota
profilometer.

153

South Dakota system also gave low values of IRI on the smoother GMPG sites, probably due to the truncation error previously described.

In addition to the truncation error described in "Profile Plots," a second roundoff effect remains due to the limited resolution of the ultrasound height sensor. In past studies, limited resolution in a profile signal has been observed to produce errors in calculating roughness indices, making the calculated numeric higher than the true value.

Waveband Indices

Figures 90 and 91 show how accurately the South Dakota system measured RMS slope over 1-octave wavebands at the time of the RPM. For the longer wavelengths represented in figure 90 , the measures from the South Dakota system tend to be too low in most instances. The results for the wavebands centered at wavelengths of 4 and 2 m, shown at the top of figure 91, show the best accuracy for this system. Except for the roughest sites (where the South Dakota measures tend to be lower than the reference values), the measures are essentially unbiased. The two plots at the bottom of figure 91 show that the measures for the wavebands centered at the shortest wavelengths are not biased, but they do include substantial random error.

As mentioned above, a second roundoff effect exists that is due to the limited resolution of the ultrasonic height sensor. This effect, which makes the calculated numeric higher than the true value, is more significant for indices covering short wavelengths. It becomes negligible for wavebands covering longer wavelengths.

Power Spectral Density (PSD) Functions

The PSD plots that were obtained from the South Dakota measurements approximately match those from the rod and level on some of the GMPG sites, but often showed reduced amplitudes over a broad range of wavenumbers. Figure 92 shows the PSD functions for the same three runs that were shown in figure 85. If the South Dakota measures were perfect, all of the PSD plots would be parallel, separated only by a factor of 3.16 (the square root of 10) on the vertical scale. The measures made at 53 and 76 km/h (33 and 47 mi/h) do match the rod and level for wavenumbers from .01 to 0.3 cycle/m (wavelengths from 100 to 3 m), but at higher wavenumbers (wavelengths shorter than 3 m) the amplitudes are disproportionately high. The PSD from the 31-km/h (19-mi/h) measure is known to be most influenced by the truncation problem, and does not match the reference PSD over any significant range of wavelengths.

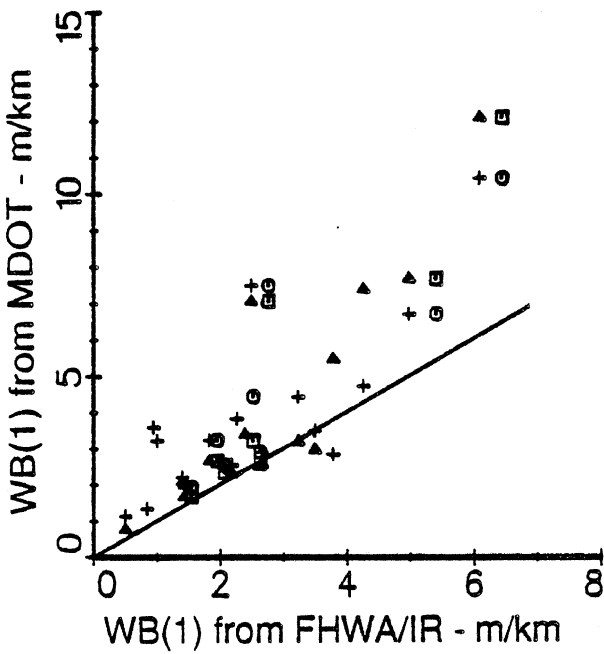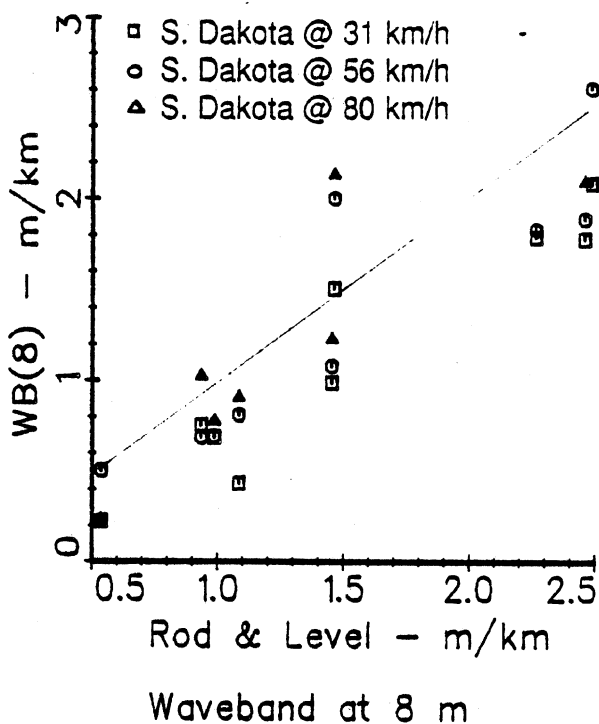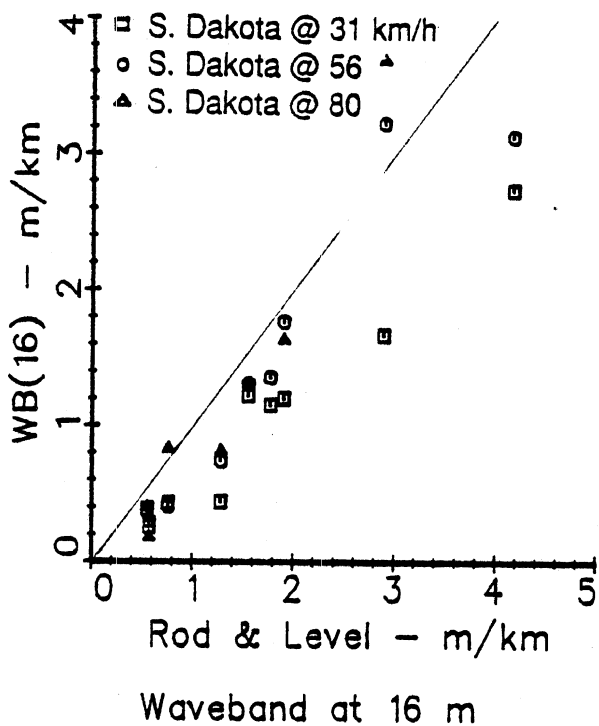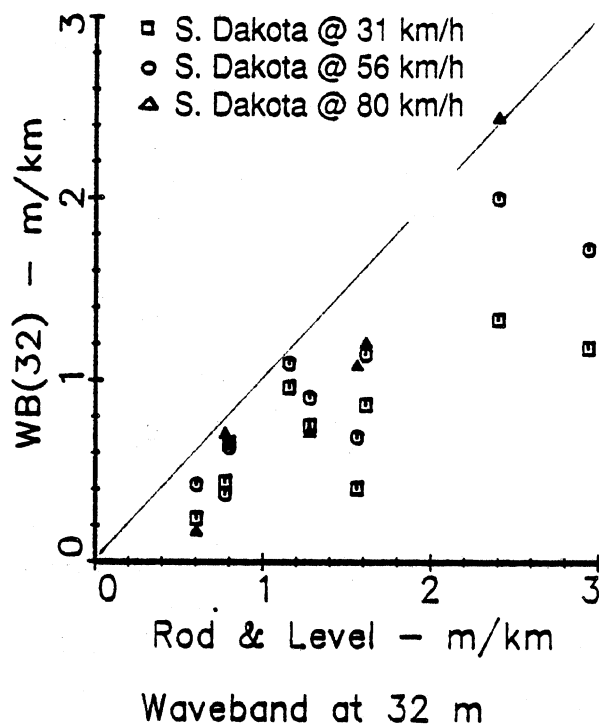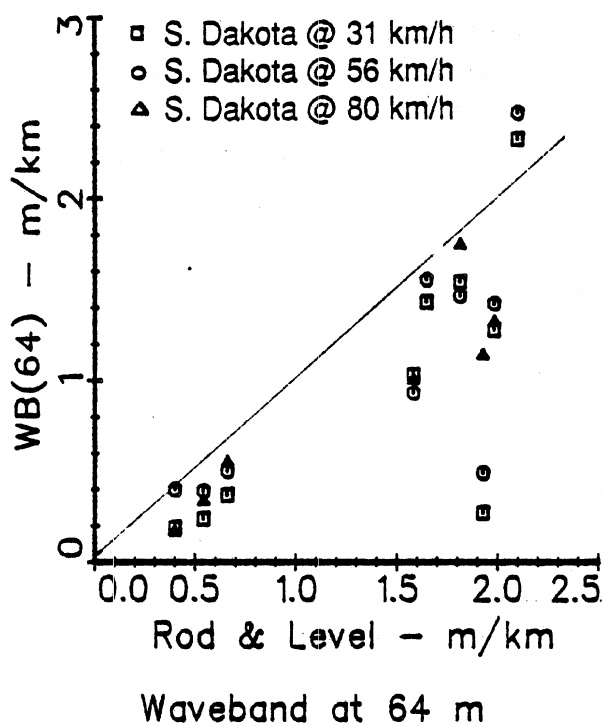Figure 90. Measurement of waveband indices for the longer wavelengths with the South Dakota profilometer.
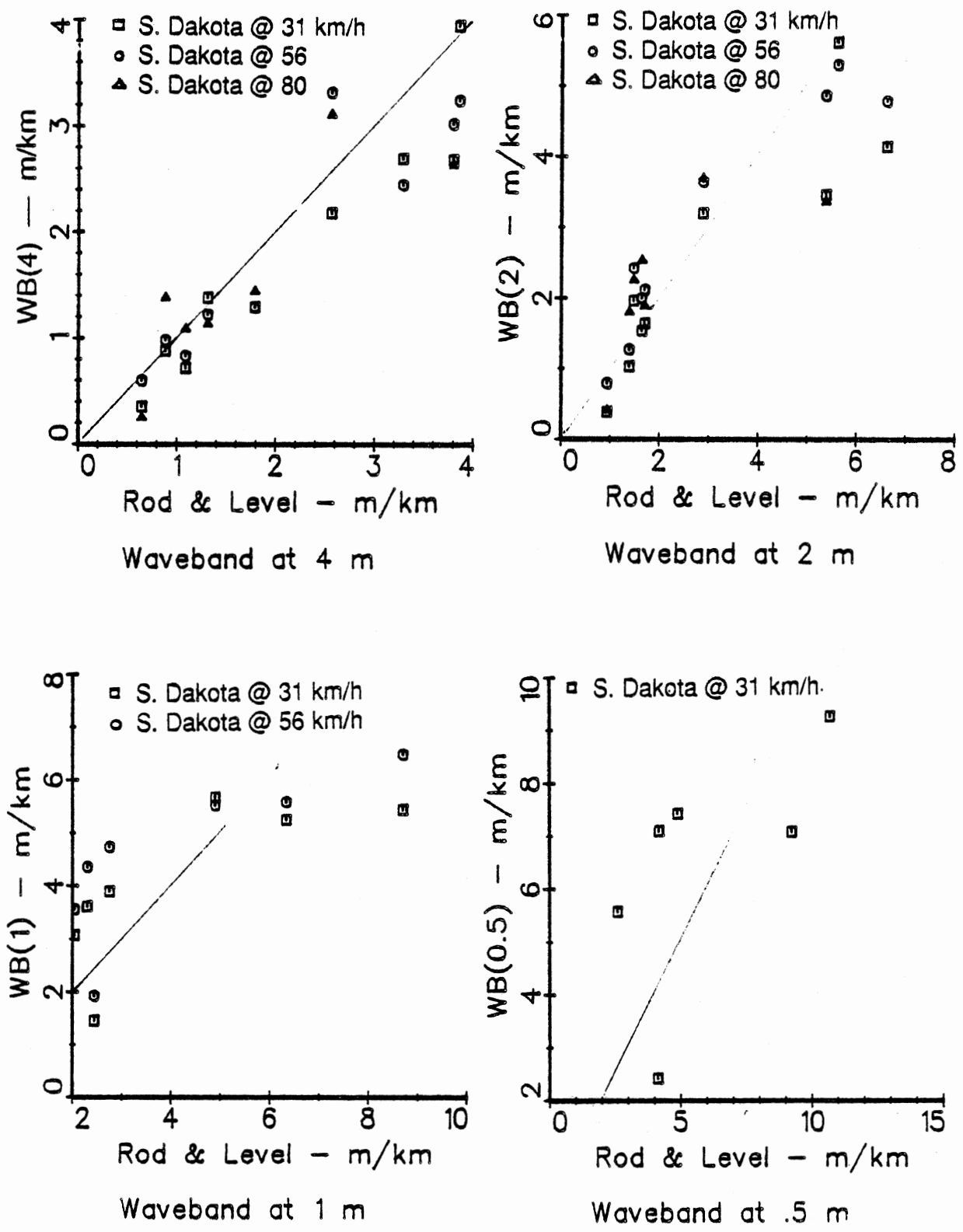
Figure 91. Measurement of waveband indices for the shorter wavelengths with the South Dakota profilometer.
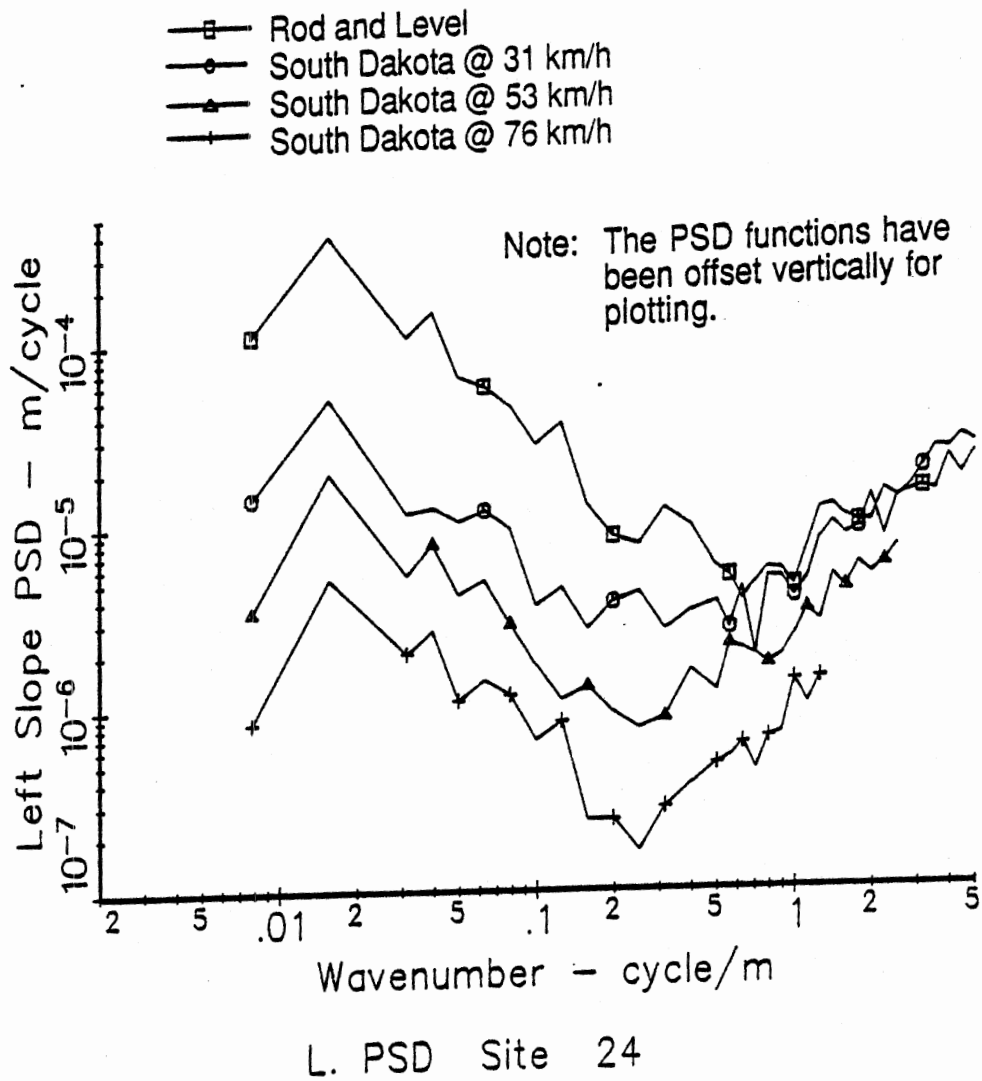
Figure 92. PSD functions from the South Dakota profilometer on a site with medium roughness.

Overall, the PSD plots show that the South Dakota system responds to a broad band of wavenumbers, but that the measures are not always accurate in amplitude. Improvements would be expected with the modification in data recording procedures to eliminate the truncation problem.

Conclusion

The profilometer built and owned by SDDOT appears to have the potential of measuring profile for moderately rough to rough roads over a full range of wavelengths. On smooth roads, the limited resolution of the ultrasonic height sensor might limit its accuracy. Due to an error in the system software, the actual limits of the instrument could not be determined from the data collected in the RPM. The error has been corrected, and another validation experiment is planned by the SDDOT to determine the accuracy.

VTI Road Surface Tester

The National Swedish Road & Traffic Research Institute (VTI) has developed a road surface tester for measurement of rut depth, roughness, macrotexture, and friction.[6] The system uses an array of laser sensors on the front bumper to sense the road surface for its many functions. An accelerometer on the bumper is used in combination with the laser sensors to compute a comfort value in the range of 0 to 9.

The VTI Road Surface Tester, shown in figure 93, was licensed to Novak, Dempsey & Associates, Inc. (317 West Colfax, Palatine, Illinois 60067) in the United States at the time of the RPM. Although the RST did not record profile at the time, it has the basic layout of the GM-type profilometer. An invitation was proffered for it to participate in the RPM, under the plan that profile recording would be added to the system by the time of the meeting. The VTI designers modified the system to record the accelerometer and laser signals on floppy disk for later profile computation. However, within the brief preparation time available, they could not verify the system. Subsequent to the RPM, the floppy disks were sent to Sweden, where profiles were computed from the data on the floppy disks. The profiles were then copied onto 9-track digital tape, and that tape was sent to UMTRI for analysis. It was soon determined that the recording attempt was unsuccessful, and therefore no profile data are available from that system.

158

Figure 93. The Swedish road Surface tester (RST).

CONCLUSIONS

Summary

The Road Profilometer Meeting (RPM) was held in Ann Arbor, Michigan to determine and compare the characteristics of profilometers in use. Twelve profilometers from different agencies were used to measure profiles of 27 test sites. Nine of the test sites were located within the General Motors Proving Grounds (GMPG) at Milford, Michigan, and static rod and level measures were obtained on those nine sites to serve as reference measures. Eleven of the twelve profilometers are GM-type profilometers, in which a vehicle is instrumented with a vertical accelerometer (to provide an inertial reference for the vertical motions of the vehicle body) and a second sensor to measure the instantaneous height of the vehicle body above the road surface. The height and integrated accelerometer data are combined to yield the profile. Participating profilometers used a variety of road-sensing systems, that included the original mechanical follower-wheel design and a number of newer noncontacting systems that measure distance through the detection of reflected ultrasound, laser light, visible light, and infrared light. A variety of computation methods were also used to process the accelerometer and distance signals to obtain the profile. One of the profilometers, the APL trailer, is not based on the GM concept and uses a completely independent design to obtain the profile.

The measured profiles were processed according to several standard analyses to determine the performance limits and expected accuracy of the profilometers. Each analysis defines an application that can be made of a profile measurement. The analyses included simple filtering (to remove long wavelengths) and plotting; quarter-car simulation, using the parameters and simulation speed recently selected to define an International Roughness Index (IRI); the Texas Mays meter calibration index (MO), based on the RMS vertical acceleration (RMSVA) analysis; a waveband analysis based on the root-mean-square (RMS) slope; and power spectral density (PSD) functions.

Data were provided from ten of the profilometers. The results from these systems indicate that they all qualify as profilometers for at least some of the applications considered. (The Pennsylvania Transportation Institute was unable to copy the measured signals from the tape recorder used in the profilometer onto a medium that could be used at UMTRI to perform the analyses. The Swedish VTI system also was unsuccessful at providing valid profile data.)

160

The main findings reported in the preceding "Results" section are summarized below, grouped according to topics related to the operation of a profilometer. Table 7 presents an overview of the results obtained with each system, and serves as a focus for the following discussion. All of the systems shown were operated over a range of speeds. For the APL trailer, different results were obtained at the different speeds, and therefore each speed is indicated. The GM-type systems all correct for the measurement speed and the results apply to all of the test speeds used.

Identification of Bad Data

The first two columns in Table 7 summarize the data from table 4 in the "Experiment" section, and are intended to give an idea of the ability of the systems to operate reliably. The first column shows how many of the sites were measured successfully, together with the number of sites that were attempted. The second column gives the percentage of invalid runs, including repeats.

The APL, FHWA, Michigan, and General Motors profilometers did not have provisions for previewing the data before submitting them to UMTRI. As a result, some bad runs were submitted that might otherwise have been noticed by the operators. As indicated in table 7, all of the bad runs from the APL trailer were due to a problem with a temporary digitizing setup. All but one of the bad runs from the FHWA systems were also due to digitizing problems. (The VTI and Pennsylvania systems also lacked the ability to preview the data, and there were no valid runs from either of those systems that were submitted.)

The rest of the systems—the South Dakota profilometer, the Minnesota, Ohio, and West Virginia 690-DNC profilometers, and the Colorado 8300 Roughness Surveyor—perform the profile calculations at the time of measurement, and also have the capability for plotting the profiles. (All but the South Dakota system are made by K. J. Law Engineers, Inc.) The Ohio and South Dakota systems had no invalid runs submitted, and the Minnesota system had but one. The West Virginia profilometer experienced computer problems during the RPM which cost a great deal of time on the part of the operating crew. As a result, the data submitted from West Virgina had not been thoroughly checked when they were submitted.

For routine use, the ability to preview data before they are transferred to another computer system would appear to be an important factor in contributing to the reliable use of the system.

161

Table 7. Overview of the profilometer results.

Profilometer	Valid Sites/ sites attempted	Bad runs *Percent*	Wavelength range[a] *m/cycle*	IRI roughness range *m/km*	IRI reproducibility *m/km*
APL @ 18 km/h	8/8	0	0.35 - 11	1 - 8	0.5
50 km/h	24/26[b]	7[b]	0.7 - 28	1 - 10	0.5
90 km/h	0/9[b]	100[b]			
Colorado (Law 8300)	10/10	0	---	1 - 5	1.
FHWA/IR	25/27	17	0.35 - 90	1 - 8	0.3
FHWA/Selcom	24/25	21	0.35 - 90	1 - 8	0.3[c]
General Motors	26/27	6	0.35 - 23	1 - 10	0.8
Michigan	20/20	0	0.35 - 90	1 - 8	0.7
Minnesota (690-DNC)	24/24	3	1.4 - 90	1 - 10	0.5
Ohio (690-DNC)	27/27	0	1.4 - 90	1 - 10	0.3
South Dakota	27/27	0	0.7 - 23	1 - 10	1.2
West Virginia (690-DNC)	14/19	17	1.4 - 90	1 - 8	0.5

Notes:

[a] The longest wavelength considered in the RPM was 90 m/cycle and the shortest was 0.35 m/cycle. Wavelengths are shown with a resolution of 1-octave.

[b] Bad runs were all due to digitizing error, not the APL trailer.

[c] The Selcom system had two "outlier" measures with errors of 1.0 m/km.

Accuracy

Assuming that invalid runs can be detected and discarded, then there is the principal question about the accuracy of the instrument. No single profilometer stood out as being the most accurate for every application, and the different systems displayed various strengths and weaknesses.

Profile Plots

Sooner or later, every profilometer will be used for the purpose of providing a plot of longitudinal profile, if it has that capability. When suitably filtered, profiles from the various systems can be compared visually with each other and with a static rod and level reference. The FHWA system (using both the Selcom and IR road sensors), the three 690-DNC systems, the APL trailer, and the Michigan profilometer all produce profile measures that match the rod and level reference when suitably filtered. The best agreement with the reference was obtained with the FHWA and 690-DNC systems, with the Michigan and APL profilometers showing a small amount of distortion in the signal. The South Dakota system produced profile measurements that varied in quality, due to an error in the system software that has since been corrected. On rougher roads, the profiles matched the rod and level with little distortion, but in others the agreement was only approximate. The General Motors profilometer also produced profile measurements that varied in quality. The profile plots never compared closely with the rod and level reference, but the measures generally replicated some surface details with little distortion.

The measured profiles will not compare well with the true profile for every type of profile filter, however. The various profilometers see different ranges of wavelengths and will only provide plots of the profile that agree with a reference when the profiles are filtered to eliminate wavelengths outside of the bandwidth of the instrument. The bandwidths are discussed below, and indicated approximately in table 7 under the "Wavelength Range" heading.

Wavelength Range

Another basis for comparison is through PSD functions, which show the profile amplitudes distributed over wavenumber (wavenumber is spatial frequency—the inverse of wavelength). The PSD functions graphically show the range of wavelengths seen by a given instrument. Waveband analysis can be used to further reduce the profile information to a series of indices that summarize the roughness content concentrate at specific

163

wavenumbers. The waveband analysis used in the RPM covered 1-octave wavebands for center wavelengths ranging from 0.5 m to 64 m. Each waveband included wavelengths from $0.71 \times \lambda$ to $1.4 \times \lambda$, where λ is the wavelength at the center of the band. Thus, the waveband analyses actually covered wavelength from 0.35 m (1.1 ft) to 90 m (297 ft). Table 7 indicates a wavelength range for each system. These ranges are given as a simple summary, with more detail being available for each system in the preceding "Results" section of this report.

The two configurations of the FHWA system and the Michigan system covered the broadest range of wavelengths, from 0.35 m up to 90 m, with the FHWA system being more accurate. The three 690-DNC systems were also extremely accurate, but they incorporate smoothing filters that attenuate wavelengths shorter than 1.4 m (4.6 ft). The APL trailer responds to wavelengths lying between the temporal frequencies 0.5 and 20 Hz at the measurement speed. For a speed of 50 km/h (31 mi/h), the wavelength range is 0.7 to 28 m. The PSD functions from the General Motors profilometer were in general agreement with the reference—even though the direct plots of profile were distorted—indicating that the measures should be valid for computing profile indices that reflect only amplitude information. The South Dakota system produced profile amplitudes that were somewhat in error due to an error in the system software that has since been corrected, and possibly also due to limitations in the ultrasonic sensor.

While the waveband analysis and the rod and level measures were limited to the wavelength range of 0.35 to 90 m, some of the systems can measure wavelengths outside of this range. The FHWA, Michigan, and General Motors profilometers all see wavelengths shorter than 0.35 m. The Michigan profilometer sees wavelengths down to 0.25 m; the General Motors system sees wavelengths shorter than the 0.20 m limit used in preparing the PSD plots; and with the Selcom laser sensor, the FHWA system sees wavelengths down to 0.25 m. Comparison with the rod and level indicates the FHWA/Selcom system was substantially more accurate at the extremely short wavelengths than any other profilometer.

Measurement of Roughness Indices

The roughness measure used in the table is the IRI—a quarter-car simulation using the parameters specified in the NCHRP 228 report, a simulation speed of 80 km/h (50 mi/h), and calculated for a single wheeltrack (rather than the half-car simulation often used with two wheeltracks). The IRI computation is the same as the "Mays Meter Simulation" available on the Law 8300 and 690-DNC systems, although the measures are given with

164

units of m/km rather than the in/mi often used (1 m/km = 63.36 in/mi.) The accuracy of each system for measuring IRI is indicated approximately by the reproducibility of the measures. Because the sites used in the RPM were selected to include "worst case" surfaces, and do not represent a normal distribution of road conditions, a statistical analysis of the roughness data would not be particularly relevant. The numbers are provided in the table just to give an approximate idea of the accuracy that can be expected from the systems when they are used on smooth and moderately rough roads, covering IRI values less than 5 m/km, and using section lengths of 161 m (1/10th mi). Generally, smaller errors can be expected when test lengths longer than 161 m are used. The values shown in the table were taken visually from the plots. The range is the maximum error that can be expected, rather than the RMS error that is often obtained from statistical analysis. Most of the profilometers showed a distributed scatter about the line of equality (the line of equality is for the condition that the measures equal the reference values), with no "outlier" points. The exception to this was the FHWA/Selcom system, which showed very little error on all but two 161 m sections, where exceptionally large errors occurred.

In addition to the IRI, another calibration index for response-type systems—the MO roughness index developed in Texas—was computed from the measured profiles. The findings involving MO closely paralleled those involving the IRI. In most cases, the relative errors in measuring MO were somewhat higher than when measuring IRI, and several of the systems showed a small but visible bias that was not present in the IRI measures. (That is, the MO measures from a particular profilometer might be consistently too low or too high.)

A Practical Limit to Accuracy

Even with a profilometer that can produce "perfect" measurements, perfect reproducibilty in measuring profile cannot be obtained in practice because there is imprecision involved in locating the wheeltrack to be profiled. A variation of at least 5 m is to be expected in locating the start of a profile measurement when the operators of the profilometer are experienced. It also appeared that a lateral imprecision of .25 m can be expected when wheeltracks are marked, and that variations of 0.5 to 1.0 m will exist when wheeltracks are not marked.

The reproducibilty levels shown in table 7 include the variation associated with different operators and drivers measuring slightly different wheeltracks. Repeatability for some of the instruments was much better, with repeat runs carefully made at the GMPG commonly showing agreement within .05 m/km for some of the systems. (The measures are tabulated

in appendix F.) This indicates the accuracy obtainable for routine use on public roads is not going to be improved by improvements to the profilometers. They are already accurate enough to achieve the practical limit imposed by the random error associated in choosing the wheeltrack for measurement.

Problems with Surface Type

The test sites were selected to include all surface types that would potentially challenge the various profilometer designs. Rather than covering a representative distribution of road conditions, the sites included most of the "worst case" surfaces for the various profilometer designs. Generally, the limitations related to surface type are due to the sensors that measure the distance between vehicle and road.

Mechanical Follower-Wheels

The early GM-type profilometers used mechanical follower-wheel systems to detect the height of the vehicle over the road. These mechanical systems introduce at least three sources of measurement error: (1) rolling nonuniformities, which are relevant only on the smoothest sites; (2) bouncing of the wheel, which occurs on rougher sites; and (3) mechanical resonances of the tire and loading suspension, which can be a problem for all roughness levels. Several measures were made with the Michigan profilometer, and dramatically demonstrated the problems of bouncing and mechanical resonance. Comparison with measures made by the same system using using a noncontacting optical height sensor show how those sources of error are eliminated by replacing the mechanical system with a noncontacting one. A problem with follower-wheels that is more visible to the practitioner is that they are easily damaged and require a great deal of maintenance. This latter problem was demonstrated during the RPM, when the follower-wheel of the Pennsylvania profilometer broke during testing.

The APL trailer has a follower-wheel integrated into its design. Unlike the follower-wheels used on GM-type profilometers, the APL trailer includes a well-damped suspension designed to keep the wheel on the ground for all roughness levels. The design also uses a motorcycle-type of tire that is much more rugged than the special urethane wheel associated with GM-type profilometers. Bounce of the follower-wheel was not a problem for any of the valid runs, which included roughness levels up to 8 m/km. (The data from the very roughest site, and the high-speed data from the other rough sites, were not valid due to an unrelated digitizing problem.) The rolling nonuniformities were shown to be negligible and no mechanical resonances were detected in any of the runs.

166

Ultrasonic Height Sensors

The Colorado and South Dakota profilometers both used ultrasonic sensors to measure vehicle height. Ultrasonic sensors are known to have difficulty when the road surface does not adequately reflect sound. The Colorado system had trouble during the RPM on the surfaces with open textures, which turn out to be poor reflectors of ultrasound. The surfaces that were eventually measured with this system included some open surface textures, yet other sites with open textures were not measured and reported. The South Dakota system, on the other hand, made measures on all of the sites, regardless of their texture. The ultrasonic sensor used by South Dakota had a limited resolution, which may degrade the ability of the system to measure profile features on smooth roads. However, another problem that was more serious (and has since been corrected) prevented the evaluation of the system on smoother roads.

Optical Height Sensors

The Michigan DOT profilometer and the three 690-DNC systems made by K. J. Law Engineers, Inc. use a similar design of an optical light sensor. The 690-DNC system owned by Ohio operated over nearly all of the surface conditions with success, proving that this design is able to deal reliably with all of the surface types included in the RPM. Due to an unrelated problem, the Michigan DOT data were not analyzed for many of the sites with surfaces that included reflectiveness changes.

The FHWA profilometer was operated using an infrared (IR) optical sensor developed by the Southwest Research Institute, under an earlier contract with FHWA. Laboratory tests with the sensor indicated that it might be unusable in a profilometer. However, the results from the RPM showed that the complete system—which included antialiasing smoothing filters—was relatively accurate for most of the conditions, even those including drastic variations in reflectiveness. On one site, where the surface had been patched extensively, the IR sensor gave unacceptable measures. Several of the roughest sites could not be processed due to a digitizing problem, and it is likely that some of the measures from the IR sensor were bad on these tests. Overall, the IR sensor appears to be suitable if the occasional failure can be detected by the operator.

Laser Height Sensors

Three systems used laser designs to sense height. In addition to the infrared sensor, the FHWA profilometer was also operated with commercially available sensors made by

the Swedish Selcom Company. On most of the surfaces, the measurements made with this system were at least as accurate as any of the other profilometers for most applications, and they were the most accurate for sensing the shortest wavelengths in the profile. However, the sensors failed on two sites. Use of this particular sensor requires that the operators are able to detect the occasional errors, but otherwise it is an appropriate choice for a profilometer. (Note that the particular model used was loaned for the project, and does not have a more advanced signal processing unit that is available and might eliminate the type of error that was observed. If purchased, the optional Receiver-Averaging board should probably be included in the package as it may correct the problem.)

The General Motors profilometer uses a laser design that is not commercially available, and which appeared to give accurate measures on all sites. It uses a larger projected image, similar to the one used in the 690-DNC and Michigan systems, to avoid the problems associated with a small dot-image used in some other laser designs. Due to a problem that was unrelated to the sensors, the profiles from this profilometer were generally not as accurate as those from some of the other profilometers. Therefore, complete evaluation of the GM laser sensor was not attempted.

The Swedish VTI system uses twelve sensors made by the Selcom Company that are not available commercially. Because the system did not make valid profile measurements, the quality of the laser sensors was not determined.

Roughness Limits

The roughness range given in table 7 indicates the range for which valid profiles were obtained with each system. The roughest site at the GMPG was about 8 m/km, but there was one public road site with a roughness of 10 m/km. Five of the systems obtained valid measures on the roughest public road site, and all but the Colorado system obtained measures on the roughest GMPG site. By way of comparison, the correlation program held in 1979 for response-type road roughness measuring systems (RTRRMSs) in the NCHRP project used the West Virginia profilometer as a reference.[9] At that time, it used mechanical follower-wheels instead of the optical height sensors. The valid range of the profilometer was determined to be about 1 to 3.5 m/km. (Rougher sites were included, but the profilometer measures were rejected as being not valid.)

Most of the profilometers that use optical or laser height sensors appear capable of measuring roads for almost any level of roughness. The roughness ranges shown in the table are limited to the range covered in the RPM, but it should be noted here that the systems can probably obtain valid measures on even rougher roads. Some failures of the

168

profilometers to measure the rougher sites were due to logistical problems. (For example, the roughest site was repaired immediately after the RPM, before measures could be made with some systems.) Failures to obtain measures with the APL trailer and FHWA systems were due to problems with temporary digitizing arrangements, which are easily corrected.

Cracks and Open Joints

Several of the systems proved that they can measure cracks in the pavement. The Selcom laser, with its tiny projected image and very high measurement update rate, is likely to detect every crack that is traversed. The "slit" images used by the Michigan and General Motors profilometers also detect cracks that are oriented transverse to the direction of travel. With different system software, the sensors used in the 690-DNC—similar in design to those used in the Michigan profilometer—might also respond to transverse cracks. These systems will also detect small openings in the joints of PCC roads that would go undetected with many other sensors.

Most roughness analyses used with measured profile—including the IRI, the MO, PSD functions, and various waveband analyses—all treat downward singularities (cracks and openings between joints) the same as upward singularities (patches and tar-strips). However, the downward singularities have no affect on vehicles, and therefore have no effect on the common perception of roughness. For example, an upward deviation of 20 mm will jolt the tire of a traversing vehicle, while a crack that is 20 mm deep will have no effect. Yet, both types of deviations will have the same effect on a roughness index or a PSD. When roughness indices such as the IRI and MO are computed from a profile that includes cracks, the roughness will not only be increased by the presence of the cracks, it will even be influenced by the depth of the cracks. This sensitivity is, of course, not appropriate. The ability to see cracks cannot really be considered a defect in the profilometer, for the cracks do exist in the pavement. (As profilometric applications develop, the ability to sense cracks may someday be considered essential.) However, because many profilometers do not detect the cracks, there is an incompatibility when applying the same analyses to profiles measured with different systems.

When profilometers are used that can detect cracks, there is a need to develop software to separate the cracks from the rest of the profile. It might appear at first that the problem could be solved with appropriate low-pass filters, such as the antialiasing filters used with many of the systems. However, a singularity such as a crack appears over a wide band of wavenumbers. (In theory, the bandwidth is infinite.) Thus, a low-pass filter will affect short wavelengths, leaving the full effects of the crack in the remaining wavelengths. Only

169

a special type of filter, designed to remove singularities in one direction—filtering out cracks while leaving patches and tar strips—would solve the problem.

Concluding Remarks

The results from the RPM show that most systems that participated in the RPM and are considered "profilometers" do, in fact, live up to that name for most applications presently made of profile data. Ten of the twelve systems provided measures that were demonstrated to be valid. All ten can be used to measure the IRI and MO roughness indices, and will give results that agree with measures made with rod and level. Different amounts of error were shown by the various systems; however, they all produced roughness measures that, on the average, lay on the same scale.

All of the profilometers can be used over a range of test speeds. The APL, Michigan, and General Motors profilometers require that test speed be constant during measurement, whereas the 690-DNC, the K. J. Law 8300 Roughness Surveyor, the FHWA, and the South Dakota system allow variations in speed during testing.

All nine of the systems that record profile (or record data later used to generate profile) can produce profiles that match a rod and level reference, when both the reference and the profilometer measure have been identically filtered to remove the longest wavelengths. (None of the profilometers can produce a profile signal that exactly matches the unfiltered rod and level reference. Additional instrumentation can be used to add this capability, but there is no reason to do so for any of the applications considered in this report.) For direct profile measurement, the different systems showed widely varying capabilities. The profiles obtained with the all of the systems compare at least approximately with the rod and level on most types of road, and several of the systems can produce profile measures that appear visually identical to the rod and level reference.

Some profilometers detect cracks and openings in the joints that are not treated realistically in the profile analyses now in use. There is a need to develop software to separate the cracks from the rest of the profile.

This experiment has proved that profilometers are generally capable of measuring road profiles with the accuracy expected. Some of the systems are so accurate that the practical limit on the reproducibility of their measures is the ability of the different operators and drivers to measure in exactly the same wheetrack. However, it was also evident that the systems did not always perform as expected. If profilometers are to become a reliable means for monitoring road roughness characteristics, more effective checks on

170

performance are needed during routine use, and standardized methods for validating the systems at periodic intervals are warranted. These needs are encompassed in two recommendations:

1. Profilometer designs should include more self-checking and diagnostic features to detect malfunctions during routine use, and alert the operator to measurements that may be in error.

2. Standardized tests and/or test methods should be developed to allow periodic validation of road profilometers. The ASTM Committee E17 on Travelled Surface Characteristics is a logical forum to address this need.

APPENDIX A: Attendees of the Road Profilometer Meeting

Peter Spellerberg	AMRL-National Bureau of Standards Building 226, Room A365 Gaithersburg, MD 20899	(301) 921-3481
John Zaniewski	· Austin Research Engineers 2600 Dellana Lane Austin, TX 78746	
Michel Gorski	Centre de Recherches Routieres Blvd. de la Woluwe 42 B-1200 Brussels, Belguim	
D. Randolph	City of Lansing Lansing, MI 48933	(517) 483-4455
Robert Clegg	City of Lansing 601 E. South Street Lansing, MI 48910	
Charles Peterson Phil McCabe Rich Griffin Robert S. Olejnik	Colorado Department of Highways 4201 E. Arkansas Ave. Denver, CO. 80222	(303) 757-9488 (303) 757-9506 (303) 757-9281
Hisao Tomita	Federal Aviation Administration 800 Independence Avenue Washington, D.C. 20591	(202) 426-2072
Rudy Hegmon Gene K. Fong	Federal Highway Administration 6300 Georgetown Pike McLean, VA 22101	(703) 285-2072 (703) 285-2363
Craig Rockafellow Phil Wesel Harold Bidwell Dave Verbrugge	General Motors Corporation GM Proving Grounds Milford, MI 48042-2001	(313) 685-6397 (313) 685-5418 (313) 685-6185 (313) 685-6185
James Strong	K.J. Law Engineers, Inc. 26341 Research Drive Farmington Hills, MI 48024	

Daniel Ducros Francois Mark	Laboratoire Central des Ponts et Chaussees BP19 44340 Bouguenais, France	
Maurice De Wilder	MAP Sarl 29 Route d'Illfurth F-68720 Illfurth, France	89/25.40.62 Telex 881 251
Tom Hattis Joe Dexter Robert Felter Leo DeFrain Tom Hathis	Michigan Department of Transportation Research Laboratory P.O. Box 30049 Lansing, MI 48909	(517) 322-1632
Marc Goess Lyle Eide	Minnesota Department of Transportation Transportation Building John Ireland Boulevard St. Paul, MN 55106	(612) 296-3167
Bob Novak Cliff Keen Nate Johnson Dave Butler	Novak, Dempsey and Associates 317 W. Colfax Palatine, IL 60067	(312) 991-0580
Emil Marginean Ed Arledge Jim McQuirt	Ohio Department of Transportation 25 S. Front Street Columbus, OH	(614) 466-2697
Mac Bryan Robin Smith	Pennsylvania State University Research Building B University Park, PA 16802	(814) 865-1891
Dave Huft Scott Stabnow	South Dakota Department of Trans. Research Program 700 E. Broadway Pierre, SD 57501	(605) 773-3871
Elson Spangler Bill Kelly	Surface Dynamics, Inc. Suite 220 800 West Long Lake Road Bloomfield Hills, MI 48013	(313) 540-8310
Tom Gillespie Mike Sayers Mike Hagan Jack Campbell Don Foster	The University of Michigan Transportation Research Institute 2901 Baxter Road Ann Arbor, MI 48109	(313) 764-2168
Mike Womack	USAF Engineering & Services Cntr HQ AFESC/RDC Tyndall AFB, FL 32403	(904) 283-6273

Cpt Norm Hannah   USAF Engineering & Services Cntr   (904) 283-6332
                    HQ AFESC/DEMP
                    Tyndall AFB, FL 32403

Don Lipscomb   West Virginia Department of High.   (304) 348-5999
Gary Garwig   312 Michigan Avenue
                    Charleston, WV

APPENDIX B: The Moving Average Filter

A profile can be smoothed at each point by considering an average over a baselength:

$$y_s(i) = \frac{1}{2k+1} \sum_{j=i-k}^{i+k} y_r(j) \tag{1}$$

$y_r(j)$ = unfiltered "raw" vertical profile elevation for sample j

$y_s(i)$ = smoothed profile elevation for sample i

k   = number of samples in 1/2 of the moving average baselength

b   = $2 \cdot k \cdot dx$ = baselength of moving average

dx   = distance between samples

In order for eq. 1 to duplicate a true moving average (as occurs in the limit when dx approaches zero), the value of k should not be too small. A value of 4 (9 points in the summation) is a reasonable lower limit. As k increases, such that the baselength is much longer than the sample interval, the equation approaches a true moving average.

The computations implied by eq. 1 can be written differently, to better reflect how the analysis is usually performed by computer:

$$y_s(i) = y_s(i-1) + \frac{1}{2k+1} [y_r(i+k) - y_r(i-k-1)] \tag{2}$$

Eq. 2 is recursive, meaning that the new value for $y_s(i)$ depends on the previous value, $y_s(i-1)$. The second form is very efficient: even if the moving average includes thousands of points, each smoothed value is calculated just from two of the original values (at sample numbers i+k and i-k-1) and the previous smoothed value.

A recursive formula such as eq. 2 requires an initialization, to obtain the first value of the smoothed signal. This value is computed using eq. 1.

The moving average analysis is a form of digital filter: it filters out short wavelengths (high frequencies), leaving the longer wavelengths (low frequencies). A filter that removes high frequencies is called a low-pass filter, and the moving average is a specific type of a digital low-pass filter. When analyzing road profile, it is usually desirable to remove the long wavelengths, leaving the roughness associated with the short waves. That is, a high-

pass filter is needed. The moving average is converted from a low-pass filter to a high-pass filter simply by subtracting the smoothed signal from the original signal:

$$y_h(i) = y_r(i) - y_s(i) \qquad (3)$$

where y_h is the high-pass filtered profile.

Figures 2 and 3 in the report show how the high-pass moving average filter affects the appearance of a measured profile. In this report, the high-pass version was used in all applications involving filtered profile plots. The low-pass (smoothing) versions was used as a part of the IRI (quarter-car simulation) computation. Further, all of the profiles obtained with the K. J. Law 690-DNC employed a 0.3048-m (1.0-ft) moving average to smooth the profiles before they were stored digitally on tape.

The moving average filters require that unfiltered data be measured on either side of the current sample. Thus, eqs. 1 through 3 cannot be used to obtain smoothed values for the first k samples of the signal, nor for the last k samples at the end. In the RPM, some of the measurements covered short distances. This is particularly true for the rod and level data. In order to compare profiles measured by different methods, it was desirable to have filtered profiles with the same number of samples as the original unfiltered profile. This meant that a special technique was needed to filter the first k and last k samples in each signal. A simple way to do this is to add k artificial samples at the beginning and end of the measurement, so that the first smoothed value from the moving average filter is at the start of the measured profile. Several schemes were tried for generating the artificial points. The intent was to use a method that results in a smoothed signal that replicates the smoothing that a draftsman might perform in preparing plots for presentation. The method that gave the best results for adding to the beginning of the profile was to use the equation

$$y_a(i) = y_r(1) + \bar{y}' \cdot (i - 1) \qquad (4)$$

where

$\bar{y}'$ = slope of profile (with respect to sample number) for the first k samples
$y_a(i)$ = artificial profile point
i = 1-k ... 0 (i ≤ 0)

Eq. 4 generates additional points that lie on a straight line that connects to the elevation of the first point of the measured profile. The slope $\bar{y}'$ is computed by a linear regression between elevation and sample number, over the first k samples.

The same method is used to generate artificial points at the end, using the equation

$$y_a(i) = y_r(n) + \bar{y}' \cdot (i - n) \tag{5}$$

where

$\bar{y}'$ = slope of profile (with respect to sample number) for the last k samples
i = n+1 ... n+k

APPENDIX C: The IRI Quarter-Car Simulation

Response-type road roughness measuring systems can be simulated using a mathematical model of the vehicle and roadmeter. The quarter-car model, shown in figure 4, has been widely used to produce the type of measure associated with response-type systems. These measures have been applied by profilometer users to maintain continuity with roughness measures made in the past, and also by users of response-type systems to obtain reference measures needed to calibrate the response-type systems. In the late 1970's, a standard set of vehicle parameters was defined and published in NCHRP Report 228.[9] Since then, the method of quarter-car simulation has been further standardized in work initiated by The World Bank. The result has been the International Roughness Index (IRI), which is defined as the roughness measure obtained using a quarter-car simulation, with the NCHRP 228 vehicle parameters, a simulation speed of 80 km/h (50 mi/h), and processing the profile for a single wheeltrack.[10, 11] (The distinction that processing is performed for a single wheeltrack comes about because quarter-car analysis can also be applied to two wheeltracks simultaneously.)

The calculation of IRI is accomplished by computing four variables as functions of the measured profile. (These four variables simulate the dynamic response of a reference vehicle, shown in figure 4, travelling over the measured profile.) The equations for the four variables are solved for each measured elevation point, except for the first point. The average slope over the first 11 m (0.5 sec at 80 km/h) is used for initializing the variables by assigning the following values:

$$Z_1' = Z_3' = (Y_a - Y_1) / 11 \tag{6}$$

$$Z_2' = Z_4' = 0 \tag{7}$$

$$a = 11 / dx + 1 \tag{8}$$

where Y_a represents the "a-th" profile elevation point that is a distance of 11 m from the start of the profile, Y_1 is the first point, and dx is the sample interval. (Thus, for a sample interval of dx = 0.25 m, eq. 6 would use the difference between the 45th elevation point and the first elevation point to establish an initial slope for the IRI computation.)

The following four recursive equations are then solved for each elevation point, from 2 to n (n = number of elevation measurements).

$$Z_1 = s_{11} \cdot Z_1' + s_{12} \cdot Z_2' + s_{13} \cdot Z_3' + s_{14} \cdot Z_4' + p_1 \cdot Y' \tag{9}$$

$$Z_2 = s_{21} \cdot Z_1' + s_{22} \cdot Z_2' + s_{23} \cdot Z_3' + s_{24} \cdot Z_4' + p_2 \cdot Y' \tag{10}$$

$$Z_3 = s_{31} \cdot Z_1' + s_{32} \cdot Z_2' + s_{33} \cdot Z_3' + s_{34} \cdot Z_4' + p_3 \cdot Y' \tag{11}$$

$$Z_4 = s_{41} \cdot Z_1' + s_{42} \cdot Z_2' + s_{43} \cdot Z_3' + s_{44} \cdot Z_4' + p_4 \cdot Y' \tag{12}$$

where

$$Y' = (Y_i - Y_{i-1}) / dx = \text{slope input} \tag{13}$$

and

$$Z_j' = Z_j \text{ from previous position, } j=1,4 \tag{14}$$

and s_{ij} and p_j are coefficients that are fixed for a given sample interval, dx. Thus, eqs. 9 through 12 are solved for each position along the wheeltrack. After they are solved for one position, eq. 14 is used to reset the values of Z_1', Z_2', Z_3', and Z_4' for the next position. Also for each position, the rectified slope (RS) of the filtered profile is computed as:

$$RS_i = |Z_3 - Z_1| \tag{15}$$

The IRI statistic is the average of the RS variable over the length of the site. Thus after the above equations have been solved for all profile points, the IRI is calculated as:

$$IRI = \frac{1}{(n-1)} \sum_{i=2}^{n} RS_i \tag{16}$$

The above procedure is valid for any sample interval between dx=.25 m and dx=.61 m (2.0 ft). For shorter sample intervals, the additional step of smoothing the profile with a 0.25-m moving average is recommended to better represent the way in which the tire of a vehicle envelops the ground. (The moving average is described in the preceding appendix.) Then the IRI is calculated by solving the equations for each averaged point using coefficients in the equations appropriate for the smaller interval.

The computed IRI will have units consistent with those used for the elevation measures and for the sample interval. For example, if elevation is measured as mm, and dx has units of meters, then IRI will have the preferred units: mm/m = m/km = slope $\times$ 10^3. The coefficients used in eqs. 9 through 12 are calculated from the equations of motion that define a quarter-car model. In the general case, they are specific to the vehicle model parameter values, simulation speed, and the sample interval. For the specific case of IRI, defined by the NCHRP 228 parameters and a standard 80 km/h simulation speed, they

179

depend only on the sample interval. Table 8 gives the necessary coefficients for most sample intervals that are likely to be selected when measuring profile with units of meters or units of feet. Complete instructions for measuring IRI are available in reference 11. The instructions include listings of computer programs that solve the equations of motion and also computer programs that calculate the coefficients.

Table 8. Coefficients for the IRI Equations.

dx = 50 mm, dt = .00225 sec

	.9998452	2.235208E-03	1.062545E-04	1.476399E-05		4.858894E-05
ST =	-.1352583	.9870245	7.098568E-02	1.292695E-02	PR =	6.427258E-02
	1.030173E-03	9.842664E-05	.9882941	2.143501E-03		1.067582E-02
	.8983268	8.617964E-02	-10.2297	.9031446		9.331372

dx = 100 mm, dt = .0045 sec

	.9994014	4.442351E-03	2.188854E-04	5.72179E-05		3.793992E-04
ST =	-.2570548	.975036	7.966216E-03	2.458427E-02	PR =	.2490886
	3.960378E-03	3.814527E-04	.9548048	4.055587E-03		4.123478E-02
	1.687312	.1638951	-19.34264	.7948701		17.65532

dx = 152.4 mm (0.50 ft), dt = .006858 sec

	.9986576	6.727609E-03	3.30789E-05	1.281116E-04		1.309621E-03
ST =	-.3717946	.9634164	-.1859178	3.527427E-02	PR =	.5577123
	8.791381E-03	8.540772E-04	.8992078	5.787373E-03		9.200091E-02
	2.388208	.2351618	-27.58257	.6728373		25.19436

dx = 166.7 mm, dt = .0075015 sec

	.9984089	7.346592E-03	-1.096989E-04	1.516632E-04		1.70055E-03
ST =	-.4010374	.9603959	-.2592032	3.790333E-02	PR =	.6602406
	1.038282E-02	1.011088E-03	.8808076	6.209313E-03		.1088096
	2.556328	.2526888	-29.58754	.6385015		27.03121

dx = 200 mm, dt = .009 sec

	.9977588	8.780606E-03	-6.436089E-04	2.127641E-04		2.885245E-03
ST =	-.4660258	.9535856	-.4602074	4.352945E-02	PR =	.9262331
	1.448438E-02	1.418428E-03	.8332105	7.105564E-03		.1523053
	2.908761	.2901964	-33.84164	.5574984		30.93289

dx = 250 mm, dt = .01125 sec

	.9966071	1.091514E-02	-2.083274E-03	3.190145E-04		5.476107E-03
ST =	-.5563044	.9438768	-.8324718	5.064701E-02	PR =	1.388776
	2.153176E-02	2.126763E-03	.7508714	8.221888E-03		.2275968
	3.335013	.3376467	-39.12762	.4347564		35.79262

dx = 304.8 mm (1.00 ft), dt = .013716 sec

	.9951219	1.323022E-02	-4.721649E-03	4.516408E-04		9.599989E-03
ST =	-.6468806	.9338062	-1.319262	5.659404E-02	PR =	1.966143
	3.018876E-02	3.010939E-03	.6487856	9.129263E-03		.3210257
	3.661957	.3772937	-43.40468	.3016807		39.74273

dx = 333.3 mm, dt = .0149985 sec

	.9942636	1.442457E-02	-6.590556E-03	5.25773E-04		1.232715E-02
ST =	-.6911992	.9287472	-1.597666	5.892596E-02	PR =	2.288865
	3.496214E-02	3.505154E-03	.5920432	9.472713E-03		.3729946
	3.775608	.3928397	-45.01348	.2341656		41.23787

dx = 500 mm, dt = .0225 sec

	.9881727	2.128394E-02	-2.520931E-02	9.923165E-04		3.703847E-02
ST =	-.928516	.9001616	-3.391369	6.280167E-02	PR =	4.319885
	6.386326E-02	6.615445E-03	.2402896	9.862685E-03		.6958473
	3.743294	.4186779	-46.67883	-.1145251		42.93555

dx = 609.6 mm (2.00 ft), dt = .027432 sec

	.9832207	2.567633E-02	-.0448194	1.291335E-03		6.159972E-02
ST =	-1.080368	.8808161	-4.54124 6	5.758515E-02	PR =	5.621614
	8.111078E-02	8.608906E-03	2.055522E-02	8.861093E-03		.898334
	3.194438	.3839011	-41.76972	-.2822351		38.57529

APPENDIX D: The Texas MO Index and RMSVA

The Texas Mays meter index, MO, is a profile analysis that produces a roughness index used to calibrate response-type road roughness measuring systems. Conceptually, it is similar to the quarter-car analysis because it defines an index computed from profile that can be used as a reference response-type system. Rather than using a quarter-car simulation, an analysis called RMSVA is employed to obtain the MO index.

RMSVA is an abbreviation for root-mean-square (RMS) vertical acceleration. Mathematically, $RMSVA_b$ is the RMS value of the variable VA_b, which is defined as:

$$VA_b(x) = [\ Y(x-b) + Y(x+b) - 2 \bullet Y(x)\ ] \bullet b^{-2} \qquad (17)$$

where $Y(x)$ is the profile elevation at position x. (Since RMSVA varies with b, the baselength is subscripted.) When b is very small, eq. 17 approximates a double differentiation, leading to the name "RMSVA." However, small values of b are not used to define the MO and similar roughness indices. Although not widely recognized, RMSVA is also equivalent to the RMS deviation at the midpoint of a rolling straightedge of length $2 \bullet b$. The equation for a mid-chord deviation is:

$$MCD(x) = [\ Y(x-b) + Y(x+b)\ ] / 2 - Y(x) \qquad (18)$$

where b is one-half of the chord length. A comparison of the above two equations shows that the right-hand side of eq. 17 is a re-scaled version of the right-hand side of eq. 18, where the scale factor is $2 \bullet b^{-2}$. This equivalence is shown in figure 6. It is sometimes easier to understand the RMSVA analysis by thinking of it as a mid-chord deviation, also called a rolling straightedge, but since it is called RMSVA by its users, that name is used here as well. (For the values of b that are normally used in Texas and elsewhere, figure 7 shows that RMSVA has no relationship whatsoever with vertical acceleration.)

Digital profile measures are typically spaced by a constant interval, and eq. 17 can be re-written using sample number rather than longitudinal distance to identify the individual profile samples:

$$VA_b(i) = [\ Y(i-k) + Y(i+k) - 2 \bullet Y(i)\ ] \bullet (k*dx)^{-2} \qquad (19)$$

182

where

i = sample number,

k = an integer used to define baselength

dx = distance between samples

b = k•dx = baselength

Since the VA value at position is calculated using the profile value b meters before and b meters after the current position, VA_b values cannot be calculated for the first and last b meters of a measured profile. The RMS value is calculated as

$$RMSVA_b = \frac{1}{(n-2 \cdot k)} \left\{ \sum_{i=k+1}^{n-k} VA_b(i)^2 \right\}^{1/2} \qquad (20)$$

These equations result in a RMSVA measure with the units: 1/length, which is appropriate for spatial acceleration. Profile elevation and longitudinal distance are both variables with units of length, but usually different units are used, and therefore care must be taken to convert RMSVA into the correct units. Since it will be seen that RMSVA is used in a regression equation to calculate a summary roughness statistic, it is critical that the exact units are used that are required for the regression equation. In the Texas method, the RMSVA measures must be converted to units of ft/sec^2. The conversion is made assuming a constant travel speed, V, and the relationship

$$RMSVA_b(time) = c \cdot RMSVA_b(distance) \qquad (21)$$

where

$$c = V^2 \qquad (22)$$

The speed that is assumed in Texas for the conversion is 80 km/h (50 mi/h). Proper units are obtained when the elevation and sample interval values are converted to units of feet, and the speed is converted to ft/sec: V = 50 mi/h = 73.33 ft/sec.

Regression analyses covering a data base of response-type measures and RMSVA values for various baselengths indicated that an excellent estimate of the response-type measure is obtained using a linear equation with two RMSVA statistics.[12] In Texas, baselengths of 4 ft and 16 ft (1.2 m and 4.9 m) are combined to arrive at an index known as the "MO":

$$MO = -20 + 23 \cdot RMSVA_4(time) + 58 \cdot RMSVA_{16}(time) \qquad (23)$$

The above equation assumes that the RMSVA numerics have been converted to units of ft/sec^2. The MO index has arbitrary units, but since it was derived to match measures from response-type systems—scaled with units of inches/mile—the MO can be considered to have units of inches/mile. For consistency with other measures, the MO data were converted to the metric slope equivalent of m/km in this report, after they were computed using eq. 23.

APPENDIX E: Power Spectral Density Functions

A general description of the power spectral density (PSD) function and its applications is available from many sources, with reference 20 being one of the best. The analysis of road profile with PSD functions is not nearly as well covered as other applications, and therefore the specific steps used to compute the PSD functions for this report are described here. The following descriptions assume that the reader is familiar with the definition of the PSD function and the basic approaches that are usually taken to transform a series of discrete measures of a variable into a series of discrete PSD values. The steps that were used to compute the PSD functions in this report were as follows:

1. The elevation profile is converted to a slope profile, by taking the difference between adjacent elevation values and dividing by the sample interval. This step is taken for several reasons. Because only a finite portion of the wheeltrack is measured, there is an effect on the PSD computation due to the abrupt start and end of the profile. The transitions are much greater for elevation profiles than for slope profile, and therefore the influence of the transitions in the computations is reduced. (Another method frequently used in other applications is to apply a tapered weighting to the signal, such as a Hanning or Hamming window. This is not recommended, because the middle of the signal assumes more significance than the beginning and end areas.) A second reason is that a profile slope has a more-or-less uniform PSD, and as a result numerical round-off and truncation errors are minimized during the FFT calculations. A third reason is that the PSD functions are desired in the form of a slope PSD, and the transformation from elevation to slope must be perfomed at some stage of the processing anyway.

2. The mean value of the slope profile is computed and subtracted from the signal.

3. The signal is padded with zeros until it contains a number of samples that is a power of two. For example, if the signal contains 6000 samples, 2192 values of zero are added to obtain a signal with 8192 points. $(8192 = 2^{13})$

4. The signal is transformed by the fast Fourier transform (FFT) into the frequency domain. The profile is now represented by $n/2$ complex coefficients that give phase and amplitude information that could be used to reconstruct the profile with a Fourier series of sinusoids. (n is the number of points transformed, which is a

power of two. If there were 8192 points in the profile signal, then there are 4096 coefficients returned.)

5. The amplitudes of the n/2 coefficients are squared and scaled to the proper units for PSD. (Phase information is not used.)

6. Adjacent PSD values are averaged to obtain smoothed PSD functions, defined at specific wavenumbers. The wavenumbers occur at 1-octave intervals for long wavelengths (each wavenumber is twice the previous value), 1/3-octave intervals for medium wavelengths (the wavenumbers increase by a factor of $2^{1/3} = 1.26$), and 1/6-octave intervals for short wavelengths (the wavenumbers increase by a factor of $2^{1/6} = 1.1225$). These wavenumbers are spread evenly on the log scale normally used for plotting PSD functions. Before averaging, the PSD values occur at wavenumbers that are equally spaced on a linear axis. Thus, there is a great deal of averaging at the higher wavenumbers, and relatively little at the low wavenumbers. For applications involving a truly random signal, the PSD function is always an estimate that becomes more representative as the length of the test approaches infinity. Greater averaging results in better PSD estimates, and there are equations used to calculate PSD accuracy based on the amount of averaging, which would be difficult to apply for this method where the averaging differs for each wavenumber. But remember that a road profile is not truly random, and that a PSD function for a road profile is not an estimate, but rather a partly reduced alternative representation. Thus, PSD statistical errors do not apply to this application, and the log averaging introduces no difficulty.

When computing the waveband indices, the same PSD computation method was used, except that averaging was performed at one octave intervals over the entire range of wavenumbers. The PSD value for each waveband was then rescaled to yield mean square slope by multiplying by the bandwidth (with units of cycle/m), and then the square root was taken to yield RMS slope.

APPENDIX F: Listing of Summary Data

The large amount of information acquired and compiled in the RPM constitues a data base that is a resource of longterm value. With additional analysis, the individual measurements could be used to answer many other questions about the repeatability, accuracy, and precision of the different systems. For that reason, the individual measurements are listed in tables in this appendix.

The first set of tables (numbers 9 through 31) list the IRI and MO indices computed from the profiles of each system over each subsection of a site. Table 9 lists the values computed from the rod and level profile, which was available on only the GMPG sites and one of the public road sites. Data for the profilometers are shown in the order of presentation in the main text of the report. Where multiple test speeds were used, values for each speed are also shown. Profiles were not recorded with the K.J. Law Model 8300 Roughness Surveyor, so only IRI values are shown. Because a large number of repeat tests were run with the Roughness Surveyor, the data are summarized in terms of the minimum, mean, and maximum.

The second set of tables (numbers 32 through 41) list the waveband amplitudes in m/km for each of the profilometers. Table 32 gives the reference values from the rod and level survey. The data for the profilometers follow in the same order as the systems were discussed in the main part of the report. No data are given for the K.J. Law Model 8300 Roughness Surveyor, because it did not record profiles for analysis.

Of special interest in tables 11 through 22 are the CP values computed by Centre de Recherches Routieres, Belgium, from the APL profile measurements. The CP is used extensively as a measure of roughness in other parts of the world. CRR staff observed at the meeting and performed separate analysis of the data obtained by the APL, as operated by LCPC staff. CP values from these measurements were provided to UMTRI for inclusion in the tables. The description of the processing is provided in the text of the following section quoted directly from the CRR report of March 11, 1986.

"Measurements performed on the General Motor's Proving Ground were recorded analogically and processed a the Belgian road Research Center using the CP scale.[21, 22]* This calculation is provided as a contribution to the evaluation of the profilometer's ability to measure profile for computing other statistics than the ones tested in the present report. The interest of this file is that it enables potentially the comparison of results of roughness evaluation of the profilometric type with a set of different measuring devices used in different countries and reduced to different roughness scales. The following cases have been compared through correlation to APL measurements performed on the same test tracks, processed to the CP scale.[10, 21, 22, 23, 24]

Rolling devices:

APL Trailer	Holland
APL Trailer	France
Winkelmesser	Switzerland
Viagraph	Belgium
High Speed Road Monitor	Great Britain
Bump Integrator	Great Britain
Mays Meter	U.S.A.
BPR Roughometer	Brazil
NAASRA Meter	Australia

Static devices:

TRRL Beam	Great Britain
Rod and Level	Brazil

Among the rolling devices different physical principles are used for referencing the profile: geometrical, inertial, dynamic responsing (quarter-car).

The characterization of evenness (roughness) that is used in Belgium is based on a geometric type of representation of the longitudinal profile. This representation makes use of a numerical filtering of the measured profile with a moving average technique. The option taken

---

* References identified by CRR can be found in the Reference section of the main text.

through this choice of representation offers the advantage of providing a straightforward geometrical interpretation, useful in practice.

The characterization of the measured profile is obtained by evaluating the difference of the surface profile from the reference line obtained by smoothing the same profile. The process of applying a moving average to the signal acts as a filter attenuating short length irregularities. For its application, this technique requires the numerically sampled signal recorded from the APL trailer. The distance marks for sampling are provided by a pulse train issued from the measuring wheel of the APL mounted as an odometer. The sample interval is such that all of the information contained within the bandwidth of the APL trailer is retained. (Information theory requires a sampling frequency at least equal to twice the higher cut-off frequency of the APL measuring device).

After the recorded profile is sampled and converted to a set of numerical values, those values are, in turn, smoothed using a moving average over an arbitrary baselength. The mean absolute value of the difference between the original profile and the smoothed one over a given section is determined. This mean value, divided by two and expressed per unit length, has been defined as the coefficient of evenness (CP: "coefficient de planeite"). The CP unit has the following dimension:

$$1 \text{ CP} = 10^{-5} \text{ m } (= 10^{4} \text{ mm}^2/\text{km})$$

Since the mean value is divided by two, one mm of the mean absolute value is equal to 50 CP units. It should be noted that the process of summation involving a moving average has a value dependent on the baselength used.

The interpretation of CP values are based on the following remarks:
- The coefficient of evenness for a given base smoothing length and a given block length is directly proportional to the mean surface area of the deviation of the measured longitudinal profile form the smoothed profile.
- The higher the coefficient of evenness for a given base length and a given block length, the poorer the quality of longitudinal evenness.
- The use of the sliding mean concept (moving average) to calculate CP values (smoothing of the profile) amounts to filtering the measured longitudinal profile. The result of this filtering is to eliminate the deformations with a longer wavelength than the base length chosen for smoothing. Thus the effect of short span deformations is separated from that of long span deformations, which makes it possible to characterize and locate the detected irregularities.

Computation in CP values of all APL test runs on the General Motor's Proving Ground were performed for the following choice of parameters:

length of sections:	100 meters and 0.1 mi.
sampling rate (digital conversion):	1/6 m at 18 km/h
	1/3 m at 54 and 90 km/h

moving average base lengths:

at 18 km/h	2.5 - 5 - 10 - 12 m
at 54 km/h	2.5 - 5 - 10 - 12 - 15 - 30 m
at 90 km/h	2.5 - 5 - 10 - 12 - 15 - 30 - 40 - 50 m

In Belgium, where the CP scale has been adopted by the State Road Association, APL and CP are used to assess level of acceptance for newly built cement concrete layers using APL at a speed of 6 m/s (21.6 km/h) and processing to CP with a 15 meters base and over a 100 meters section. APL and CP are also used on national networks and highways to monitor pavement roughness for the purpose of maintenance management. This is done a two possible speeds, depending on rideability condition:

54 km/h:	CP bases 2.5, 10 and 30 meters, 100 m sections
72 km/h:	CP bases 2.5, 10 and 40 meters, 100 m sections

The CP scale is implemented in Marocco and is in a process of implementation in France".

Table 9. Summary of the IRI and MO values from the rod and level profiles

Site	IRI m/km	MO m/km
19.10	8.27	5.04
20.10	7.23	4.85
21.10	4.89	3.25
22.10	7.66	5.32
23.10	2.44	1.76
24.10	2.88	2.16
25.10	3.00	1.72
26.10	1.96	0.96
26.20	1.40	0.68
27.10	2.57	1.51
27.20	2.30	1.31

Table 10. Summary of the IRI and MO values from the APL

Site	IRI m/km 50 km/h	MO m/km 50 km/h	Site	IRI m/km 18 km/h	IRI m/km 50 km/h	IRI m/km 90 km/h	MO m/km 18 km/h	MO m/km 50 km/h	MO m/km 90 km/h
1.1	8.24	5.35	16.1	-	4.50	-	-	2.82	-
			16.2	-	3.64	-	-	2.31	-
4.1	4.48	2.85	16.3	-	2.36	-	-	1.49	-
4.2	4.60	2.97	16.4	-	2.29	-	-	1.38	-
4.3	4.11	2.67							
4.4	2.08	1.24	17.1	-	0.91	-	-	0.35	-
4.5	2.86	1.63	17.2	-	0.87	-	-	0.36	-
			17.3	-	0.96	-	-	0.44	-
5.1	2.77	1.76	17.4	-	1.00	-	-	0.44	-
5.2	3.15	1.97							
5.3	2.82	1.88	19.1	6.43	6.96	6.84	4.04	4.11	3.89
			19.2	3.90	2.74	2.75	2.21	1.37	1.28
6.1	1.48	0.76							
6.2	1.53	0.85	20.1	6.52	6.65	7.83	4.22	4.07	4.55
6.3	1.35	0.65	20.2	5.57	4.84	5.80	2.56	2.27	2.64
6.4	1.24	0.58							
			21.1	-	5.74	-	-	3.72	-
7.1	1.78	0.99							
7.2	1.46	0.80	22.1	6.62	7.37	-	4.94	4.96	-
7.3	2.69	1.77	22.2	7.91	6.41	-	4.94	4.02	-
7.4	2.23	1.28							
7.5	2.14	1.21	23.1	2.33	2.53	3.04	1.42	1.63	2.05
			23.2	-	4.57	6.04	-	3.00	2.78
8.1	2.52	1.29							
8.2	2.74	1.30	24.1	3.14	3.09	3.46	1.92	2.02	2.25
8.3	3.81	3.55	24.2	2.66	3.01	3.07	1.61	1.97	1.97
9.1	1.48	0.69	25.1	2.95	3.08	2.98	1.88	1.77	1.69
9.2	1.41	0.65	25.2	2.62	2.84	3.16	1.55	1.74	1.84
			25.3	3.42	3.35	3.94	2.02	1.91	2.21
10.1	1.77	1.01							
10.2	1.44	0.77	26.1	2.04	2.44	2.64	1.19	1.53	1.72
10.3	1.81	1.01	26.2	1.52	1.57	1.71	0.76	0.81	0.83
10.4	1.94	1.16	26.3	1.47	1.45	1.30	0.68	0.74	0.57
12.1	1.86	1.25	27.1	1.99	2.31	2.15	1.17	1.42	1.18
			27.2	1.93	1.96	2.20	1.14	1.18	1.22
13.1	2.62	1.71	27.3	1.55	1.79	2.07	0.87	1.07	1.14
13.2	2.35	1.80							
13.3	2.57	1.71							
13.4	2.11	1.20							
14.1	1.61	0.89							
14.2	1.83	1.00							
15.1	2.95	1.78							
15.2	3.26	2.20							
15.3	2.71	1.95							
15.4	3.44	2.42							
15.5	4.01	2.82							

Table 11. Summary of the CP values from the APL on site 19

Test site number : 19   12 mi   Coming (Holden Area)   0, 3 mi

APL speed : 18 km/h   (5 m/s)   Sample rate 1/6 m

Distance (m)	CP	Bases m	2.5	5	10	12	15	30	40	50
0 - 100 m			98	102	109	110				
100 - 200 m			110	127	187	202				
200 - 300 m			94	117	127	130				
300 - 400 m			57	66	87	93				
400 - 500 m										
500 - 600 m •										
Distance (mi)										
0 - 0.1 mi			103	107	114	116				
0.1 - 0.2 mi			93	122	167	179				
0.2 - 0.3 mi			60	65	75	79				
0.3 - 0.4 mi										

APL speed : 54 km/h (15 m/s)   Sample rate 1/3 m

Distance (m)	CP	Bases m	2.5	5	10	12	15	30	40	50
0 - 100 m			·99	99	110	116	130	224		
100 - 200 m			122	154	211	235	267	366		
200 - 300 m			89	105	135	148	171	254		
300 - 400 m			41	52	66	76	99	176		
400 - 500 m										
500 - 600 m										
Distance (mi)										
0 - 0.1 mi			110	122	160	175	196	290		
0.1 - 0.2 mi			88	108	136	151	179	270		
0.2 - 0.3 mi			45	52	60	65	77	135		
0.3 - 0.4 mi										

APL speed : 90 km/h (25 m/s)   Sample rate 1/3 m

Distance (m)	CP	Bases m	2.5	5	10	12	15	30	40	50
0 - 100 m			99	100	109	114	128	244	307	362
100 - 200 m			110	146	209	235	268	386	434	512
200 - 300 m			98	116	150	163	190	331	416	491
300 - 400 m			43	48	64	73	93	173	207	249
400 - 500 m										
500 - 600 m										
Distance (mi)										
0 - 0.1 mi			104	119	161	176	196	312	369	413
0.1 - 0.2 mi			91	112	139	153	181	311	380	479
0.2 - 0.3 mi			46	49	61	68	83	158	193	226
0.3 - 0.4 mi										

Table 12. Summary of the CP values from the APL on site 20

Test site number : 20	12 mi Going (Holden Area)	0, 3 mi

APL speed : 18 km/h (5 m/s) Sample rate 1/6 m

Distance (m)	CP	Bases m	2,5	5	10	12	15	30	40	50
0 - 100 m			52	54	58	59				
100 - 200 m			73	84	106	113				
200 - 300 m			104	151	202	208				
300 - 400 m			77	78	100	111				
400 - 500 m										
500 - 600 m										
Distance (mi)										
0 - 0.1 mi			64	69	81	86				
0.1 - 0.2 mi			89	123	170	180				
0.2 - 0.3 mi			79	79	86	88				
0.3 - 0.4 mi										

APL speed : 54 km/h (15 m/s) Sample rate 1/3 m

Distance (m)	CP	Bases m	2,5	5	10	12	15	30	40	50
0 - 100 m			66	65	75	85	102	171		
100 - 200 m			71	92	128	143	170	266		
200 - 300 m			113	162	228	254	293	384		
300 - 400 m			63	68	85	97	123	244		
400 - 500 m										
500 - 600 m										
Distance (mi)										
0 - 0.1 mi			67	73	96	110	135	218		
0.1 - 0.2 mi			98	135	185	204	235	328		
0.2 - 0.3 mi			73	76	91	98	113	187		
0.3 - 0.4 mi										

APL speed : 90 km/h (25 m/s) Sample rate 1/3 m

Distance (m)	CP	Bases m	2,5	5	10	12	15	30	40	50
0 - 100 m			69	68	82	93	114	203	220	252
100 - 200 m			74	100	139	154	189	312	361	398
200 - 300 m			130	174	235	263	306	447	508	569
300 - 400 m			85	87	103	113	137	277	340	380
400 - 500 m										
500 - 600 m										
Distance (mi)										
0 - 0.1 mi			68	74	101	118	148	246	255	262
0.1 - 0.2 mi			113	146	193	212	246	386	466	558
0.2 - 0.3 mi			88	90	105	113	127	214	247	281
0.3 - 0.4 mi										

Table 13. Summary of the CP values from the APL on site 21

Test site number : 21   Pontiac Trail Coming (Holden Area)   0, 3 mi

APL speed : 18 km/h   (5 m/s)   Sample rate 1/6 m

Distance (m)	CP	Bases m	2,5	5	10	12	15	30	40	50
0 - 100 m			103	147	240	260				
100 - 200 m			94	122	191	220				
200 - 300 m			56	76	118	135				
300 - 400 m			140	144	209	227				
400 - 500 m										
500 - 600 m										
Distance (mi)										
0 - 0.1 mi			104	140	217	239				
0.1 - 0.2 mi			79	100	157	180				
0.2 - 0.3 mi			100	125	185	201				
0.3 - 0.4 mi										

APL speed : 54 km/h (15 m/s)   Sample rate 1/3 m

Distance (m)	CP	Bases m	2,5	5	10	12	15	30	40	50
0 - 100 m			93	140	242	279	340	654		
100 - 200 m			85	121	235	297	401	639		
200 - 300 m			80	104	184	226	298	520		
300 - 400 m			126	164	251	285	336	508		
400 - 500 m										
500 - 600 m										
Distance (mi)										
0 - 0.1 mi			99	144	264	317	405	710		
0.1 - 0.2 mi			94	110	180	214	274	467		
0.2 - 0.3 mi			111	175	299	360	466	933		
0.3 - 0.4 mi										

APL speed : 90 km/h (25 m/s)   Sample rate 1/3 m

Distance (m)	CP	Bases m	2,5	5	10	12	15	30	40	50
0 - 100 m			161	215	347	404	510	1184	1607	1729
100 - 200 m			178	240	371	446	577	892	1052	1227
200 - 300 m			149	189	305	362	468	831	1062	1186
300 - 400 m			121	161	253	290	350	619	774	830
400 - 500 m										
500 - 600 m										
Distance (mi)										
0 - 0.1 mi			198	263	417	491	628	1218	1558	1716
0.1 - 0.2 mi			136	163	250	292	372	647	830	971
0.2 - 0.3 mi			134	208	344	399	499	1053	426	1312
0.3 - 0.4 mi										

Table 14. Summary of the CP values from the APL on site 22

Test site number : 22   Pontiac Trail Going (Holden Area)   0,3 mi

APL speed : 18 km/h (5 m/s)   Sample rate 1/6 m

Distance (m)	CP	Bases m	2,5	5	10	12	15	30	40	50
0 - 100 m			110	144	197	217				
100 - 200 m			111	139	188	201				
200 - 300 m			65	95	160	183				
300 - 400 m			117	150	213	240				
400 - 500 m										
500 - 600 m										
Distance (mi)										
0 - 0,1 mi			114	147	198	216				
0,1 - 0,2 mi			86	117	176	199				
0,2 - 0,3 mi			100	132	207	231				
0,3 - 0,4 mi										

APL speed : 54 km/h (15 m/s)   Sample rate 1/3 m

Distance (m)	CP	Bases m	2,5	5	10	12	15	30	40	50
0 - 100 m			163	228	326	365	416	738		
100 - 200 m			103	134	209	241	302	540		
200 - 300 m			112	180	288	350	459	703		
300 - 400 m			115	171	305	357	436	748		
400 - 500 m										
500 - 600 m										
Distance (mi)										
0 - 0,1 mi			147	199	288	322	369	631		
0,1 - 0,2 mi			121	192	326	391	504	831		
0,2 - 0,3 mi			101	142	219	252	304	565		
0,3 - 0,4 mi										

APL speed : 90 km/h (25 m/s)   Sample rate 1/3 m

Distance (m)	CP	Bases m	2,5	5	10	12	15	30	40	50
0 - 100 m			174	235	335	380	440	798	1128	1339
100 - 200 m			160	226	398	499	681	1206	1233	1161
200 - 300 m			225	423	797	914	1055	1156	1210	1223
300 - 400 m			131	186	289	340	435	849	1123	1213
400 - 500 m										
500 - 600 m										
Distance (mi)										
0 - 0,1 mi			167	224	323	373	459	834	1064	1180
0,1 - 0,2 mi			197	353	686	813	989	1234	1287	1284
0,2 - 0,3 mi			178	286	507	578	665	1062	1311	1380
0,3 - 0,4 mi										

Table 15. Summary of the CP values from the APL on site 23

Test site number : 23   Sound Test Coming   (Holden Area)   0. 3 mi

APL speed : 18 km/h   (5 m/s)   Sample rate 1/6 m

Distance (m)	CP	Bases m	2,5	5	10	12	15	30	40	50
0 - 100 m			55	74	94	104				
100 - 200 m			32	41	56	60				
200 - 300 m			39	51	86	96				
300 - 400 m			40	58	106	120				
400 - 500 m										
500 - 600 m										
Distance (mi)										
0 - 0.1 mi			46	61	78	87				
0.1 - 0.2 mi			37	50	83	91				
0.2 - 0.3 mi			52	80	120	131				
0.3 - 0.4 mi										

APL speed : 54 km/h (15 m/s)   Sample rate 1/3 m

Distance (m)	CP	Bases m	2,5	5	10	12	15	30	40	50
0 - 100 m			53	73	109	138	189	407		
100 - 200 m			34	54	100	119	156	313		
200 - 300 m			36	54	97	115	144	302		
300 - 400 m			43	71	128	148	176	264		
400 - 500 m										
500 - 600 m										
Distance (mi)										
0 - 0.1 mi			45	61	96	120	165	358		
0.1 - 0.2 mi			37	59	108	127	159	310		
0.2 - 0.3 mi			69	103	153	171	196	280		
0.3 - 0.4 mi										

APL speed : 90 km/h   (25 m/s)   Sample rate 1/3 m

Distance (m)	CP	Bases m	2,5	5	10	12	15	30	40	50
0 - 100 m			50	74	113	140	191	432	580	676
100 - 200 m			40	61	113	138	183	423	599	734
200 - 300 m			36	54	102	127	173	386	513	588
300 - 400 m			47	76	137	159	194	337	477	695
400 - 500 m										
500 - 600 m										
Distance (mi)										
0 - 0.1 mi			44	65	104	129	176	405	554	673
0.1 - 0.2 mi			39	60	113	136	178	383	524	646
0.2 - 0.3 mi			75	116	166	187	220	364	499	639
0.3 - 0.4 mi										

Table 16. Summary of the CP values from the APL on site 24

Test site number : 24	Sound Test Going	(Holden Area)	0.3 mi

APL speed : 18 km/h (5 m/s) Sample rate 1/6 m

Distance (m) CP Bases m	2,5	5	10	12	15	30	40	50
0 - 100 m	72	113	184	207				
100 - 200 m	39	48	69	76				
200 - 300 m	41	60	102	112				
300 - 400 m	42	50	74	84				
400 - 500 m								
500 - 600 m								
Distance (mi)								
0 - 0.1 mi	58	87	139	155				
0.1 - 0.2 mi	43	60	96	105				
0.2 - 0.3 mi	41	52	93	107				
0.3 - 0.4 mi								

APL speed : 54 km/h (15 m/s) Sample rate 1/3 m

Distance (m) CP Bases m	2,5	5	10	12	15	30	40	50
0 - 100 m	72	113	193	231	291	446		
100 - 200 m	38	57	100	124	166	344		
200 - 300 m	43	70	133	161	207	356		
300 - 400 m	40	55	95	114	148	260		
400 - 500 m								
500 - 600 m								
Distance (mi)								
0 - 0.1 mi	59	92	156	187	235	367		
0.1 - 0.2 mi	42	64	117	142	188	364		
0.2 - 0.3 mi	44	67	138	169	225	434		
0.3 - 0.4 mi								

APL speed : 90 km/h (25 m/s) Sample rate 1/3 m

Distance (m) CP Bases m	2,5	5	10	12	15	30	40	50
0 - 100 m	103	154	268	331	452	1070	1454	1646
100 - 200 m	43	64	119	146	196	447	598	704
200 - 300 m	47	71	129	157	207	407	572	724
300 - 400 m	38	57	117	148	198	384	519	558
400 - 500 m								
500 - 600 m								
Distance (mi)								
0 - 0.1 mi	80	119	206	252	340	789	1078	1248
0.1 - 0.2 mi	45	67	126	155	207	443	609	739
0.2 - 0.3 mi	43	70	149	187	251	491	593	665
0.3 - 0.4 mi								

Table 17. Summary of the CP values from the APL on site 25 (first pass)

Test site number : 25   Left lane, Accoustic Area   0.4 mi

APL speed : 18 km/h   (5 m/s)   Sample rate 1/6 m

Distance (m)	CP	Bases m	2,5	5	10	12	15	30	40	50
0 - 100 m			47	70	97	100				
100 - 200 m			51	73	107	115				
200 - 300 m			44	61	73	74				
300 - 400 m			43	58	73	77				
400 - 500 m			49	70	104	109				
500 - 600 m			53	68	79	79				
Distance (mi)										
0 - 0.1 mi			50	75	111	118				
0.1 - 0.2 mi			44	60	71	71				
0.2 - 0.3 mi			47	64	92	97				
0.3 - 0.4 mi			57	75	87	89				

APL speed : 54 km/h (15 m/s)   Sample rate 1/3 m

Distance (m)	CP	Bases m	2,5	5	10	12	15	30	40	50
0 - 100 m			46	73	106	111	114	115		
100 - 200 m			50	74	121	143	185	314		
200 - 300 m			42	60	79	86	100	170		
300 - 400 m			44	66	85	87	95	101		
400 - 500 m			52	78	113	119	122	128		
500 - 600 m			47	61	70	71	74	82		
Distance (mi)										
0 - 0.1 mi			49	77	124	140	165	231		
0.1 - 0.2 mi			42	60	76	83	97	154		
0.2 - 0.3 mi			48	74	103	107	110	116		
0.3 - 0.4 mi			52	69	86	88	94	103		

APL speed : 90 km/h (25 m/s)   Sample rate 1/3 m

Distance (m)	CP	Bases m	2,5	5	10	12	15	30	40	50
0 - 100 m			47	79	116	120	123	127	138	160
100 - 200 m			49	71	115	140	182	333	388	431
200 - 300 m			38	56	73	81	95	155	182	212
300 - 400 m			40	62	83	87	95	101	103	115
400 - 500 m			48	75	113	121	123	126	126	136
500 - 600 m			49	62	73	74	77	87	93	112
Distance (mi)										
0 - 0.1 mi			48	77	125	140	164	237	268	294
0.1 - 0.2 mi			41	59	75	82	97	158	184	219
0.2 - 0.3 mi			45	70	103	109	113	116	118	131
0.3 - 0.4 mi			54	71	87	89	93	107	113	119

Table 18. Summary of the CP values from the APL on site 25 (second pass)

Test site number : 25 Left lane Accoustic Area   0. 4 mi

APL speed : 18 km/h   (5 m/s) Second Passage   Sample rate 1/6 m

Distance (m)	CP	Bases m	2,5	5	10	12	15	30	40	50
0 - 100 m			47	70	95	98				
100 - 200 m			53	74	110	118				
200 - 300 m			51	64	73	73				
300 - 400 m			45	62	76	79				
400 - 500 m			49	71	103	107				
500 - 600 m			49	64	76	77				

Distance (mi)

Distance (mi)			2,5	5	10	12	15	30	40	50
0 - 0.1 mi			51	75	112	119				
0.1 - 0.2 mi			48	62	72	72				
0.2 - 0.3 mi			47	66	92	96				
0.3 - 0.4 mi			54	72	84	86				

APL speed : 54 km/h (15 m/s)   Sample rate 1/3 m

Distance (m)	CP	Bases m	2,5	5	10	12	15	30	40	50
0 - 100 m										
100 - 200 m										
200 - 300 m										
300 - 400 m										
400 - 500 m										
500 - 600 m										

Distance (mi)

Distance (mi)										
0 - 0.1 mi										
0.1 - 0.2 mi										
0.2 - 0.3 mi										
0.3 - 0.4 mi										

APL speed : 90 km/h (25 m/s)   Sample rate 1/3 m

Distance (m)	CP	Bases m	2,5	5	10	12	15	30	40	50
0 - 100 m										
100 - 200 m										
200 - 300 m										
300 - 400 m										
400 - 500 m										
500 - 600 m										

Distance (mi)

Distance (mi)										
0 - 0.1 mi										
0.1 - 0.2 mi										
0.2 - 0.3 mi										
0.3 - 0.4 mi										

Table 19. Summary of the CP values from the APL on site 26 (first pass)

Test site number : 26   Center Lane,   Accoustic Area   0.4 mi

APL speed : 18 km/h   (5 m/s)   Sample rate 1/6 m

Distance (m)	CP	Bases m	2,5	5	10	12	15	30	40	50
0 - 100 m			25	27	32	32				
100 - 200 m			31	40	75	90				
200 - 300 m			28	32	45	50				
300 - 400 m			27	32	44	46				
400 - 500 m			30	36	55	60				
500 - 600 m			27	30	34	35				
Distance (mi)										
0 - 0.1 mi			26	32	53	61				
0.1 - 0.2 mi			29	33	47	51				
0.2 - 0.3 mi			29	34	50	54				
0.3 - 0.4 mi			27	30	38	40				

APL speed : 54 km/h (15 m/s)   Sample rate 1/3 m

Distance (m)	CP	Bases m	2,5	5	10	12	15	30	40	50
0 - 100 m			19	24	29	30	33	40		
100 - 200 m			32	49	111	143	197	374		
200 - 300 m			22	32	55	67	87	159		
300 - 400 m			27	38	56	61	68	80		
400 - 500 m			24	36	56	63	73	102		
500 - 600 m			23	32	38	40	46	67		
Distance (mi)										
0 - 0.1 mi			25	37	74	94	127	220		
0.1 - 0.2 mi			24	33	55	65	81	148		
0.2 - 0.3 mi			25	37	57	63	72	93		
0.3 - 0.4 mi			22	32	40	44	50	81		

APL speed : 90 km/h (25 m/s)   Sample rate 1/3 m

Distance (m)	CP	Bases m	2,5	5	10	12	15	30	40	50
0 - 100 m			24	28	33	34	37	50	65	96
100 - 200 m			33	51	113	145	202	404	487	537
200 - 300 m			28	33	52	61	78	137	170	221
300 - 400 m			23	33	56	62	70	93	110	139
400 - 500 m			23	34	54	60	70	98	94	97
500 - 600 m			19	23	33	36	44	76	90	111
Distance (mi)										
0 - 0.1 mi			28	39	74	93	125	236	287	321
0.1 - 0.2 mi			28	35	56	66	84	144	178	227
0.2 - 0.3 mi			23	34	56	63	71	95	100	120
0.3 - 0.4 mi			20	25	36	40	48	88	102	117

Table 20. Summary of the CP values from the APL on site 26 (second pass)

Test site number : 26 Center Lane Accoustic Area	0.4 mi

APL speed : 18 km/h   (5 m/s) Second Passage   Sample rate 1/6 m

Distance (m)	CP	Bases m	2,5	5	10	12	15	30	40	50
0 - 100 m			23	25	29	30				
100 - 200 m			27	35	70	85				
200 - 300 m			27	30	43	47				
300 - 400 m		.	27	32	44	47				
400 - 500 m			27	34	52	57				
500 - 600 m			24	27	33	34				
Distance (mi)										
0 - 0.1 mi			24	30	50	58				
0.1 - 0.2 mi			27	31	44	48				
0.2 - 0.3 mi			28	33	51	55				
0.3 - 0.4 mi			24	27	35	37				

APL speed : 54 km/h (15 m/s) Second Passage   Sample rate 1/3 m

Distance (m)	CP	Bases m	2,5	5	10	12	15	30	40	50
0 - 100 m			20	25	30	31	32	37		
100 - 200 m			32	49	108	140	194	367		
200 - 300 m			24	33	59	71	91	162		
300 - 400 m			23	36	54	60	66	75		
400 - 500 m			24	35	54	61	73	102		
500 - 600 m			21	30	35	38	43	64		
Distance (mi)										
0 - 0.1 mi			26	38	74	93	126	214		
0.1 - 0.2 mi			25	34	55	65	82	149		
0.2 - 0.3 mi			23	35	54	61	71	92		
0.3 - 0.4 mi			21	31	40	43	48	79		

APL speed : 90 km/h (25 m/s)   Sample rate 1/3 m

Distance (m)	CP	Bases m	2,5	5	10	12	15	30	40	50
0 - 100 m										
100 - 200 m										
200 - 300 m										
300 - 400 m										
400 - 500 m										
500 - 600 m										
Distance (mi)										
0 - 0.1 mi										
0.1 - 0.2 mi										
0.2 - 0.3 mi										
0.3 - 0.4 mi										

Table 21. Summary of the CP values from the APL on site 27 (first pass)

Test site number : 27 Right Lane, Accoustic Area			0.4 mi

APL speed : 18 km/h (5 m/s)   Sample rate 1/6 m

Distance (m)	CP	Bases m	2.5	5	10	12	15	30	40	50
0 - 100 m			22	27	39	43				
100 - 200 m			30	47	88	104				
200 - 300 m			32	42	65	68				
300 - 400 m			34	47	74	79				
400 - 500 m			30	35	51	58				
500 - 600 m			28	35	52	59				
Distance (mi)										
0 - 0.1 mi			26	37	64	73				
0.1 - 0.2 mi			32	44	65	69				
0.2 - 0.3 mi			31	38	60	67				
0.3 - 0.4 mi			28	36	55	61				

APL speed : 54 km/h (15 m/s)   Sample rate 1/3 m

Distance (m)	CP	Bases m	2.5	5	10	12	15	30	40	50
0 - 100 m			21	32	51	60	76	121		
100 - 200 m			33	59	115	147	203	393		
200 - 300 m			32	57	96	109	132	258		
300 - 400 m			30	44	74	85	100	129		
400 - 500 m			28	43	72	86	108	165		
500 - 600 m			27	42	69	81	101	167		
Distance (mi)										
0 - 0.1 mi			28	47	92	115	156	279		
0.1 - 0.2 mi			30	49	81	91	112	217		
0.2 - 0.3 mi			30	45	76	89	110	160		
0.3 - 0.4 mi			25	38	65	79	105	188		

APL speed : 90 km/h (25 m/s)   Sample rate 1/3 m

Distance (m)	CP	Bases m	2.5	5	10	12	15	30	40	50
0 - 100 m			23	32	53	61	77	127	155	192
100 - 200 m			34	60	127	162	222	429	495	514
200 - 300 m			28	49	84	95	116	231	292	341
300 - 400 m			31	45	74	87	107	175	234	284
400 - 500 m			24	36	68	83	106	157	150	158
500 - 600 m			25	41	73	89	113	204	234	250
Distance (mi)										
0 - 0.1 mi			30	47	95	118	160	290	334	357
0.1 - 0.2 mi			27	46	77	89	112	219	276	327
0.2 - 0.3 mi			29	42	75	89	112	174	201	229
0.3 - 0.4 mi			24	37	67	82	106	196	224	244

Table 22. Summary of the CP values from the APL on site 27 (second pass)

Test site number : 27   Right Lane   Accoustic Area   0. 4 mi

APL speed : 18 km/h   (5 m/s) Second Passage   Sample rate 1/6 m

Distance (m)	CP	Bases m	2,5	5	10	12	15	30	40	50
0 - 100 m			22	29	40	43				
100 - 200 m			29	47	86	101				
200 - 300 m			31	42	68	71				
300 - 400 m			33	47	74	80				
400 - 500 m			28	35	54	61				
500 - 600 m			28	36	54	60				
Distance (mi)										
0 - 0.1 mi			26	38	64	73				
0.1 - 0.2 mi			31	43	66	71				
0.2 - 0.3 mi			30	39	62	69				
0.3 - 0.4 mi			28	36	58	65				

APL speed : 54 km/h (15 m/s) Second Passage   Sample rate 1/3 m

Distance (m)	CP	Bases m	2,5	5	10	12	15	30	40	50
0 - 100 m			23	34	52	60	76	115		
100 - 200 m			33	57	110	140	197	392		
200 - 300 m			33	57	94	107	131	254		
300 - 400 m			30	44	74	85	100	135		
400 - 500 m			26	40	69	83	106	159		
500 - 600 m			27	42	67	81	100	157		
Distance (mi)										
0 - 0.1 mi			29	48	89	113	153	274		
0.1 - 0.2 mi			31	48	79	88	110	213		
0.2 - 0.3 mi			29	43	73	87	107	158		
0.3 - 0.4 mi			26	39	66	82	108	184		

APL speed : 90 km/h (25 m/s)   Sample rate 1/3 m

Distance (m)	CP	Bases m	2,5	5	10	12	15	30	40	50
0 - 100 m										
100 - 200 m										
200 - 300 m										
300 - 400 m										
400 - 500 m										
500 - 600 m										
Distance (mi)										
0 - 0.1 mi										
0.1 - 0.2 mi										
0.2 - 0.3 mi										
0.3 - 0.4 mi										

Table 23. Summary of the IRI values from the K.J. Law Model 8300 Roughness Surveyor

Site	IRI m/km		
	Minimum	Mean	Maximum
3.1	3.85	4.97	5.95
4.1	4.29	4.70	5.05
4.2	4.36	4.54	4.80
4.3	3.69	4.02	4.34
4.4	2.13	2.26	2.35
4.5	2.84	3.10	3.35
5.1	2.18	2.45	2.90
5.2	2.65	2.88	3.16
5.3	2.07	2.27	2.67
5.4	4.58	4.58	4.58
6.1	0.93	1.03	1.17
6.2	1.22	1.29	1.40
6.3	0.82	0.95	1.06
6.4	0.88	0.98	1.09
8.1	2.27	2.50	2.73
9.1	1.29	1.62	1.77
9.2	1.52	1.71	1.88
9.3	1.78	1.95	2.07
9.4	1.69	1.93	2.11
9.5	1.58	1.84	2.13
10.1	1.58	1.78	2.00
10.2	1.61	1.82	2.05
10.3	1.63	1.89	2.04
10.4	2.26	2.42	2.81
11.1	1.52	1.59	1.72
11.2	1.72	1.82	1.99
11.3	1.52	1.62	1.72
11.4	1.47	1.58	1.69
11.5	2.40	2.59	2.95
12.1	1.40	1.64	2.49
12.2	1.78	1.79	1.80
12.3	2.83	2.83	2.83
13.1	2.26	2.36	2.49
13.2	2.04	2.24	3.01
13.3	2.64	2.86	3.41
13.4	1.66	2.04	2.57
13.5	2.18	2.66	3.25

Table 24. Summary of the IRI and MO values from the FHWA/IR profilometer

Site	IRI m/km 80 km/h	MO m/km 80 km/h
4.1	4.99	3.62
4.2	4.67	3.29
4.3	4.35	3.10
4.4	2.30	1.42
5.1	2.40	1.61
5.2	3.03	2.09
5.3	2.49	1.74
6.1	1.42	0.97
6.2	1.57	1.05
6.3	1.27	0.79
6.4	1.18	0.63
7.1	1.87	1.17
7.2	1.50	0.93
7.3	2.84	2.06
7.4	2.62	1.78
7.5	2.26	1.42
8.1	2.79	1.47
8.2	2.96	1.65
8.3	4.35	3.99
9.1	1.58	0.83
9.2	1.34	0.71
9.3	1.86	1.01
9.4	1.71	0.90
10.1	1.81	1.11
10.2	1.60	0.86
10.3	1.83	1.10
10.4	2.04	1.22
11.1	1.87	1.26
11.2	2.09	1.33
11.3	2.05	1.27
11.4	1.86	1.11
12.1	1.82	1.43
13.1	2.67	2.04
13.2	2.55	2.24
13.3	2.83	2.15
13.4	1.99	1.53
14.1	1.68	0.98
14.2	2.12	1.28
15.1	5.96	4.53
15.2	3.69	2.60
15.3	3.45	2.30
15.4	3.76	2.77
15.5	5.09	3.79

Site	IRI m/km 32 km/h	IRI m/km 56 km/h	IRI m/km 80 km/h	MO m/km 32 km/h	MO m/km 56 km/h	MO m/km 80 km/h
16.1	-	-	4.67	-	-	3.05
16.2	-	-	4.01	-	-	2.87
16.3	-	-	2.40	-	-	1.58
16.4	-	-	2.72	-	-	2.80
17.1	-	-	0.96	-	-	0.42
17.2	-	-	0.91	-	-	0.36
17.3	-	-	0.97	-	-	0.52
17.4	-	-	0.94	-	-	0.47
18.1	-	-	2.89	-	-	2.42
18.2	-	-	2.24	-	-	1.70
19.1	7.68	6.65	-	4.78	4.29	-
19.2	3.52	3.34	-	2.23	2.13	-
20.1	7.16	7.57	-	4.77	4.92	-
20.2	5.78	5.94	-	2.86	2.93	-
21.1	5.70	5.82	-	4.32	4.42	-
21.2	9.81	9.99	-	6.50	6.62	-
22.1	8.33	8.22	-	6.27	6.28	-
22.2	8.67	8.64	-	6.11	6.22	-
23.1	2.39	2.44	2.43	1.68	1.70	1.71
23.2	3.85	3.88	4.00	2.93	2.81	2.90
24.1	2.98	2.93	2.85	2.23	2.16	2.05
24.2	2.98	3.01	3.11	2.07	2.13	2.15
25.1	3.07	3.10	3.10	2.05	2.01	2.02
25.2	2.74	2.69	2.81	1.74	1.72	1.81
25.3	3.60	3.60	3.50	2.23	2.21	2.18
26.1	2.16	-	2.12	1.30	-	1.31
26.2	1.32	-	1.37	0.67	-	0.68
26.3	1.06	-	1.14	0.44	-	0.48
27.1	2.31	2.23	2.31	1.48	1.40	1.34
27.2	1.81	1.85	1.80	1.14	1.12	1.10
27.3	1.61	1.65	1.63	0.96	0.96	0.95

Table 25. Summary of the IRI and MO values from the FHWA/Selcom profilometer

Site	IRI m/km 32 km/h	IRI m/km 80 km/h	MO m/km 32 km/h	MO m/km 80 km/h
4.1	-	4.89	-	3.54
4.2	-	4.71	-	3.27
4.3	-	4.38	-	3.16
4.4	-	2.33	-	1.46
4.5	-	3.15	-	2.06
5.1	-	2.51	-	1.89
5.2	-	3.28	-	2.32
6.1	-	1.42	-	1.02
6.2	-	1.59	-	1.12
6.3	-	1.25	-	0.83
6.4	-	1.12	-	0.60
7.1	-	2.01	-	1.31
7.2	-	1.57	-	1.00
7.3	-	3.22	-	2.66
7.4	-	3.17	-	. 2.67
8.1	-	2.78	-	1.60
8.2	-	3.48	-	2.03
9.1	-	1.60	-	0.85
9.2	-	1.36	-	0.74
9.3	-	1.83	-	1.04
9.4	-	1.76	-	0.99
10.1	-	1.91	-	1.17
10.2	-	1.64	-	0.96
10.3	-	1.91	-	1.22
10.4	-	2.08	-	1.30
11.1	-	1.86	-	1.32
11.2	-	2.26	-	1.46
11.3	-	2.13	-	1.56
11.4	-	1.89	-	1.13
12.1	-	1.55	-	0.92
13.1	-	2.71	-	2.16
13.2	-	2.68	-	2.26
13.3	-	2.78	-	2.25
13.4	-	2.10	-	1.98
14.1	1.99	-	1.17	-
16.1	-	4.95	-	3.34
16.2	-	3.84	-	2.77
16.3	-	2.40	-	1.60
16.4	-	2.57	-	2.44

Site	IRI m/km 32 km/h	IRI m/km 56 km/h	IRI m/km 80 km/h	MO m/km 32 km/h	MO m/km 56 km/h	MO m/km 80 km/h
17.1	-	-	0.98	-	-	0.45
17.2	-	-	0.92	-	-	0.38
17.3	-	-	0.97	-	-	0.50
17.4	-	-	1.00	-	-	0.53
18.1	-	-	3.09	-	-	2.49
19.1	7.44	6.58	-	4.77	4.43	-
19.2	3.57	3.67	-	2.47	2.59	-
20.1	6.91	-	-	4.70	-	-
20.2	6.15	-	-	3.19	-	-,
21.1	-	5.68	-	-	3.81	-
22.1	8.11	8.02	-	6.21	6.21	-
22.2	8.42	8.52	-	5.84	5.86	-
23.1	2.37	2.38	2.39	1.72	1.70	1.72
23.2	3.77	3.84	3.99	2.87	2.87	2.97
24.1	3.22	3.74	4.10	2.61	3.13	3.61
24.2	3.39	3.87	4.44	2.75	3.16	3.70
25.1	-	3.09	3.03	-	2.13	2.08
25.2	-	2.74	2.80	-	1.76	1.79
25.3	-	3.68	3.65	-	2.31	2.33
26.1	2.04	1.95	1.94	1.24	1.16	1.12
26.2	1.23	1.27	1.21	0.60	0.62	0.58
26.3	1.07	1.08	1.10	0.45	0.45	0.45
27.1	2.48	2.63	2.40	1.86	2.02	1.74
27.2	2.08	2.21	2.08	1.60	1.71	1.50
27.3	1.89	2.09	2.08	1.45	1.65	1.63

Table 26. Summary of the IRI and MO values from the GMPG profilometer

Site	IRI m/km 24	IRI m/km 56	IRI m/km 80 km/h	MO m/km 24	MO m/km 56	MO m/km 80 km/h
1.1	-	8.27	-	-	5.55	-
1.2	-	6.98	-	-	4.92	-
2.1	-	11.09	-	-	8.33	-
2.2	-	5.57	-	-	4.14	-
3.1	6.85	7.82	-	6.28	6.88	-
4.1	-	5.28	-	-	3.91	-
4.2	-	4.44	-	-	2.87	-
4.3	-	5.01	-	-	3.35	-
4.4	-	2.35	-	-	1.34	-
4.5	-	3.58	-	-	2.24	-
5.1	-	3.03	-	-	1.87	-
5.2	-	2.99	-	-	2.11	-
6.1	-	1.57	-	-	0.91	-
6.2	-	1.33	-	-	0.71	-
6.3	-	1.30	-	-	0.74	-
7.1	-	1.83	-	-	1.07	-
7.2	-	2.32	-	-	1.77	-
7.3	-	2.72	-	-	1.66	-
7.4	-	2.64	-	-	1.52	-
8.1	-	2.89	-	-	1.54	-
8.2	-	2.86	-	-	1.57	-
9.1	-	-	1.49	-	-	0.74
9.2	-	-	1.37	-	-	0.71
9.3	-	-	2.00	-	-	1.08
9.4	-	-	1.99	-	-	1.09
10.1	-	-	1.80	-	-	1.00
10.2	-	-	1.71	-	-	0.90
10.3	-	-	1.93	-	-	1.15
11.1	-	-	2.22	-	-	1.41
11.2	-	-	2.21	-	-	1.31
11.3	-	-	2.16	-	-	1.19
11.4	-	-	2.31	-	-	1.47
12.1	-	-	2.22	-	-	1.58
13.1	-	-	2.33	-	-	1.69
13.2	-	-	2.63	-	-	2.11
13.3	-	-	2.51	-	-	1.82
13.4	-	-	2.50	-	-	1.84
14.1	-	-	1.88	-	-	1.11
14.2	-	-	2.19	-	-	1.23

Site	IRI m/km 24	IRI m/km 56	IRI m/km 80 km/h	MO m/km 24	MO m/km 56	MO m/km 80 km/h
16.1	-	-	4.11	-	-	2.74
16.2	-	-	3.46	-	-	2.26
16.3	-	-	2.53	-	-	1.66
16.4	-	-	2.11	-	-	1.42
17.1	-	-	0.92	-	-	0.35
17.2	-	-	0.87	-	-	0.32
17.3	-	-	0.95	-	-	0.45
17.4	-	-	0.90	-	-	0.38
18.1	-	3.46	-	-	2.77	-
19.1	7.90	10.05	7.60	5.13	5.80	4.63
19.2	4.09	3.37	3.33	2.40	1.83	1.93
20.1	7.63	7.36	7.62	4.76	4.83	4.89
20.2	4.88	4.92	5.70	2.53	2.47	2.61
21.1	8.10	8.63	6.28	6.44	6.06	4.24
21.2	11.66	8.41	6.82	6.86	5.70	4.80
22.1	9.21	7.98	8.45	7.49	6.17	6.44
22.2	9.62	-	7.52	6.39	-	5.02
23.1	3.00	-	2.66	1.78	-	1.54
23.2	4.62	-	4.11	2.97	-	-
24.1	3.40	2.71	3.01	2.18	1.72	1.94
24.2	3.34	-	2.76	2.21	-	1.84
25.1	3.73	3.33	2.86	2.25	2.04	1.71
25.2	4.00	-	3.17	2.57	-	2.03
25.3	4.38	-	3.44	-	-	2.00
26.1	1.74	1.37	1.33	0.76	0.70	0.58
26.2	1.49	1.33	1.24	0.65	0.63	0.56
26.3	1.41	-	1.06	-	-	0.42
27.1	2.22	1.86	1.79	1.25	1.15	1.09
27.2	2.18	1.91	1.89	1.18	1.15	1.08
27.3	1.87	-	1.43	-	-	0.83

Table 27. Summary of the IRI and MO values from the Minnesota profilometer

Site	IRI m/km 48 km/h	IRI m/km 80 km/h	MO m/km 48 km/h	MO m/km 80 km/h
1.1	10.22	-	6.92	-
1.2	6.89	-	4.68	-
2.1	8.37	-	6.47	-
2.2	4.84	-	3.49	-
3.1	-	5.34	-	5.21
4.1	-	4.72	-	3.33
4.2	-	4.40	-	2.94
4.3	-	3.98	-	2.79
4.4	-	2.26	-	1.39
4.5	-	2.34	-	1.54
5.1	-	2.26	-	1.43
5.2	-	2.96	-	1.89
5.3	-	2.28	-	1.46
6.1	-	1.19	-	0.68
6.2	-	1.43	-	0.88
6.3	-	1.13	-	0.59
6.4	-	1.18	-	0.66
7.1	-	1.55	-	0.95
7.2	-	1.51	-	0.84
7.3	-	2.26	-	1.36
7.4	-	2.09	-	1.20
7.5	-	1.72	-	0.88
9.1	-	1.49	-	0.74
9.2	-	1.22	-	0.57
9.3	-	1.82	-	0.97
9.4	-	1.65	-	0.83
10.1	-	1.83	-	1.05
10.2	-	1.36	-	0.69
10.3	-	1.69	-	0.93
10.4	-	2.14	-	1.31
11.1	-	1.87	-	1.12
11.2	-	1.93	-	1.18
11.3	-	1.95	-	1.15
11.4	-	1.71	-	0.96
12.1	-	1.87	-	1.28
13.1	-	2.48	-	1.75
13.2	-	2.23	-	1.72
13.3	-	2.80	-	2.18
13.4	-	1.88	-	1.24

Site	IRI m/km 24 km/h	IRI m/km 48 km/h	IRI m/km 80 km/h	MO m/km 24 km/h	MO m/km 48 km/h	MO m/km 80 km/h
14.1	-	-	1.49	-	-	0.79
14.2	-	-	1.90	-	-	1.09
15.1	-	3.15	-	-	2.38	-
15.2	-	3.55	-	-	2.41	-
15.3	-	2.59	-	-	1.78	-
15.4	-	2.99	-	-	2.34	-
15.5	-	3.77	-	-	2.84	-
16.1	-	-	3.87	-	-	2.56
16.2	-	-	3.71	-	-	2.55
16.3	-	-	2.29	-	-	1.46
16.4	-	-	2.45	-	-	1.81
17.1	-	-	0.99	-	-	0.40
17.2	-	-	0.92	-	-	0.36
17.3	-	-	0.98	-	-	0.48
17.4	-	-	1.03	-	-	0.48
18.1	-	2.63	-	-	2.02	-
18.2	-	2.02	-	-	1.48	-
21.1	4.67	4.62	5.03	3.21	3.16	3.65
21.2	8.83	8.71	8.84	5.53	5.47	5.54
22.1	7.57	7.64	-	5.59	5.55	-
22.2	7.88	8.19	-	5.61	5.76	-
23.1	2.33	2.42	2.52	1.56	1.59	1.80
23.2	3.46	3.53	3.52	2.35	2.44	2.38
24.1	2.44	2.45	2.49	1.58	1.54	1.59
24.2	2.91	2.70	2.70	1.88	1.80	1.77
25.1	3.04	3.09	3.12	2.01	2.03	2.06
25.2	2.53	2.61	2.61	1.59	1.61	1.62
25.3	2.99	2.95	3.02	1.70	1.69	1.73
26.1	2.04	1.99	1.87	1.28	1.27	1.15
26.2	1.06	0.99	1.02	0.45	0.41	0.44
26.3	0.89	0.84	0.80	0.28	0.26	0.26
27.1	2.40	2.35	2.37	1.59	1.55	1.52
27.2	1.71	1.75	1.79	1.03	1.03	1.07
27.3	1.62	1.52	1.58	0.90	0.81	0.85

Table 28. Summary of the IRI and MO values from the Ohio profilometer

Site	IRI m/km 48 km/h	IRI m/km 80 km/h	MO m/km 48 km/h	MO m/km 80 km/h
1.1	7.70	-	5.03	-
1.2	6.22	-	4.14	-
2.1	8.58	-	6.63	-
2.2	4.68	-	3.27	-
3.1	5.67	-	5.83	-
4.1	-	4.82	-	3.42
4.2	-	4.40	-	3.00
4.3	-	4.60	-	3.23
4.4	-	2.36	-	1.51
4.5	-	2.89	-	1.80
5.1	2.41	2.44	1.73	1.75
5.2	3.46	3.18	2.34	2.16
5.3	2.67	2.52	1.92	1.81
6.1	1.34	1.36	0.78	0.79
6.2	1.47	1.50	0.93	0.96
6.3	1.19	1.17	0.62	0.61
6.4	1.16	1.14	0.60	0.59
7.1	1.80	1.82	1.09	1.11
7.2	1.43	1.45	0.81	0.83
7.3	2.53	2.83	1.68	2.00
7.4	2.33	2.36	1.58	1.54
7.5	2.39	1.98	1.34	1.08
8.1	2.73	2.77	1.39	1.43
8.2	3.22	3.49	1.67	1.77
8.3	4.14	4.23	3.52	3.19
9.1	-	1.40	-	0.66
9.2	-	1.32	-	0.63
9.3	-	1.65	-	0.90
9.4	-	1.70	-	0.85
10.1	-	1.80	-	1.08
10.2	-	1.52	-	0.78
10.3	-	1.71	-	0.95
10.4	-	2.03	-	1.17
10.5	-	1.62	-	0.90
11.1	-	1.93	-	1.19
11.2	-	2.04	-	1.28
11.3	-	1.99	-	1.17
11.4	-	1.74	-	0.97
12.1	-	1.60	-	1.17
13.1	-	2.59	-	1.87
13.2	-	2.17	-	1.84
13.3	-	2.63	-	2.04
13.4	-	2.02	-	1.40

Site	IRI m/km 24 km/h	IRI m/km 48 km/h	IRI m/km 80 km/h	MO m/km 24 km/h	MO m/km 48 km/h	MO m/km 80 km/h
14.1	-	-	1.52	-	-	0.82
14.2	-	-	1.91	-	-	1.05
15.1	-	2.63	2.62	-	1.68	1.61
15.2	-	3.49	3.78	-	2.69	2.49
15.3	-	2.58	3.09	-	1.82	1.98
15.4	-	3.15	3.90	-	2.30	2.54
15.5	-	5.37	6.24	-	3.64	4.34
16.1	-	-	4.31	-	-	2.72
16.2	-	-	3.93	-	-	2.75
16.3	-	-	2.33	-	-	1.50
16.4	-	-	2.30	-	-	1.47
16.5	-	-	.	-	-	-
17.1	-	-	0.87	-	-	0.34
17.2	-	-	0.82	-	-	0.27
17.3	-	-	0.84	-	-	0.37
17.4	-	-	0.99	-	-	0.43
18.1	-	-	2.98	-	-	2.52
18.2	-	-	2.25	-	-	1.60
19.1	6.46	7.12	6.52	4.19	4.43	4.07
19.2	4.66	4.69	3.95	2.77	2.81	2.33
20.1	6.61	6.42	7.71	4.37	4.29	4.77
20.2	4.12	3.91	6.08	2.34	2.16	2.83
21.1	5.88	5.70	-	4.52	4.15	-
21.2	11.00	10.81	-	6.71	6.66	-
22.1	7.68	7.03	-	5.78	5.33	-
22.2	9.17	9.10	-	6.33	6.16	-
23.1	2.49	2.33	-	1.80	1.69	-
23.2	4.38	4.21	-	3.33	3.21	-
24.1	2.91	2.83	-	1.96	1.95	-
24.2	2.97	3.07	-	1.96	2.04	-
25.1	3.16	3.17	3.19	2.15	2.08	2.16
25.2	2.59	2.71	2.78	1.60	1.66	1.68
25.3	2.92	2.92	2.99	1.76	1.67	1.76
26.1	1.87	1.92	1.89	1.25	1.26	1.23
26.2	0.93	0.96	1.01	0.41	0.40	0.44
26.3	0.80	0.73	0.74	0.26	0.21	0.23
27.1	2.52	2.52	2.52	1.59	1.58	1.62
27.2	1.92	1.89	1.87	1.20	1.15	1.19
27.3	1.58	1.63	1.73	0.80	0.87	0.90

Table 29. Summary of the IRI and MO values from the West Virginia profilometer

Site	IRI m/km			MO m/km		
	24 km/h	48 km/h	80 km/h	24 km/h	48 km/h	80 km/h
2.1	-	8.14	-	-	6.07	-
2.2	-	4.54	-	-	3.33	-
6.1	-	1.24	-	-	0.67	-
6.2	-	1.40	-	-	0.84	-
6.3	-	1.07	-	-	0.53	-
6.4	-	1.05	-	-	0.49	-
7.1	-	1.56	-	-	0.95	-
7.2	-	1.35	-	-	0.71	-
7.3	-	2.25	-	-	1.33	-
7.4	-	2.03	-	-	1.23	-
7.5	-	1.81	-	-	1.00	-
9.1	-	1.34	-	-	0.65	-
9.2	-	1.21	-	-	0.59	-
9.3	-	1.55	-	-	0.80	-
9.4	-	1.47	-	-	0.72	-
10.1	-	1.64	-	-	0.91	-
10.2	-	1.31	-	-	0.64	-
10.3	-	1.63	-	-	0.93	-
11.1	-	1.68	-	-	1.01	-
11.2	-	1.92	-	-	1.29	-
11.3	-	1.89	-	-	1.08	-
11.4	-	1.64	-	-	0.92	-
18.1	-	2.72	-	-	2.09	-
18.2	-	1.96	-	-	1.40	-
19.1	9.07	6.42	-	5.24	4.30	-
19.2	3.36	5.65	-	2.02	2.70	-
20.1	6.66	7.73	-	4.33	4.68	-
20.2	6.15	3.08	-	2.85	1.86	-
23.1	2.25	7.03	-	1.50	5.27	-
23.2	3.25	7.82	-	2.18	5.41	-
24.1	2.38	-	-	1.52	-	-
24.2	2.66	-	-	1.71	-	-
25.1	2.68	2.81	2.88	1.68	1.89	1.90
25.2	2.21	2.40	2.31	1.31	1.49	1.43
25.3	2.38	2.61	2.62	1.35	1.54	1.52
26.1	1.89	1.89	1.98	1.21	1.22	1.28
26.2	0.97	0.95	0.93	0.39	0.39	0.39
26.3	0.72	0.73	0.78	0.21	0.21	0.22
27.1	2.15	2.18	2.40	1.34	1.39	1.47
27.2	1.62	1.59	1.63	0.96	0.96	0.98
27.3	1.43	1.46	1.48	0.73	0.76	0.77

Table 30. Summary of the IRI and MO values from the Michigan DOT profilometer

Site	IRI m/km 55 km/h	IRI m/km 82 km/h	MO m/km 55 km/h	MO m/km 82 km/h	Site	IRI m/km 55 km/h	IRI m/km 82 km/h	MO m/km 55 km/h	MO m/km 82 km/h
6.1	1.69	1.55	1.20	1.06	17.1	-	0.82	-	0.38
6.2	1.67	1.84	1.18	1.37	17.2	-	0.70	-	0.27
6.3	1.37	1.38	0.78	0.84	17.3	-	0.91	-	0.48
6.4	1.17	1.26	0.69	0.71	17.4	-	0.97	-	0.47
7.1	1.72	1.67	1.12	1.16	19.1	11.52	9.47	6.62	5.81
7.2	2.02	1.95	1.27	1.29	19.2	4.33	3.60	2.62	2.25
7.3	3.02	2.98	1.98	2.02					
7.4	2.78	2.73	1.95	1.96	20.1	8.37	7.58	5.40	5.03
7.5	2.57	2.47	1.62	1.52	20.2	7.58	6.66	3.63	3.19
8.1	3.10	2.96	1.72	1.63	21.1	6.13	6.86	4.34	4.94
8.2	3.05	3.38	1.75	1.88	21.2	10.58	10.72	6.86	6.85
8.3	4.18	4.29	3.21	3.15					
					22.1	9.15	8.86	6.86	6.76
10.1	-	1.73	-	1.02	22.2	10.18	9.80	6.90	6.49
10.2	-	1.49	-	0.85					
10.3	-	1.82	-	1.13	23.1	2.60	2.60	1.82	1.90
					23.2	3.93	3.87	2.89	2.87
11.1	-	1.93	-	1.18					
11.2	-	2.34	-	1.52	24.1	3.17	3.53	2.28	2.64
11.3	-	2.07	-	1.33	24.2	3.40	3.32	2.27	2.36
11.4	-	2.01	-	1.32					
					25.1	3.31	3.29	2.30	2.29
13.1	-	2.70	-	2.17	25.2	3.10	3.09	1.95	1.90
13.2	-	2.68	-	2.44	25.3	2.87	2.73	1.67	1.60
13.3	-	2.85	-	2.22					
13.4	-	2.04	-	1.51	26.1	2.19	2.13	1.50	1.41
					26.2	1.15	1.18	0.53	0.56
16.1	4.11	3.92	2.69	2.70	26.3	0.98	1.08	0.44	0.52
16.2	4.11	3.94	2.99	2.86					
16.3	2.70	2.58	1.81	1.74	27.1	2.92	2.92	1.83	1.84
16.4	2.52	2.49	1.69	1.66	27.2	2.12	2.03	1.26	1.25
					27.3	1.80	1.73	1.26	1.04

Table 31. Summary of the IRI and MO values from the South Dakota profilometer

Site	IRI 31	56	80 km/h	MO 31	56	80 km/h	Site	IRI 31	56	80 km/h	MO 31	56	80 km/h
1.1	6.95	6.00	5.99	4.44	4.54	4.33	14.1	-	1.80	2.51	-	1.00	1.39
1.2	4.46	5.38	5.27	3.07	3.92	4.03	14.2	-	1.87	2.20	-	1.11	1.20
2.1	-	-	-	5.62	5.56	-	15.1	-	4.09	3.76	-	2.37	2.32
2.2	-	-	-	2.07	2.63	-	15.2	-	4.05	4.61	-	2.63	2.77
							15.3	-	3.85	4.24	-	2.17	2.45
3.1	-	-	-	-	4.55	-	15.4	-	3.82	4.01	-	2.31	2.38
							15.5	-	4.61	4.68	-	3.24	3.05
4.1	-	4.17	4.27	-	2.86	2.81							
4.2	-	4.67	4.53	-	3.09	2.98	16.1	-	-	2.78	-	-	2.02
4.3	-	4.32	4.25	-	2.82	2.87	16.2	-	-	3.52	-	-	2.25
4.4	-	2.71	2.99	-	1.79	1.83	16.3	-	-	2.94	-	-	1.78
4.5	-	2.93	2.67	-	1.80	1.70	16.4	-	-	2.99	-	-	1.81
5.1	-	2.34	2.68	-	1.50	1.70	17.1	-	-	1.30	-	-	0.63
5.2	-	3.31	3.71	-	2.02	2.26	17.2	-	-	1.23	-	-	0.65
5.3	-	2.57	3.00	-	1.86	2.20	17.3	-	-	1.66	-	-	0.90
							17.4	-	-	1.24	-	-	0.69
6.1	-	2.13	2.92	-	1.28	1.69							
6.2	-	1.84	1.83	-	1.16	1.11	18.1	-	3.35	3.54	-	2.58	2.61
6.3	-	1.92	2.00	-	1.04	1.21	18.2	-	2.59	3.29	-	1.79	2.19
6.4	-	1.53	1.50	-	0.94	0.84							
							19.1	5.46	6.03	-	3.47	3.71	-
7.1	-	1.02	1.47	-	0.63	0.87	19.2	2.78	3.26	-	1.74	2.07	-
7.2	-	2.15	2.39	-	1.28	1.41							
7.3	-	1.81	2.37	-	1.33	1.63	20.1	5.01	5.99	5.18	3.24	3.97	3.35
7.4	-	1.26	1.71	-	0.71	1.01	20.2	5.72	5.75	4.30	2.82	2.86	2.34
7.5	-	2.89	2.69	-	2.19	1.61							
							21.1	4.01	5.86	5.90	2.87	4.37	4.51
8.1	-	3.19	3.16	-	1.91	1.80	21.2	6.99	8.59	7.31	4.67	5.32	4.91
8.2	-	2.65	2.65	-	1.56	1.48							
8.3	-	3.48	3.84	-	2.63	2.83	22.1	6.89	6.56	-	5.15	5.07	-
							22.2	5.62	6.62	-	3.72	4.69	-
9.1	-	-	1.84	-	-	1.03							
9.2	-	-	1.92	-	-	1.02	23.1	1.22	1.79	2.41	0.69	1.07	1.55
9.3	-	-	1.86	-	-	0.96	23.2	2.59	3.24	3.86	1.80	2.24	2.59
9.4	-	-	1.60	-	-	0.91							
							24.1	3.03	3.28	3.24	2.09	2.25	2.16
10.1	-	-	1.57	-	-	0.85	24.2	3.17	3.01	3.19	2.18	2.09	1.98
10.2	-	-	1.95	-	-	1.02							
10.3	-	-	1.92	-	-	1.09	25.1	2.60	2.79	2.81	1.70	1.71	1.82
10.4	-	-	2.24	-	-	1.31	25.2	2.51	2.76	2.78	1.48	1.62	1.73
							25.3	3.08	2.85	3.32	1.83	1.77	1.98
11.1	-	-	2.66	-	-	1.60							
11.2	-	-	2.39	-	-	1.41	26.1	1.21	1.46	1.01	0.89	0.94	0.81
11.3	-	-	1.06	-	-	0.58	26.2	0.24	1.25	0.26	0.01	0.64	-
11.4	-	-	1.52	-	-	0.93	26.3	0.22	0.62	0.28	-	0.24	-
12.1	-	-	2.18	-	-	1.37	27.1	2.65	2.50	3.71	1.81	1.91	2.39
							27.2	1.73	1.74	3.46	0.96	1.25	2.03
13.1	-	-	2.73	-	-	1.97	27.3	1.79	1.89	3.65	0.93	1.14	2.09
13.2	-	-	2.87	-	-	2.08							
13.3	-	-	3.12	-	-	2.18							
13.4	-	-	2.58	-	-	1.69							

Table 32. Summary of waveband values for the rod and level measurements

Site	128 m	64 m	32 m	16 m	8 m	4 m	2 m	1 m	0.5 m
19	0.76	1.65	1.16	1.77	2.26	3.29	6.61	8.70	10.70
20	0.76	1.58	1.28	1.90	2.46	3.80	5.37	6.34	9.23
21	0.83	1.81	2.40	2.89	1.46	2.57	2.88	2.75	2.60
22	0.88	2.10	2.94	4.17	2.49	3.87	5.61	4.90	4.89
23	0.93	1.93	1.56	1.28	1.08	1.09	1.39	2.45	4.13
24	0.93	1.98	1.61	1.55	1.45	1.31	1.48	2.31	4.18
25	0.29	0.54	0.80	0.55	0.99	1.79	1.70	2.05	3.70
26	0.28	0.40	0.60	0.57	0.54	0.65	0.94	-	-
27	0.20	0.66	0.77	0.76	0.93	0.89	1.65	-	-

Table 33. Summary of waveband values for the APL

Site	128 m 18	50	90 km/h	64 m 18	50	90 km/h	32 m 18	50	90 km/h	16 m 18	50	90 km/h
1	-	0.17	-	-	0.49	-	-	1.05	-	-	1.90	-
4	-	0.15	-	-	0.65	-	-	1.37	-	-	1.16	-
5	-	0.13	-	-	0.35	-	-	0.93	-	-	0.69	-
6	-	0.10	-	-	0.20	-	-	0.57	-	-	0.65	-
7	-	0.07	-	-	0.45	-	-	0.87	-	-	1.05	-
8	-	0.12	-	-	0.42	-	-	0.81	-	-	0.76	-
10	-	0.07	-	-	0.33	-	-	0.66	-	-	0.74	-
12	-	0.09	-	-	0.29	-	-	0.71	-	-	0.82	-
13	-	0.02	-	-	0.11	-	-	0.39	-	-	0.86	-
14	-	0.01	-	-	0.12	-	-	0.35	-	-	0.70	-
15	-	0.05	-	-	0.26	-	-	0.80	-	-	0.85	-
16	-	0.03	-	-	0.17	-	-	0.89	-	-	1.43	-
17	-	0.04	-	-	0.11	-	-	0.49	-	-	0.50	-
19	0.01	0.15	0.22	0.08	0.74	1.24	0.26	1.20	0.84	1.24	1.66	1.42
20	0.04	0.15	0.13	0.12	0.70	1.52	0.30	1.05	1.10	1.39	1.91	1.96
21	-	0.40	-	-	1.08	-	-	1.87	-	-	2.99	-
22	0.07	0.56	-	0.20	1.58	-	0.43	1.97	-	2.48	3.77	-
23	0.02	0.16	0.26	0.07	0.88	1.72	0.25	1.42	1.97	0.79	1.27	1.47
24	0.03	0.22	0.43	0.08	0.80	1.69	0.31	1.47	1.71	1.01	1.57	1.52
25	0.05	0.08	0.16	0.13	0.19	0.41	0.39	0.83	0.85	0.81	0.48	0.62
26	0.05	0.26	0.24	0.07	0.39	0.43	0.16	0.78	0.60	0.34	0.58	0.59
27	0.02	0.07	0.08	0.04	0.29	0.56	0.14	0.78	0.79	0.52	0.75	0.90

Site	8 m 18	50	90 km/h	4 m 18	50	90 km/h	2 m 18	50	90 km/h	1 m 18
1	-	2.90	-	-	3.80	-	-	8.01	-	-
4	-	1.26	-	-	1.83	-	-	2.57	-	-
5	-	1.07	-	-	1.49	-	-	2.08	-	-
6	-	0.76	-	-	0.63	-	-	0.88	-	-
7	-	0.69	-	-	0.95	-	-	1.30	-	-
8	-	0.78	-	-	2.13	-	-	2.76	-	-
10	-	1.04	-	-	0.91	-	-	0.59	-	-
12	-	0.76	-	-	0.68	-	-	0.68	-	-
13	-	0.84	-	-	1.39	-	-	2.43	-	-
14	-	0.81	-	-	0.90	-	-	0.87	-	-
15	-	1.15	-	-	2.00	-	-	3.45	-	-
16	-	1.57	-	-	1.74	-	-	1.84	-	-
17	-	0.49	-	-	0.55	-	-	0.58	-	-
19	2.17	2.23	1.38	3.27	2.97	3.33	4.68	5.04	5.67	5.62
20	2.38	2.36	2.03	3.28	3.38	3.72	4.99	4.62	6.11	5.84
21	-	1.66	-	-	2.30	-	-	4.13	-	-
22	2.26	1.91	-	4.24	3.67	-	4.98	4.75	-	4.04
23	1.07	1.15	1.42	1.07	1.19	1.21	1.52	1.31	1.84	2.60
24	1.43	1.43	1.55	1.38	1.31	1.42	2.06	1.62	2.02	2.91
25	1.13	0.94	0.86	1.70	1.90	1.93	1.86	1.70	1.64	2.51
26	0.51	0.59	0.60	0.65	0.74	0.70	1.31	1.09	1.29	1.88
27	0.83	0.96	0.89	0.82	0.88	0.88	1.38	1.24	1.43	2.03

Table 34. Summary of waveband values for the FHWA/IR profilometer

Site	128 m 32	56	80 km/h	64 m 32	56	80 km/h	32 m 32	56	80 km/h	16 m 32	56	80 km/h	8 m 32	56	80 km/h
2	-	5.42	-	-	1.59	-	-	3.30	-	-	2.61	-	-	3.49	-
5	-	-	2.01	-	-	1.40	-	-	1.08	-	-	0.74	-	-	0.97
6	-	-	1.52	-	-	1.30	-	-	0.87	-	-	0.63	-	-	0.80
7	-	-	1.88	-	-	1.44	-	-	1.10	-	-	1.11	-	-	0.78
8	-	-	1.58	-	-	1.37	-	-	1.03	-	-	0.75	-	-	0.83
9	-	-	0.20	-	-	0.31	-	-	0.38	-	-	0.50	-	-	0.95
10	-	-	0.45	-	-	1.07	-	-	0.76	-	-	0.82	-	-	1.04
11	-	-	0.51	-	-	0.34	-	-	0.51	-	-	0.96	-	-	0.83
12	-	-	0.43	-	-	0.98	-	-	0.84	-	-	0.87	-	-	0.59
13	-	-	0.25	-	-	0.38	-	-	0.44	-	-	0.94	-	-	0.91
14	-	-	0.56	-	-	0.48	-	-	0.50	-	-	0.80	-	-	0.87
15	-	-	1.00	-	-	1.02	-	-	0.93	-	-	1.07	-	-	1.17
16	-	-	1.20	-	-	0.65	-	-	1.01	-	-	1.39	-	-	1.66
17	-	-	0.31	-	-	0.34	-	-	0.55	-	-	0.50	-	-	0.57
18	-	-	3.45	-	-	1.55	-	-	1.43	-	-	1.20	-	-	1.37
19	1.01	0.79	0.66	1.79	1.71	-	1.20	1.29	-	1.74	1.65	-	2.09	2.33	-
20	1.21	0.71	0.72	1.51	1.53	-	1.31	1.26	-	1.78	1.89	-	2.49	2.65	-
21	2.24	1.48	1.20	2.56	2.29	-	2.42	2.39	-	3.31	3.39	-	1.56	1.81	-
22	2.79	1.53	1.02	2.89	2.46	-	2.99	2.87	-	4.07	4.09	-	2.64	2.81	-
23	0.69	0.84	0.86	1.78	1.80	1.86	1.41	1.42	1.45	1.16	1.15	1.21	1.12	1.17	1.19
24	1.01	0.97	0.87	2.05	1.94	1.89	1.65	1.57	1.57	1.55	1.47	1.52	1.44	1.41	1.28
25	0.19	0.19	0.23	0.47	0.47	0.54	0.86	0.84	0.85	0.48	0.50	0.52	0.86	1.00	0.91
26	0.12	-	0.25	0.51	-	0.44	0.57	-	0.59	0.56	-	0.54	0.52	-	0.58
27	0.18	0.21	0.18	0.59	0.59	0.62	0.80	0.82	0.83	0.74	0.74	0.77	0.89	0.94	0.92

Site	4 m 32	56	80 km/h	2 m 32	56	80 km/h	1 m 32	56	80 km/h	0.5 m 32	56	80 km/h
2	-	3.98	-	-	4.22	-	-	5.28	-	-	5.44	-
5	-	-	1.23	-	-	1.89	-	-	1.74	-	-	2.23
6	-	-	0.60	-	-	0.80	-	-	1.60	-	-	1.91
7	-	-	0.91	-	-	1.44	-	-	2.32	-	-	3.96
8	-	-	1.95	-	-	3.13	-	-	4.23	-	-	5.94
9	-	-	0.80	-	-	0.75	-	-	1.00	-	-	1.79
10	-	-	0.79	-	-	0.73	-	-	1.01	-	-	1.49
11	-	-	1.03	-	-	1.13	-	-	1.81	-	-	3.16
12	-	-	0.39	-	-	0.42	-	-	0.57	-	-	1.11
13	-	-	1.46	-	-	2.70	-	-	3.74	-	-	5.69
14	-	-	0.88	-	-	1.08	-	-	1.09	-	-	1.52
15	-	-	2.37	-	-	4.72	-	-	9.35	-	-	13.46
16	-	-	1.83	-	-	2.64	-	-	5.04	-	-	6.52
17	-	-	0.54	-	-	0.71	-	-	0.84	-	-	1.55
18	-	-	1.28	-	-	1.63	-	-	1.97	-	-	2.81
19	3.29	2.92	-	5.82	4.77	-	7.32	5.87	-	8.16	7.25	-
20	3.92	3.82	-	5.06	5.46	-	5.66	6.25	-	6.18	6.79	-
21	3.23	3.33	-	3.53	3.61	-	3.01	3.04	-	2.29	2.49	-
22	3.69	3.78	-	6.38	6.41	-	5.49	5.20	-	4.82	4.46	-
23	1.15	1.15	1.11	1.41	1.44	1.44	2.46	2.45	2.34	3.25	3.29	3.13
24	1.36	1.31	1.13	1.63	1.61	1.56	2.31	2.28	2.31	4.61	4.71	5.13
25	1.82	1.78	1.72	1.44	1.59	1.57	2.00	1.91	1.86	3.33	3.05	3.02
26	0.67	-	0.62	0.87	-	0.90	1.15	-	1.18	1.62	-	1.69
27	0.86	0.84	0.84	0.98	0.99	1.01	1.33	1.34	1.34	2.30	2.46	2.15

Table 35. Summary of waveband values for the FHWA/Selcom profilometer

Site	128 m 32	56	80 km/h	64 m 32	56	80 km/h	32 m 32	56	80 km/h	16 m 32	56	80 km/h	8 m 32	56	80 km/h
4	-	-	1.80	-	-	2.26	-	-	1.69	-	-	1.23	-	-	1.28
5	-	-	2.06	-	-	1.47	-	-	1.17	-	-	0.76	-	-	1.17
6	-	-	1.56	-	-	1.29	-	-	0.89	-	-	0.61	-	-	0.76
7	-	-	1.75	-	-	1.39	-	-	1.05	-	-	1.08	-	-	0.77
8	-	-	1.19	-	-	1.37	-	-	1.05	-	-	0.82	-	-	0.83
9	-	-	0.18	-	-	0.29	-	-	0.38	-	-	0.49	-	-	0.98
10	-	-	0.54	-	-	1.10	-	-	0.79	-	-	0.76	-	-	1.04
11	-	-	0.52	-	-	0.36	-	-	0.52	-	-	0.94	-	-	0.80
12	-	-	0.39	-	-	0.92	-	-	0.97	-	-	0.90	-	-	0.62
17	-	-	0.36	-	-	0.35	-	-	0.54	-	-	0.53	-	-	0.53
19	0.93	0.81	-	1.67	1.67	-	1.21	1.23	-	1.69	1.76	-	2.12	2.19	-
20	0.67	-	-	1.52	-	-	1.25	-	-	1.85	-	-	2.39	-	-
21	-	1.34	-	-	2.25	-	-	2.60	-	-	3.10	-	-	1.69	-
22	1.53	1.33	-	2.53	2.26	-	2.89	2.69	-	4.37	4.29	-	2.51	2.59	-
23	0.87	0.84	0.91	1.85	1.79	1.86	1.44	1.45	1.47	1.21	1.17	1.19	1.04	1.12	1.09
24	0.75	0.83	0.84	1.86	1.83	1.85	1.58	1.62	1.61	1.46	1.45	1.51	1.11	1.31	1.22
25	-	0.23	0.22	-	0.52	0.52	-	0.84	0.86	-	0.49	0.49	-	0.91	0.91
26	0.13	0.20	0.27	0.55	0.38	0.40	0.60	0.60	0.61	0.56	0.53	0.55	0.50	0.51	0.49
27	0.26	0.20	0.18	0.61	0.63	0.64	0.83	0.83	0.83	0.74	0.74	0.75	0.86	0.88	0.88

Site	4 m 32	56	80 km/h	2 m 32	56	80 km/h	1 m 32	56	80 km/h	0.5 m 32	56	80 km/h
4	-	-	1.94	-	-	2.70	-	-	2.69	-	-	3.32
5	-	-	1.40	-	-	2.06	-	-	1.99	-	-	2.74
6	-	-	0.64	-	-	0.83	-	-	1.81	-	-	2.77
7	-	-	1.16	-	-	2.07	-	-	4.73	-	-	9.70
8	-	-	1.79	-	-	2.99	-	-	5.14	-	-	7.63
9	-	-	0.77	-	-	0.83	-	-	1.25	-	-	3.13
10	-	-	0.86	-	-	0.91	-	-	1.43	-	-	3.07
11	-	-	1.04	-	-	1.25	-	-	2.15	-	-	4.84
12	-	-	0.49	-	-	0.67	-	-	0.88	-	-	1.22
17	-	-	0.57	-	-	0.73	-	-	0.97	-	-	1.62
19	3.22	3.15	-	5.58	4.75	-	7.54	6.29	-	10.66	10.99	-
20	3.68	-	-	4.97	-	-	6.19	-	-	8.98	-	-
21	-	2.53	-	-	3.62	-	-	3.64	-	-	3.14	-
22	4.45	4.58	-	5.31	5.41	-	5.12	5.10	-	5.57	5.54	-
23	1.08	1.10	1.07	1.47	1.41	1.44	2.64	2.57	2.42	4.96	4.14	4.04
24	1.21	1.33	1.48	2.04	2.44	2.84	4.30	6.26	7.51	11.52	14.55	16.75
25	-	1.77	1.75	-	1.59	1.51	-	1.97	2.43	-	4.57	4.63
26	0.56	0.55	0.51	0.77	0.78	0.71	0.98	1.02	0.93	1.64	1.61	1.50
27	0.94	0.88	0.89	1.28	1.49	1.36	2.94	3.33	2.98	7.48	8.88	7.52

Table 36. Summary of waveband values for the GMPG profilometer

Site	128 m 24	56	80 km/h	64 m 24	56	80 km/h	32 m 24	56	80 km/h	16 m 24	56	80 km/h	8 m 24	56	80 km/h
1	-	0.09	-	-	0.61	-	-	1.60	-	-	1.74	-	-	2.51	-
2	-	0.13	-	-	0.50	-	-	2.64	-	-	2.53	-	-	3.05	-
4	-	0.11	-	-	0.78	-	-	1.49	-	-	1.22	-	-	1.23	-
5	-	0.10	-	-	0.41	-	-	0.97	-	-	0.81	-	-	1.25	-
6	-	0.08	-	-	0.33	-	-	0.64	-	-	0.54	-	-	0.61	-
7	-	0.05	-	-	0.53	-	-	0.87	-	-	1.03	-	-	0.69	-
8	-	0.08	-	-	0.45	-	-	0.74	-	-	0.59	-	-	0.64	-
9	-	-	0.03	-	-	0.10	-	-	0.30	-	-	0.47	-	-	1.09
10	-	-	0.06	-	-	0.33	-	-	0.55	-	-	0.71	-	-	1.17
11	-	-	0.05	-	-	0.12	-	-	0.45	-	-	0.97	-	-	0.98
12	-	-	0.02	-	-	0.34	-	-	0.83	-	-	0.77	-	-	0.87
13	-	-	0.03	-	-	0.09	-	-	0.40	-	-	0.86	-	-	1.02
16	-	-	0.07	-	-	0.22	-	-	0.83	-	-	1.44	-	-	1.60
17	-	-	0.01	-	-	0.14	-	-	0.39	-	-	0.34	-	-	0.31
18	-	0.04	-	-	0.43	-	-	1.24	-	-	1.04	-	-	1.55	-
19	0.09	0.15	0.04	0.57	0.73	0.56	0.97	1.23	1.15	1.70	1.95	2.48	2.09	2.45	2.12
20	0.06	0.07	0.09	0.53	0.65	0.55	0.98	0.95	0.99	1.75	1.77	2.39	2.03	2.79	2.81
21	0.41	0.23	0.22	1.37	1.13	1.16	1.76	1.95	1.43	3.62	3.22	3.22	1.62	2.51	2.14
22	0.51	0.34	0.39	1.58	1.07	1.17	1.87	2.32	2.41	3.84	4.25	5.17	2.06	2.49	3.09
23	0.09	-	0.21	0.56	-	0.43	1.06	-	0.92	0.98	-	0.86	1.14	-	1.00
24	0.13	0.22	0.15	0.74	0.92	0.74	1.26	1.02	0.98	1.38	1.35	1.58	1.09	1.00	1.36
25	0.06	0.11	0.20	0.15	0.15	0.22	0.73	0.51	0.49	0.53	0.61	0.57	0.74	1.03	0.79
26	0.01	0.07	0.05	0.14	0.14	0.11	0.50	0.40	0.46	0.57	0.52	0.48	0.41	0.39	0.50
27	0.02	0.04	0.05	0.22	0.24	0.22	0.67	0.61	0.65	0.74	0.84	0.76	0.74	0.92	1.01

Site	4 m 24	56	80 km/h	2 m 24	56	80 km/h	1 m 24	56	80 km/h	0.5 m 24	56	80 km/h	0.25 m 24	56	80 km/h
1	-	3.98	-	-	6.93	-	-	10.65	-	-	15.90	-	-	20.19	-
2	-	5.95	-	-	4.87	-	-	5.23	-	-	6.67	-	-	7.38	-
4	-	2.44	-	-	2.73	-	-	2.49	-	-	2.92	-	-	4.01	-
5	-	1.83	-	-	2.33	-	-	2.12	-	-	2.63	-	-	3.80	-
6	-	0.87	-	-	0.81	-	-	1.58	-	-	2.24	-	-	2.99	-
7	-	1.20	-	-	1.40	-	-	2.25	-	-	3.87	-	-	5.59	-
8	-	2.56	-	-	3.07	-	-	4.21	-	-	6.26	-	-	6.08	-
9	-	-	0.91	-	-	0.77	-	-	1.15	-	-	2.29	-	-	1.72
10	-	-	0.83	-	-	0.72	-	-	1.14	-	-	1.90	-	-	1.65
11	-	-	1.22	-	-	1.16	-	-	1.67	-	-	2.35	-	-	1.83
12	-	-	0.87	-	-	1.21	-	-	1.46	-	-	1.89	-	-	1.47
13	-	-	1.62	-	-	2.40	-	-	3.18	-	-	4.64	-	-	2.90
16	-	-	1.90	-	-	1.75	-	-	3.05	-	-	4.34	-	-	2.82
17	-	-	0.46	-	-	0.62	-	-	0.91	-	-	1.45	-	-	1.11
18	-	1.82	-	-	2.09	-	-	2.36	-	-	3.53	-	-	5.00	-
19	4.45	3.94	3.39	5.74	8.07	5.22	5.77	9.09	6.42	8.09	11.51	6.71	11.77	11.78	3.94
20	3.86	3.93	3.80	5.65	5.04	5.37	5.00	6.00	6.20	6.87	7.00	6.11	9.45	7.81	3.07
21	6.27	3.98	2.55	4.82	8.07	4.22	3.99	6.84	4.90	3.24	6.81	5.78	3.83	10.60	3.99
22	7.01	5.06	4.30	6.48	4.88	5.23	4.05	4.43	4.14	4.68	4.14	5.07	5.12	3.96	3.95
23	1.22	-	1.18	2.20	-	1.92	2.25	-	2.37	4.42	-	3.29	5.47	-	1.93
24	1.49	1.05	1.33	2.08	1.52	1.48	2.40	2.41	2.49	4.95	4.71	4.42	10.42	9.41	3.55
25	2.60	2.29	2.02	1.86	1.68	1.39	1.98	2.15	1.92	3.71	3.84	3.20	7.44	6.67	2.37
26	0.60	0.80	0.59	0.98	0.75	0.75	0.79	1.03	1.12	1.46	1.98	1.74	2.37	2.70	1.23
27	0.80	1.05	0.93	1.55	1.04	0.97	1.30	1.44	1.46	2.78	2.84	2.55	6.36	5.31	2.17

Table 37. Summary of waveband values for the Minnesota profilometer

Site	128 m 24	48	80 km/h	64 m 24	48	80 km/h	32 m 24	48	80 km/h	16 m 24	48	80 km/h
1	-	1.49	-	-	1.32	-	-	1.30	-	-	1.81	-
2	-	1.68	-	-	1.51	-	-	3.31	-	-	2.63	-
4	-	-	1.01	-	-	1.91	-	-	1.69	-	-	1.13
5	-	-	0.88	-	-	1.26	-	-	0.96	-	-	0.64
6	-	-	0.84	-	-	1.20	-	-	1.01	-	-	0.58
7	-	-	0.44	-	-	1.26	-	-	1.01	-	-	0.99
9	-	-	0.07	-	-	0.24	-	-	0.36	-	-	0.48
10	-	-	0.18	-	-	0.79	-	-	0.86	-	-	0.77
11	-	-	0.17	-	-	0.24	-	-	0.49	-	-	0.91
12	-	-	0.42	-	-	0.62	-	-	0.56	-	-	0.86
13	-	-	0.08	-	-	0.35	-	-	0.44	-	-	0.87
14	-	-	0.12	-	-	0.32	-	-	0.43	-	-	0.68
15	-	0.23	-	-	0.57	-	-	0.92	-	-	0.82	-
16	-	-	0.29	-	-	0.54	-	-	0.95	-	-	1.25
17	-	-	0.18	-	-	0.36	-	-	0.56	-	-	0.46
18	-	0.48	-	-	0.88	-	-	1.19	-	-	0.98	-
21	0.93	0.87	0.94	2.16	1.97	2.10	2.39	2.25	2.47	2.97	2.89	3.34
22	1.22	1.18	-	2.86	2.82	-	2.82	2.65	-	4.25	4.29	-
23	0.47	0.35	0.34	2.10	2.00	1.98	1.46	1.39	1.41	1.11	1.10	1.14
24	0.60	0.63	0.61	1.61	1.52	1.53	1.67	1.57	1.57	1.33	1.24	1.21
25	0.39	0.38	0.38	0.57	0.52	0.51	0.90	0.87	0.88	0.56	0.57	0.57
26	0.24	0.35	0.27	0.47	0.49	0.48	0.63	0.66	0.64	0.56	0.56	0.57
27	0.28	0.29	0.29	0.69	0.64	0.66	0.81	0.80	0.83	0.84	0.85	0.86

Site	8 m 24	48	80 km/h	4 m 24	48	80 km/h	2 m 24	48	80 km/h	1 m 24	48	80 km/h
1	-	2.91	-	-	4.84	-	-	9.15	-	-	7.64	-
2	-	2.97	-	-	3.75	-	-	4.37	-	-	4.52	-
4	-	-	1.23	-	-	1.89	-	-	2.46	-	-	2.11
5	-	-	0.88	-	-	1.20	-	-	1.77	-	-	1.57
6	-	-	0.68	-	-	0.63	-	-	0.74	-	-	1.21
7	-	-	0.54	-	-	0.73	-	-	1.03	-	-	1.33
9	-	-	0.93	-	-	0.77	-	-	0.79	-	-	1.07
10	-	-	0.89	-	-	0.71	-	-	0.70	-	-	1.03
11	-	-	0.74	-	-	0.98	-	-	1.11	-	-	1.49
12	-	-	0.58	-	-	0.48	-	-	0.98	-	-	1.77
13	-	-	0.83	-	-	1.44	-	-	2.47	-	-	3.04
14	-	-	0.70	-	-	0.85	-	-	1.03	-	-	1.21
15	-	1.08	-	-	1.94	-	-	3.30	-	-	5.05	-
16	-	-	1.54	-	-	1.78	-	-	1.83	-	-	2.98
17	-	-	0.52	-	-	0.54	-	-	0.73	-	-	1.02
18	-	1.18	-	-	1.12	-	-	1.27	-	-	1.79	-
21	1.80	1.68	1.75	2.25	2.11	2.66	2.48	2.50	2.76	1.82	1.86	2.32
22	2.71	2.61	-	3.45	3.40	-	5.28	5.38	-	4.47	4.17	-
23	1.09	1.06	1.08	1.06	1.09	1.26	1.36	1.53	1.88	1.99	2.01	2.34
24	0.95	0.98	0.99	0.97	0.97	0.98	1.41	1.36	1.51	1.81	1.95	2.24
25	0.86	0.81	0.87	1.54	1.54	1.54	1.51	1.52	1.51	1.55	1.85	1.93
26	0.47	0.43	0.43	0.42	0.39	0.43	0.64	0.58	0.59	0.67	0.61	0.63
27	0.82	0.84	0.82	0.77	0.76	0.78	0.99	0.95	0.98	1.17	1.26	1.38

Table 38. Summary of waveband values for the Ohio profilometer

Site	128 m 24	48	80 km/h	64 m 24	48	80 km/h	32 m 24	48	80 km/h	16 m 24	48	80 km/h
1	-	1.44	-	-	1.45	-	-	1.15	-	-	1.78	-
2	-	1.59	-	-	1.58	-	-	3.30	-	-	2.58	-
4	-	-	1.00	-	-	1.91	-	-	1.64	-	-	1.21
5	-	0.81	0.81	-	1.21	1.21	-	1.07	0.99	-	0.67	0.71
6	-	0.91	0.91	-	1.21	1.20	-	0.88	0.89	-	0.57	0.57
7	-	0.47	0.48	-	1.27	1.27	-	1.01	1.00	-	1.01	1.05
8	-	0.77	0.76	-	1.17	1.17	-	1.06	1.09	-	0.83	0.79
9	-	-	0.09	-	-	0.23	-	-	0.36	-	-	0.48
10	-	-	0.18	-	-	0.80	-	-	0.81	-	-	0.71
11	-	-	0.16	-	-	0.24	-	-	0.49	-	-	0.89
12	-	-	0.46	-	-	0.60	-	-	0.54	-	-	0.77
13	-	-	0.08	-	-	0.33	-	-	0.46	-	-	0.86
14	-	-	0.11	-	-	0.33	-	-	0.44	-	-	0.72
15	-	0.28	0.31	-	0.61	0.62	-	0.96	0.96	-	0.78	0.79
16	-	-	0.32	-	-	0.55	-	-	0.94	-	-	1.31
17	-	-	0.17	-	-	0.36	-	-	0.58	-	-	0.45
18	-	-	0.50	-	-	0.86	-	-	1.15	-	-	0.97
19	0.51	0.21	0.22	1.60	1.59	1.56	1.20	1.17	1.15	1.76	1.77	1.71
20	0.69	0.30	0.27	1.24	1.45	1.47	1.21	1.21	1.24	1.88	1.82	1.97
21	0.75	0.89	-	2.05	2.18	-	2.59	2.65	-	3.67	3.52	-
22	0.87	1.19	-	2.57	2.79	-	2.41	2.38	-	4.07	3.56	-
23	0.37	0.36	-	1.78	1.97	-	1.60	1.60	-	1.39	1.31	-
24	0.83	0.75	-	1.53	1.67	-	1.64	1.69	-	1.49	1.48	-
25	0.55	0.40	0.39	0.75	0.50	0.56	0.89	0.89	0.89	0.65	0.59	0.65
26	0.49	0.34	0.35	0.91	0.52	0.52	0.70	0.67	0.67	0.58	0.57	0.56
27	0.64	0.27	0.26	0.77	0.65	0.65	0.83	0.84	0.84	0.87	0.85	0.86

Site	8 m 24	48	80 km/h	4 m 24	48	80 km/h	2 m 24	48	80 km/h	1 m 24	48	80 km/h
1	-	2.92	-	-	3.73	-	-	7.40	-	-	8.15	-
2	-	3.14	-	-	3.77	-	-	4.24	-	-	4.52	-
4	-	-	1.38	-	-	1.99	-	-	2.67	-	-	2.29
5	-	1.09	1.15	-	1.44	1.39	-	1.90	1.82	-	1.77	1.54
6	-	0.75	0.77	-	0.65	0.64	-	0.77	0.77	-	1.45	1.49
7	-	0.69	0.69	-	0.93	0.93	-	1.32	1.33	-	1.91	1.88
8	-	0.82	0.93	-	1.86	1.75	-	3.04	3.10	-	4.10	3.92
9	-	-	1.00	-	-	0.67	-	-	0.69	-	-	1.04
10	-	-	1.03	-	-	0.74	-	-	0.71	-	-	0.95
11	-	-	0.81	-	-	1.04	-	-	1.10	-	-	1.37
12	-	-	0.52	-	-	0.47	-	-	0.61	-	-	0.76
13	-	-	0.87	-	-	1.47	-	-	2.52	-	-	2.96
14	-	-	0.73	-	-	0.86	-	-	0.97	-	-	1.01
15	-	1.18	1.19	-	2.07	2.22	-	3.76	4.24	-	5.61	6.84
16	-	-	1.68	-	-	1.93	-	-	2.11	-	-	4.10
17	-	-	0.56	-	-	0.54	-	-	0.67	-	-	0.86
18	-	-	1.32	-	-	1.45	-	-	1.84	-	-	2.11
19	2.31	2.16	2.20	3.44	3.51	3.03	4.62	5.18	4.80	4.42	5.48	5.13
20	2.51	2.58	2.87	3.51	3.52	3.82	4.73	4.54	5.53	4.74	4.88	5.54
21	1.86	1.94	-	3.68	3.17	-	3.34	3.25	-	2.50	2.42	-
22	2.69	2.35	-	3.79	3.70	-	5.85	5.54	-	4.17	3.66	-
23	1.21	1.15	-	1.25	1.20	-	1.32	1.12	-	1.69	1.80	-
24	1.43	1.47	-	1.30	1.24	-	1.39	1.40	-	1.80	1.77	-
25	0.92	0.86	0.96	1.76	1.66	1.78	1.30	1.48	1.32	1.70	1.72	1.77
26	0.40	0.41	0.43	0.37	0.40	0.43	0.46	0.51	0.55	0.47	0.51	0.54
27	0.86	0.84	0.88	0.82	0.84	0.84	1.21	1.21	1.22	1.36	1.37	1.33

Table 39. Summary of waveband values for the West Virginia profilometer

Site	128 m 24	48	80 km/h	64 m 24	48	80 km/h	32 m 24	48	80 km/h	16 m 24	48	80 km/h
2	-	0.55	-	-	1.27	-	-	3.11	-	-	2.71	-
6	-	0.34	-	-	0.74	-	-	0.85	-	-	0.60	-
7	-	0.16	-	-	0.91	-	-	0.97	-	-	0.98	-
9	-	0.03	-	-	0.17	-	-	0.36	-	-	0.51	-
10	-	0.07	-	-	0.60	-	-	0.77	-	-	0.75	-
11	-	0.06	-	-	0.18	-	-	0.48	-	-	0.95	-
18	-	0.11	-	-	0.63	-	-	1.13	-	-	1.01	-
19	0.18	0.43	-	1.63	1.48	-	1.21	1.14	-	1.75	1.75	-
20	0.16	0.15	-	1.46	1.55	-	1.28	1.17	-	2.01	1.74	-
23	0.36	1.37	-	1.94	2.93	-	1.40	2.60	-	1.13	4.03	-
24	0.52	-	-	1.46	-	-	1.60	-	-	1.26	-	-
25	0.43	0.43	0.41	0.61	0.54	0.54	0.93	0.90	0.90	0.57	0.55	0.56
26	0.46	0.36	0.39	0.53	0.51	0.52	0.69	0.66	0.69	0.55	0.56	0.58
27	0.23	0.29	0.30	0.57	0.62	0.63	0.83	0.82	0.86	0.79	0.81	0.88

Site	8 m 24	48	80 km/h	4 m 24	48	80 km/h	2 m 24	48	80 km/h	1 m 24	48	80 km/h
2	-	2.82	-	-	3.22	-	-	3.98	-	-	3.97	-
6	-	0.69	-	-	0.55	-	-	0.67	-	-	1.37	-
7	-	0.60	-	-	0.72	-	-	0.97	-	-	1.40	-
9	-	0.82	-	-	0.65	-	-	0.64	-	-	1.02	-
10	-	0.85	-	-	0.66	-	-	0.60	-	-	0.89	-
11	-	0.65	-	-	0.95	-	-	1.05	-	-	1.78	-
18	-	1.10	-	-	1.13	-	-	1.38	-	-	1.78	-
19	2.12	2.47	-	3.24	3.45	-	7.52	4.70	-	8.36	4.71	-
20	2.36	1.93	-	3.32	3.12	-	5.01	6.24	-	4.99	6.76	-
23	1.01	2.49	-	1.02	2.94	-	1.27	5.23	-	1.79	3.99	-
24	0.96	-	-	0.80	-	-	1.36	-	-	1.63	-	-
25	0.83	0.81	0.75	1.22	1.40	1.44	1.33	1.26	1.43	1.41	1.50	1.66
26	0.42	0.42	0.37	0.32	0.36	0.37	0.55	0.50	0.50	0.50	0.61	0.58
27	0.78	0.83	0.72	0.63	0.65	0.67	0.92	0.81	0.97	0.97	1.09	1.09

Table 40. Summary of waveband values for the Michigan DOT profilometer

Site	128 m 55 km/h	128 m 82 km/h	64 m 55 km/h	64 m 82 km/h	32 m 55 km/h	32 m 82 km/h	16 m 55 km/h	16 m 82 km/h	8 m 55 km/h	8 m 82 km/h
4	1.88	-	2.57	-	2.69	-	1.46	-	1.46	-
5	1.33	-	1.91	-	1.45	-	1.16	-	1.27	-
6	1.52	1.50	1.67	1.69	1.32	1.34	0.68	0.68	0.75	0.76
7	0.67	0.70	1.51	1.51	1.20	1.22	1.26	1.28	0.75	0.73
8	1.13	0.84	1.76	1.53	1.15	1.18	0.90	0.84	1.04	0.78
9	-	0.27	-	0.51	-	0.66	-	1.14	-	1.61
10	-	0.31	-	0.83	-	0.90	-	0.92	-	1.00
11	-	0.53	-	0.61	-	1.24	-	2.15	-	1.79
16	0.85	1.01	0.73	0.81	1.00	1.03	1.55	1.53	1.75	1.62
17	-	0.28	-	0.42	-	0.65	-	0.46	-	0.58
19	0.16	0.26	1.72	1.69	1.25	1.18	1.82	1.82	2.46	2.36
20	0.64	0.44	1.48	1.53	1.30	1.25	2.07	2.08	2.81	2.50
21	3.13	2.78	4.22	3.32	2.20	2.79	3.40	4.02	1.72	1.99
22	0.78	0.76	3.36	3.20	2.27	2.71	4.66	4.96	3.17	2.31
23	0.17	0.13	2.39	2.35	1.63	1.61	1.29	1.33	1.12	1.16
24	2.28	1.12	2.31	2.11	1.66	1.90	1.51	1.73	1.38	1.68
25	0.44	0.57	1.08	1.03	1.25	1.17	0.80	0.84	1.15	1.05
26	0.23	0.29	1.05	0.76	1.10	0.93	0.76	0.69	0.51	.0.49
27	0.20	0.36	0.75	0.78	0.79	0.75	1.26	1.15	0.92	0.93

Site	4 m 55 km/h	4 m 82 km/h	2 m 55 km/h	2 m 82 km/h	1 m 55 km/h	1 m 82 km/h	0.5 m 55 km/h	0.5 m 82 km/h
4	2.27	-	3.04	-	2.76	-	3.67	-
5	2.01	-	3.03	-	3.40	-	7.00	-
6	0.67	0.64	1.07	1.07	2.08	2.20	4.46	2.67
7	1.26	0.91	2.49	1.34	5.48	2.84	10.50	4.68
8	2.37	1.62	4.32	3.29	7.39	4.74	17.37	7.72
9	-	1.18	-	1.99	-	3.59	-	6.50
10	-	0.99	-	1.59	-	3.22	-	6.49
11	-	2.06	-	2.09	-	3.83	-	5.51
16	1.83	1.88	1.85	1.90	2.97	3.51	6.05	7.15
17	-	0.59	-	0.91	-	1.34	-	1.87
19	4.13	3.37	9.57	7.93	12.11	10.44	14.80	15.58
20	4.20	3.93	6.56	5.70	7.69	6.72	9.03	8.09
21	3.12	3.28	3.39	4.37	3.21	4.45	2.75	3.49
22	4.34	4.45	7.20	6.55	7.07	7.49	7.80	10.58
23	1.15	1.16	1.53	1.58	2.57	2.89	4.26	4.40
24	1.36	1.64	1.74	2.10	2.65	3.24	5.72	6.64
25	1.69	1.74	1.63	1.60	2.33	2.55	4.56	4.68
26	0.46	0.46	0.56	0.57	0.78	1.13	1.49	1.48
27	0.87	0.87	1.16	1.11	1.67	1.92	3.45	3.58

Table 41. Summary of waveband values for the South Dakota profilometer

Site	128 m 31	56	80 km/h	64 m 31	56	80 km/h	32 m 31	56	80 km/h	16 m 31	56	80 km/h
1	2.28	4.89	3.48	2.44	3.05	2.07	1.37	2.96	2.17	1.43	1.93	1.86
2	3.33	2.98	-	0.79	1.12	-	2.04	2.14	-	1.90	2.23	-
4	-	1.13	1.17	-	1.76	1.69	-	1.36	1.38	-	1.14	1.06
5	-	1.32	1.31	-	0.97	0.99	-	0.85	0.81	-	0.71	0.59
6	-	1.06	1.27	-	0.98	1.09	-	0.83	0.90	-	0.56	0.56
7	-	0.92	1.00	-	0.65	0.86	-	0.60	0.76	-	0.53	0.75
8	-	1.42	2.17	-	1.26	1.94	-	0.72	1.32	-	0.69	0.61
9	-	-	0.11	-	-	0.16	-	-	0.24	-	-	0.37
10	-	-	0.22	-	-	0.44	-	-	0.40	-	-	0.44
11	-	-	0.33	-	-	0.23	-	-	0.48	-	-	0.77
12	-	-	0.36	-	-	0.44	-	-	0.51	-	-	0.62
13	-	-	0.15	-	-	0.27	-	-	0.36	-	-	0.66
14	-	0.12	0.08	-	0.25	0.24	-	0.35	0.41	-	0.65	0.75
15	-	0.80	0.76	-	0.68	0.71	-	0.81	0.85	-	0.96	1.02
16	-	-	0.54	-	-	0.45	-	-	0.82	-	-	1.07
17	-	-	0.16	-	-	0.35	-	-	0.46	-	-	0.42
18	-	1.07	1.57	-	0.94	0.88	-	1.10	1.06	-	0.87	1.11
19	0.74	0.34	-	1.43	1.55	-	0.96	1.09	-	1.15	1.36	-
20	0.34	0.29	0.29	1.03	0.93	1.00	0.75	0.90	0.71	1.20	1.76	1.63
21	0.52	0.75	0.80	1.54	1.46	1.75	1.33	1.99	2.43	1.67	3.22	3.69
22	2.24	2.89	-	2.32	2.47	-	1.18	1.72	-	2.74	3.13	-
23	0.11	0.12	0.29	0.27	0.49	1.14	0.40	0.69	1.08	0.44	0.74	0.81
24	0.61	0.53	0.47	1.28	1.42	1.32	0.87	1.14	1.20	1.22	1.31	1.31
25	0.15	0.20	0.15	0.24	0.39	0.34	0.65	0.63	0.65	0.39	0.37	0.40
26	0.10	0.09	0.09	0.19	0.40	0.17	0.24	0.43	0.16	0.26	0.30	0.18
27	0.16	0.19	0.24	0.37	0.50	0.55	0.44	0.37	0.70	0.43	0.41	0.83

Site	8 m 31	56	80 km/h	4 m 31	56	80 km/h	2 m 31	56	80 km/h	1 m 31	56	80 km/h	0.5 m 31 km/h
1	2.43	2.79	2.89	3.35	3.02	3.18	5.77	4.46	4.45	8.61	7.26	-	14.01
2	2.53	2.83	-	3.04	3.11	-	3.17	3.48	-	4.99	5.05	-	7.06
4	-	1.15	1.13	-	1.75	1.79	-	2.79	2.74	-	4.03	-	-
5	-	0.95	0.96	-	1.27	1.37	-	2.08	2.37	-	3.13	-	-
6	-	0.76	0.72	-	0.88	0.86	-	1.27	1.64	-	2.27	-	-
7	-	0.61	0.60	-	0.85	0.90	-	1.22	1.47	-	1.93	-	-
8	-	1.01	0.78	-	1.61	1.79	-	2.68	2.98	-	4.13	-	-
9	-	-	0.62	-	-	0.84	-	-	1.46	-	-	-	-
10	-	-	0.68	-	-	0.79	-	-	1.45	-	-	-	-
11	-	-	0.75	-	-	0.92	-	-	1.47	-	-	-	-
12	-	-	0.68	-	-	0.88	-	-	1.33	-	-	-	-
13	-	-	0.86	-	-	1.54	-	-	2.72	-	-	-	-
14	-	0.72	0.75	-	1.06	1.16	-	1.47	2.13	-	2.60	-	-
15	-	1.26	1.08	-	2.03	2.01	-	3.41	3.48	-	6.77	-	-
16	-	-	1.22	-	-	1.54	-	-	1.90	-	-	-	-
17	-	-	0.44	-	-	0.70	-	-	1.08	-	-	-	-
18	-	1.05	1.26	-	1.50	1.56	-	2.20	2.34	-	3.85	-	-
19	1.79	1.83	-	2.69	2.44	-	4.14	4.78	-	5.43	6.48	-	9.25
20	1.78	1.89	2.09	2.68	3.02	2.63	3.46	4.86	3.36	5.25	5.58	-	7.07
21	1.50	2.00	2.14	2.18	3.31	3.11	3.19	3.65	3.69	3.90	4.73	-	5.57
22	2.09	2.61	-	3.94	3.24	-	5.62	5.30	-	5.67	5.51	-	7.42
23	0.43	0.81	0.91	0.72	0.83	1.09	1.03	1.27	1.80	1.46	1.92	-	2.42
24	0.99	1.08	1.23	1.38	1.22	1.14	1.96	2.42	2.26	3.61	4.36	-	7.09
25	0.69	0.69	0.78	1.29	1.29	1.44	1.64	2.12	1.89	3.07	3.56	-	-
26	0.22	0.50	0.23	0.35	0.60	0.25	0.39	0.79	0.41	0.34	1.25	-	-
27	0.76	0.69	1.03	0.88	0.98	1.38	1.53	2.00	2.53	3.60	3.21	-	-

REFERENCES

[1] E. Spangler and W. Kelly, "GMR Road Profilometer - A Method for Measuring Road Profile." HRR121, Highway Research Board, 1966.

[2] "Analyseur de Profil en Long - APL 72." Bulletin 1BAC76, Laboratoire Central de Ponts et Chaussees, 58 Boulevard Lefebvre, 75732 Paris Cedex 15, France.

[3] P. B. Still and P. G. Jordan, "Evaluation of the TRRL high-speed profilometer." TRRL Laboratory Report 922, Crowthorne, UK, 45 pp.

[4] D. L. Huft, "South Dakota Profilometer." TRR 1000, Surface Properties-Vehicle Interaction, Transportation Research Board,1984.

[5] G. S. Preston, S. Macintyre, and T. L. Yang, Noncontact Road Profiling System. FHWA Report No. FHWA/RD-82/062, August 1982.

[6] P. Arnberg, "The Laser Road Surface Tester." Swedish National Road & Traffic Research Institute, Report No. 255A, 1983.

[7] J. D. Campbell and M. W. Sayers, "An Infrared Distance Sensor, Analysis and Test Results" The University of Michigan Transportation Research Instutute, Report No. UMTRI-84-14, March 1984, 114 pp.

[8] J. D. King and S.A. Cerwin, "System for Inventorying Road Surface Topography (SIRST)." FHWA Report No. FHWA/RD-82/062, August 1982.

[9] T. D. Gillespie, M. Sayers, and L. Segel, "Calibration of Response-Type Road Roughness Measuring Systems." NCHRP Report No. 228, December 1980, 88 pp.

[10] M. Sayers, T. D. Gillespie, and C. Queiroz, "The International Road Roughness Experiment: Establishing Correlation and a Calibration Standard for Measurements," World Bank Technical Paper No. 45, The World Bank, Washington DC, January 1986, 453 pp.

[11] M. Sayers, T. D. Gillespie, and W. D. Paterson, "Guidelines for Conducting and Calibrating Road Roughness Measurements," World Bank Technical Paper No. 46, The World Bank, Washington DC, January 1986, 87 pp.

[12] W. R. Hudson, D. Halbach, J. P. Zaniewski, and L. Moser, "Root-Mean-Square Vertical Acceleration as a Summary Roughness Statistic," Measuring Road Roughness and Its Effects on User Cost and Comfort, ASTM STP 884, T. D. Gillespie and M. Sayers, Eds., American Society for Testing and Materials, Philadelphia, 1985, pp 3-24.

[13] C. V. Queiroz, "A Procedure for Obtaining a Stable Roughness Scale from Rod and Level Profiles." Working Document #22, Research on the Interrelationships between Costs of Highway Construction, Maintenance, and Utilization, Empresa Brasileria de Planejamente de Transportes (GEIPOT), Brasilia, July 1979.

[14] J. Lucas and A. Viano, "Systematic Measurement of Evenness on the Road Network: High Output Longitudinal Profile Analyser." LCPC Report No. 101, June 1979.

[15] D. M. Ducros, "Mesure de 'Uni des Couches de Chaussees avec l'Analyseur Dynamique de Profile en Long Type APL 25." Laboratoire Central des Ponts et Chaussees, January 1980.

[16] "Descriptive Specification for the Model 8300 Road Roughness Surveyor." K. J. Law Engineers, Inc., Farmington, Michigan, November 1983.

[17] R. J. Chaka, "The Design and Development of a Highway Speed Road Profilometer." SAE Paper No. 780064, 1978.

[18] U.S. Patent No. 4,422,322, issued Dec. 27, 1983.

[19] G. K. Watugala and G. F. Hayhoe, "Simulation of Road Meters by Separate Analysis of Accelerometer and Height Sensor Data." Measuring Road Roughness and Its Effects on User Cost and Comfort, ASTM STP 884, T. D. Gillespie and Michael Sayers, Eds., American Society for Testing and Materials, Philadelphia, 1985, pp 48-65.

[20] J. S. Bendat and A. G. Piersol, Engineering Applications of Correlation and Spectral Analysis. John Wiley and Sons, New York, 1980.

[21] M. B. Gorski, "Etude de l'uni longitudinal revetements routiers." CR 15/81, Centre de Recherches Routieres, Bruxelles, Belgique, 1981.

[22] M. B. Gorski, "L'exploitation a grand rendement de l'analyseur de profil en long et ses possibilites d'adaptation aux differentes techniques de chaussees dans differents pays." International Road Federation, Xth IRF World Meeting, Rio de Janiero, October 1984.

[23] M. B. Gorski, "The implication of the International Road Roughness Experiment for Belgium." 65th Annual Meeting of the Transportation Research Board, Washington DC, January 1986, (To be published).

[24] D. R. C. Cooper and J. C. Young (Transport and Road Research Laboratory, Great Britain) and M. B. Gorski (Belgium Road Research Center), "Comparisons between the High-Speed Road Monitor and the CRR Analyseur de Profil en Long." Joint report TRRL-BRRC, (To be published).